

**PHOTOCHEMISTRY OF TRIPTYCENE-1,4-QUINONE AND
THE CONTROL OF REACTION MULTIPLICITY
IN THE SOLID STATE**

By
Janet Nathalie Gamlin

B.Sc. (Hons), University of British Columbia, 1991

A THESIS SUBMITTED IN PARTIAL FULFILLMENT OF
THE REQUIREMENTS FOR THE DEGREE OF
DOCTOR OF PHILOSOPHY

in
THE FACULTY OF GRADUATE STUDIES
(DEPARTMENT OF CHEMISTRY)

We accept this thesis as conforming
to the required standard

THE UNIVERSITY OF BRITISH COLUMBIA

JUNE 1996

© Janet N. Gamlin, 1996

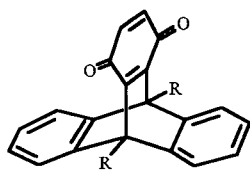
In presenting this thesis in partial fulfilment of the requirements for an advanced degree at the University of British Columbia, I agree that the Library shall make it freely available for reference and study. I further agree that permission for extensive copying of this thesis for scholarly purposes may be granted by the head of my department or by his or her representatives. It is understood that copying or publication of this thesis for financial gain shall not be allowed without my written permission.

Department of CHEMISTRY

The University of British Columbia
Vancouver, Canada

Date June 28 / 96

ABSTRACT



- 63 R = H
69 R = CH₃
72 R = CH₂OCH₃

Three triptycene-1,4-quinone derivatives were synthesized and their photochemical rearrangements investigated in solution and in the solid state. The substituents at the 9,10-bridgehead positions affected the outcome of the photochemical reactions in some novel and unexpected ways. Upon direct irradiation of triptycene **63** in acetonitrile in the absence of oxygen, formation of the corresponding dibenzosemibullvalene derivative arising from the di- π -methane rearrangement was observed. Photolysis of the methyl substituted compound **69** led to the formation of the corresponding dibenzosemibullvalene compound as well as a dark blue norcaradiene derivative resulting from a carbene intermediate. Triptycene **72** also rearranged to a small extent to a norcaradiene derivative, but primarily underwent a γ -hydrogen abstraction reaction giving a colorless dihydrofuran derivative. Additionally, a dark orange benz[*a*]aceanthrylene derivative was isolated. Photolysis of triptycene **63** in the presence of oxygen gave a unique triketone derivative. Irradiation of triptycene **63** in chlorinated solvents resulted in chlorinated triptycene quinones. All three starting triptycene-1,4-quinones were found to be photochemically inert in the crystalline state. The photoproduct structures were supported by X-ray crystallographic analysis, and possible mechanisms for their formation are presented and discussed.

The ability to enhance triplet photochemical behavior of a probe molecule in the solid state was tested by introducing either heavy atoms, which enhance intersystem crossing, or

sensitizers, which promote triplet-triplet energy transfer. The efficiency of intersystem crossing as well as triplet-triplet energy transfer was studied by forming salts between photochemically reactive carboxylic acids and either alkali metal hydroxides or organic amines containing an acetophenone moiety. Promising triplet-triplet energy transfer results were established by irradiating salts formed between a β,γ -unsaturated keto-acid and several different sensitizer amines.

The singlet/triplet photoreactivity of a series of monosubstituted dibenzobarrelene carboxylates (probe molecules) was also analyzed in the crystalline state and in solution. The Li^+ , Na^+ , K^+ , Rb^+ and Cs^+ salts of the carboxylates as well as salts with various ammonium ion sensitizer components were prepared in order to control the reaction multiplicity in the solid state by the heavy atom effect or by triplet-triplet energy transfer. By monitoring the ratio of singlet photoproduct (dibenzocyclooctatetraene) to triplet photoproduct (dibenzo-semibullvalene), the effects of heavy atoms linked to a probe molecule were studied. A general explanation for the increase in triplet product formation in the solid state upon the introduction of heavy atoms was suggested. Solid state triplet-triplet energy transfer was also successfully demonstrated in the salts containing the amine sensitizers. The X-ray crystal structures of the salts were studied in order to establish a correlation between the geometric arrangement of the donor and acceptor and the increase in triplet state reactivity. The observed difference in efficiency of the sensitizers was proposed to result from different excited states.

TABLE OF CONTENTS

Abstract	ii
Table of Contents	iv
List of Figures	x
List of Tables	xvi
List of Graphs	xviii
Acknowledgments	xix
Dedication	xx

INTRODUCTION	1
---------------------------	---

CHAPTER 1 PHOTOCHEMICAL INTRODUCTION	1
---	---

1.1. General.....	1
1.2. Solid State Organic Photochemistry	2
1.2.1. The Topochemical Principle	3
1.2.2. Topotactic Reactions.....	6
1.2.3. Solid State Reaction Efficiency.....	7
1.2.4. Photochemical Reactivity of Organic Salts.....	8
1.3. The Di- π -Methane Rearrangement	9
1.3.1. Reaction Mechanism	10
1.3.2. Reaction Multiplicity	14
1.3.3. Regioselectivity of the Di- π -Methane Rearrangement	15
1.3.4. Photochemistry of Dibenzobarrelene Derivatives	17
1.3.5. The Oxadi- π -Methane Rearrangement	20
1.4. The Norrish Type II Reaction	22
1.5. The Excited State.....	25
1.5.1. Triplet-Triplet Energy Transfer.....	26
1.5.2. The Heavy Atom Effect.....	29

1.5.3. The Heavy Atom Effect in Zeolites.....	33
1.6. Objectives of Present Research.....	35

RESULTS AND DISCUSSION..... 41

PART I PHOTOCHEMISTRY OF

TRIPTYCENE-1,4-QUINONE 41

CHAPTER 2 GENERAL ORGANIC SYNTHESIS..... 41

2.1. Preparation of 9,10-Dihydro-9,10[1',2']benzoanthracene-1,4-dione (63).....	41
2.2. Synthesis of Anthracene Derivatives.....	42
2.3. Preparation of 9,10-Disubstituted-9,10-dihydro-9,10[1',2']benzoanthracene-1,4-dione Derivatives	43
2.4. Preparation of 5- and 6-Chloro-9,10-dihydro-9,10[1',2']benzoanthracene-1,4-diones	45

CHAPTER 3 PHOTOCHEMICAL STUDIES OF 9,10-DIHYDRO-9,10[1',2']

BENZENOANTHRACENE-1,4-DIONE (63**)..... 47**

3.1. Photochemical Results Upon Direct Irradiation of 63	48
3.1.1. Structure Elucidation of Semibullvalene 80	49
3.1.2. Regioselectivity of Semibullvalene Photoproduct Formation	51
3.2. Photochemical Results Upon Irradiation of 63 in Acetone	53
3.2.1. Structural Assignment of Triketone 81	53
3.2.2. Mechanistic Speculation on the Formation of Triketone 81	57
3.3. Photolysis of Quinone 63 in Chlorinated Solvents.....	61
3.3.1. Structural Assignment	62
3.3.2. Mechanism for Formation of Chlorinated Product 75	65
3.3.3. Mechanism of Formation of Chlorinated Photoproduct 74	68
3.4. Solid State Reactivity of Triptycene-1,4-quinone (63).....	71

CHAPTER 4 PHOTOCHEMICAL STUDIES OF 9,10-DIHYDRO-9,10-DIMETHYL-9,10[1',2']BENZENOANTHRACENE-1,4-DIONE (69)	77
4.1. Photochemical Results Upon Direct Irradiation	77
4.1.1. Photoproduct Structure Elucidation.....	77
4.1.2. Mechanism of Formation of Semibullvalene 102 and Norcaradiene Derivative 103.....	83
4.1.3. The Midnight- Blue Color of Norcaradiene 103	86
4.1.4. Solvatochromic Effect of Norcaradiene 103.....	90

CHAPTER 5 PHOTOCHEMICAL STUDIES OF 9,10-BIS(METHOXYMETHYL)-9,10-DIHYDRO-9,10[1',2']BENZENOANTHRACENE-1,4-DIONE (72)	93
5.1. Photorearrangement of 72 in Acetonitrile.....	93
5.1.1. Structure Elucidation of Photoproducts 103, 110 and 111	94
5.1.2. Mechanism for Formation of Dihydrobenzofuran 111	99
5.1.3. Structure-Reactivity Analysis of Quinone 72.....	102
5.1.4. Structure Elucidation of Product 112.....	104
5.1.5. Mechanism for the Formation of Benz[<i>a</i>]aceanthrylene 112.....	107

PART II THE CONTROL OF REACTION MULTIPLICITY IN THE SOLID STATE: IONIC SENSITIZERS AND IONIC HEAVY ATOM EFFECTS	111
--	-----

CHAPTER 6 GENERAL ORGANIC SYNTHESIS	112
6.1. Preparation of β , γ -Unsaturated Ketones.....	112
6.2. Preparation of <i>p</i> -Acetyl- <i>N,N</i> -dimethylbenzylamine (128).....	113
6.3. Preparation of 9,10-Dihydro-9,10-ethenoanthracene Acids.....	114

CHAPTER 7 THE PHOTOCHEMISTRY OF β , γ -UNSATURATED

KETONES	116
7.1. The Solution Phase Photochemistry of Pentanone Derivative 121	116
7.2. The Solid State Photochemistry of Pentanone Derivative 121 and its Alkali Salts	117
7.3. The Photochemistry of Ionic Sensitizer Salts of Pentanone Derivative 121	118
7.4. The Solution Phase Photochemistry of Hexanone Derivative 125	121

CHAPTER 8 THE PHOTOCHEMISTRY OF 9,10-DIHYDRO-9,10-ETHENO

ANTHRACENE DERIVATIVES	127
8.1. Photolysis of 11-Hydroxymethyl-9,10-dihydro-9,10-ethenoanthracene (131)..	127
8.2. Triplet-Triplet Energy Transfer in Zeolites	129
8.3. Photolysis of 13-(11-Methyl-9,10-dihydro-9,10-ethenoanthracenyl) succinate (132)	131
8.4. The Heavy Atom Effect in the Photochemistry of Succinate 132	133
8.5. Photolysis of 13-(11-Methyleneoxy-9,10-dihydro-9,10-ethenoanthracenyl) acetic Acid (133)	135
8.6. The Heavy Atom Effect in the Photolysis of Acetic Acid Derivative 133	137
8.7. Structural Elucidation of Cyclooctatetraene and Semibullvalene Photoproducts	143

CHAPTER 9 TRIPLET-TRIPLET ENERGY TRANSFER

IN A TWO-COMPONENT CRYSTALLINE SYSTEM	146
9.1. Photochemical Results Upon Irradiation of Salts 164 , 166 , and Complex 165	146
9.2. Structure-Reactivity Analysis of Salts 164 , 166 , and Complex 165	151
9.3. UV/VIS Analysis of Salts 164 , 166 , and Complex 165	157
9.4. Energy State Analysis of Salts 164 , 166 and Complex 165	159

EXPERIMENTAL	161
CHAPTER 10 PREPARATION OF SUBSTRATES	161
10.1. General Procedures.....	161
10.2. Preparation of Photochemical Substrates.....	165
10.2.1. 9,10[1',2']Benzenoanthracene-1,4-dione Derivatives.....	165
10.2.2. 2-(1-Cyclopentenyl)cyclopentanones and 2-(1-Cyclohexenyl) cyclohexanones.....	186
10.2.3. 9,10-Dihydro-9,10-ethenoanthracene Derivatives	198
10.3. Salt Formation of Photochemical Substrates.....	207
10.3.1. Sensitizer Salts Formed with 2-(1-Cyclopentenyl)cyclopentanone Derivative 121.....	207
10.3.2. Alkali Metal Salts Formed with 9,10-Dihydro-9,10-ethenoanthracene Derivatives	210
10.3.2.1. Alkali Metal Salts Formed with Succinate Derivative 132....	210
10.3.2.2. Alkali Metal Salts Formed with Acetic Acid Derivative 133.....	213
10.3.3. Sensitizer Salts Formed with Acetic Acid Derivative 133.....	218
CHAPTER 11 PHOTOCHEMICAL STUDIES	223
11.1. General Procedures.....	223
11.2. Photolysis of Substrates	225
11.2.1. Photolysis of 9,10[1',2']Benzenoanthracene-1,4-dione Derivatives in Solution.....	225
11.2.2. Photolysis of 2-(1-Cyclopentenyl)cyclopentanone Derivative 121 in Solution.....	237
11.2.3. Photolysis of 9,10-Dihydro-9,10-ethenoanthracene Derivatives in Solution.....	239
11.2.4. Photolysis of 9,10-Dihydro-9,10-ethenoanthracene Derivatives in the Solid State	252

11.3. Photochemical Studies of Salts.....	253
11.3.1. Photolysis of Sensitizer Salts Formed with 2-(1-Cyclopentenyl)cyclo- pentanone Derivative 121	253
11.3.2. Photolysis of Alkali Metal Salts of 9,10-Dihydro-9,10-ethenoanthracene Derivatives.....	255
11.3.3. Photolysis of Sensitizer Salts Formed with Acetic Acid Derivative 133.....	258
REFERENCES	260

LIST OF FIGURES

Figure	Caption	Page
1.01.	Photochemistry of <i>trans</i> -Cinnamic Acid (1) in the Crystalline State and Solution.....	4
1.02.	Cohen's Concept of Reaction Cavity.....	5
1.03.	Photodimerization of Cyclopentanone 5.....	6
1.04.	Plots of Changes in Quantum Yield as a Function of Reaction Progress.....	8
1.05.	Photodimerization of Acridizinium Salt 7.....	9
1.06.	Mechanism of the Di- π -Methane Rearrangement.....	10
1.07.	Experimental Exploration of Biradical I in the Di- π -Methane Rearrangement.....	12
1.08.	Deuterium Labeling Experiment.....	13
1.09.	Multiplicity-Dependent Photochemistry of Barrelene.....	15
1.10.	Regioselective Di- π -Methane Rearrangements.....	16
1.11.	Photorearrangement of Dibenzobarrelene Derivative 27.....	18
1.12.	Enantioselective Photorearrangement of Dibenzobarrelene 30.....	19
1.13.	Photorearrangements of β , γ -Unsaturated Ketones.....	20
1.14.	State-Selectivity of β , γ -Unsaturated Ketone Photochemistry.....	21
1.15.	Reaction Pathways for ODPM Rearrangement and [1,3]-Acyl Shift.....	22
1.16.	Norrish Type II Reaction Mechanism.....	23

1.17.	Representation of Hydrogen Abstraction Geometry and Arrangement of Atomic Orbitals.....	24
1.18.	Energy Diagram for Selected Transitions	25
1.19.	Benzoyl (Donor)-Naphthyl (Acceptor) Systems 43 and 44	28
1.20.	Experimental Example of the External Heavy Atom Effect	30
1.21.	Experimental Example of the Internal Heavy Atom Effect	30
1.22.	Photolysis of β , γ -Unsaturated Ketone 51a and 51b	31
1.23.	Photolysis of Enone 54	32
1.24.	Xanthone	33
1.25.	11,12-Diester-9,10-ethenoanthracene Derivatives.....	36
1.26.	Series of Triptycene-1,4-quinone Studied.....	37
1.27.	β , γ -Unsaturated Ketone and Sensitizers Selected for the Study of Triplet-Triplet Energy Transfer	38
1.28.	Series of 9,10-Dihydro-9,10-ethenoanthracene Derivatives and Sensitizers.....	39
2.01.	Preparation of 9,10-Dihydro-9,10[1',2']benzenoanthracene-1,4-dione (63)	41
2.02.	Preparation of 9,10-Bis(chloromethyl)anthracene (64), 9,10-Dimethylanthracene (65) and 9,10-Bis(methoxymethyl)anthracene (66).....	42
2.03.	Preparation of 9,10-Dihydro-9,10-dimethyl-9,10[1',2']benzenoanthracene-1,4-dione (69)	43
2.04.	Preparation of 9,10-Bis(methoxymethyl)-9,10-dihydro-9,10[1',2']benzenoanthracene-1,4-dione (72)	44

2.05.	Structures of 5-Chlorotriptycene-1,4-quinone (73) and 6-Chlorotriptycene-1,4-quinone (74).....	45
2.06.	Possible Chlorinated 2 : 1 Adducts 77a-d.....	46
2.07.	Preparation of 5-Chloroanthracene (79a) and 6-Chloroanthracene (79b).....	46
3.01.	Numbering System for Triptycene-1,4-quinone (63) and its Charge-Transfer Excited State (63a).....	47
3.02.	Dibenzosemibullvalene 80 from the Irradiation of Triptycene-1,4-quinone (63).....	48
3.03.	¹ H NMR Spectrum of Dibenzosemibullvalene 80.....	50
3.04.	Regioselectivity of the Di- π -Methane Rearrangement of 63.....	52
3.05.	Triketone 81 from the Irradiation of Triptycene-1,4-quinone (63).....	53
3.06.	Cyclopenten-3,5-dione (82).....	54
3.07.	¹ H NMR Spectrum of Triketone 81.....	55
3.08.	X-ray Crystal Structure of Triketone 81.....	56
3.09.	Proposed Mechanism for Formation of Triketone 81.....	57
3.10.	Carbene Mechanism for Formation of Triketone 81.....	58
3.11.	Reaction Pathway Between Carbene 87 and Molecular Oxygen.....	59
3.12.	Carbene Trapping Mechanism.....	60
3.13.	Chlorinated Photoproducts from the Irradiation of Triptycene-1,4-quinone (63).....	61
3.14.	¹ H NMR Spectrum of Triptycene-1,4-quinone (63).....	63

3.15.	¹ H NMR NOE Experiment for Triptycene-1,4-quinone (63).....	64
3.16.	Addition of Hydrogen Chloride to 1,4-Benzoquinone (60), Followed by Oxidation.....	66
3.17.	Proposed Mechanism for Formation of Chlorinated Product 75.....	67
3.18.	Addition of Chlorine Atom at Carbon 4a of Intermediate 96.....	68
3.19.	Proposed Mechanism for Formation of Chlorinated Photoproduct 74.....	69
3.20.	Proposed Mechanism for Hydrogen Chloride Formation	70
3.21.	Packing Diagram for Triptycene-1,4-quinone (63).....	72
3.22.	X-ray Crystallographic Structure of Triptycene-1,4-quinone (63).....	73
3.23.	Intramolecular Distances between Ring Centers 1, 2 and 3	74
3.24.	Example of an Unreactive Photoreaction in the Solid State.....	75
3.25.	Crystal Lattice Steric Effects in Compound 100	76
4.01.	Photolysis of 69 in Acetonitrile	77
4.02.	¹ H NMR Spectrum of Norcaradiene 103	79
4.03.	X-ray Crystallographic Structure of Norcaradiene 103	82
4.04.	Photolysis of Triptycene 104.....	83
4.05.	Trapping of Carbene 104a.....	84
4.06.	Proposed Mechanism for Formation of Photoproducts 102 and 103	85
4.07.	Charge-Transfer from an Excited Donor (D*) to Acceptor (A)	87
4.08.	Naphth[2,3- <i>a</i>]azulene-5,12-dione (108) and Norcaradiene 103.....	88
4.09.	Example of a Photochromic 9,10-Ethenoanthracene Derivative 109	89

4.10.	UV/VIS Absorption Spectrum of 103 in Acetonitrile and Chloroform.....	91
5.01.	Photolysis of 72 in Acetonitrile	93
5.02.	¹ H NMR Spectrum of Dihydrofuran Derivative 111	96
5.03.	Mechanism for the Formation of Dihydrofuran Derivative 114	100
5.04.	Mechanism for the Formation of Dihydrofuran Derivative 111	101
5.05.	X-ray Crystal Structure of Quinone 72.....	103
5.06.	¹ H NMR Spectrum of Benz[<i>a</i>]aceanthrylene Derivative 112.....	105
5.07.	Photoreaction of 1,4-Dimethoxytiptycene (115).....	108
5.08.	Proposed Mechanism for the Formation of Benz[<i>a</i>]aceanthrylene 112	109
6.01.	Preparation of 2-(1-Cyclopentyl)cyclopentanone (121).....	112
6.02.	Preparation of 2-(1-Cyclohexenyl)cyclohexanone (125).....	113
6.03.	Preparation of <i>p</i> -Acetyl- <i>N,N</i> -dimethylbenzylamine (128).....	114
6.04.	Preparation of 9,10-Dihydro-9,10-ethenoanthracene Acid 132 and 133	115
7.01.	Photolysis of Keto-Acid 121	116
7.02.	Photolysis and Work-Up of Salts 138, 139 and 140.....	119
7.03.	1(1-Cyclohexen-1-yl)-2-oxocyclohexaneacetic Acid (125).....	121
7.04.	Rearrangement of 2-Cyclohexenyldenecyclohexanone (123) and 2-(1-Cyclohexenyl)cyclohexanone (123a)	122
7.05.	Dieneone 142 Studied by Direct Irradiation.....	123

7.06.	X-ray Crystallographic Structure of Keto-Acid 125.....	124
7.07.	Stereo Diagram of Keto-Acid 125, Showing Hydrogen Bonding.....	125
8.01.	Photolysis of Dibenzobarrelene 131.....	127
8.02.	Photolysis of Succinate 132.....	132
8.03.	Photolysis of Acetic Acid Derivative 133.....	136
8.04.	Tub-shape of Cyclooctatetraene (163a).....	144
9.01.	Photolysis of Salts 164, 166 and Complex 165.....	146
9.02.	Stern-Volmer Equation.....	147
9.03.	Packing Diagram and Stereoview of Salt 164.....	152
9.04.	Packing Diagram and Stereoview of Complex 165.....	153
9.05.	Packing Diagram and Stereoview of Salt 166.....	154
9.06.	Different Representation of Packing Diagrams for Salts 164 and 166.....	156
9.07.	UV/VIS Absorption Spectrum of Salt 166 in Methanol.....	157
9.08.	Structural Comparison of 4'-Aminobutyrophenone (168) and 4'-Piperazinoacetophenone (167).....	158
9.09.	Examples of Different States for Aryl Ketones.....	160

LIST OF TABLES

Figure	Caption	Page
I	Angles Between the Quinone and Benzene Moieties.....	71
II	Intermolecular and Intramolecular Distances Between Ring Centers.....	75
III	^1H NMR (500 MHz) and ^{13}C NMR (125 MHz) Data for Norcaradiene 103.....	80
IV	^1H NMR Data (500 MHz) for Norcaradiene 103.....	81
V	UV/VIS Absorption Data for Norcaradiene 103.....	90
VI	UV/VIS Absorption Data for Benzoquinone.....	90
VII	^1H NMR (500 MHz) and ^{13}C NMR (125 MHz) Data for Dihydrofuran 111.....	97
VIII	^1H NMR Data (500 MHz) for Dihydrofuran 111.....	98
IX	Crystallographically Determined Angles for Quinone 72.....	104
X	^1H NMR (500 MHz) and ^{13}C NMR (125 MHz) Data for Benz[<i>a</i>]aceanthrylene Derivative 112.....	106
XI	^1H NMR Data (500 MHz) for Benz[<i>a</i>]aceanthrylene Derivative 112.....	107
XII	Hydrogen Abstraction Geometric Parameters for 125.....	126
XIII	Photolysis Results of Alcohol 131.....	128
XIV	Zeolite Photolysis Results.....	130
XV	Photolysis Results of Succinate 132.....	133
XVI	Photolysis of Acetic Acid Derivative 133.....	137
XVII	Relationship between Lifetime and Concentration of a Quencher.....	148

XVIII	Solid State Photolysis Results of Sensitizer Salts 164, 166 and Complex 165	149
XIX	Distances (< 7.5 Å) Between Chromophores.....	155
XX	Photoproduct Mixture Composition of Derivatives 131, 132 and 133a	252
XXI	Photoproduct Mixture Composition of Salts 138, 139 and 140	254
XXII	Photoproduct Mixture Composition of Salts 153 and 154	255
XXIII	Photoproduct Mixture Composition of Salts 158 to 162.....	257
XXIV	Photoproduct Mixture Composition of Salts 164, 166 and Complex 165.....	258

LIST OF GRAPHS

Figure	Caption	Page
I	Irradiation Results of Alkali Salts of Succinate 132	135
II	Irradiation Results of Alkali Salts of Acetic Acid 133	138
III	Conversion versus Irradiation Time Experiments.....	141
IV	Irradiation Results of Methyl Ester of Acid 133 in Alkali-Containing Zeolites.....	142
V	Reactant Conversion of Salts 164, 166 and Complex 165 versus Irradiation Time.....	150

ACKNOWLEDGMENTS

I would like to thank my research supervisor Professor John R. Scheffer for his valuable guidance, his encouragement and the many helpful suggestions he has offered. His expertise and dedication in the field of photochemistry have been a source of inspiration to me.

I would also like to extend my gratitude to Professor James Trotter and the members of his research group, Dr. Gunnar Olovsson, Dr. Bozena Borecka and Dr. Tai Yu Fu, who are responsible for the X-ray structures in this thesis. Also, special thanks go to the members of the NMR laboratory, Mass-Spec facilities, Mr. Peter Borda and the attentive staff of the departmental services.

Furthermore, I would like to express my thankfulness to my co-workers in the lab, especially Matt Netherton and Dr. Heiko Ihmels for proof-reading my thesis. Their thoroughness, promptness and invaluable comments were very much appreciated. Special recognition also goes to Jeffery Raymond for his encouragement.

Finally, I am also grateful for all the help I have received from my friends in the department, who have made my life at U.B.C. a zestful and memorable experience.

DEDICATION

To my parents

INTRODUCTION

CHAPTER 1 PHOTOCHEMICAL INTRODUCTION

1.1. General

In the early 20th century, photochemists made use of the sun as a radiation source in order to induce chemical reactions, as demonstrated by Ciamician, who conducted his research on the roof of the chemical research building in Bologna.¹ Nowadays, experiments are more carefully controlled and the use of narrower bands of electromagnetic radiation enables researchers to investigate photochemical reactions systematically.

There are many areas of photochemistry that have been addressed increasingly over the years. Among them is synthetic organic photochemistry. Light can be remarkably selective causing chemical reactions. A structurally simple molecule may be converted by the process of irradiation into a rather complex structure, which might be otherwise difficult to synthesize.

Another more recent area of interest that photochemists are concerned with is the development of devices that can be reversibly written and read by light.² Compounds that exhibit photochromism, a photoinduced transformation photochemically or thermally reversible, resulting in molecules with different electronic properties,³ are used in the development of Photochromic Microimage Processing leading to ultramicrofilms.⁴ Through this technique a standard size book page can be reduced to less than 1 mm in height. Further development in the field of organic photochemistry may offer promising advancements in the field of computers and electronics.

1.2. Solid State Organic Photochemistry

The history of solid state chemistry dates back to 1828 when Friedrich Wöhler observed the thermal transformation of crystalline ammonium cyanate into urea.⁵ Combining photochemistry and solid state reactivity, Trommsdorff⁶ showed in 1834 that crystals of santonin, much later shown to have the skeleton of a sesquiterpene, turned yellow and cleaved when exposed to sunlight. During the late 19th and early 20th centuries, a greater understanding of the interaction of matter with light was obtained as a wide variety of photochemical reactions were investigated by the pioneers of photochemistry.⁷ As technology advanced, X-ray crystallography was used as a tool to explore molecular conformation and packing arrangements of starting materials and products in the crystal, providing a greater insight into structure-reactivity relationships.

Extensive research in the field of solid state organic photochemistry has shown that the molecular crystal lattice plays an important role in controlling organic photoreactivity.⁸ This work has demonstrated that photoreactions are capable of giving different products in the solid and solution states as a result of changes in reaction regio-, stereo- and enantioselectivity. Entirely different photoproducts may arise from solid state irradiation experiments as a result of physical restraints restricting the movements found in the solution phase. Reactions in the solid state are governed by two important factors, namely the conformation and the packing arrangement of the reacting molecules. In isotropic phases, a flexible molecule may adopt many conformations due to fast equilibrium between them. However, in the crystalline state, the molecule will rarely take up

more than one conformation and most commonly crystallizes in or near its minimum energy conformation.⁹ Increased selectivity arises from the limited motion in crystals which consequently affects reactions that are sensitive to the conformation of the reactant. Furthermore, the packing of the reactant in a crystal is important, since the anisotropic environment of the crystal lattice can affect the course of the reaction by restricting the movement within the crystal. Using X-ray crystallography, mechanistic information on the preferred interatomic distances and angles required for a reaction to proceed can be determined. A number of review articles dealing with differential reactivity in solution and the solid-state have appeared in recent years.¹⁰

1.2.1. The Topochemical Principle

The topochemical principle was proposed in 1918 by Kohlshutter,¹¹ who stated that "reactions in solids are dependent on the constraining three dimensional environment in which the molecules exist". This first principle of solid state chemical reactivity recognized the restrictive environment a crystal may impose on a given reaction. More than 40 years later, the topochemical postulate was reinvestigated with the introduction of X-ray crystallography by Schmidt and co-workers,¹² who examined the [2+2] photocycloaddition reaction of *trans*-cinnamic acid derivatives in the crystalline phase. Figure 1.01 illustrates the three packing forms (α , β , γ) for unsubstituted and/or substituted *trans*-cinnamic acids. In order for a photocycloaddition to occur, the center-to-center distance between the two neighboring double bonds was proposed to be less than 4.2 Å. Furthermore, the parallel alignment of the reacting double bonds played an important role in the reaction.

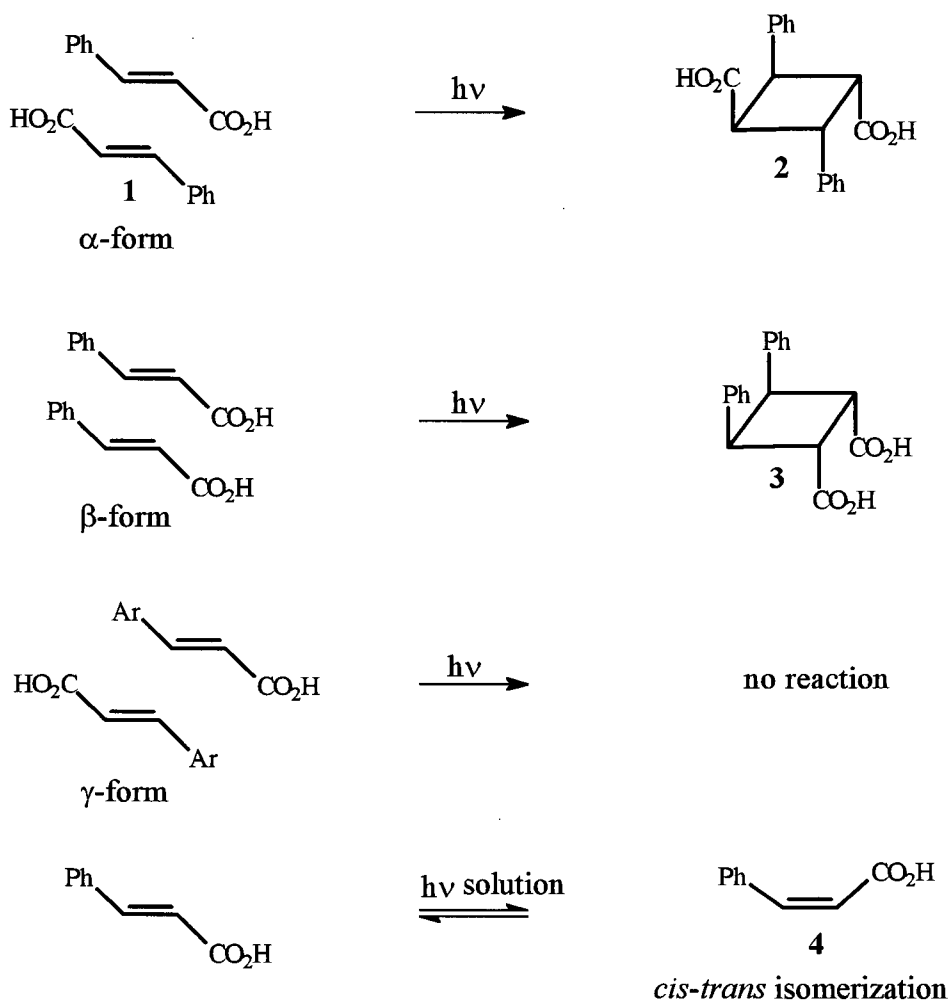


Figure 1.01. Photochemistry of *trans*-Cinnamic Acid (1) in the Crystalline State and Solution.

Hence, by determining the intermolecular distances and orientations between the reactive centers of *trans*-cinnamic acid, Schmidt demonstrated that solid state reactions are controlled by strict size and shape limitations. A “reaction cavity” can be thought of as arising from the non-bonding repulsive interactions between a reacting molecule and its closest neighbors. This concept was first introduced by Cohen,¹³ who visualized a reacting molecule in a crystal as a substance

that was residing in a cavity created by its neighboring molecules, whose shape resembled the packing of the crystal. As the reaction would proceed, the surface of the cavity walls could become distorted as a result of pressure exerted by atomic movement. According to Cohen,¹³ the closely packed crystal lattice restricted the degree of distortion of the cavity wall.

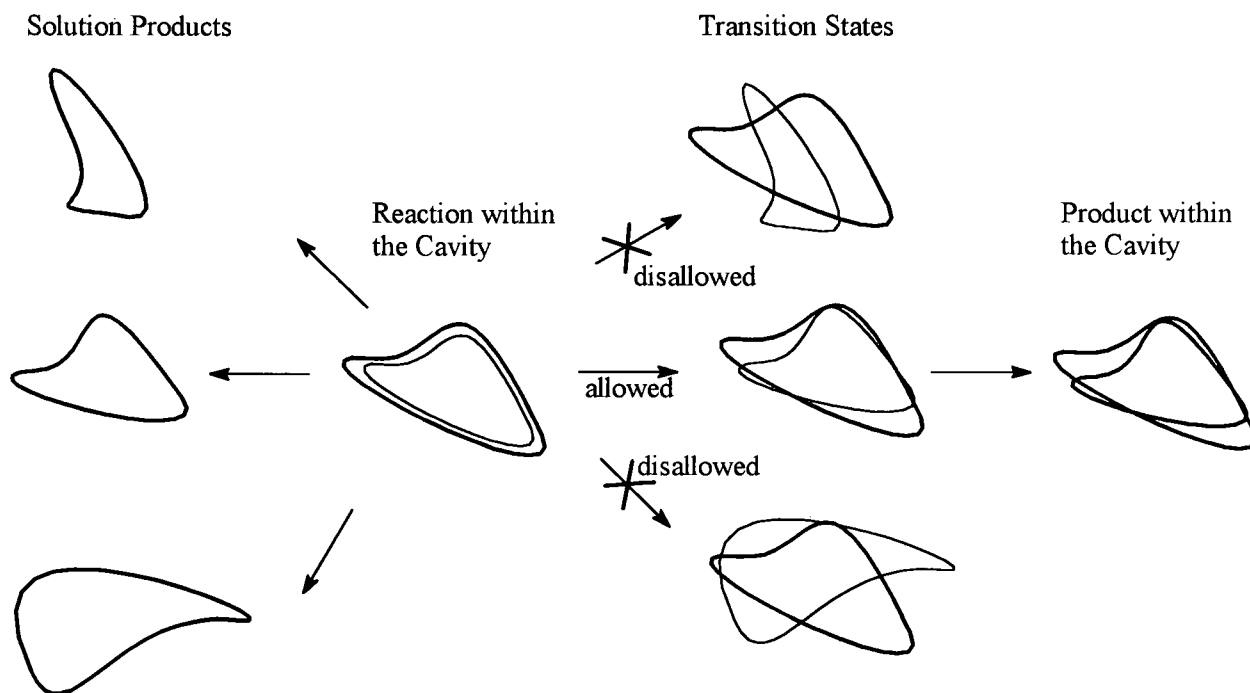


Figure 1.02. Cohen's Concept of Reaction Cavity.

As indicated in Figure 1.02, the reaction proceeding from within the cavity walls is not only limited by the number of reaction partners (if any) but also by the extent of molecular displacement and conformational motions.¹⁴ Hence, a reaction is predicted to be topochemically feasible if the shape and size of the transition state resembles the cavity.

The concept of the reaction cavity has further been explored by Ramamurthy *et al.*,¹⁵ who investigated the reactivity in a variety of organized and constrained media such as organic inclusion hosts, zeolites, micelles and liquid crystals.

1.2.2. Topotactic Reactions

One goal of research in organic solid state photochemistry is the discovery of single crystal-to-single-crystal transformations, known as topotactic reactions.¹⁶ This rare phenomenon occurs when a single crystal of the reactant retains its singularity while being smoothly and continuously transformed into a single crystal of the product. One reaction that has been extensively studied by Jones *et al.*¹⁷ is the photodimerization of 2-benzylidene-5-benzyl cyclopentanone (**5**) in the solid state. Photolysis of crystalline compound **5** resulted in a complete conversion to the [2+2] adduct **6** with the retention of molecular single crystallinity. The packing arrangement of the reactant and product showed that the reaction involved relatively small amounts of molecular and atomic motion, which was demonstrated by following the topotactic process by X-ray crystallography.

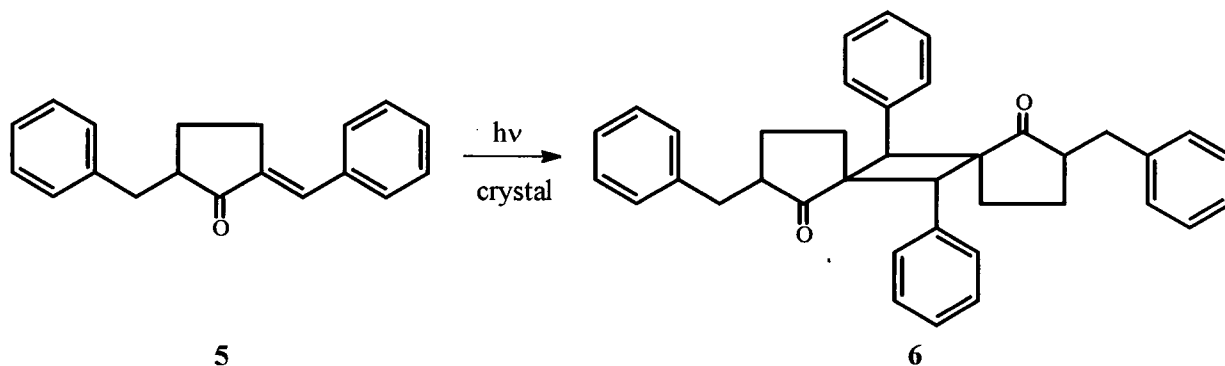


Figure 1.03. Photodimerization of Cyclopentanone **5**.

1.2.3. Solid State Reaction Efficiency

The photochemical conversion of a reactant to a photoproduct in the solid state is usually limited, as the reactivity often changes as a function of reaction progress. The quantum yield of a photochemical reaction is defined as the number of moles of product formed divided by the number of photons absorbed by the system.¹⁸ Ideally, the quantum yield in a solid state reaction remains unaltered from the lowest to the highest conversion values as shown in the first order plot in Figure 1.04 (a).¹⁴ However, most commonly, the environment and/or crystal phase may continuously change, leading to a decrease in quantum yield as a function of time (Figure 1.04 (b)). Once the product formation begins, the reacting species in the lattice may absorb the light resulting in poor photon penetration through the crystal. The light absorbing properties of the reactant may also be diminished by the generation of defects in the lattice. These are formed by the different three-dimensional geometries corresponding to the reactants and products. Scattering of light back to the surface will take place and the reaction of the crystal will be inhibited. Reaction efficiency may also be reduced by prolonged photolysis as a result of the crystal cracking or becoming cloudy. Melting of the crystal may facilitate the reaction leading to fewer constraints on molecular motion (Figure 1.04 (c)), or even result in the formation of different products.

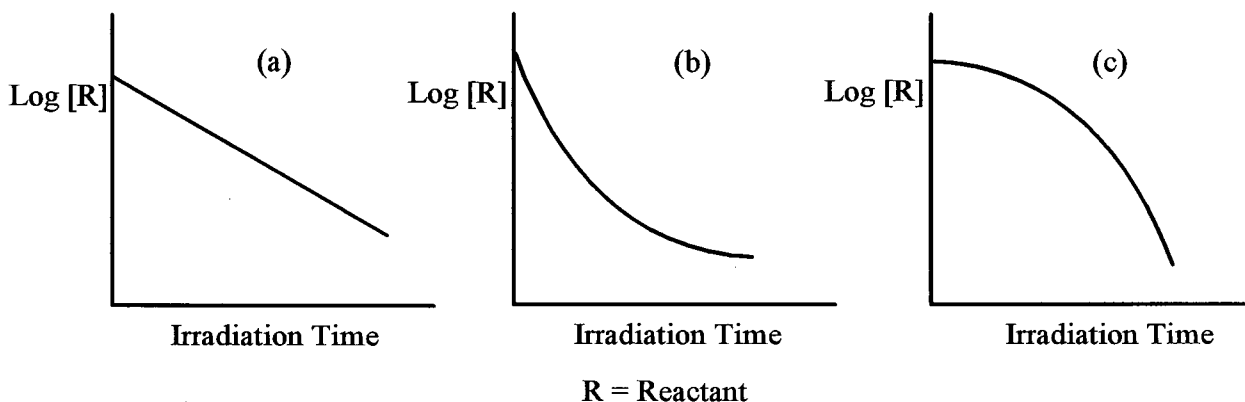


Figure 1.04. Plots of Changes in Quantum Yield as a Function of Reaction Progress.

1.2.4. Photochemical Reactivity of Organic Salts

Research in solid state organic photochemistry has concentrated primarily on the chemical reactivity of molecular crystals. An attractive system that has not received much attention is a crystal that is ionic in nature, such as a salt of the type RCOOM^+ or RNH_3^+X^- . Whereas molecular crystals are held together by relatively weak dipole-dipole and van der Waals attractive forces, and sometimes by hydrogen bonding, ionic crystals are held together by relatively strong Coulombic attractive forces. This difference gives salts the advantage of being not only high melting solids, reducing the chances of crystal breakdown, but may also lead to higher conversions without the loss of crystallinity and topochemical control. Jones and co-workers¹⁹ showed, for example, that acridizinium salts underwent topotactic transformations upon irradiation in the solid state yielding the [4+4] photodimer **8**.

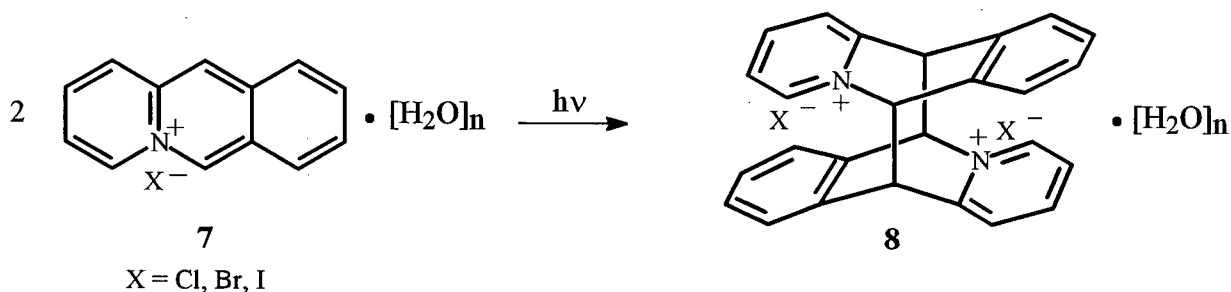


Figure 1.05. Photodimerization of Acridizinium Salt 7.

Upon photolysis, single-crystal-to-single crystal conversion was observed in the halide salts of 7 resulting in the corresponding dimer 8. X-ray structure analysis showed that the dimerization process requires a substantial amount of movement in the crystal lattice.

1.3. The Di- π -Methane Rearrangement

The photoreaction investigated in this thesis is the di- π -methane rearrangement, a photo-induced unimolecular process, recognized as one of the most general and thoroughly studied of all organic photoreactions.²⁰ This photochemical reaction is known to occur in compounds possessing two π -bonds separated by an sp^3 hybridized carbon atom. Upon irradiation, the compounds can be converted into products containing a vinylcyclopropane moiety. The mechanism was first proposed by Howard Zimmerman in 1967, who postulated that the initial step involves bonding between C2 and C4 to afford a 1,4 biradical (9a), followed by a homolytic cyclopropane ring cleavage to give a 1,3 biradical (9b) and subsequent ring closure to the vinylcyclopropane unit (10).²¹ Figure 1.06 shows the mechanism for the simplest case of 1,4-pentadiene.

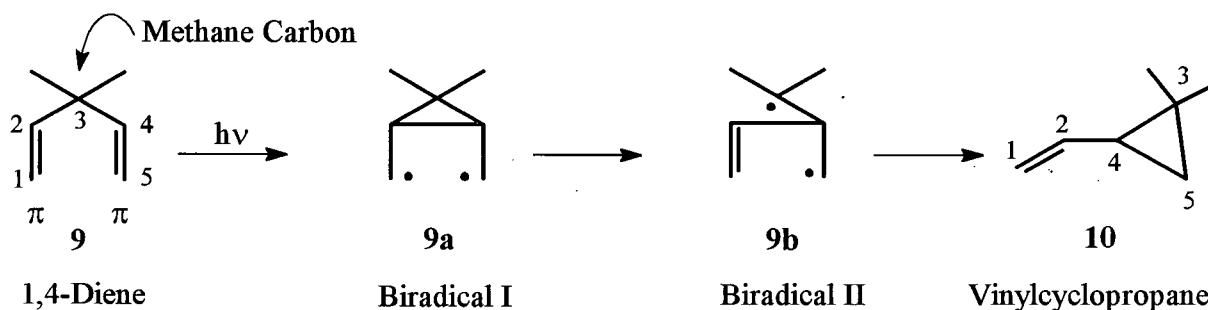


Figure 1.06. Mechanism of the Di- π -Methane Rearrangement.

The π -moieties may be either isolated or conjugated and may be part of a cyclic or an acyclic system. The biradical species **9a** and **9b** were first considered by Zimmerman as approximations of species involved, but recently Zimmerman *et al.*²² provided evidence that biradical **9a** is a true thermally equilibrated intermediate.

1.3.1. Reaction Mechanism

Despite extensive investigations of the di- π -methane rearrangement over the last three decades, the mechanistic pathway has still not been completely delineated. In order to confirm the existence of the cyclopropylidene biradical **9a** (Figure 1.06), Zimmerman chose to explore the di- π -methane rearrangement of dideuterio-*m*-cyanodibenzobarrelene **11**.²³ The irradiation experiment with acetophenone in benzene was shown to be regioselective giving semibullvalene **12** as the sole product. Figure 1.07 depicts the four possible reaction pathways. The experimental results indicated that the reaction followed pathway I demonstrating that the initial bridging step was favored by the cyanobenzo ring, rather than the benzo ring. Also, in reaction pathway I the

cyano-group stabilized biradical I (11a). Conversely, pathway II resulted in the cyano-stabilization of biradical II (11d). Reaction pathways III and IV did not apply as they did not afford an odd-electron stabilization by the cyano-substituent. The regioselectivity was proposed to be controlled by the formation of the lowest-energy biradical I. Zimmerman²³ also conducted *ab initio* theoretical calculations in order to explore the existence of biradical I further.

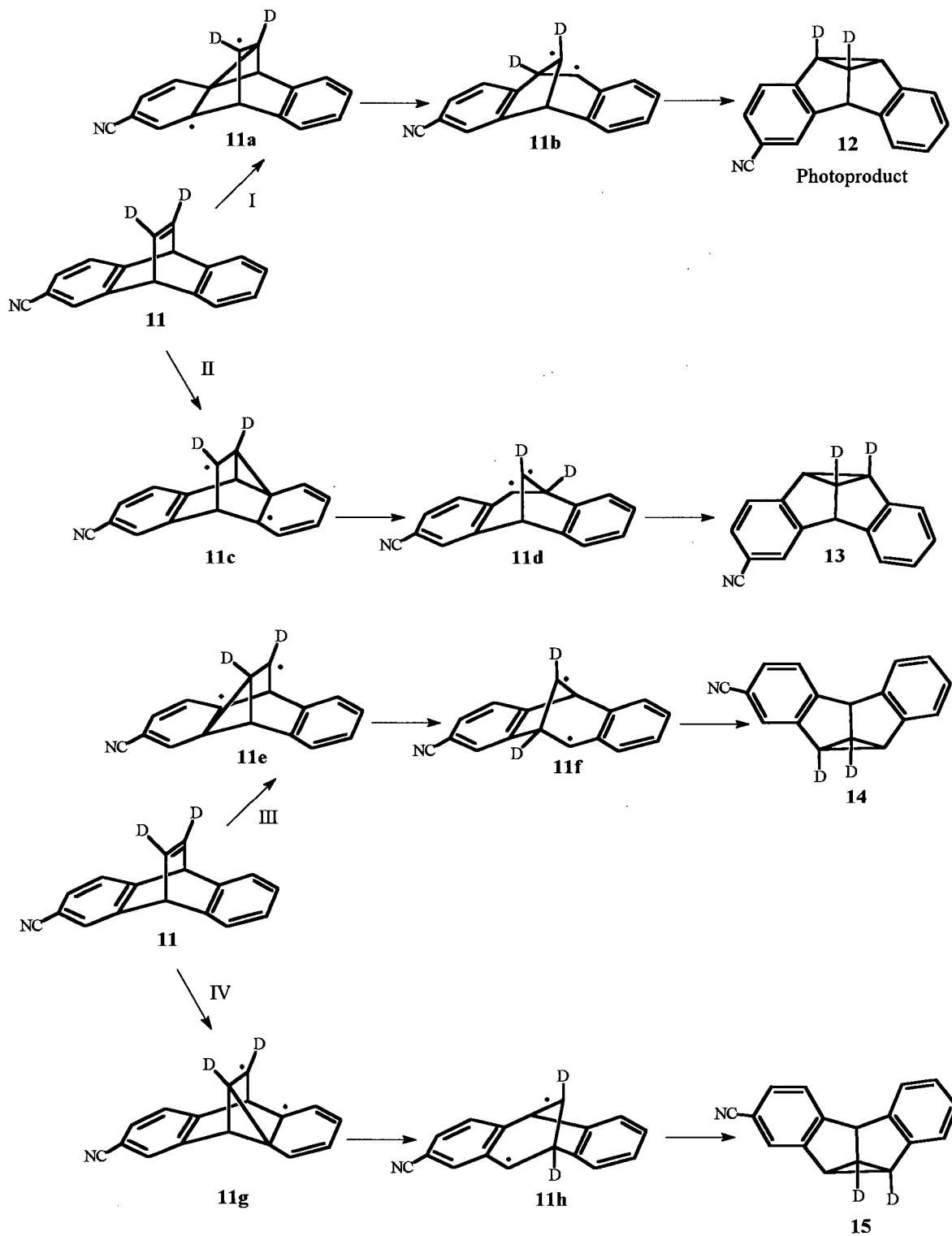


Figure 1.07. Experimental Exploration of Biradicals I in the Di- π -Methane Rearrangement of Cyanodibenzobarrelene 11.

In order to verify the 1,3-biradical II (9b, Figure 1.06) in the di- π -methane rearrangement of bicyclic barrelene systems, Zimmerman conducted deuterium labeling experiments.^{21b,21c} The results showed that triplet-sensitized irradiation of barrelene 16 led to a 1 : 1 ratio of semibullvalenes 17 and 18 as a result of radical coupling reactions occurring in the biradical resonance structures of 16b and 16c. This evidence supported the presence of the 1,3-biradical, acting as an actual intermediate.

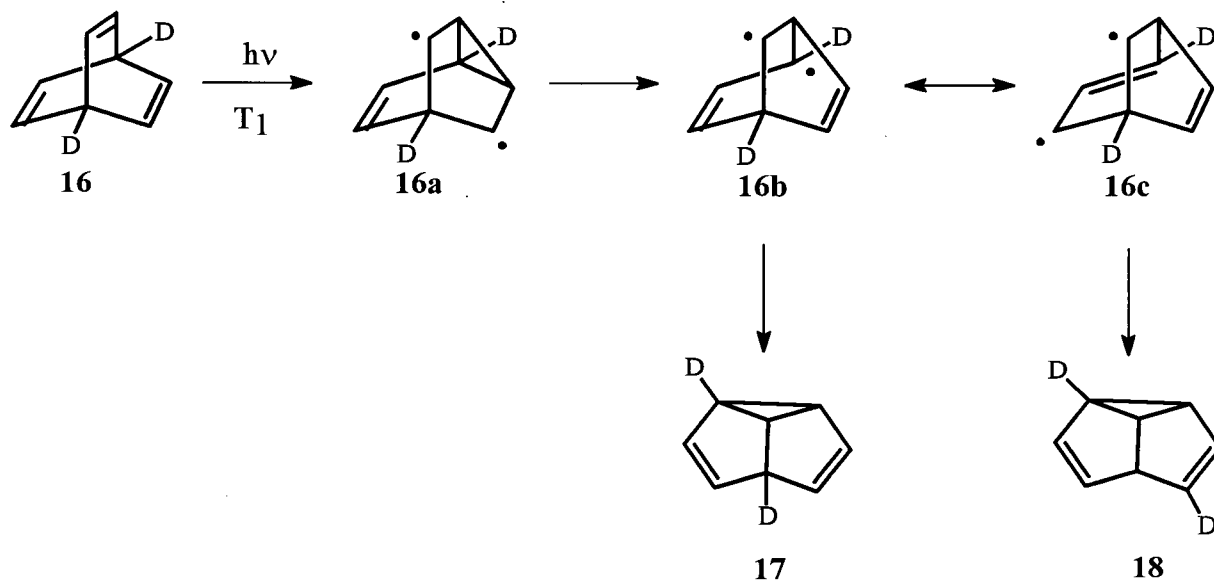


Figure 1.08. Deuterium Labeling Experiment.

1.3.2. Reaction Multiplicity

Another aspect to be considered is the multiplicity-dependency of the di- π -methane rearrangement.²⁴ Generally, acyclic compounds rearrange via their singlet excited states, whereas cyclic compounds undergo the rearrangement efficiently through their triplet excited states.²⁵ This can be explained in terms of how the geometry of the diene unit favors a particular reaction pathway. The competing pathways consist of *cis-trans* isomerization²⁶ and [2+2] cycloaddition.²⁷ A comparison of the rate constants for each of these processes^{20a} shows that the triplet state of an acyclic system favors *cis-trans* isomerization over the di- π -methane rearrangement. However, a cyclic system that is unable to *cis-trans* isomerize prefers the latter pathway.



where CA = Cycloaddition Reactions

DPM = Di- π -Methane Rearrangement

CTI = *Cis-Trans* Isomerization

Hence, the di- π -methane rearrangement of acyclic diene systems generally occurs from the singlet excited state and is often in competition with cycloaddition reactions. The barrelene system (Figure 1.09) illustrates distinct reactivity of a substrate based on the multiplicity of the excited state. This cyclic di- π -methane system rearranges to semibullvalene **20** upon triplet-sensitized photolysis as shown by Zimmerman and co-workers,²¹ whereas direct irradiation results in a [2+2]

cycloaddition forming the quadricyclene-like intermediate **19c**, followed by the thermally allowed [4+2] retrocycloaddition to give **19d**. This intermediate then rearranges to produce cyclooctatetraene **21**.²⁸

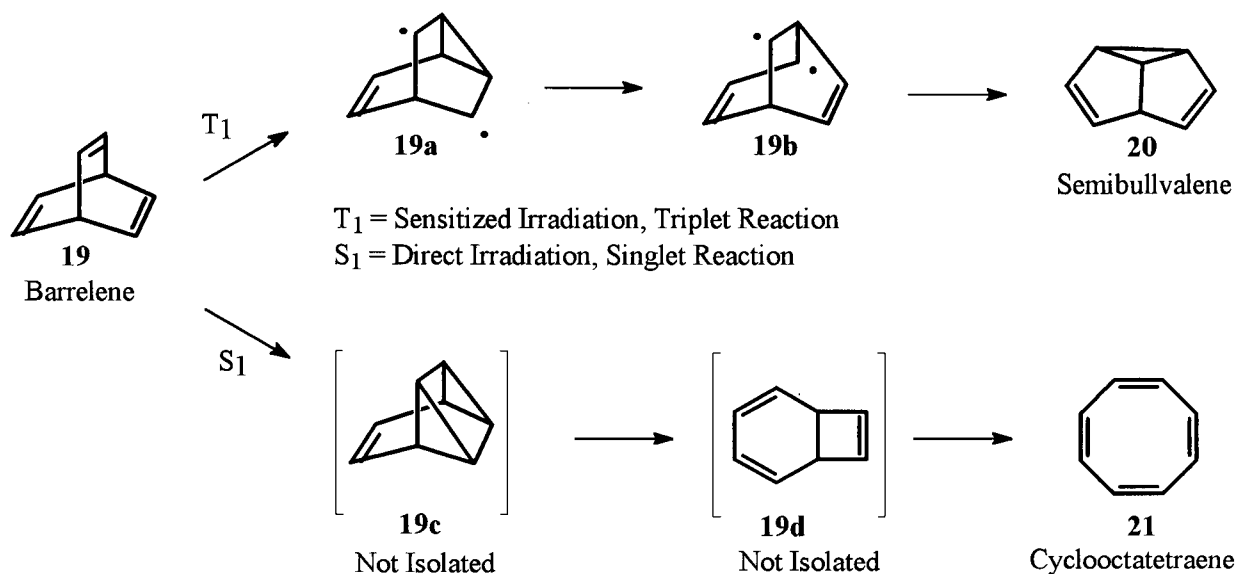


Figure 1.09. Multiplicity-Dependent Photochemistry of Barrelene.

1.3.3. Regioselectivity of the Di- π -Methane Rearrangement

In addition to the formation of distinct photoproducts arising from different excited states, the di- π -methane rearrangement can also yield regioisomeric products resulting from two differentially substituted π -bonds, as shown in Figure 1.10.^{20a} Regioselectivity studies have played an important role in understanding and establishing the reaction mechanism. For instance, the regioselectivity has been correlated with different stabilities of the two possible biradical species that can be formed in the initial step of the reaction mechanism.²⁰ If the π -bonds of the diene

system are part of an aromatic unit, the reaction will proceed in such a manner that the aromaticity will be re-established in the final product. Additionally, initial bonding usually gives the more stable intermediate.

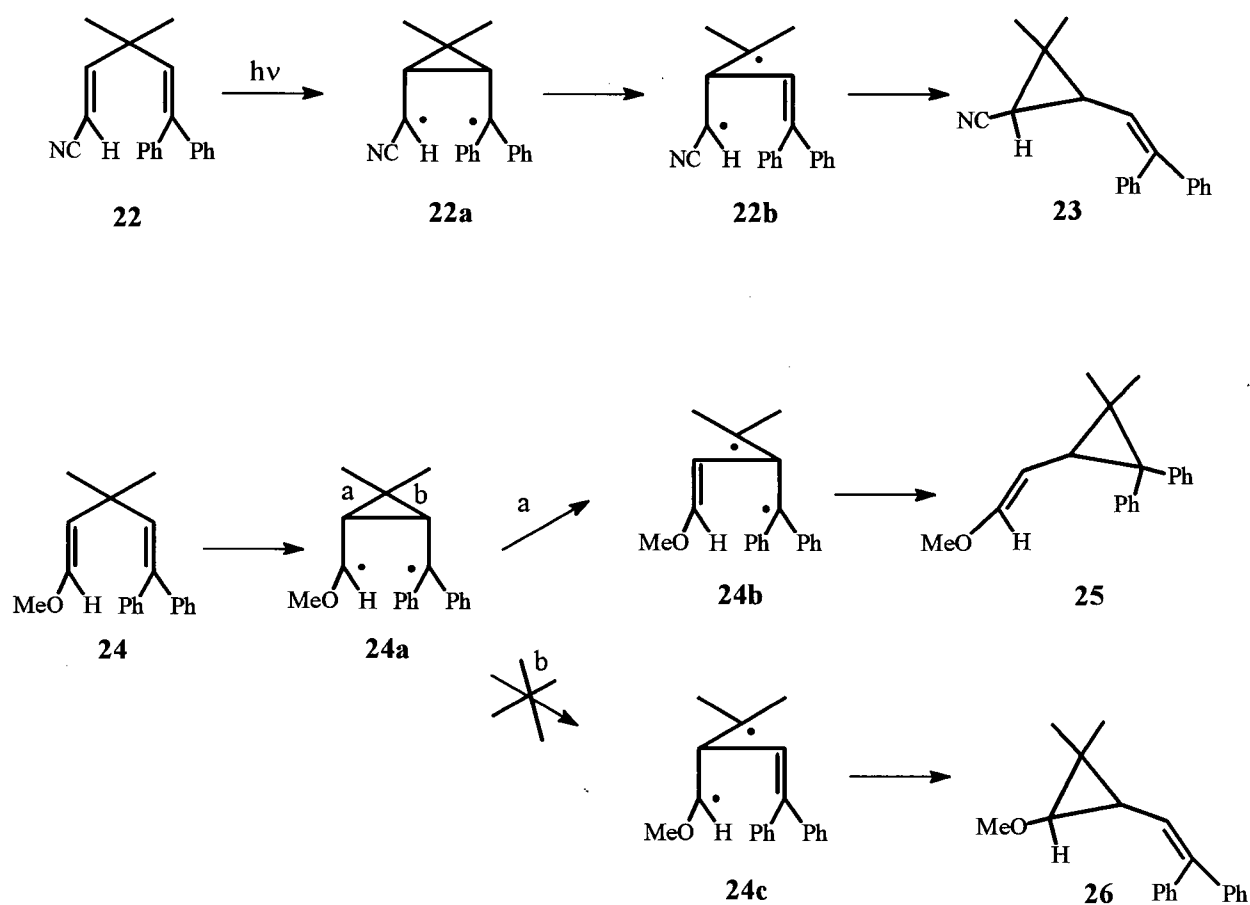


Figure 1.10. Regioselective Di- π -Methane Rearrangements.

Hence, an electron withdrawing group will likely be part of the final cyclopropyl ring (**23**), whereas an electron donating group will be attached to the double bond of the product (**25**), due to the reduced ability of the radical to delocalize.^{20a} The carbinyl carbons of the cyclopropyldicarbonyl biradical (**22a** or **24a**) are believed to be electron rich. Opening of the

cyclopropyl ring was proposed to result in the transfer of this negative charge onto the carbon which participates in the double bond formation. An electron withdrawing substituent may aid the neighboring carbonyl carbon in maintaining its electron-rich character and in not taking part in the formation of the π -bond (23). On the other hand, an electron donating group may act as a driving force for the adjacent carbonyl carbon to participate in the ring opening step, converting it into the π -bonded carbon(25).

1.3.4. Photochemistry of Dibenzobarrelene Derivatives

The study of barrelenes has been expanded to include the photoreactions of benzobarrelenes,^{29,30} dibenzobarrelenes³¹ and notably to various ester derivatives^{32, 33, 34} of the same. The possibility of obtaining different regioisomers from photoreactions of unsymmetrically substituted dibenzobarrelenes has also been explored. The first report of a photochemical study of this type, by Ciganek,³² dates back to 1966. As seen from Figure 1.11, dibenzobarrelene ester 27 has four initial bonding possibilities. The reaction pathway involving initial benzo-benzo bridging may be ruled out, due to the loss of aromaticity in two phenyl rings as opposed to the disruption of only one aromatic ring occurring in benzo-vinyl bonding. This leaves two reaction pathways, the first involving benzo-vinyl bonding on the unsubstituted side, the second benzo-vinyl bonding on the ester side. Pathway "a" is preferred as a result of the radical stabilization by the ester carbonyl group leading to the formation of the dibenzosemibullvalene derivative 28.

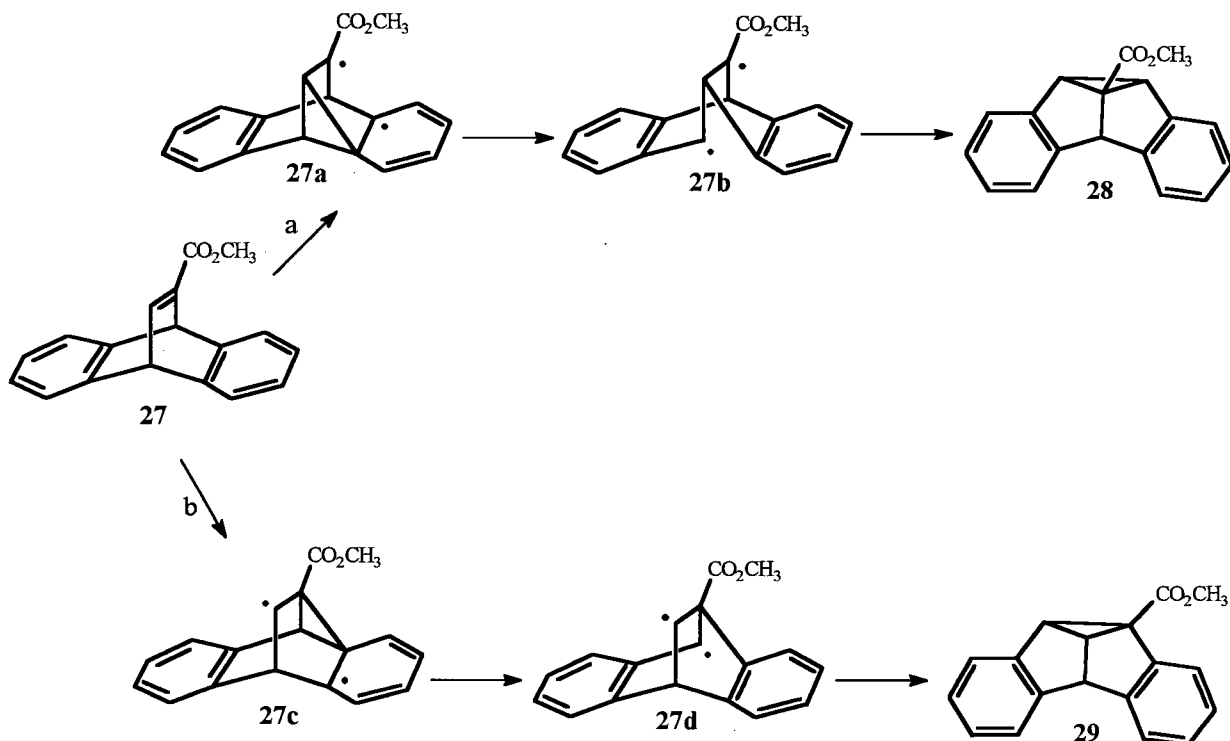


Figure 1.11. Photorearrangement of Dibenzobarrelene Derivative 27.

The mechanism postulated for this transformation is in agreement with Zimmerman's proposal. Ciganek also demonstrated that solution irradiation of the dimethyl dibenzobarrelene diester derivative resulted in a dibenzosemibullvalene photoproduct. More recent studies investigating the photolysis of dibenzobarrelene diesters in the solid state have been carried out by Scheffer, Trotter and co-workers,³⁵ who conducted structure-correlation experiments. Dibenzobarrelene derivative 30 was investigated in solution and the solid state.^{35a} One interesting aspect of this compound was that it was found to crystallize in two different dimorphic forms, belonging to the achiral space group *Pcba* or the chiral space group *P2₁2₁2₁*.

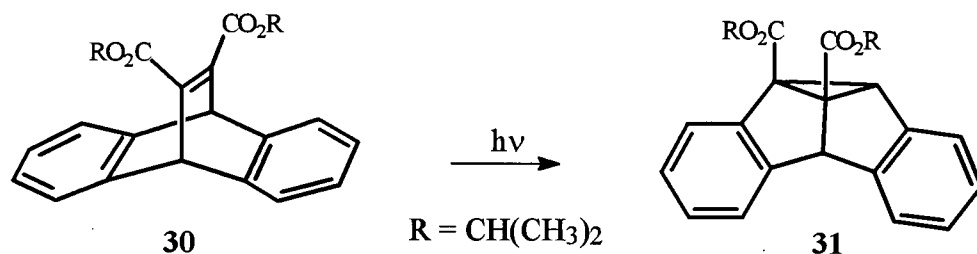


Figure 1.12. Enantioselective Photorearrangement of Dibenzobarrelene 30.

Photolysis of diester **30** in solution or in a single *Pcba* crystal gave a racemic mixture of semibullvalene **31**, whereas single crystal photolysis of the chiral $P2_12_12_1$ morphology led to the formation of photoproduct **31** with >95% enantiomeric excess. The initial bridging step was suggested to be the source of enantioselectivity resulting in different reaction pathways. Crystallographic analysis was used to determine the absolute configuration of the starting material and its photoproduct in order to differentiate between the different pathways. Furthermore, the lattice environment of the starting material was analyzed showing that steric crowding would hinder one of the bonding routes.

1.3.5. The Oxadi- π -Methane Rearrangement

Another example of a di- π -methane rearrangement is the structurally analogous oxadi- π -methane (ODPM) rearrangement.³⁶ This rearrangement takes place upon triplet excitation of a β , γ -unsaturated ketone **32**, and leads to a cyclopropyl ketone **34** formed via a formal 1,2-sigmatropic acyl shift accompanied by ring closure. Upon direct irradiation of the same ketone, a 1,3-sigmatropic acyl shift³⁷ is often observed, resulting in photoproducts of general structure **33**. The competition between the 1,2-acyl shift pathway occurring from the lowest excited triplet state (π , π^*) and the 1,3-acyl shift from the lowest excited singlet state (n , π^*) is dependent on the structure of the molecule.

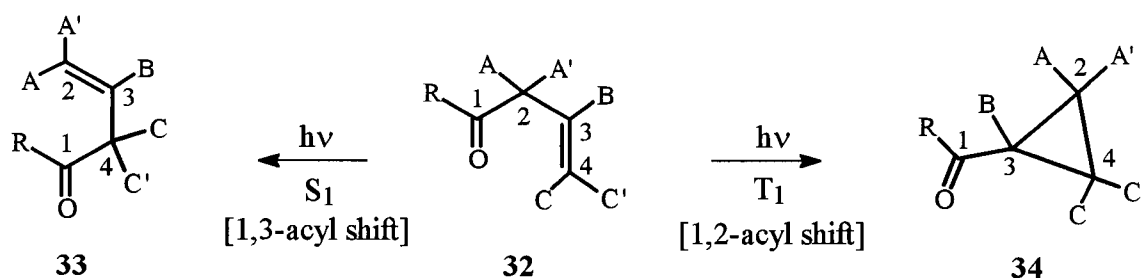


Figure 1.13. Photorearrangements of β , γ -Unsaturated Ketones.

The current state of understanding of the mechanism of the above processes is summarized in Figure 1.14, according to Demuth.³⁸ Investigations showed that the 1,3-acyl shift arises not only from the singlet state, but also through intersystem crossing from the singlet (S_1) to the triplet state (T_2). The ODPM rearrangement is thought to proceed through the T_1 state involving an initial 1,2-acyl shift.

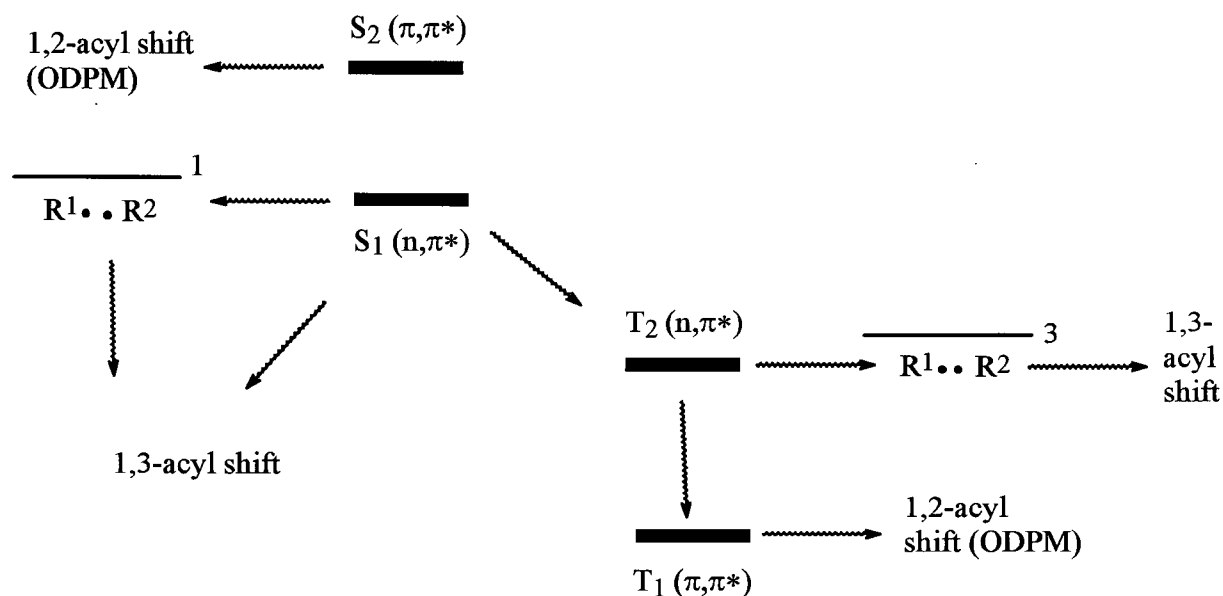


Figure 1.14. State-Selectivity of β, γ -Unsaturated Ketone Photochemistry.

The ODPM rearrangement and the 1,3-acyl shift have been the subject of many reviews^{39,40} and the possible reaction mechanisms are illustrated in Figure 1.15. The ODPM reaction pathway is analogous to the di- π -methane rearrangement suggesting the presence of biradicals **35a** and **35b**. However, the 1,3-acyl shift has been proposed to involve two competitive routes via either a free radical pair **35c** (i.e. a fragmentation-recombination mechanism) or via a quasi-concerted process demonstrated by intermediate **35d**. Recent theoretical studies have been conducted by Wilsey *et al.*⁴¹ who explored the reaction pathways of the 1,3- and 1,2-acyl shifts by investigating the existence and nature of the “classical” proposed reaction intermediates computationally. Their results supported the reaction pathways represented in Figure 1.15.

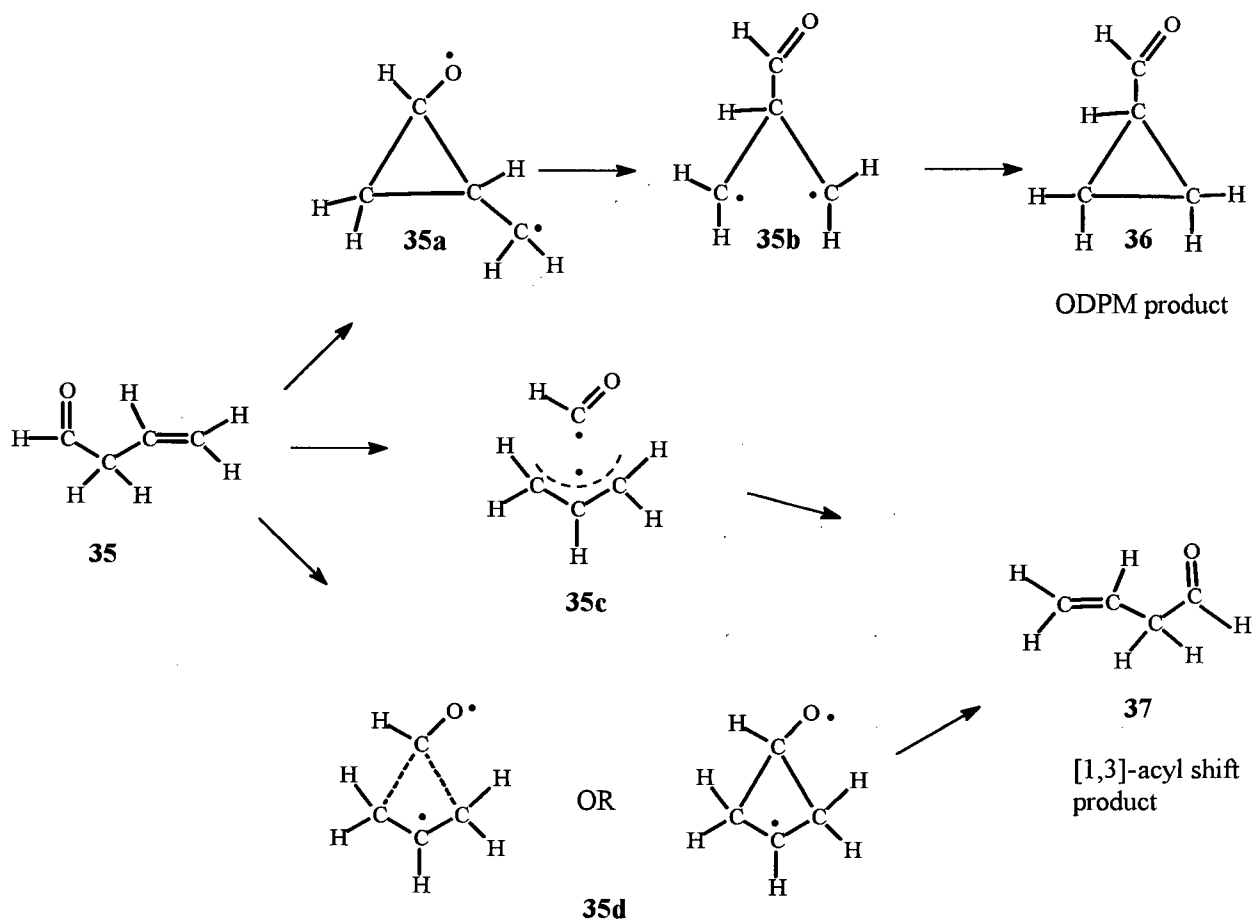


Figure 1.15. Reaction Pathways for ODPM Rearrangement and [1,3]-Acyl Shift.

1.4. Norrish Type II Reaction

Another common type of photochemical reaction is the Norrish type II reaction, which involves the intramolecular abstraction of a γ -hydrogen atom by a carbonyl oxygen atom.⁴² The hydrogen abstraction by the excited carbonyl group is suggested to result in the formation of a 1,4-hydroxybiradical intermediate **38a**, which may either cyclize to the cyclobutanol **39** (Yang reaction) or fragment to the alkene **42** and enol **40** products (Figure 1.16).⁴²

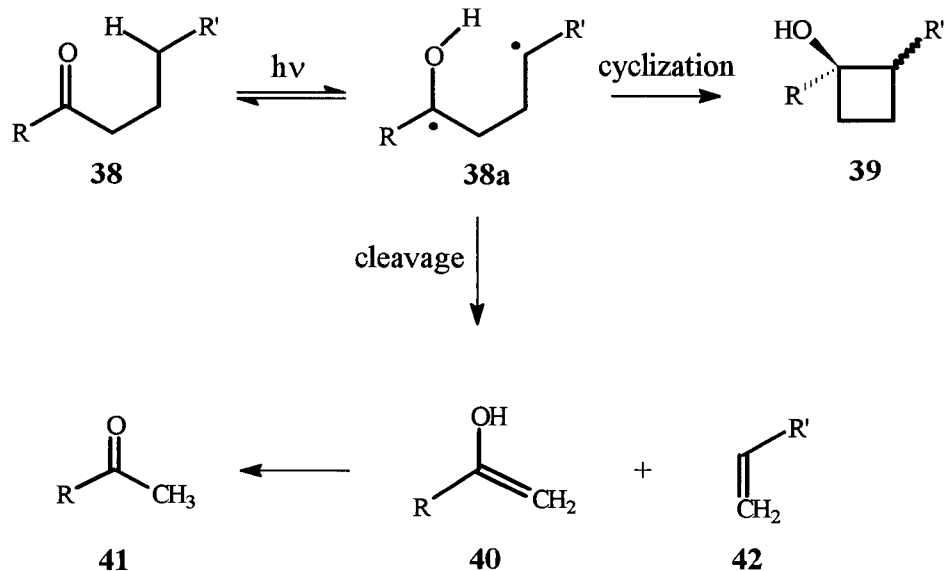


Figure 1.16. Norrish Type II Reaction Mechanism.

The Norrish type II reaction has been widely used to create relatively strained ring systems in natural product synthesis,⁴³ and much attention has been devoted to the mechanistic aspects of the process, particularly those concerning the 1,4-biradical intermediate.⁴⁴ The determination of the geometric requirements for the initial hydrogen abstraction was also of interest. Wagner *et al.*⁴⁵ suggested that the geometry for the γ -hydrogen abstraction would involve a strain-free, chair-like, six-membered transition state. However, later work by Scheffer, Trotter and co-workers^{46,47} demonstrated that a chair-like transition state is not essential in the crystalline state. Irradiation of α -cycloalkylacetophenones in the solid state showed three types of γ -hydrogen abstraction geometries: - chair-like, boat-like and half-chair-like.⁴⁷ Four parameters were proposed to describe the hydrogen abstraction geometry: (i) d , the distance between the carbonyl oxygen and the γ -hydrogen; (ii) ω , the angle between the $O\cdots H\gamma$ vector and the carbonyl mean

plane; (iii) θ , the angle between the carbonyl oxygen, the γ -hydrogen and the γ -carbon; and (iv) Δ , the angle between the carbonyl carbon, the carbonyl oxygen and the γ -hydrogen.

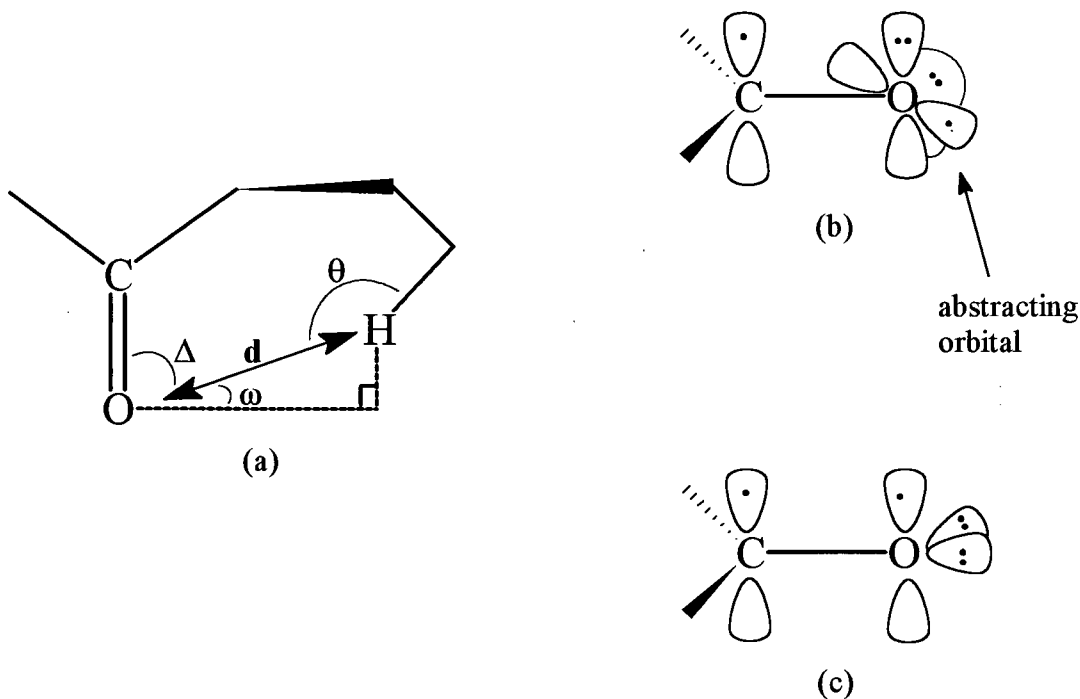


Figure 1.17. (a) Representation of Hydrogen Abstraction Geometry, (b) and (c) Arrangement of Atomic Orbitals.

The optimal values of these four parameters for a hydrogen abstraction involving the n,π^* excited state of a carbonyl compound have been suggested by Scheffer *et al.*⁴⁷ The ideal value for the distance is *ca.* 2.7 Å, which originates from the sum of the van der Waals radii for hydrogen and oxygen (2.72 Å).⁴⁸ The preferred value of Δ lies between 90° and 120° and depends on the nature of the atomic orbitals containing the n -electrons, that can be represented by two types of models. The Kasha Model⁴⁹ (Figure 1.17 (b)) demonstrates the involvement of a 2p orbital,

forming an angle of 90° with the C=O axis. Alternatively, the second model, the “rabbit ear” model⁵⁰ (Figure 1.17 (c)), has an sp^2 hybridized atomic orbital leading to an orientation of 120° with respect to the C=O axis. In the case of the angle ω , the most favorable value is $\omega = 0^\circ$, in which case the hydrogen is coplanar with the n-orbital on oxygen. The abstracting orbital is thought to be the non-bonding p_y orbital on oxygen, which lies in the π -bond nodal plane, represented by the Kasha Model (Figure 1.17 (b)). In the case of the angle θ , a linear arrangement is thought to be preferred ($\theta = 180^\circ$), however, departures from this value have been observed.⁵¹

1.5. The Excited State

When an organic molecule absorbs light, a molecular excited state is produced. In the ground state of most organic molecules, electrons exist in pairs with anti-parallel spins. This is referred to as the ground singlet state (S_0). Upon irradiation with ultraviolet or visible light, a photon may be absorbed, promoting an electron to the first excited singlet state (S_1).

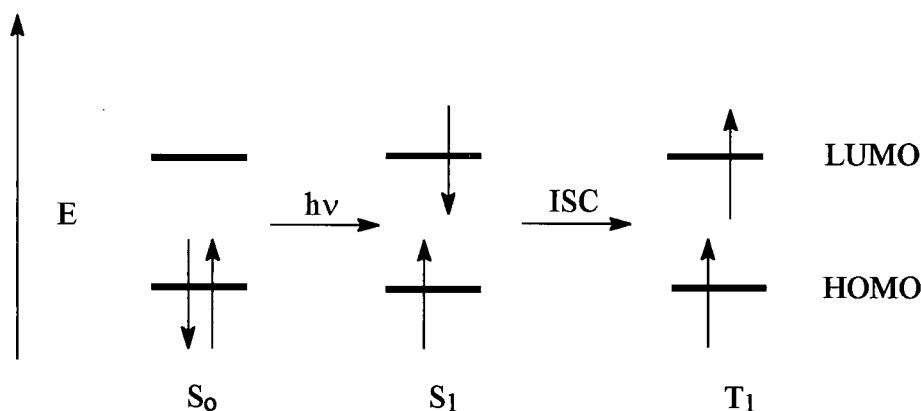


Figure 1.18. Energy Diagram for Selected Transitions.

As a result of spin-orbit coupling, an electron can flip its spin, resulting in a configuration with parallel spins called the triplet excited state (T_1). This non-radiative transition between vibronic states is referred to as intersystem crossing (ISC), a process that is formally spin-forbidden. Spin-orbit coupling results from the mixing of an electron's spin-magnetic moment ($s = \pm 1/2$) with the electron's orbital angular momentum ($l = 0, 1, 2, \dots$) and depends on the relative orientation between the spin and orbital magnetic moments. Furthermore, spin-orbit coupling is most effective between states which involve both changes in electron spin and orbital types $^1(n, \pi^*) \rightarrow ^3(\pi, \pi^*)$ and can be enhanced by the presence of either paramagnetic compounds (i.e. O_2 , NO, *etc.*), or heavy atoms (I, Br, K, Rb, *etc.*). Other photochemical processes a molecule can undergo after excitation include chemical reaction, fluorescence ($S_1 \rightarrow S_0 + h\nu$), phosphorescence ($T_1 \rightarrow S_0 + h\nu$) or internal conversion (e.g. $S_1 \rightarrow S_0 + \text{heat}$), a non-radiative process that occurs between two electronic states of equal multiplicity.

1.5.1. Triplet-Triplet Energy Transfer

Sensitization methods provide a powerful technique leading to products from the triplet state without obtaining the competing products arising from the singlet state. A triplet-triplet energy transfer (triplet sensitization) involves the transfer of triplet energy from an electronically excited molecule (donor) to its ground state neighbor (acceptor), which then becomes electronically excited.



This bimolecular process is more likely to occur if the excited state of the donor is long-lived (e.g., $\tau_T = 10^{-4}$ s for acetophenone). The use of a triplet sensitizer (donor) will enable an acceptor molecule to be excited to its triplet state without having directly absorbed a photon. Compounds containing carbonyl groups, such as acetone ($E_T = 78$ kcal/mol),⁵² acetophenone ($E_T = 74$ kcal/mol) and benzophenone ($E_T = 69$ kcal/mol), have high-energy triplet states and are examples of commonly used sensitizers. The donor triplet state must be of higher energy than the acceptor triplet state to provide for successful exothermic energy transfer. Effective exchange interactions are also facilitated if the donor and acceptor molecules come into close proximity on the order of 10-15 Å.⁵³ Intramolecular energy transfer has been investigated by Zimmerman *et al.*,⁵⁴ amongst others, who conducted experiments involving the excitation ($\lambda \geq 350$ nm) of the benzoyl (donor)-naphthyl (acceptor) system 43. At this wavelength only the benzoyl moiety ($n-\pi^*$) was excited, leading to through space energy transfer to the naphthyl group, from which phosphorescence was detected. A triplet-triplet energy transfer efficiency of 100% was observed when the average separation between donor and acceptor, created by a spacer group, was 7 Å. Steroid 44,⁵⁵ although not as efficient ($\phi = 35\%$), is another example of a compound that can undergo intramolecular triplet-triplet energy transfer. In this case the estimated distance between donor and acceptor lies around 14 Å, thus giving evidence that triplet-triplet energy transfer is distance dependent.

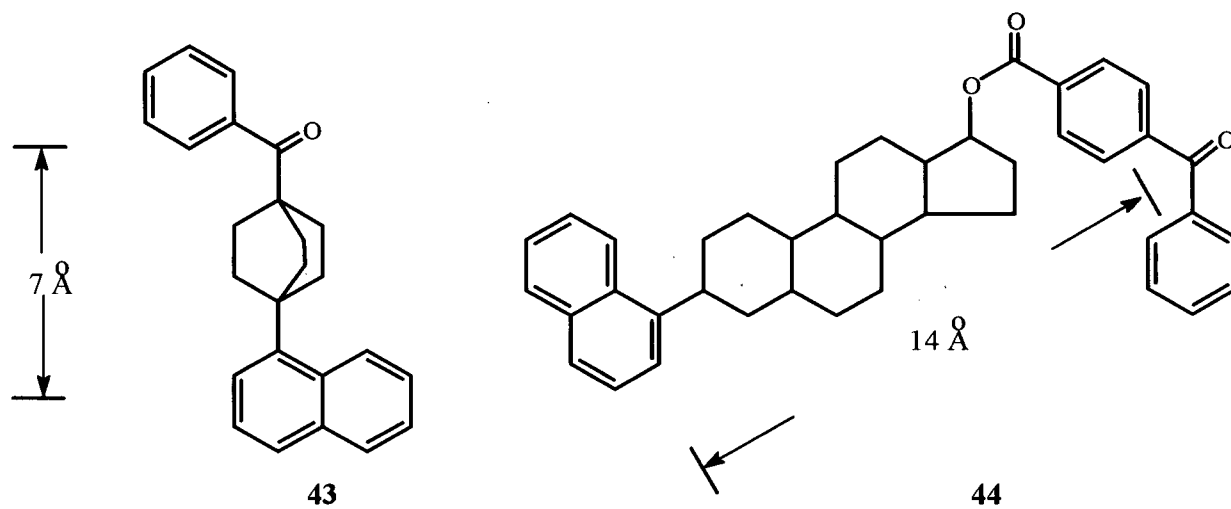


Figure 1.19. Benzoyl (Donor)-Naphthyl (Acceptor) Systems 43 and 44.

1.5.2. The Heavy Atom Effect

An alternative method for generating triplet state-derived photoproducts is by taking advantage of the heavy atom effect. In this case, the triplet state results from intersystem crossing (ISC) from the singlet state. For compounds with large S_1 - T_1 energy gaps, such as alkenes, ISC is very inefficient by itself. Although ISC is spin forbidden, these radiative and radiationless transitions may be enhanced in the presence of atoms possessing a high atomic number. This is referred to as the heavy atom effect and is brought about by the interaction between spin-orbit coupling, among the spin magnetic moment and the orbital angular moment, and a nuclear charge.⁵⁶ By directly relating the magnitude of the nuclear magnetic field from the motion of the nucleus to the size of the nuclear charge, and therefore atomic number, spin-orbit coupling is found to increase with increasing atomic number.⁵⁷ The heavy atom may either be attached to the molecule (internal)⁵⁸ or be located in the reaction medium (external).⁵⁹ One of the first examples of an external heavy atom effect was given by Cowan and Drisko,⁶⁰ who investigated the photochemistry of acenaphthylene **45** in different solvents. Compound **45** was shown to dimerize to the *trans* dimer **47** from the T_1 state, whereas the *cis* dimer **46** was obtained from the S_1 state. Photolysis in benzene or cyclohexane yielded the *cis* dimer as the major product. However, irradiation in *n*-propyl bromide, a heavy atom solvent, resulted in an increase of the triplet-derived *trans* dimer. This data indicated an increase in ISC from $S_1 \rightarrow T_1$ due to external heavy atom perturbation.

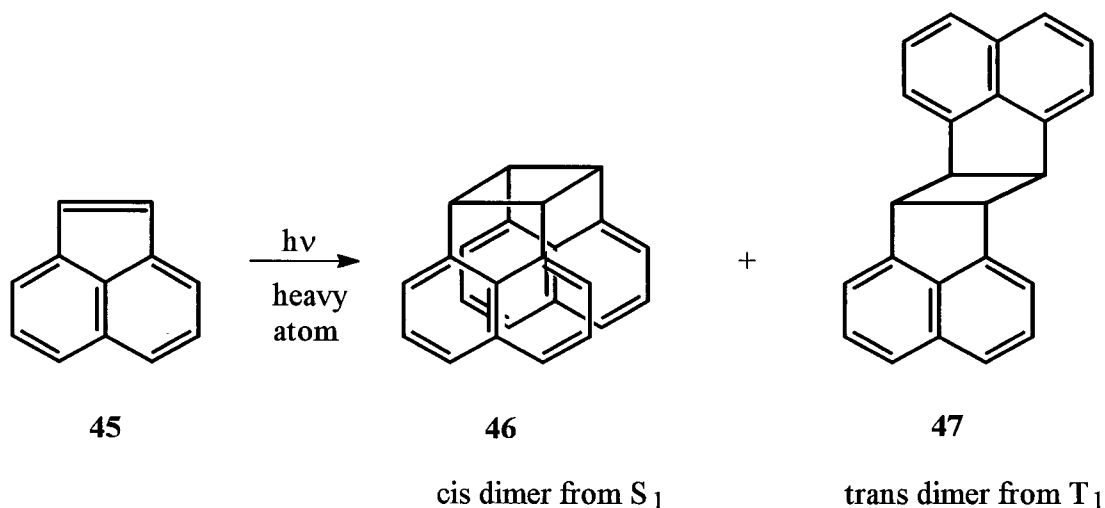


Figure 1.20. Experimental Example of the External Heavy Atom Effect.

A great number of investigations of the heavy atom effect involve halogens. However, other atoms of high atomic weight have been shown to lead to similar results. An internal heavy atom effect was found when α -methylmercuridiazocetonitrile **48** was photolyzed.⁶¹ Direct irradiation in *cis*-2-butene resulted in a non-stereospecific 1:1 ratio of the *cis* and *trans* products of **50**. However, the reaction of diazoacetone nitrile with *cis*-2-butene was known to be stereospecific resulting from a singlet carbene. As a result, compound **48** was believed to undergo ISC to the triplet state in the presence of the mercury as the heavy atom.

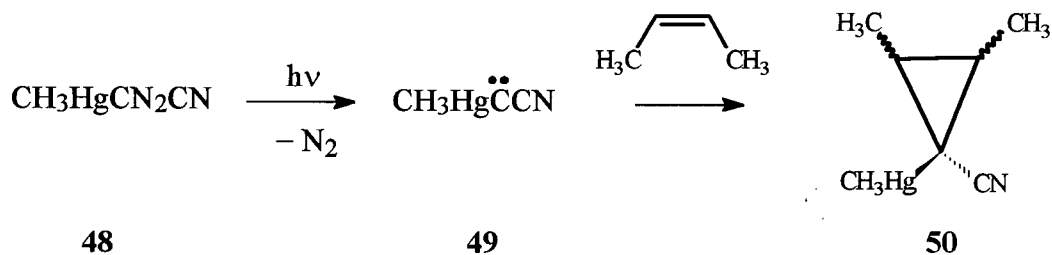


Figure 1.21. Experimental Example of the Internal Heavy Atom Effect.

An internal heavy atom effect has also been observed by Givens *et al.*,⁶² who detected an increase in $T_1 \rightarrow S_0$ radiationless decay. The author reported on the photochemistry of the halogenated β,γ -unsaturated ketones **51a** or **51b**. These compounds are known to undergo either an oxadi- π -methane rearrangement (ODPM) from the T_1 (π, π^*) state or a 1,3-acyl shift (AS) from $S_1(n, \pi^*)$ or $T_2(n, \pi^*)$. Upon irradiation, the quantum yields of the sensitized ODPM reactions were decreased with the introduction of the heavy atoms chlorine or bromine. Furthermore, the triplet-sensitized reaction also resulted in less 1,3-acyl shift product formation. These results, which were supported by phosphorescence quenching studies, led to the conclusion that the heavy atom effect increases the radiationless decay rate for the triplet states.

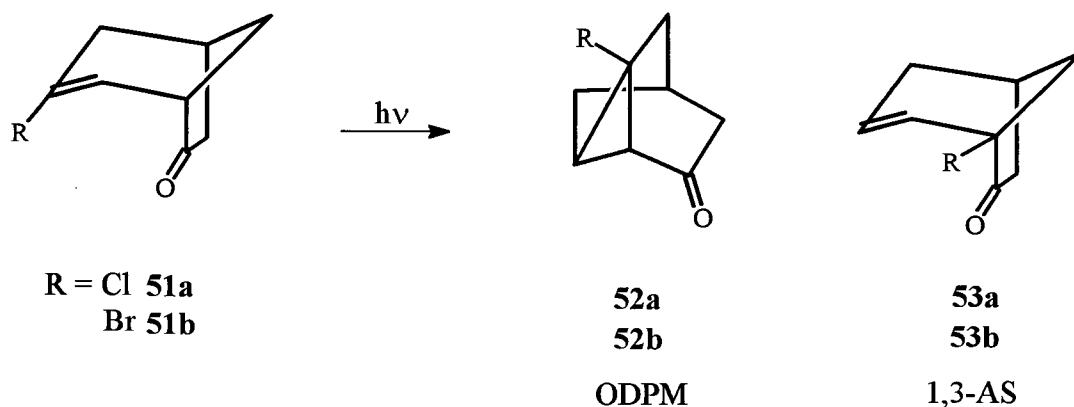


Figure 1.22. Photolysis of β,γ -Unsaturated Ketones **51a** and **51b**.

An example of an external heavy atom-induced $S_1 \rightarrow T_2$ intersystem crossing process was provided by Schuster *et al.*,⁶³ who irradiated 3-methyl-3-(1-cyclopentenyl)butan-2-one (**54**) in the presence of xenon. Enone **54** is known to undergo the 1,3-acyl shift to give product **56** upon direct or sensitized irradiation from the $S_1(n, \pi^*)$ or $T_2(n, \pi^*)$ states. Additionally, upon

1.5.3. The Heavy Atom Effect in Zeolites

The heavy atom effect has also been investigated in zeolite environments. These molecules may be viewed as an open structure of silica in which a number of tetrahedral sites have been substituted with aluminum.⁶⁵ Hence, the framework consists of pores, channels and cages. As a result of the substitution of trivalent aluminum ions for a fraction of tetravalent silicon ions at lattice positions, a negatively charged network is obtained. This must be balanced by other counterions. The pioneers in this area, Turro and Ramamurthy *et al.*⁶⁶ studied the photophysics and photochemistry of molecules in zeolites, focusing on the changes in electronic excited states and reactivities of guest molecules. Recently, the phosphorescence properties of xanthone have been investigated in alkali metal cation-exchanged zeolites by Anpo *et al.*⁶⁷ A weak fluorescence spectrum was observed with Li^+ and Na^+ cations. However, by changing the alkali metals to Rb^+ and Cs^+ , phosphorescence increased remarkably. Overall, an enhancement of the phosphorescence of xanthone was observed by changing the alkali metal cations from Li^+ , Na^+ , K^+ , Rb^+ to Cs^+ . Anpo *et al.* suggested that intersystem crossing in xanthone was enhanced by the presence of the alkali metals.

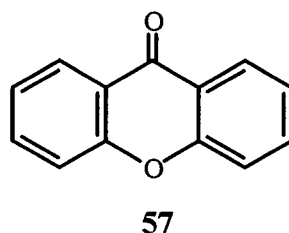


Figure 1.24. Xanthone (57).

Another example of the heavy atom cation effect in zeolite systems was demonstrated by Ramamurthy *et al.*,⁶⁸ who examined the photophysical properties of aromatic and olefinic compounds in these environments. The effect that heavy atoms exert on the guest molecule was established by monitoring the phosphorescence to fluorescence ratio from several aromatics (naphthalene, anthracene, phenanthrene) and olefins (*trans*-stilbenes). The intensity ratios were observed to increase as lighter cations were substituted by heavier ones in the order of $\text{Li}^+ < \text{Na}^+ < \text{K}^+ < \text{Rb}^+ < \text{Cs}^+ < \text{Tl}^+$. The results showed that it is possible to control the extent of the excited singlet and triplet interconversion of the guest molecule by introducing different exchange cations into the zeolites. Ramamurthy *et al.*⁶⁹ also reported on the study of a bimolecular photoreaction within the zeolite framework in the presence of heavy atoms. By varying the exchangeable cations, the multiplicity of the reactive state could be controlled. The chosen molecule for these studies was acenaphthylene (45), which was known to dimerize in solution forming the *cis* 46 and *trans* 47 dimers (Figure 1.20). The singlet excited state yields mainly the *cis* dimer, whereas the triplet state gives both the *cis* and *trans* dimers. The triplet yields and lifetimes of acenaphthylene in the zeolite were obtained by monitoring the intensity of the T-T absorption at 470 nm via flash photolysis techniques.⁷⁰ Zeolites containing the Li^+ and Na^+ cations did not show any triplet absorption, indicating that the dimerization originated from the excited singlet state. However, high triplet yields were obtained in the zeolites containing, K^+ , Rb^+ , Cs^+ and Tl^+ which could be attributed to the heavy atom effect. Although this paper demonstrated an increase in the intensity of the T-T absorption with increasing mass of the cation, the product distribution of *cis* and *trans* dimers was not as expected, leading to a decrease in *trans* dimer yield for Rb^+ , Cs^+ and Tl^+ zeolites. The different product ratios were proposed to result from the limited space in the zeolite

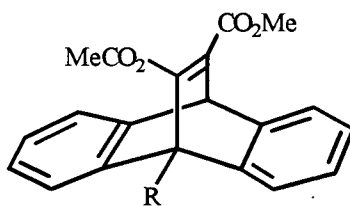
cavity. In contrast to the *cis* dimer with a length (7 Å) that could occupy a single cage, the *trans* isomer was thought to be too extended (14 Å) taking up two cages within the zeolite.

1.6. Objectives of Present Research

As previously mentioned, solid state organic photochemistry is an area that is receiving an increasing amount of attention, as it is important and interesting to understand how a molecular crystal lattice affects organic photoreactivity. The overall objective of this thesis is to investigate how different media, either solution or the solid state, influence the photoreactivity of a probe molecule. By preparing a number of related compounds and applying X-ray crystallography, a correlation may be drawn between the reactivity in the solid state and the structure. Before fully exploring the solid state reactivity of a compound, the photochemistry in an isotropic medium needs to be investigated. This thesis is divided into two parts: (I) the photochemistry of triptycene-1,4-quinone and (II) the control of reaction multiplicity in the solid state, which discusses triplet-triplet energy transfer and the heavy atom effect.

In Part I, the photoreactivity of triptycene-1,4-quinone is presented and discussed. The carbon skeleton of this compound (**63**) resembled that of previously investigated dibenzobarrelene diesters.^{71,72} For example, compound **58a** (Figure 1.25) is known to undergo the di- π -methane rearrangement in solution and the solid state.⁷¹ Introducing 9,10-substituents at the bridgehead positions⁷² resulted in dibenzobarrelenes exhibiting photochromism, changing them from colorless to dark blue or green as a result of irradiation in the solid state. One possible explanation for the

photochromism is photoinduced electron transfer between electron donating and electron accepting groups in the molecule.

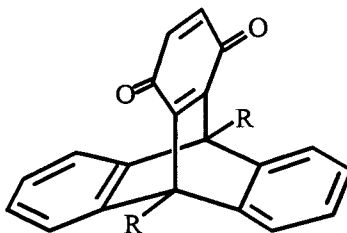


58 (a-d)

- a** R = H ⁷¹
- b** R = CHO ^{72a,b}
- c** R = CH₂Cl ^{72a,b}
- d** R = CO₂Me ^{72c}

Figure 1.25. 11,12-Diester-9,10-ethenoanthracene Derivatives.

Triptycene-1,4-quinone was chosen to study photoinduced electron transfer further in such systems. By investigating the photoreactions or lack thereof in the solid state, it was anticipated that some insight would be gained on the influence of crystal packing on the availability of reaction pathways. With the intention of comparing the reactivity of triptycene-1,4-quinone and two of its derivatives in solution and the solid state, experiments in solution were carried out first.



- 63 R = H, Chapter 3
 69 R = CH₃, Chapter 4
 72 R = CH₂OCH₃, Chapter 5

Figure 1.26. Series of Triptycene-1,4-quinones Studied.

Part I of this thesis is divided into three chapters discussing the photorearrangements of triptycene-1,4-quinone and two 9,10-dialkyl-substituted derivatives. The photoreactivity of triptycene-1,4-quinone in solution was examined, as it brought about some unexpected and interesting results. Irradiation of the triptycene-1,4-quinones led to the isolation and characterization of different photoproducts depending on the solvents used and the absence or presence of oxygen. Mechanistic pathways leading to the formation of the various photoproducts are presented and discussed. Furthermore, the photoreactivity of the substituted quinones provides insight into the solid state photochromism of certain 9,10-ethenoanthracene derivatives.

Part II of the thesis deals with the control of singlet/triplet photoreactivity of two different probe molecules in the solid state. Up to now, studies of the chemical reactivity of organic crystals have been primarily concerned with materials involving one pure component only. This may be explained by the fact that two-component solid solutions existing over a wide concentration range are relatively uncommon. In solution phase photochemistry, reaction

multiplicity can often be directed by the use of sensitizers. In the crystalline state, however, this is difficult to achieve. This obstacle could be overcome by forming a salt between a probe molecule that would exhibit a differential singlet/triplet reactivity and a counterion that would selectively populate the triplet excited state. This project was aimed at controlling the reaction multiplicity of an electronically excited probe molecule in the solid state by introducing heavy atoms or sensitizers. The first section of Part II reports on the results obtained by applying the "ionic sensitizer" concept to the carboxylic acid of a β,γ -unsaturated ketone **121** (Figure 1.27) through salt formation with a number of appropriate sensitizers containing an amine functionality.

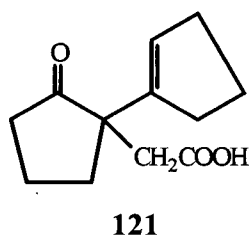
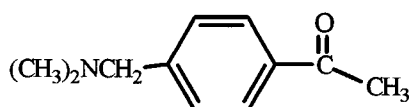
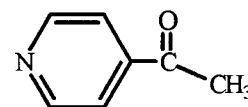
**136****128****137**

Figure 1.27. β,γ -Unsaturated Ketone and Sensitizers Selected for the Study of Triplet-Triplet Energy Transfer.

Additionally, the solid and solution state photochemistry of three 9,10-dihydro-9,10-ethenoanthracene derivatives (Figure 1.28) has been investigated in order to establish their singlet and triplet photoreactivity. The later part of the thesis is concerned with the effects that heavy

atoms (Li^+ , Na^+ , K^+ , Rb^+ , Cs^+) and three different sensitizers exert on the photochemical behavior of 9,10-dihydro-9,10-ethenoanthracene derivative **132**. X-ray crystallography was employed to investigate the geometric relationship between the sensitizer and the probe molecule in order to explain the efficiency of triplet-triplet energy transfer.

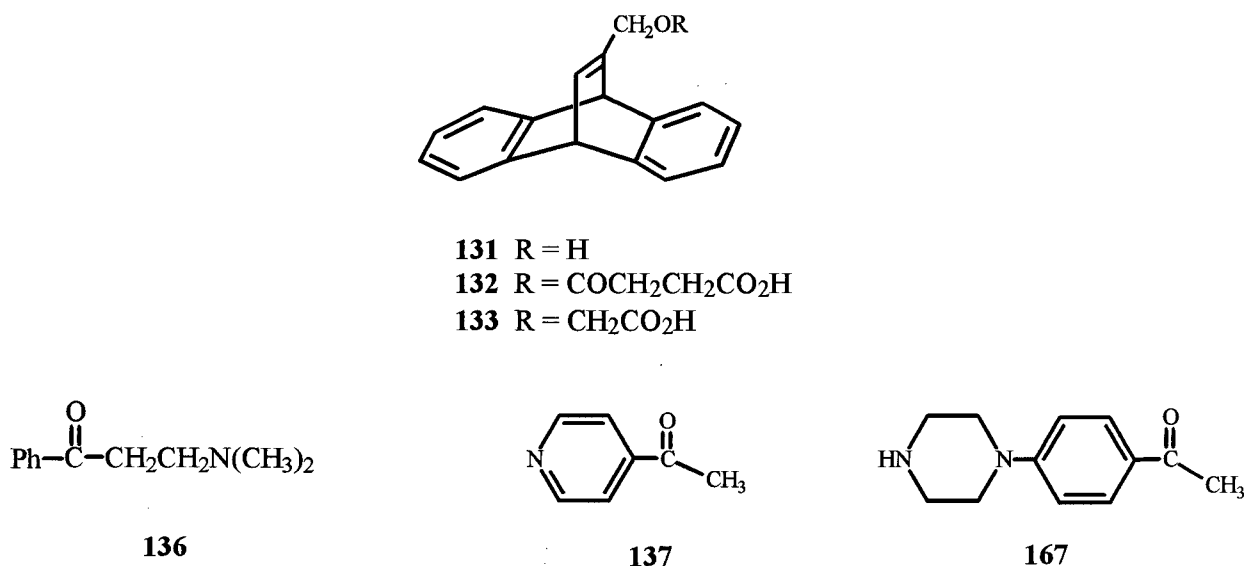


Figure 1.28. Series of 9,10-Dihydro-9,10-ethenoanthracene Derivatives and Sensitizers.

The successful experiments demonstrating the control of reaction multiplicity in the solid state expand the field of organic photochemistry in this medium. Triplet as well as singlet excited state properties can now be investigated in the solid state by applying X-ray crystallography as a tool to correlate structure and reactivity. These positive results open up the possibility of performing triplet energy quenching studies in the crystalline state, an area that has yet to be explored. Furthermore, as already accomplished in solution,⁷³ Stern-Volmer type kinetic studies could be carried out in the solid state through quantum yield determinations. By studying the

photochemical and photophysical behavior of organic compounds in a variety of solid environments, such as salts, zeolites and polymers, more may be learned about controlling chemical reactivity in ordered media.

RESULTS AND DISCUSSION

PART I PHOTOCHEMISTRY OF TRIPTYCENE-1,4-QUINONE

CHAPTER 2 GENERAL ORGANIC SYNTHESIS

2.1. Preparation of 9,10-Dihydro-9,10[1',2']benzenoanthracene-1,4-dione (63)

9,10-Dihydro-9,10[1',2']benzenoanthracene-1,4-dione (63), also known as triptycene-1,4-quinone, was first synthesized by Clar⁷⁴ in 1931 and later by Bartlett.⁷⁵ This sequence involved an initial Diels-Alder addition between *p*-benzoquinone and anthracene to give adduct 61, followed by aromatization with hydrobromic acid to 1,4-dihydroxytriptycene 62 and an oxidation with potassium bromate (Figure 2.01).

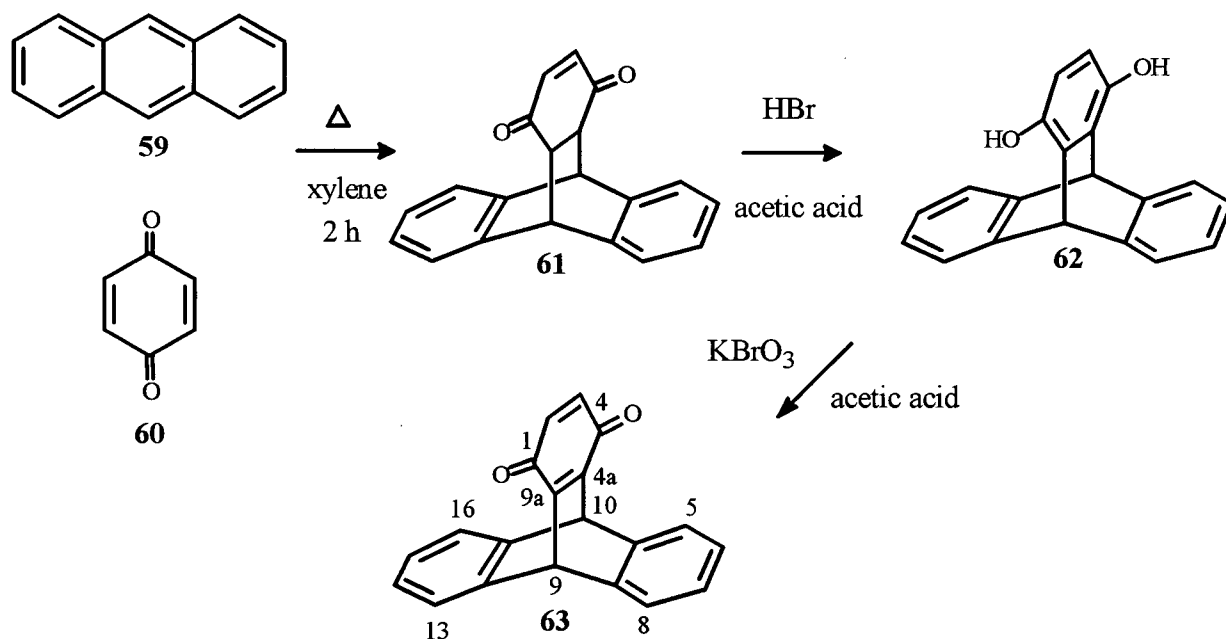


Figure 2.01. Preparation of 9,10-Dihydro-9,10[1',2']benzenoanthracene-1,4-dione (63).

2.2. Synthesis of Anthracene Derivatives

9,10-Dimethylantracene (65) was prepared by reduction of 9,10-bis(chloromethyl)anthracene (64) with lithium aluminum hydride according to the procedure by Kirby *et al.*⁷⁶ 9,10-Bis(methoxymethyl)anthracene (66) was obtained by refluxing 9,10-bis(chloromethyl)anthracene (64) in a solution of methanol with potassium hydroxide according to Miller *et al.*⁷⁷ The parent compound for both syntheses was prepared by adding anthracene and paraformaldehyde to a solution of dioxane and concentrated hydrochloric acid saturated with hydrogen chloride gas.⁷⁷

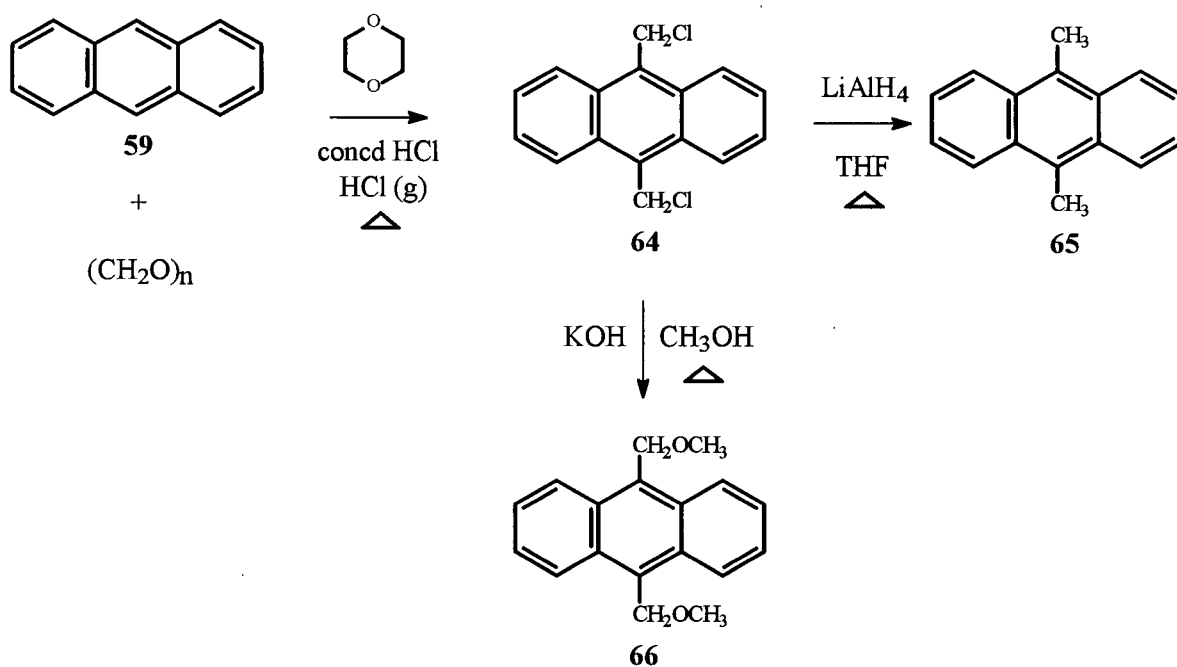


Figure 2.02. Preparation of 9,10-Bis(chloromethyl)anthracene (64), 9,10-Dimethylantracene (65) and 9,10-Bis(methoxymethyl)anthracene (66).

2.3. Preparation of 9,10-Disubstituted-9,10-dihydro-9,10[1',2']benzenoanthracene-1,4-dione Derivatives

9,10-Dihydro-9,10-dimethyl[1',2']benzenoanthracene-1,4-dione (**69**), otherwise known as 9,10-dimethyl triptycene-1,4-quinone,⁷⁸ and 9,10-bis(methoxymethyl)-9,10-dihydro-9,10[1',2']-benzenoanthracene-1,4-dione (9,10-bis(methoxymethyl)triptycene-1,4-quinone) (**72**), were synthesized by oxidation of the corresponding hydroquinones (**68** and **71**) with potassium bromate. The hydroquinones were prepared according to the literature procedure through the Diels-Alder addition of *p*-benzoquinone to either 9,10-dimethylantracene or 9,10-bis(methoxymethyl)anthracene, followed by base-catalyzed aromatization.⁷⁹

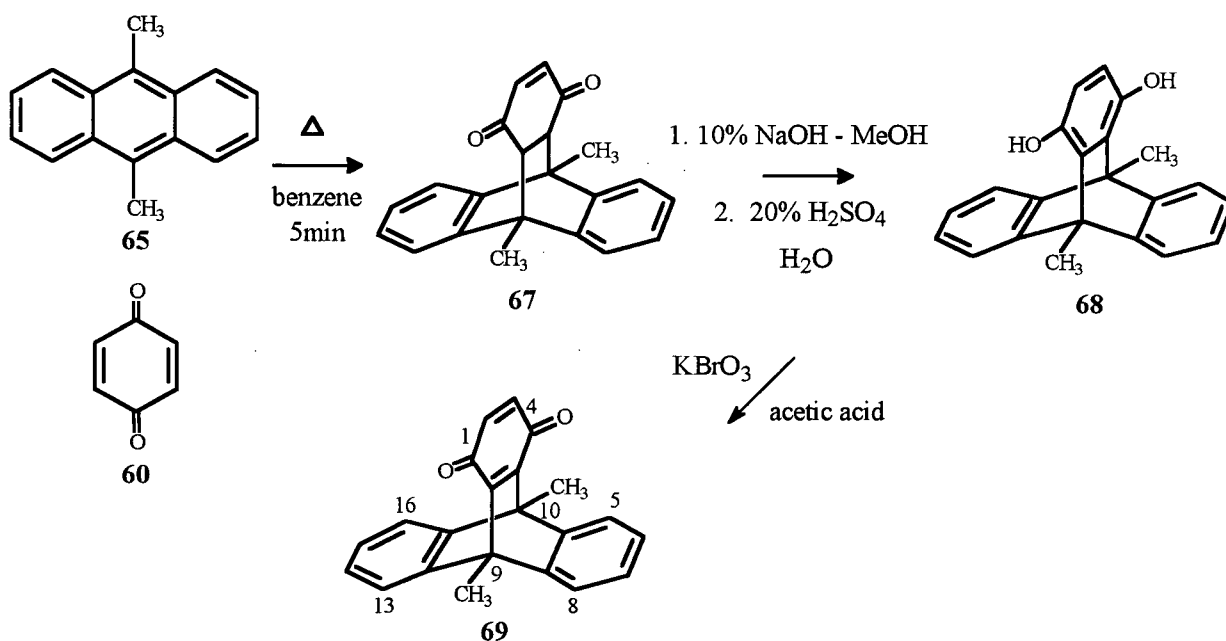


Figure 2.03. Preparation of 9,10-Dihydro-9,10-dimethyl-9,10[1',2']benzenoanthracene-1,4-dione (**69**).

In the case of **72**, difficulties arose in the base-catalyzed aromatization step and the concentration of the base had to be reduced. The aromatization of the Diels-Alder adduct **70** was also attempted with hydrobromic acid, but this did not result in the desired hydroquinone **71**.

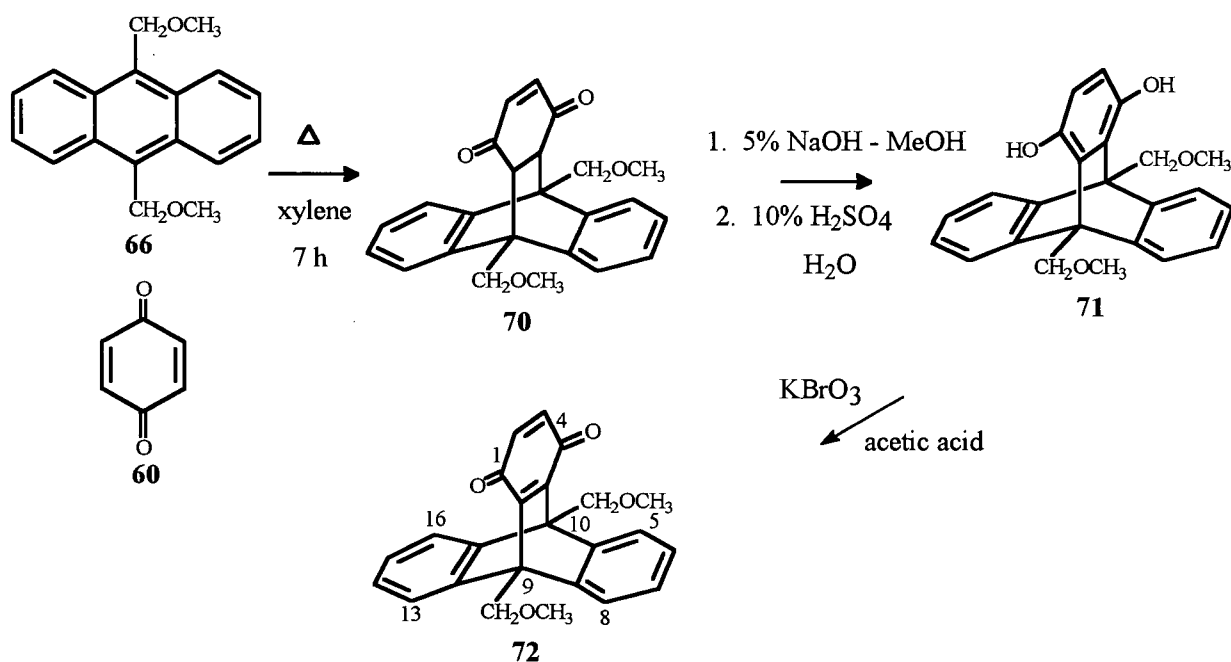


Figure 2.04. Preparation of 9,10-Bis(methoxymethyl)-9,10-dihydro-9,10[1',2'] benzenoanthracene-1,4-dione (**72**).

The Diels-Alder addition between 9,10-bis(methoxymethyl)anthracene and benzoquinone proceeded in high yield (90%), although the reaction time to form **70** was prolonged (7 h) compared to the adduct formation times of **61** (2 h) and **67** (1 min). Although not as efficient as the methyl groups, the methoxymethyl substituents apparently act as electron donating groups, to promote the cycloaddition. Since 9,10-bis(chloromethyl)anthracene (**64**) had already been prepared, an experiment was also conducted to add this diene to the dienophile benzoquinone.

However, this reaction led to no distinct product formation for reasons that are unclear at this point.

2.4. Preparation of 5- and 6-Chloro-9,10-dihydro-9,10[1',2']benzenoanthracene-1,4-diones

Two chlorinated derivatives of triptycene-1,4-quinone were prepared in order to confirm the structure of an isolated photoproduct and verify the position of the chlorine atom (see Chapter 3.3). The synthesized compounds were 5-chlorotriptycene-1,4-quinone (73) and 6-chlorotriptycene-1,4-quinone (74), a compound that had been prepared by a six step synthesis described by Hashimoto *et al.*⁸⁰ Improving upon this lengthy synthesis, both chlorinated quinones were obtained by the same procedures as for triptycene-1,4-quinone 63, giving 5-chlorotriptycene-1,4-quinone (73) and 6-chlorotriptycene-1,4-quinone (74). The spectral data of 74 was found to be identical to that reported in the literature.⁸⁰

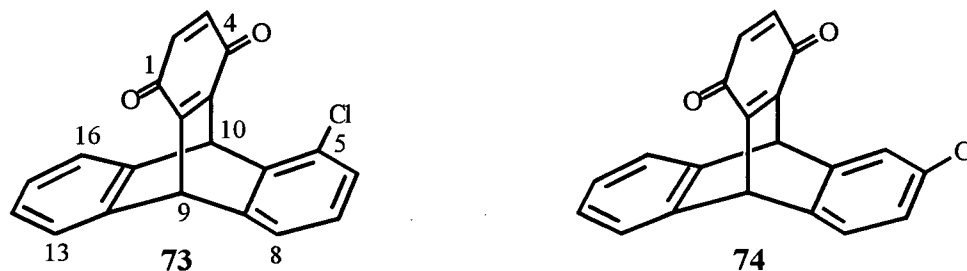


Figure 2.05. Structures of 5-Chlorotriptycene-1,4-quinone (73) and 6-Chlorotriptycene-1,4-quinone (74).

The reduced yield in the case of 74 can be attributed to the formation of one or a mixture of the 2 : 1 adducts 77a-d (i.e. two molecules of anthracene and one molecule of benzoquinone, Figure 2.06). The structural elucidation was based on comparing the spectral data to the corresponding 1 : 1 adduct 74. The mass spectrum shows the characteristic pattern of a structure with two chlorine atoms with a peak ratio of 9 : 6 : 1 corresponding to the molecular ion peak at m/e 528, $M+2$ at m/e 530 and $M+4$ at m/e 532. The disappearance of the quinone vinyl hydrogens in the 1H NMR gave a clear indication that a second cycloaddition had occurred. However, the exact position of the second chlorine atom could not be determined.

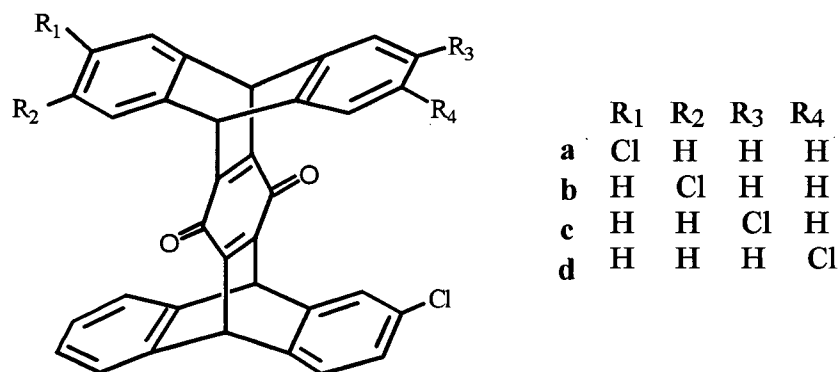


Figure 2.06. Possible Chlorinated 2 : 1 Adducts 77a-d.

The required chlorinated anthracene derivatives were obtained by reduction of the corresponding anthraquinone with zinc powder and acetic acid (Figure 2.07).^{81,82}

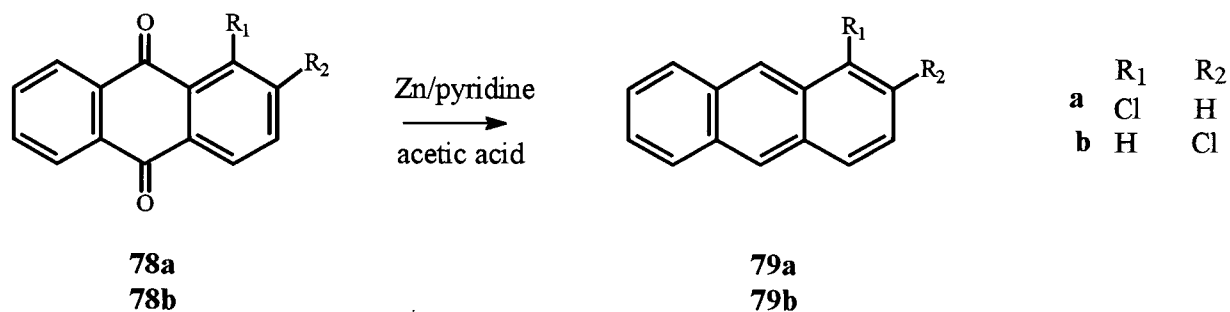


Figure 2.07. Preparation of 5-Chloroanthracene (79a) and 6-Chloroanthracene (79b).

CHAPTER 3 PHOTOCHEMICAL STUDIES OF

9,10-DIHYDRO-9,10[1',2']BENZENOANTHRACENE-1,4-DIONE (63)

In the past, 9,10-dihydro-9,10[1',2']benzenoanthracene-1,4-dione (63) has received a great deal of attention concerning its photophysical properties. Iwamura and Makino⁸³ as well as Murata *et al.*⁸⁴ and Kitaguchi⁸⁵ have demonstrated that this compound, along with several derivatives, possesses a charge transfer excited state (Figure 3.01) resulting from intramolecular electron transfer from one of the aromatic rings to the quinone ring.

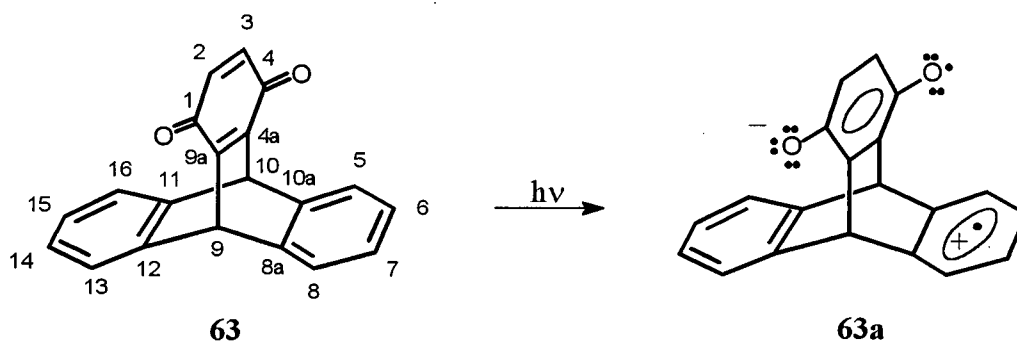


Figure 3.01. Numbering System for Triptycene-1,4-quinone (63) and its Charge-Transfer Excited State (63a).

Photochemically, triptycene-1,4-quinone (63) has been studied by Kitaguchi,⁸⁶ who investigated its photoreduction in the presence of xanthene as a hydrogen atom donor and determined the quantum yield ($\Phi = 0.35$). However, Kitaguchi did not report any unimolecular photoreactivity of this system. Triptycene-1,4-quinone possesses the skeleton of a di- π -methane reactant in which the 1,4-pentadiene moiety is replaced by a benzene and quinone ring

respectively. This prompted the question whether a dipolar CT excited state would interfere with the photochemistry of quinone **63**.

3.1. Photochemical Results Upon Direct Irradiation of **63**

Irradiation of triptycene-1,4-quinone through Pyrex ($\lambda \geq 290$ nm) in deoxygenated acetonitrile, methanol or ethanol led to a single photoproduct isolated as yellow needles (80%), and assigned as the di- π -methane rearranged product **80** (Figure 3.02) based on its spectroscopic properties.

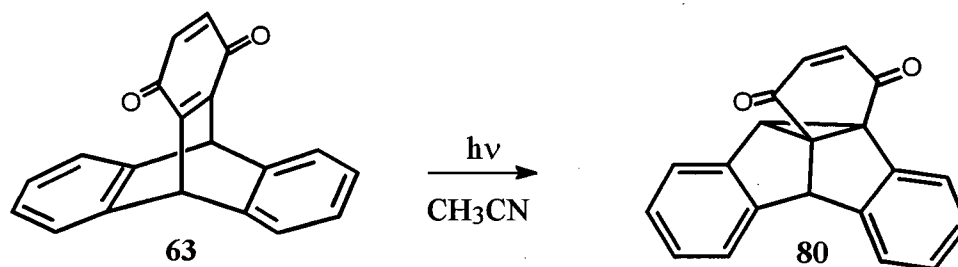


Figure 3.02. Dibenzosemibullvalene **80** from the Irradiation of Triptycene-1,4-quinone (**63**).

This conversion of triptycene quinone to photoproduct **80**, a dibenzosemibullvalene, is analogous to the well established di- π -methane rearrangement of other 9,10-ethenoanthracene derivatives as discussed in the Introduction.

3.1.1. Structure Elucidation of Semibullvalene 80

The ^1H NMR spectrum of dibenzosemibullvalene **80** (Figure 3.03) was compared to structures containing the semibullvalene skeleton that had been investigated previously.⁸⁷ The multiplet at δ 8.05-7.97 ppm can be assigned to the aromatic hydrogen H-1 (Figure 3.03). The downfield position of this hydrogen may be explained by the deshielding effect of the anisotropic cone⁸⁸ of the carbonyl group, situated closest to the aromatic ring at this position. The remaining seven aromatic hydrogens are represented by a multiplet at δ 7.35-7.03 ppm. The vinyl hydrogens H-2' and H-3' are observed at δ 6.63 ppm as a singlet. The singlet at δ 5.13 ppm is assigned to hydrogen H-4b at the doubly benzylic position. This downfield position may result from the deshielding effect of the two aromatic rings. The more shielded hydrogen at δ 4.37 ppm is attributed to the cyclopropyl methine H-8b. Such chemical shifts are characteristic of dibenzosemibullvalenes and the assignment of the structure was supported by correlation of ^1H NMR spectral interpretation to X-ray crystal structures reported by Scheffer *et al.*⁸⁹ The IR spectrum, with a carbonyl band at 1677 cm^{-1} , and the mass spectrum, with a parent mass of m/e 284, also support the structure assigned to photoproduct **80**.

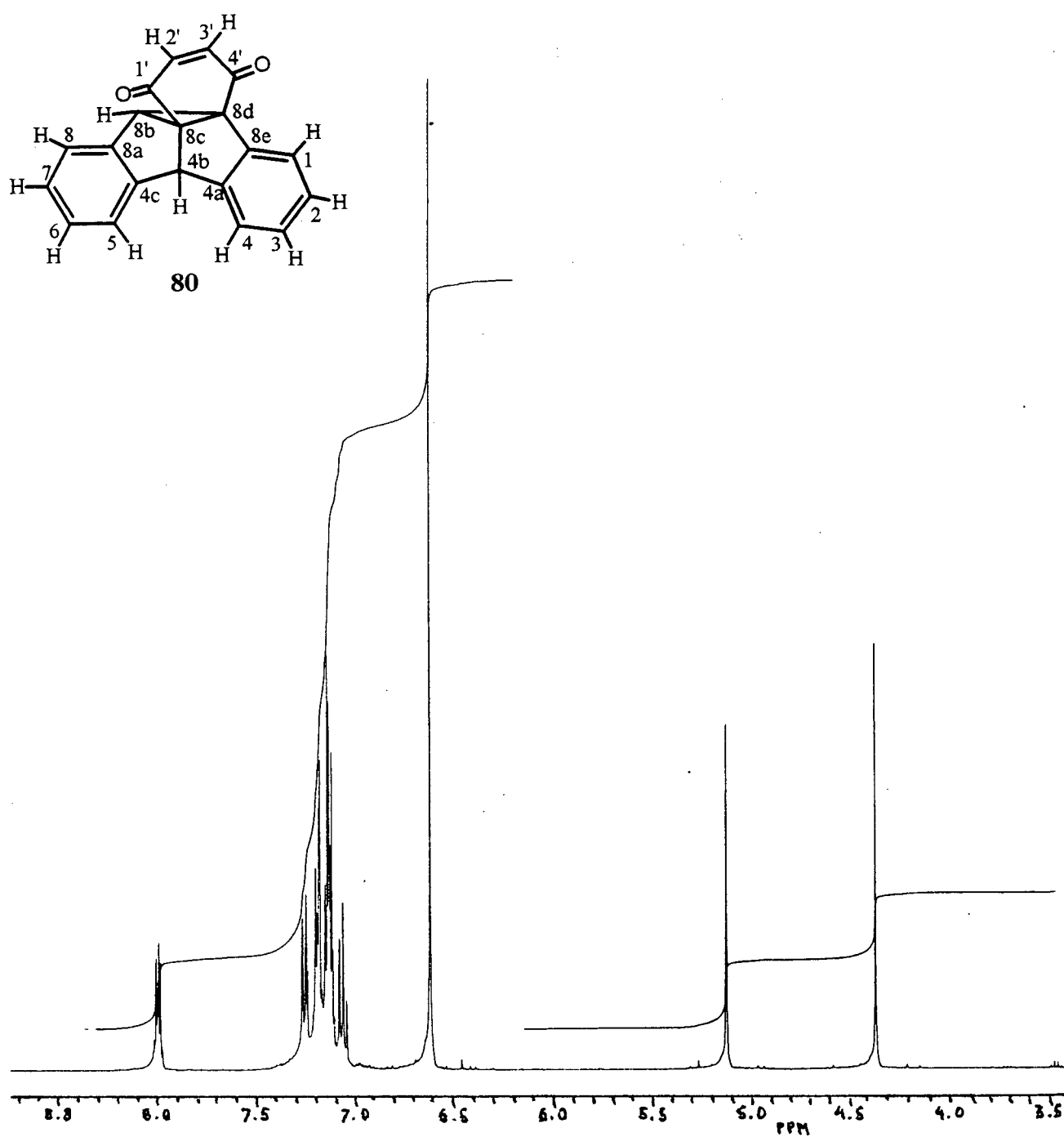


Figure 3.03. ^1H NMR Spectrum of Dibenzosemibullvalene 80.

3.1.2. Regioselectivity of Semibullvalene Photoproduct Formation

The formation of semibullvalene **80** may be rationalized by comparing the relative stabilities of intermediates **63b** and **63e** (Figure 3.04) that would result from the two possible bridging pathways: (a) benzo-benzo bridging [i.e. bonding between C(8a) and C(12)] and (b) benzo-quinone bridging [i.e. bonding between C(4a) and C(10a)]. If the reaction proceeds through pathway (a) the aromaticity would be lost in both benzenoid rings, as seen in biradical **63b**. However, if the benzo-quinone bridging pathway (b) would be followed, only one benzenoid ring would be disrupted, whereas the second odd electron would be stabilized by the adjacent carbonyl group of the quinone ring. Reaction pathway (b) is preferred since it involves the more stable biradical **63e** affecting only one of the benzenoid rings instead of two. This regiochemistry is in accord with the work of Zimmerman *et al.*,⁹⁰ who showed that initial bridging to form the more stable cyclopropyldicarbonyl 1,4-biradical intermediate is product-determining in such compounds. There appears to be no need to invoke a CT excited state for this process, although its participation cannot be ruled out.

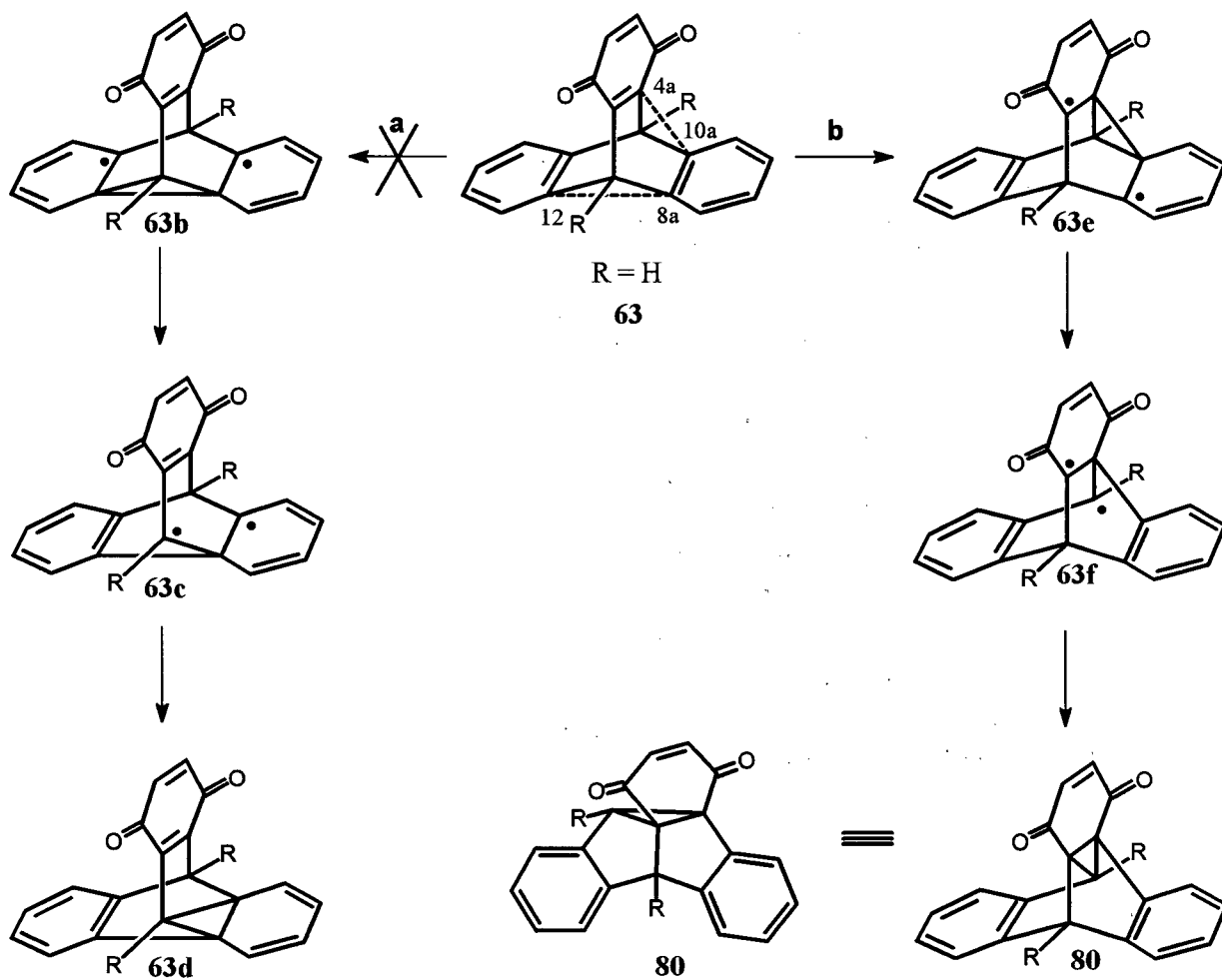


Figure 3.04. Regioselectivity of the Di- π -Methane Rearrangement of 63.

3.2. Photochemical Results Upon Irradiation of 63 in Acetone

The photolysis of triptycene-1,4-quinone (**63**) in deoxygenated acetone resulted in the formation of the dibenzosemibullvalene product **80**, the same photoproduct that had been obtained from direct irradiation experiments. However, when air was present, a different photoproduct was detected by gas chromatographic (GC) analysis. Optimization of the experimental conditions in air-saturated acetone led to a maximum isolated yield of 18% of triketone **81** (Figure 3.05).

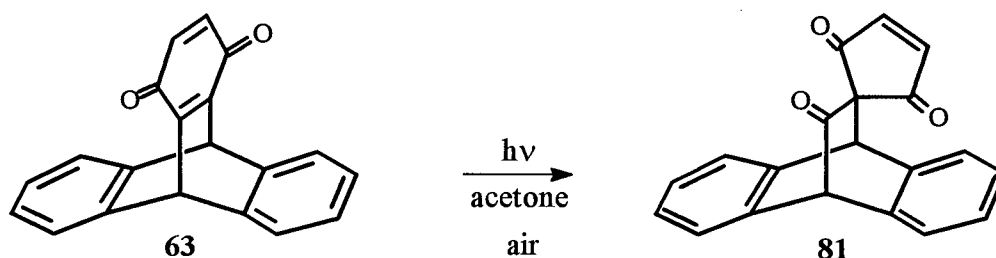


Figure 3.05. Triketone **81** from the Irradiation of Triptycene-1,4-quinone (**63**).

3.2.1. Structural Assignment of Triketone **81**

The structure of triketone **81** was initially assigned by spectral analysis and then confirmed by X-ray crystal analysis. In order to obtain a mass spectrum of triketone **81**, desorption chemical ionization (DCI + NH₃) was used to ionize the sample resulting in a base peak of M+18 at *m/e* 318. The M+1 peak at *m/e* 301 indicates that an additional oxygen atom has been added to the initial skeleton, which has an M+1 peak at *m/e* 285. The infrared spectrum also reveals the

presence of two types of carbonyl stretches: a strong band at 1709 and a medium band at 1760 cm^{-1} . The lower stretching frequency was compared to the vibrations of the carbonyl groups of cyclopenten-3,5-dione (**82**), which occur at 1718 cm^{-1} (nujol).⁹¹

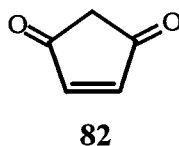


Figure 3.06. Cyclopenten-3,5-dione (**82**).

Peak assignment of the ^1H NMR spectrum was done by comparing the triketone **81** to the starting material **63**. A noticeable change was observed in the chemical shift of the vinyl hydrogens, initially at δ 6.59 ppm, which moved further downfield to δ 7.38 ppm. This chemical shift can be compared to the shift of the vinyl hydrogens of cyclopenten-3,5-dione (**82**) at δ 7.31 ppm.⁹² The bridgehead hydrogens shifted upfield from the initial singlet at δ 5.79 ppm to two distinct singlets at δ 4.98 and 4.47 ppm.

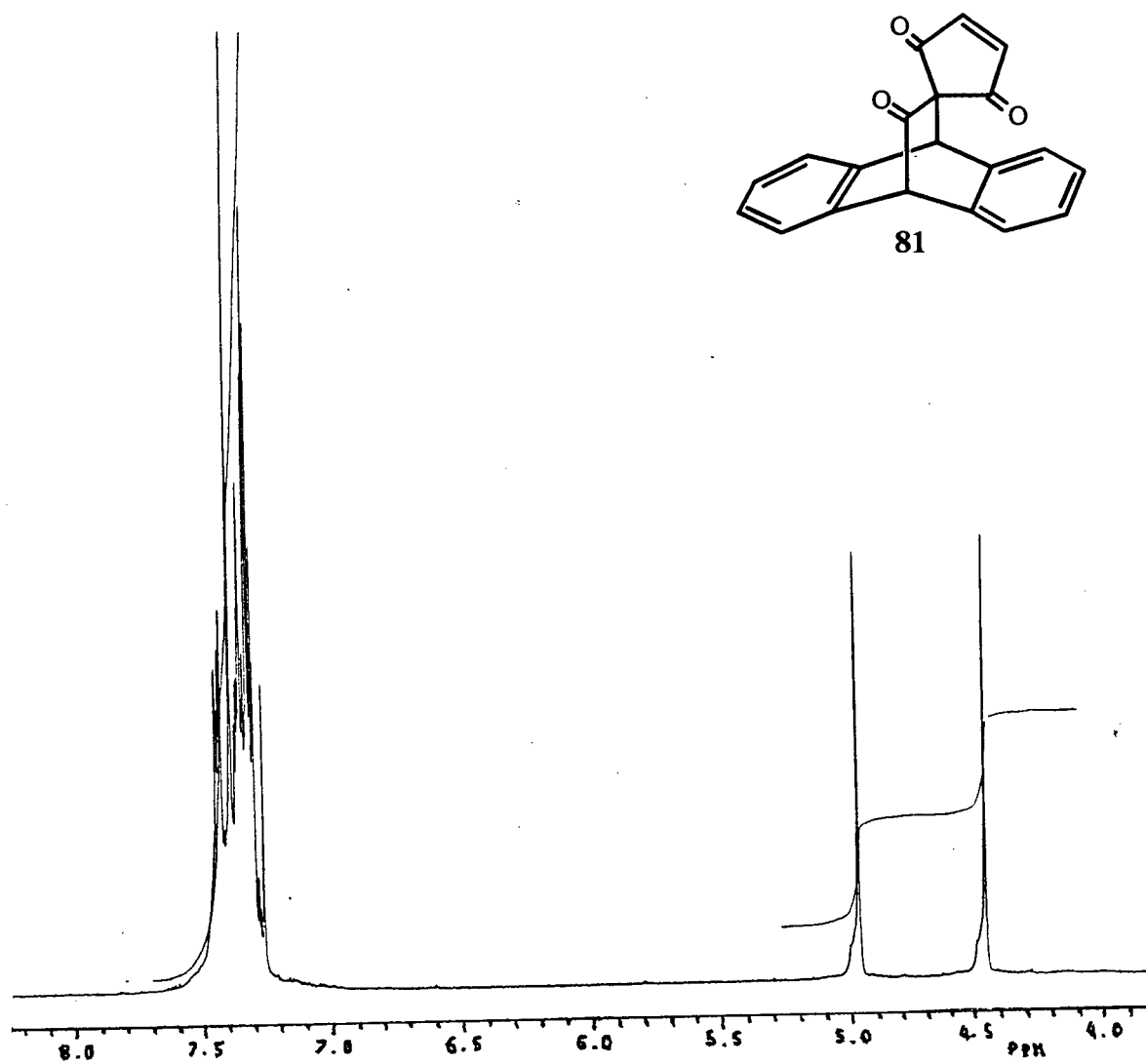


Figure 3.07. ¹H NMR Spectrum of Triketone 81.

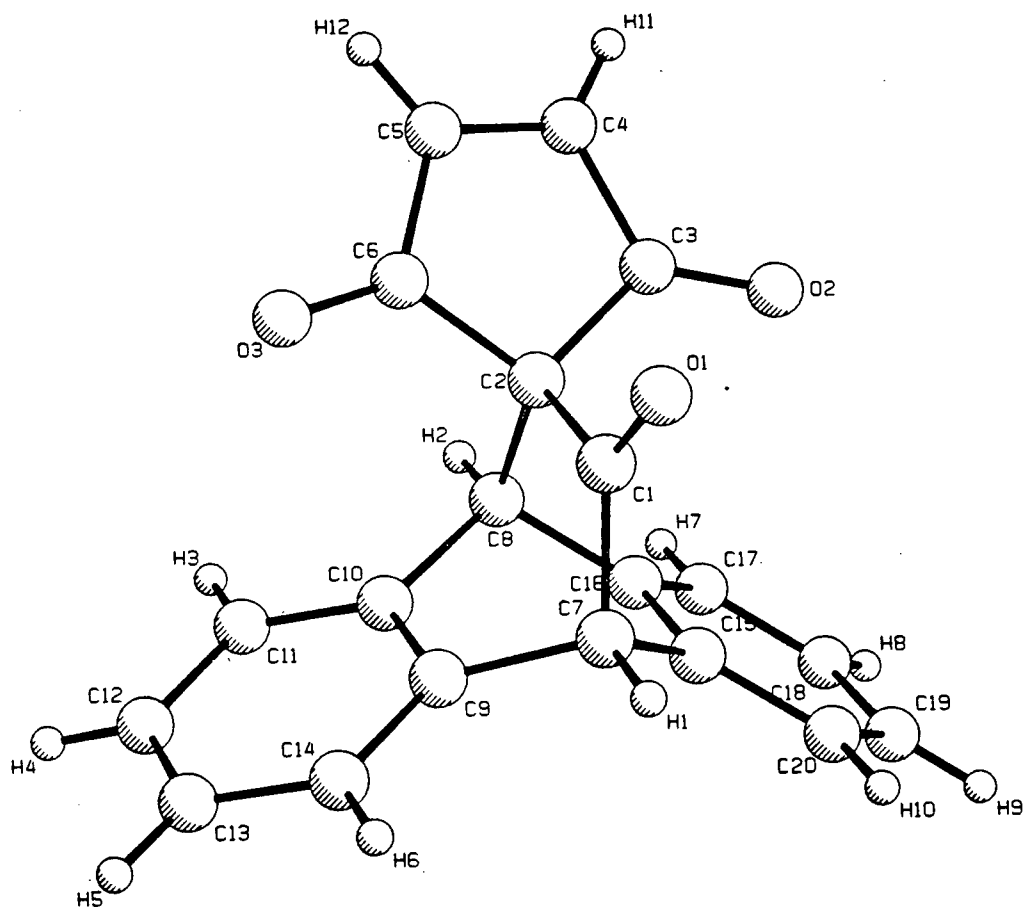


Figure 3.08. X-ray Crystal Structure of Triketone 81. Space Group $Pna2_1$ (#33);

$a = 12.274(3) \text{ \AA}$, $b = 7.957(3) \text{ \AA}$, $c = 15.444(3) \text{ \AA}$, $Z = 4$, $R = 3.7\%$.

3.2.2. Mechanistic Speculations on the Formation of Triketone 81

A possible mechanism for the photochemical reaction leading to the formation of triketone 81 is depicted in Figure 3.09. The reaction pathway is believed to proceed through the cyclopropyldicarbonyl biradical 63e, which could either undergo the di- π -methane rearrangement in the absence of oxygen to give semibullvalene 80 (Figure 3.04, pathway (b)), or be trapped by dissolved oxygen from an air-saturated acetone solution. Intermediate 83 could then abstract a hydrogen from the solvent, followed by homolysis and rearrangement of biradical 85 to triketone 81.

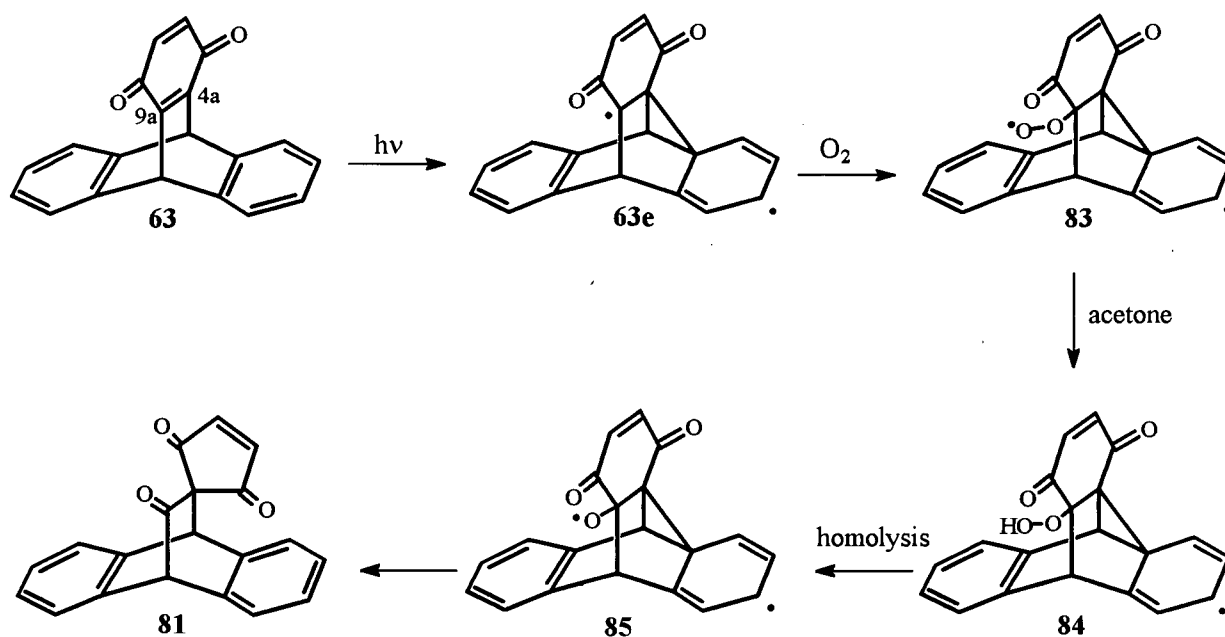


Figure 3.09. Proposed Mechanism for Formation of Triketone 81.

An alternative mechanism could involve the participation of the charge transfer excited state species **63a** (Figure 3.01), which could capture dissolved oxygen at positions C(4a) or C(9a). The reaction pathway would then progress by a mechanism similar to that described above and be completed by an electron return step to the benzene ring. However, the proposed mechanism described in Figure 3.09 appears to be more promising, as it involves the already established biradical **63e**.

The possibility of the reaction proceeding through a carbene mechanism was also considered as shown in Figure 3.10.

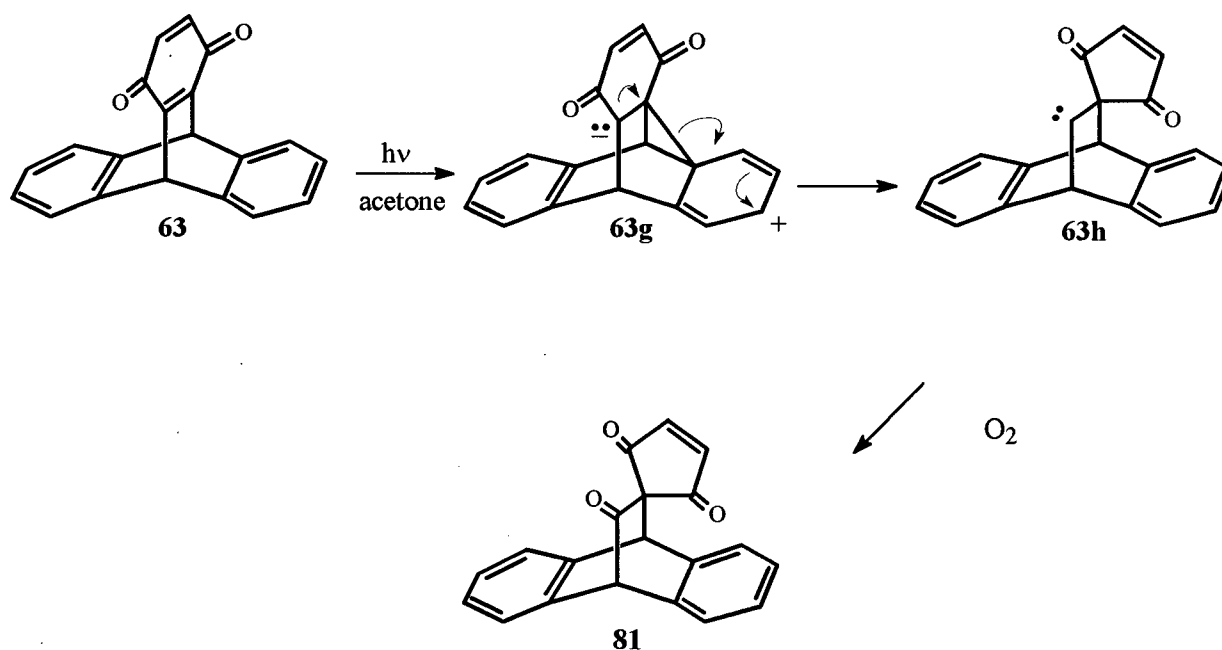


Figure 3.10. Carbene Mechanism for Formation of Triketone **81**.

Although not completely ruled out, the carbene mechanism (Figure 3.10) for the formation of triketone **81** is less likely, as a carbene trapping experiment failed to produce positive results. This was conducted by irradiating triptycene **63** in methanol. The resulting photoproduct was determined to be dibenzosemibullvalene **80** as mentioned in Section 3.1, after isolation by chromatography. Trapping experiments are often performed in order to determine the presence of a carbene. The mechanism, involving the insertion of methanol into the arylcarbene **92**, generated by the photolysis of diazo compound **91** is illustrated in Figure 3.12. This experiment provided evidence for the involvement of the carbene **92** in the product formation step.⁹⁴

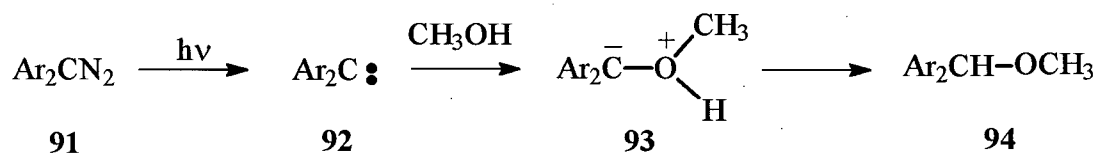


Figure 3.12. Carbene Trapping Mechanism.

3.3.1. Structural Assignment

The mass spectra of compounds **75** and **74** clearly indicate that one hydrogen atom has been substituted by a chlorine atom, resulting in the characteristic isotopic pattern for chlorine. The relative abundance of the peaks occurs in a 3 : 1 ratio corresponding to the molecular ion peak at m/e 318 and the M+2 peak at m/e 320. Compound **76** shows a molecular ion peak at m/e 352, an M+2 peak at m/e 354 and an M+4 peak at m/e 356 in the ratio of 9 : 6 : 1, a characteristic pattern for a compound containing two chlorine atoms. The structure of the benzoquinone ring was not altered, since the carbonyl absorption bands remained in the typical range of 1675-1655 cm^{-1} , established by the IR spectra. In order to determine at what position the addition of the chlorine atoms occurred, the ^1H NMR spectra of the chlorinated products were compared to the spectrum of the starting material triptycene-1,4-quinone (**63**). The ^1H NMR spectrum of **75** clearly shows the loss of one of the vinyl hydrogens. The ^1H NMR spectrum of **74**, however, indicates the loss of one hydrogen at an aromatic position. In order to determine the assignments of the aromatic hydrogens, an NOE NMR experiment was performed with triptycene-1,4-quinone (**63**) (Figure 3.15). On the one hand, irradiation of the bridgehead hydrogens H-9 and H-10 at δ 5.79 ppm led to the disappearance of the multiplet at δ 7.10-6.95 ppm. On the other hand, irradiation at δ 7.01 ppm resulted in the disappearance of the peak at δ 5.79 ppm. Irradiation at δ 7.4 ppm had no effect on the multiplet at δ 7.01 ppm and singlet at δ 5.79 ppm. Hence, the multiplet at δ 7.50-7.35 ppm can be assigned to the hydrogen atoms at the α -position of the aromatic rings, whereas the multiplet at δ 7.10-6.95 ppm corresponds to hydrogen atoms β on the aromatic rings.

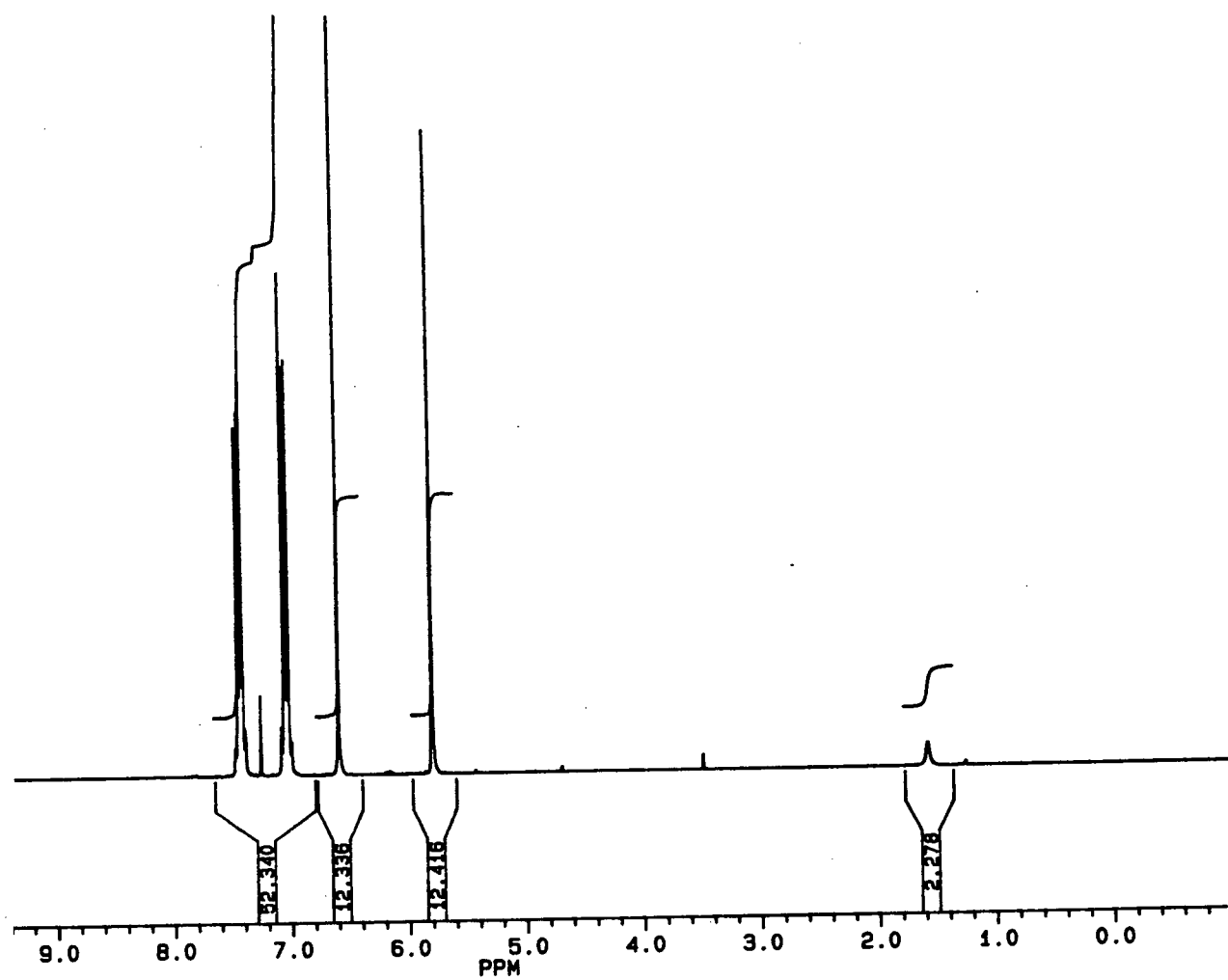


Figure 3.14. ^1H NMR Spectrum of Triptycene-1,4-quinone (63).

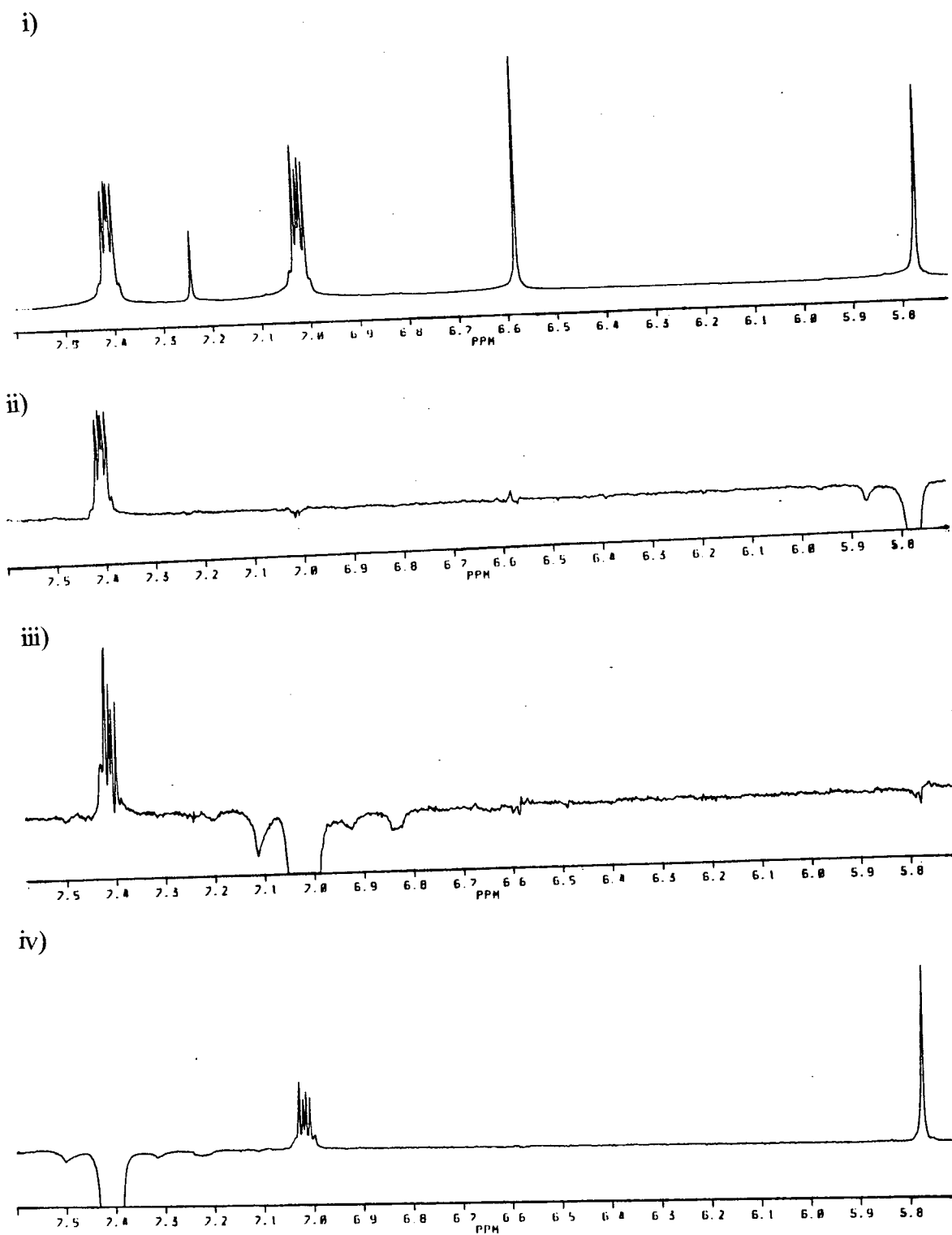


Figure 3.15. ¹H NMR NOE Experiment for Triptycene-1,4-quinone (63), (i) No Irradiation, (ii) Irradiation at δ 5.79 ppm, (iii) Irradiation at δ 7.01 ppm, (iv) Irradiation at δ 7.4 ppm.

The ^1H NMR spectrum of the chlorinated product **74** lacks one hydrogen in the upfield aromatic region, positioning the chlorine atom beta (β) on the aromatic ring. In order to establish the structure further, two triptycene-1,4-quinone adducts were synthesized with chlorine atoms at either the α or β positions on one of the benzene rings (see Chapter 2, Figure 2.05, p 45). Comparing the spectral data of the authentic samples to the spectral data of photoproduct **74** confirmed the assignment.

3.3.2. Mechanism of Formation of Chlorinated Product **75**

The photoreaction of **63** in chloroform was monitored by gas chromatography, which showed that the dichlorinated species **76** only formed after the appearance of monochlorinated products **75** and **74** in solution. Furthermore, upon irradiation in either chloroform or carbon tetrachloride, the solution tested positive for the presence of hydrogen chloride. A control experiment was conducted by stirring triptycene-1,4-quinone (**63**) dissolved in acetone in a 15% aqueous hydrogen chloride solution and monitoring the reaction by GC. After one hour product **75** could be detected and hence the possibility that **75** or **76** could be true photoproducts was ruled out.

Based on the assumption that hydrogen chloride is formed during the photolysis, the formation of **75** can be explained in terms of the analogous reaction between 1,4-benzoquinone (**60**) and hydrogen chloride which dates back to the 19th century.⁹⁵ Detailed mechanistic studies on the hydrogen chloride reaction with quinonoid systems were later pursued by Adams.⁹⁶ As seen from Figure 3.16 (a), the electrophilic part of hydrogen chloride was proposed to bind to the carbonyl group and the nucleophilic part attaches to the β -carbon. This results in the hydroxydienone **60a** which enolizes to the phenol **60b**. Upon oxidation by an unreacted quinone molecule in the reaction mixture, as described by Cason *et al.*,⁹⁷ quinone **60c** will be obtained (Figure 3.16 (b)).

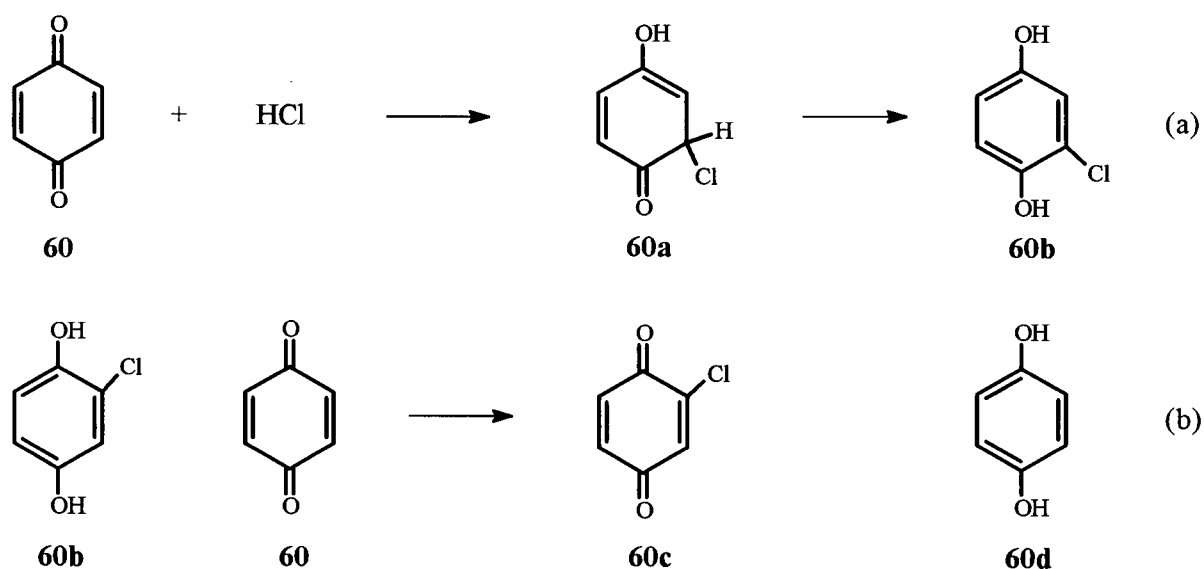


Figure 3.16. Addition of Hydrogen Chloride to 1,4-Benzoquinone (**60**), Followed by Oxidation.

The above reaction pathways may be applied to triptycene-1,4-quinone (**63**), which possesses the quinone moiety. During the photolysis hydroquinone **95a** is believed to be oxidized by an unreacted quinone **63** molecule to give product **75**.

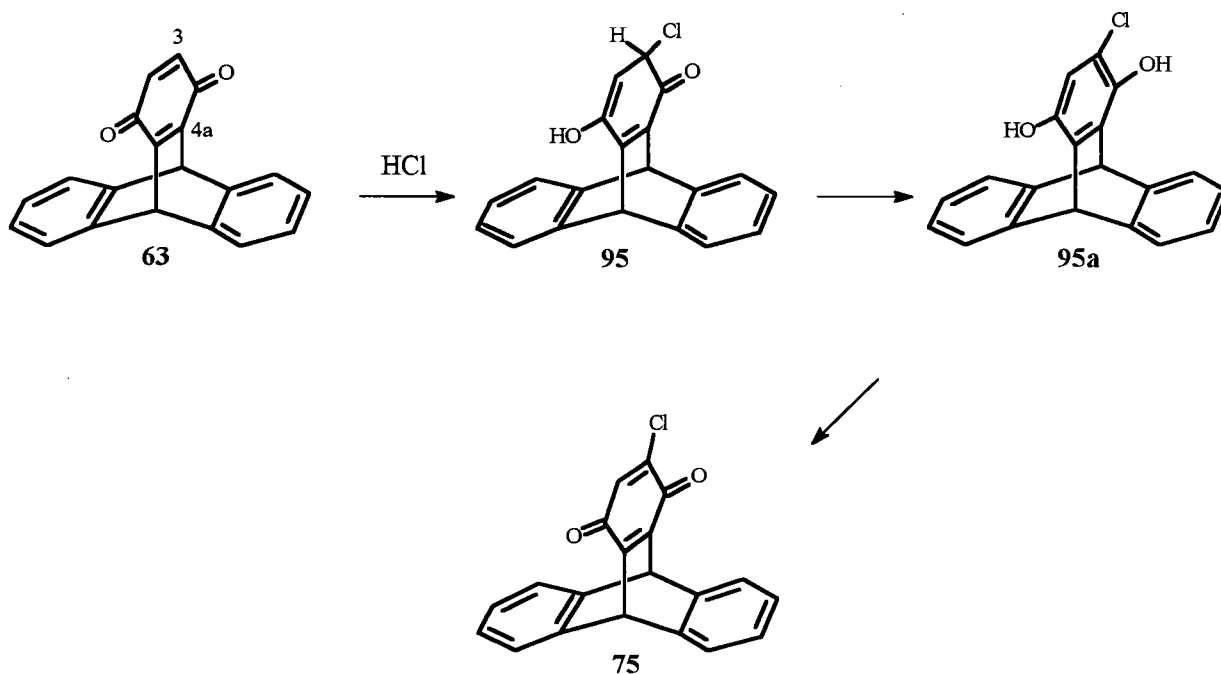


Figure 3.17. Proposed Mechanism for Formation of Chlorinated Product **75**.

As illustrated by Figure 3.17, the chlorine addition is only observed at position C3. This may be explained by the lack of a hydrogen atom at position C4a, which is required for the enolization step to form the corresponding hydroquinone. If the addition did occur, elimination of the chlorine atom would likely result, driven by the ketonization step (Figure 3.18).

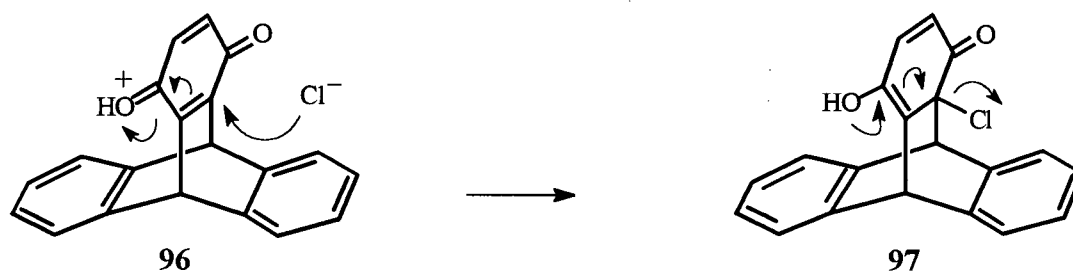


Figure 3.18. Addition of Chlorine Atom at Carbon 4a of Intermediate 96.

3.3.3. Mechanism of Formation of Chlorinated Photoproduct 74

The unusual chlorination of the aromatic ring of triptycene-1,4-quinone (63) was quite puzzling and a control experiment was conducted showing that benzene could not be chlorinated under the same irradiation conditions. The chlorinated photoproduct 74 may originate from the cyclopropyldicarbonyl biradical 63e (Figure 3.19) which was proposed earlier in this thesis as a common intermediate for semibullvalene 80 and triketone 81. A chlorine atom from the solvent could be abstracted by intermediate 63e resulting in radical 99. In chloroform, the hydrogen could then be abstracted by the solvent radical giving dichloromethane and photoproduct 74. A gas chromatographic analysis of the volatile reaction product, dichloromethane, was not performed as it would have been very difficult to trace such minute quantities in the chloroform reaction mixture. In the case of carbon tetrachloride, the abstraction of a chlorine radical would result in a $\cdot\text{CCl}_3$ radical. Upon the abstraction of a hydrogen atom from intermediate 99, chloroform would be the obtained byproduct. The lack of substitution at position C(5) of the benzene ring may be explained by sterically hindering interactions between the incoming chlorine atom and the bridgehead hydrogen at the position C(10) of 63.

As previously noted, the participation of a charge-transfer excited state is not required for the reaction to proceed, but can not be excluded at this point.

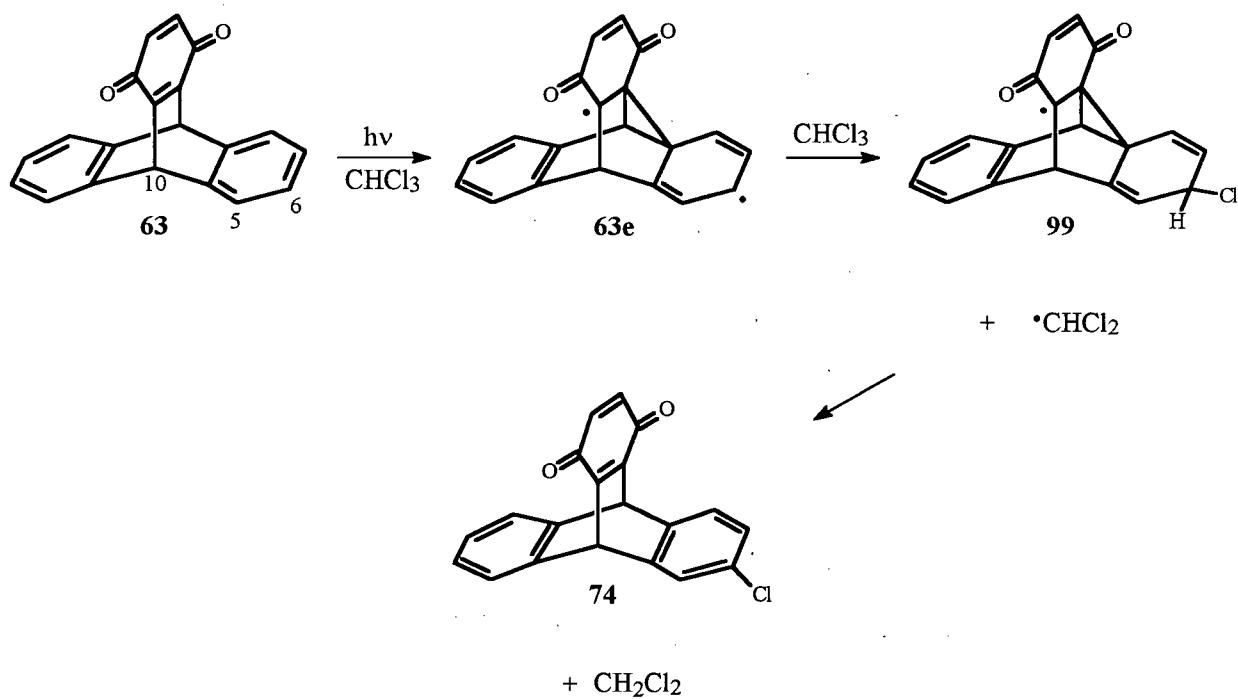


Figure 3.19. Proposed Mechanism for Formation of Chlorinated Photoproduct 74.

The above reaction pathway leading to photoproduct **74** may also give an insight into the presence of hydrogen chloride in the reaction mixture. As illustrated by Figure 3.20, the chlorinated intermediate **99** is proposed to undergo a reversible loss of the chlorine atom forming quinone **63**. If this is the case, the resulting chlorine atom may abstract a hydrogen from chloroform yielding hydrogen chloride.⁹⁸ The presence of hydrogen chloride in the carbon tetrachloride reaction mixture may result from the small quantities of chloroform being formed during the photolysis reaction.

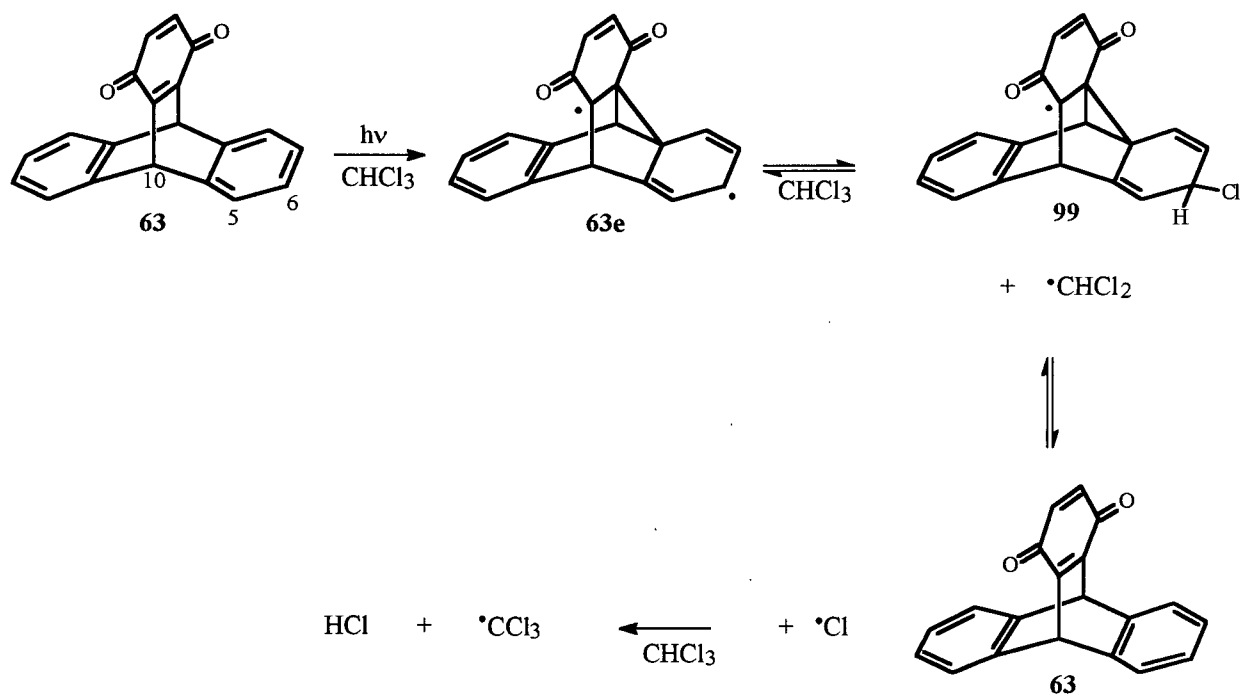


Figure 3.20. Proposed Mechanism for Hydrogen Chloride Formation.

3.4. Solid State Reactivity of Triptycene-1,4-quinone (63)

The photochemistry of 9,10-ethenoanthracene derivatives in the solid state has been well documented by Scheffer *et al.*⁹⁹ as these molecules possess interesting photochemical reactivity. In view of further exploring these systems, the solid state reactivity of triptycene-1,4-quinone (63) was investigated.

Unexpectedly, however, irradiation of triptycene-1,4-quinone in the solid state through Pyrex ($\lambda \geq 290\text{nm}$) for 8 h led to no reaction. In order to provide insight into this lack of reactivity in the solid state, the X-ray crystal and molecular structure was determined and analyzed. As seen from the packing diagram in Figure 3.21, the bridgehead carbons (C9 and C10) of the individual molecules are tetrahedral (109.5°). These angles, between each V-shaped cleft, are slightly deviated (4°) due to strain (Table I). Cyclopropyldicarbonyl biradical 63e formation would require that one of the aromatic rings and the quinone ring would move together to approximately 60° .

Table I Angles Between the Quinone and Benzene Moieties (see Figure 3.23)

Atoms	Angles ($^\circ$)
C8a, C9, C12	106.2
C9a, C9, C8a	105.5
C9a, C9, C12	105.4

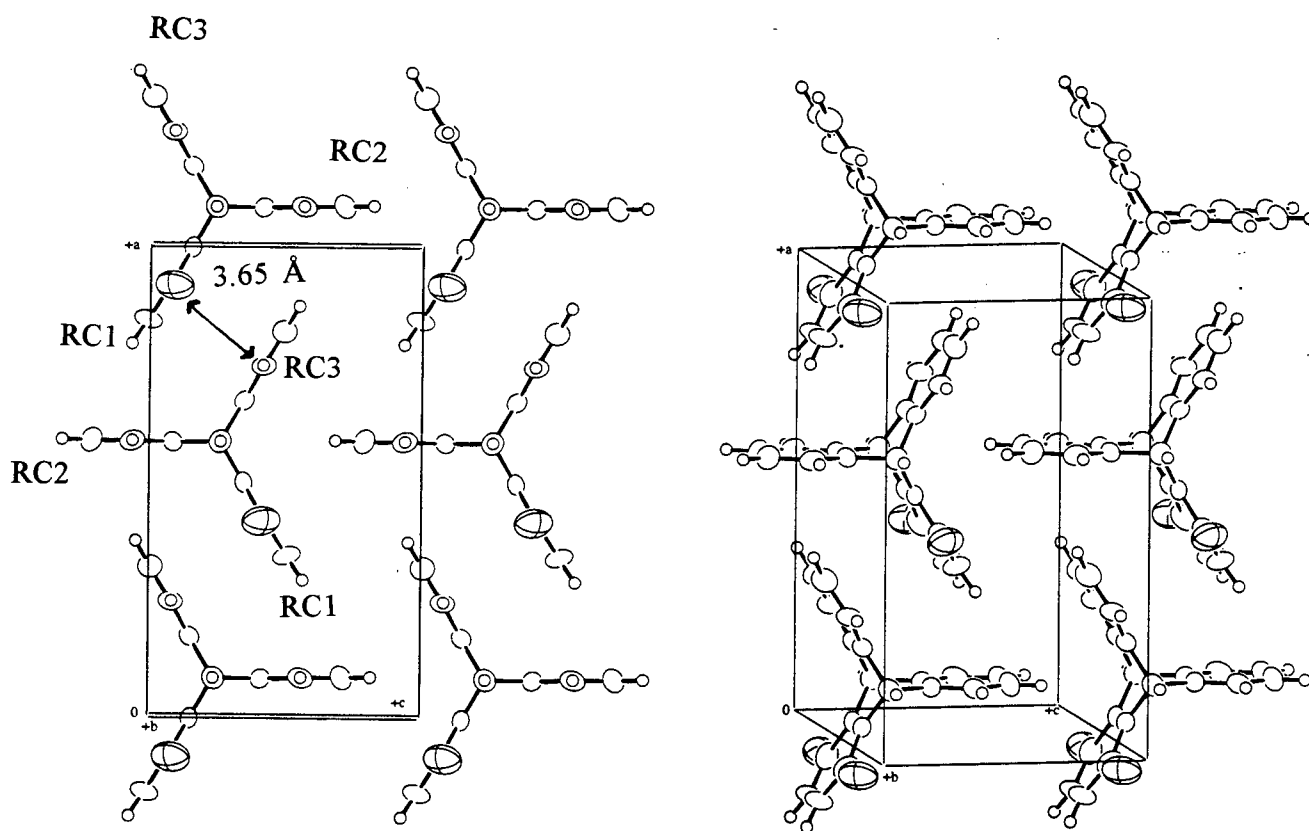


Figure 3.21. Packing Diagram for Triptycene-1,4-Quinone (63).

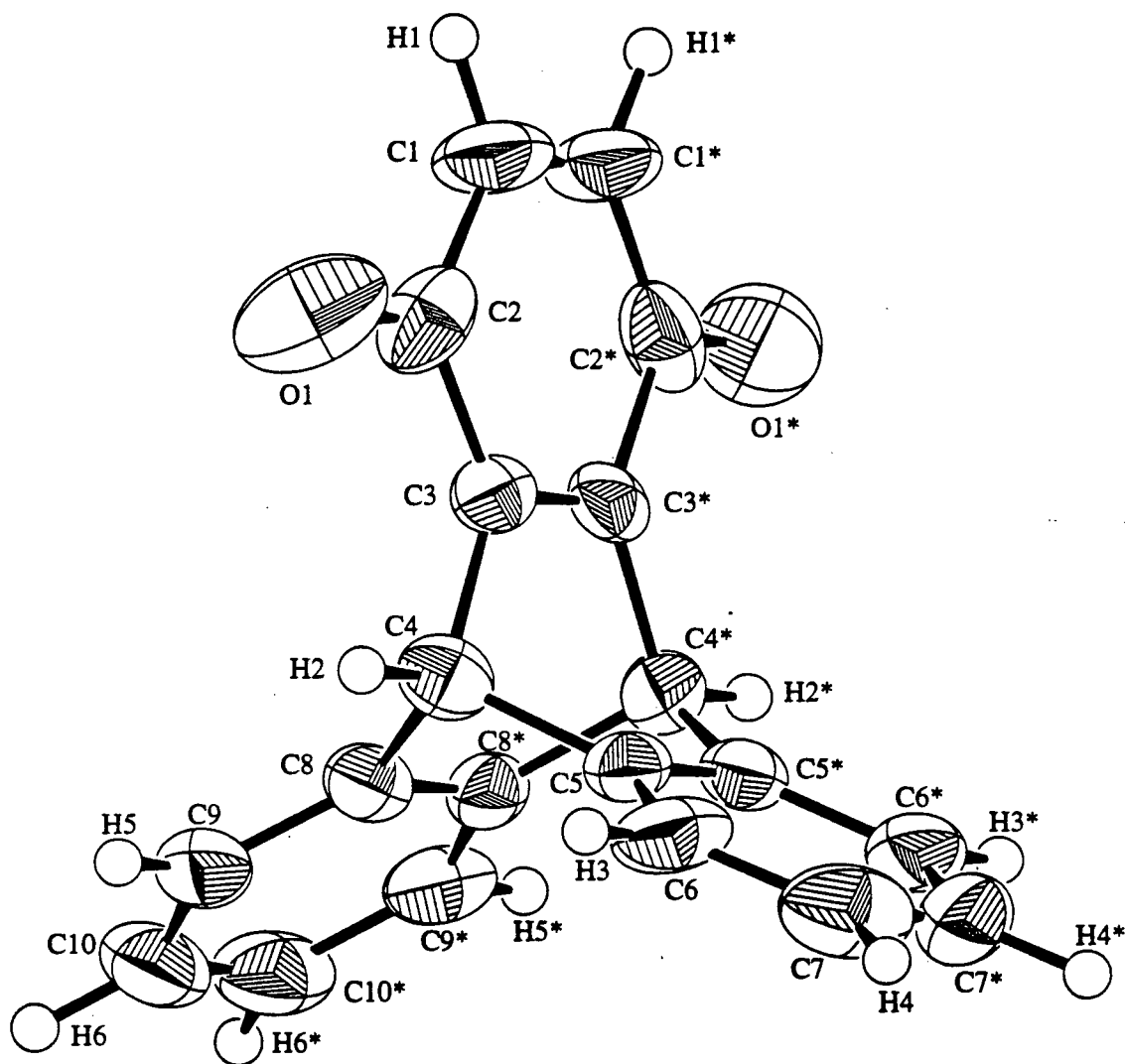


Figure 3.22. X-ray Crystallographic Structure of Triptycene-1,4-quinone (63). Space Group *Pnma* (#62), $a = 13.979(2)\text{\AA}$, $b = 12.608(7)\text{\AA}$, $c = 8.024(2)\text{\AA}$, $Z = 4$, $R = 5.9\%$. The structure is represented, showing its crystallographic numbering system, which takes the symmetry of the molecule into account. This numbering system differs from the up-to-now applied IUPAC system.

As shown by Figure 3.23 and Table II, the center-to-center (represented as RC) intramolecular distances between the separate rings range between 4.45 and 4.58 Å, permitting initial di- π -methane bridging. However, the illustration of the molecular stacking of 63 (Figure 3.21), indicates that each molecule is very close to its neighbors with distances ranging between 3.65 to 4.80 Å (Table II). The quinone and aromatic rings of adjacent molecules in the crystal appear to be almost interlocked, which may explain the possible hindrance of the benzo-quinone bridging step. Figure 3.23 depicts the two possibilities for the initial bonding process: (i) bonding between the quinone ring RC1 and benzene ring RC2 and (ii) bonding between the quinone ring RC1 and the benzene ring RC3. The packing diagram of quinone 63 (Figure 3.21) reveals that pathway (i) may be sterically impeded by the short distance between benzene ring RC3 and benzene ring RC2 of adjacent molecules (4.74 Å) and the even smaller intermolecular distance between benzene ring RC3 and quinone ring RC1 (3.65 Å). Additionally, process (ii) may be hindered by the vicinity of the intruding hydrogens of the aromatic ring RC2 to quinone ring RC1 and benzene ring RC3 of the neighboring molecule, given by the distances 3.37 Å and 3.28 Å, respectively (Figure 3.21).

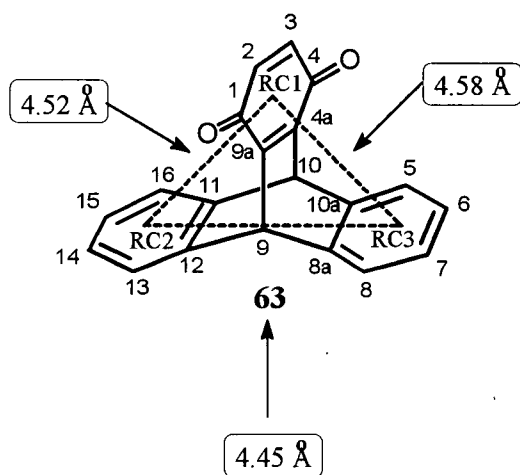


Figure 3.23. Intramolecular Distances between Ring Centers 1, 2 and 3.

Table II Intermolecular and Intramolecular Distances Between Ring Centers

Ring Centers	Intermolecular Distances (Å)		Ring Centers	Intramolecular Distances (Å)
RC1-RC2	4.80		RC1-RC2	4.52
RC1-RC3	3.65		RC1-RC3	4.58
RC2-RC3	4.74		RC2-RC3	4.45

Previous research by Scheffer *et al.*¹⁰⁰ has demonstrated that bridging motions in the solid state may be hindered by the presence of aromatic rings from adjacent molecules in the clefts.

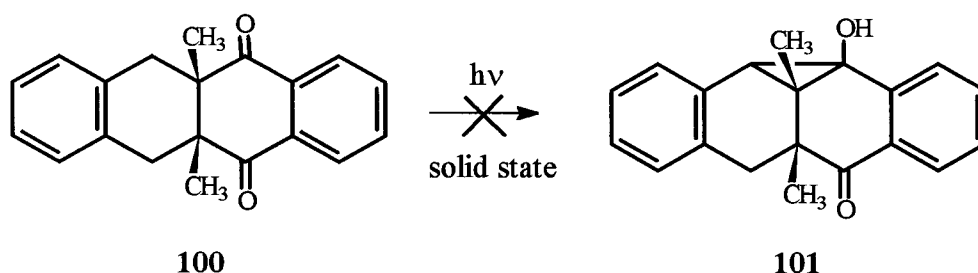


Figure 3.24. Example of an Unreactive Photoreaction in the Solid State.

The initial reaction step in compound 100 was believed to be hindered by the presence of a methyl group from an adjacent molecule, which was at a distance of 4.12 Å and 4.75 Å from the center of either aromatic ring. The center-to-center distances between the two aromatic rings was shown to be 6.48 Å (Figure 3.25). After the reaction, the aromatic center-to-center distance was estimated from Dreiding models to have decreased to 4.1 Å, reducing the distances between the methyl carbon and the aromatic rings to 2.6 and 3.0 Å respectively. Adding the van der Waals radii of the methyl group (2.0 Å)¹⁰¹ and the van der Waals half "thickness" of an aromatic ring

(1.7 Å) together resulted in a sum (3.7 Å) greater than the distances between the methyl group and the rings, prohibiting the photoreaction in the solid state.

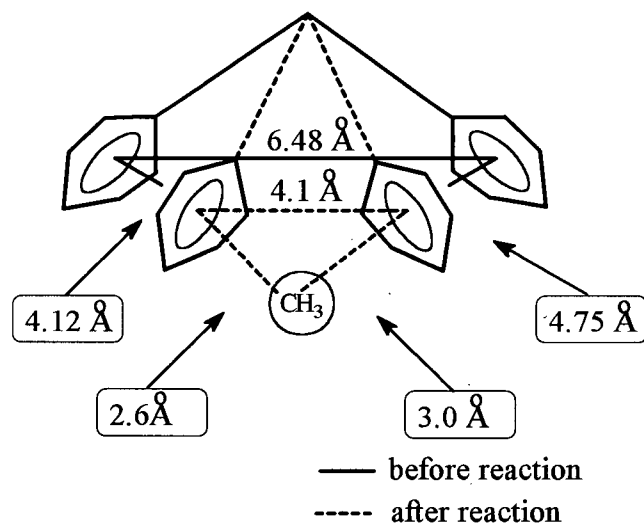


Figure 3.25. Crystal Lattice Steric Effects in Compound 100.

Applying this hypothesis to triptycene-1,4-quinone (**63**) may explain the lack of reactivity. The already relatively short distances between the hydrogen attached to carbon 14 at RC2 with respect to RC1 and RC3 are believed to decrease considerably upon the bridging process, making it difficult to accommodate the aromatic ring RC2, resulting in the photostability of **63**.

CHAPTER 4 PHOTOCHEMICAL STUDIES OF

9,10-DIHYDRO-9,10-DIMETHYL-9,10[1',2']BENZENOANTHRACENE-1,4-DIONE (69)

4.1. Photochemical Results Upon Direct Irradiation

Irradiation at $\lambda \geq 300$ nm of 9,10-dimethyltritycene-1,4-quinone (69) in deoxygenated acetonitrile resulted in a purple solution (4.5 h). Two photoproducts were isolated, the di- π -methane photoproduct 102 (yellow needles, 28%) and the norcaradiene photoproduct 103 (blue black prisms, 23%).

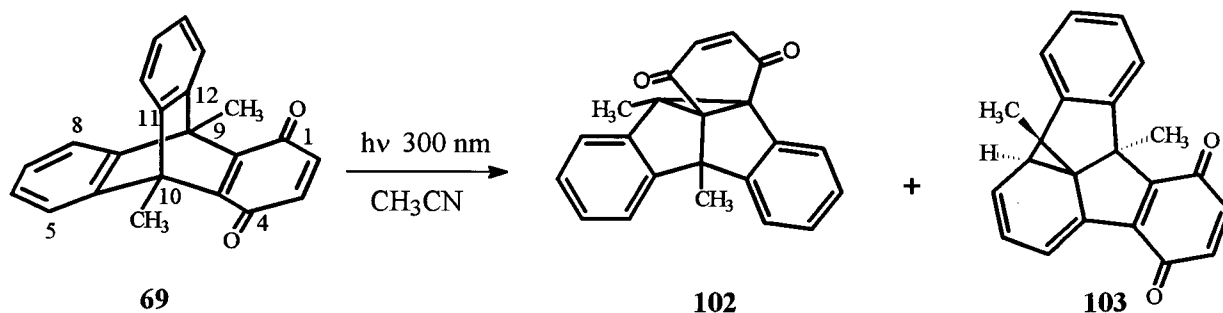


Figure 4.01. Photolysis of 69 in Acetonitrile.

4.1.1. Photoproduct Structure Elucidation

The elucidation of the structure of photoproduct 102 was facilitated by its similarity to the di- π -methane photoproduct analogue 80 (Figure 3.02). The ^1H NMR spectrum shows the presence of one aromatic hydrogen as a doublet at δ 7.80 ppm ($J = 7$ Hz), and a multiplet at δ

7.20-7.02 ppm, corresponding to the remaining seven hydrogens. The vinyl hydrogens of the quinone ring can be assigned to the AB system at δ 6.74 ppm ($J = 10\text{Hz}$). The remaining two singlets at δ 2.13 and 1.98 ppm represent the methyl substituents. The IR spectrum displaying the carbonyl band at 1668 cm^{-1} and the mass spectrum with a parent mass of m/e 312 are also consistent with the assignment of the proposed photoproduct 102.

The structure of norcaradiene 103 was elucidated on the basis of the spectral data collected. The IR spectrum shows the presence of two carbonyl bands (1664 cm^{-1} and 1645 cm^{-1}), with the latter being shifted to lower frequencies due to extended conjugation with the diene ring. The mass spectrum of compound 103 has a base peak at m/e 297, which results from the loss of one methyl group from the molecular ion peak at m/e 312. The ^1H NMR spectrum of norcaradiene 103 (Figure 4.02) reveals the presence of one aromatic ring. The quinone vinyl hydrogens H-3 and H-4 are represented by an AB system at δ 6.65 ppm ($J = 10\text{ Hz}$). The former second aromatic ring, however, is replaced by a diene system. The assignments of the hydrogens of the diene ring are based on the coupling constants (J), corresponding to the doublet at δ 6.98 ppm (H-17, $J = 6\text{ Hz}$), the doublet of doublets at δ 6.31 ppm (H-18, $J = 9\text{ Hz}$ and $J = 6\text{ Hz}$) and the doublet of doublets at δ 6.03 ppm (H-19, $J = 9\text{ Hz}$ and $J = 5\text{ Hz}$). The doublet at δ 2.55 ppm represents the cyclopropyl hydrogen (H-20, $J = 5\text{ Hz}$). Due to the lack of symmetry of the molecule a single peak is observed for each methyl group (Me-21 at δ 1.50 ppm and Me-22 at δ 1.06 ppm). To further verify the structure, an HMQC NMR experiment (Heteronuclear Multi-Quantum Correlation) as well as an HMBC NMR experiment (Heteronuclear Multi-Bond Correlation) were conducted. The assignments are given in Table III.

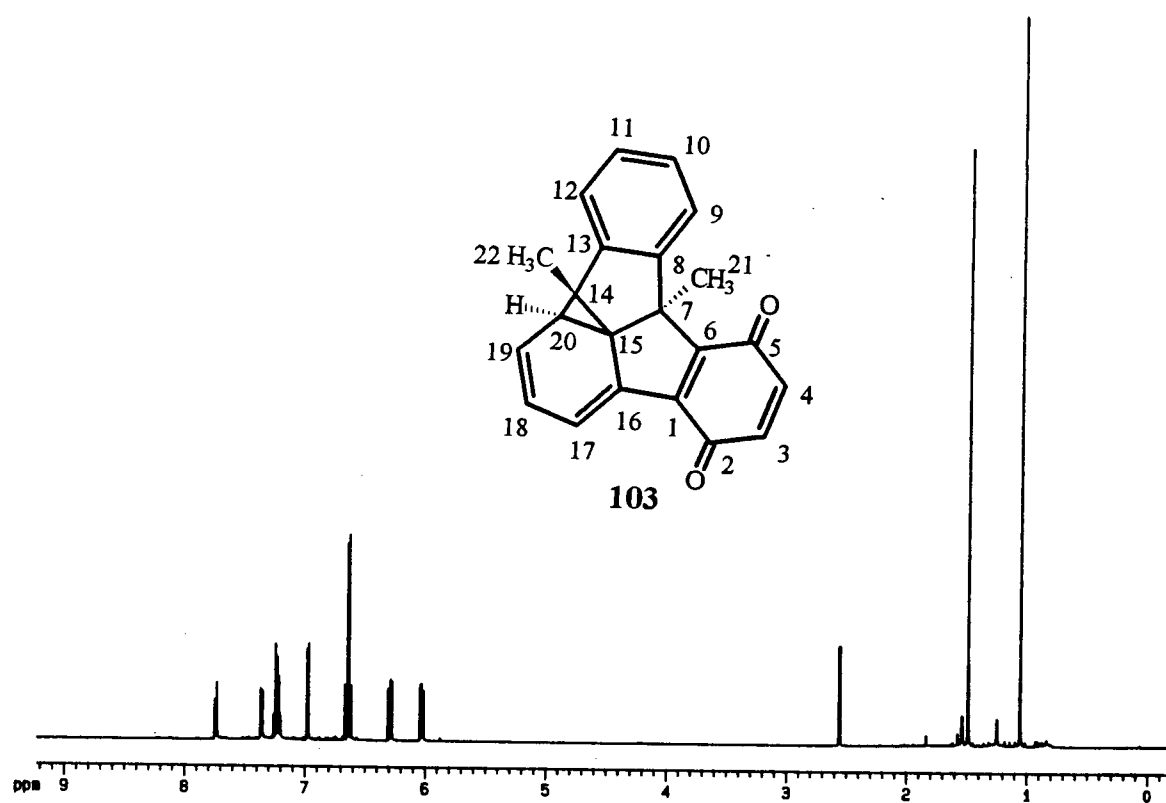
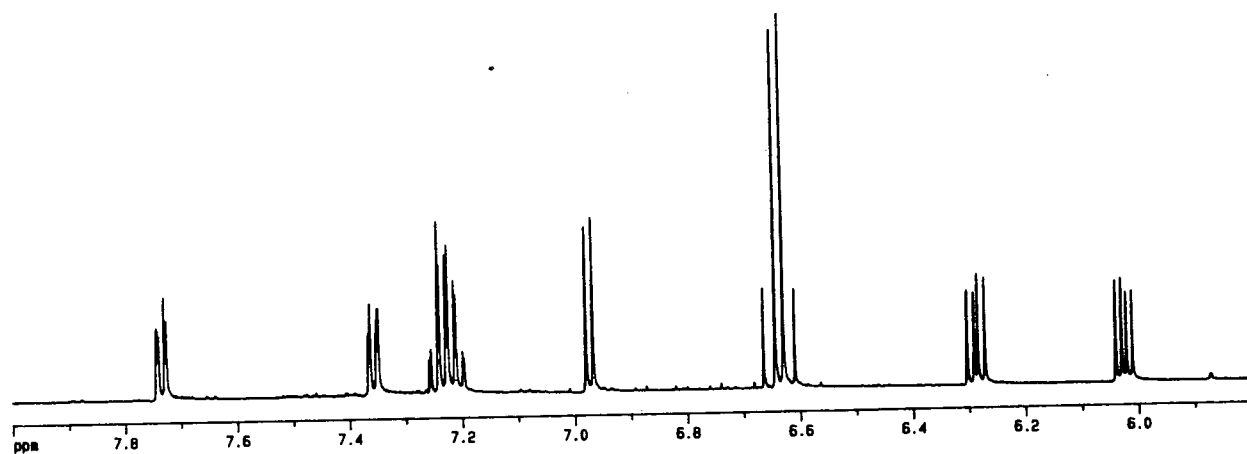
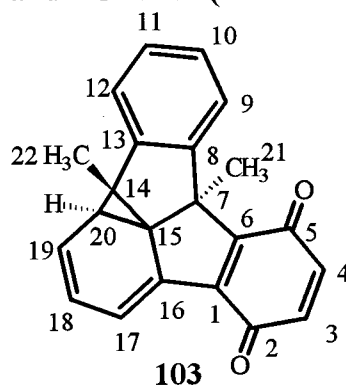


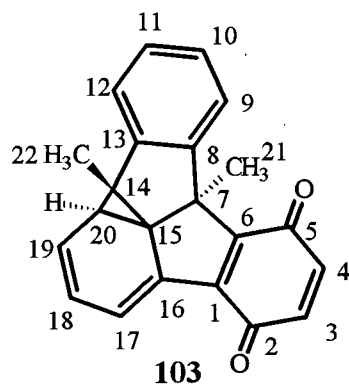
Figure 4.02. ¹H NMR Spectrum of Norcaradiene 103.

Table III ^1H NMR (500 MHz) and ^{13}C NMR (125 MHz) Data for Norcaradiene 103^a

E N T R Y	Carbon Assign- ment	^{13}C NMR Spectrum (125 MHz) δ ppm, APT ^b	HMQC ^1H NMR Correlations (500 MHz) δ ppm (Assignment)	^1H - ^{13}C HMBC Long-range Correlations
a	1	141.89		H-3 & 4, H-17
b	2 & 5	186.11, 185.87		H-3 & 4
c	3 & 4	137.87(-ve), 136.19(-ve)	6.03 & 6.31 (H-3 & 4)	
d	6	149.51		H-3 & 4, Me-21
e	7	61.01		H-19, Me-21
f	8	146.45		H-9, H-10 & 11, Me-21
g	9 & 12	124.97(-ve), 126.74(-ve)	7.78-7.69 & 7.40- 7.30 (H-9 & 12)	H-10, H-11
h	10 & 11	127.14(-ve), 128.01(-ve)	7.28-7.19 (H-10 & 11)	H-9, H-12
i	13	148.17		H-10 & 11, H-12, H-20, Me-22
j	14	21.99		Me-22
k	15	56.88		H-19, H-20, Me-21, Me-22
l	16	134.89		H-18
m	17	121.84(-ve)	6.98 (H-17)	H-18
n	18	126.32(-ve)	6.31 (H-18)	H-17, H-20
o	19	126.65(-ve)	6.02 (H-19)	H-17, H-20
p	20	37.82(-ve)	2.55 (H-20)	H-19
q	21	23.88(-ve)	1.50 (Me-21)	
r	22	10.77(-ve)	1.06 (Me-22)	H-20

a -The assignments and chemical shifts of the ^{13}C NMR spectrum are listed in columns II and III, respectively. Column IV shows the ^1H NMR signal(s) which correlate(s) with the carbon of columns II and III, as obtained from the HMQC experiment (1 bond correlation). The last column lists the hydrogen(s) which correlate(s) with the ^{13}C NMR signal of column II and III as obtained from the HMBC experiments (2 and 3 bonds correlation(s)).

b - The results of the APT experiments are given in parentheses (-ve for CH and CH_3 carbon signals).

Table IV ^1H NMR Data (500 MHz) for Norcaradiene 103

Entry	Hydrogen Assignment	^1H -NMR (500 MHz) δ ppm (mult., J (Hz))	COSY Correlations
a	H-3 & 4	6.65 (AB system, $J = 10$)	
b	H-9 & 12	7.78-7.69 (m), 7.40-7.30 (m)	H-10 & 11
c	H-10 & 11	7.28-7.19 (m)	H-9 & 12
d	H-17	6.98 (d, $J = 6$)	H-18
e	H-18	6.31 (dd, $J = 6$ & 9)	H-17, H-19
f	H-19	6.03 (dd, $J = 9$ & 5)	H-18, H-20
g	H-20	2.55 (d, $J = 5$)	H-19
h	Me-21	1.50 (s)	
i	Me-22	1.06 (s)	

The proposed structure of norcaradiene 103 was later confirmed by X-ray crystal analysis. The X-ray structure shown in Figure 4.03 demonstrates that the methyl groups C21 and C22 are *anti* to each other, and the methyl group C21, which is closer to the quinone ring, is *syn* to the cyclopropyl hydrogen H10.

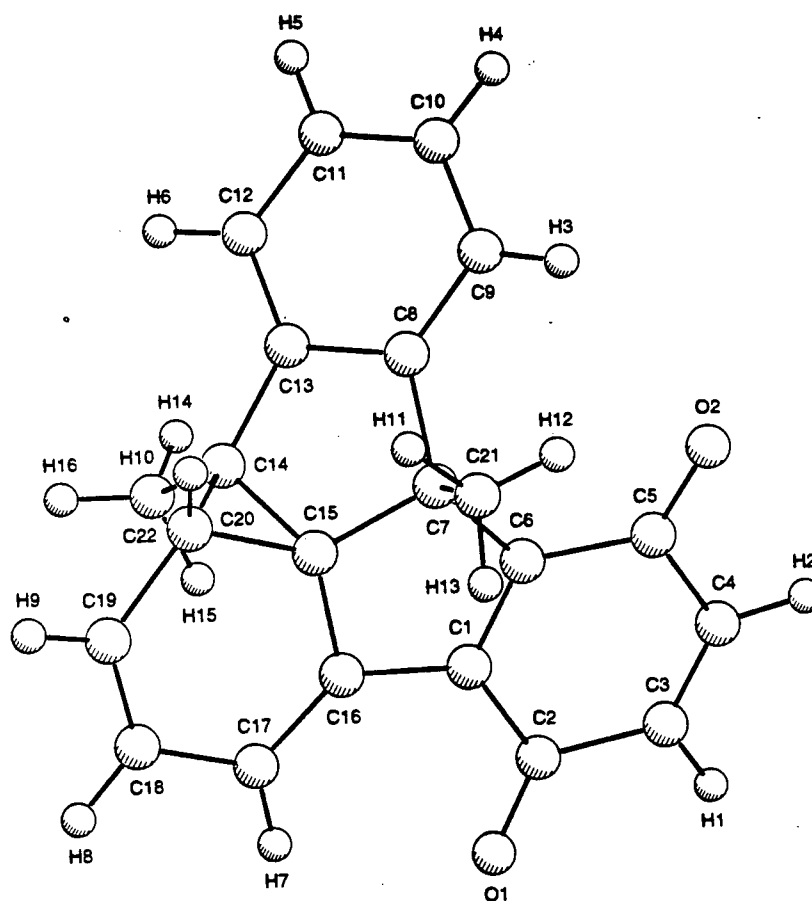


Figure 4.03. X-ray Crystallographic Structure of Norcaradiene 103. Space Group $P2_1/n$ (#14),

$a = 8.114(3) \text{ \AA}$, $b = 11.966(3) \text{ \AA}$, $c = 16.694(3) \text{ \AA}$, $\beta = 95.53(2)^\circ$, $Z = 4$, $R = 3.7\%$.

4.1.2. Mechanism of Formation of Semibullvalene 102 and Norcaradiene Derivative 103

Photoproduct 102 is analogous to the previously discussed photoproduct 80, which resulted from the di- π -methane rearrangement of triptycene-1,4-quinone (63). As shown by Scheffer and co-workers,¹⁰² 9,10-bridgehead substitution can have a profound effect on the photochemistry of 9,10-ethenoanthracene derivatives. This is also the case for the irradiation of quinone 69. The formation of photoproduct 103 can be related to the work of Walsh¹⁰³ and Turro *et al.*,¹⁰⁴ who in 1969 studied the photochemical behavior of triptycene (104) and isolated a similar norcaradiene derivative (106) upon irradiation in solution. These results contrasted former photochemical results with barrelene and its benzo derivatives, which were found to rearrange to semibullvalene and cyclooctatetraene derivatives upon irradiation, as discussed in the Introduction.

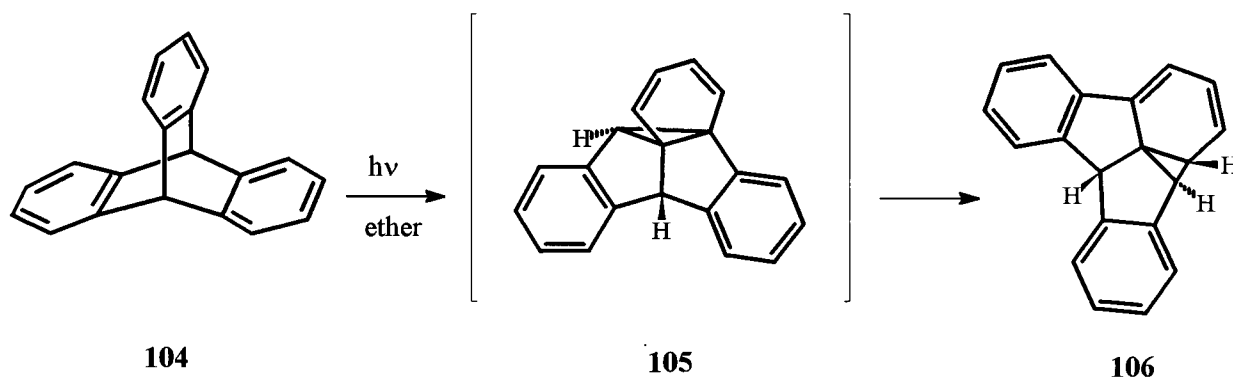


Figure 4.04. Photolysis of Triptycene 104.

Initially, Turro¹⁰⁴ proposed that photoproduct 106 was formed by a 1,5-sigmatropic rearrangement of semibullvalene 105, which was not isolated by him or Walsh. Iwamura and co-

workers^{105, 106} later proposed that this reaction proceeds through a carbene mechanism. This hypothesis was supported by trapping of the carbene intermediate **104a** with methanol, leading to the isolation of compound **107**. Additionally, molecular models were used to demonstrate the favorable position of the divalent carbon atom with respect to the aromatic carbons of the fluorene ring **104a**.

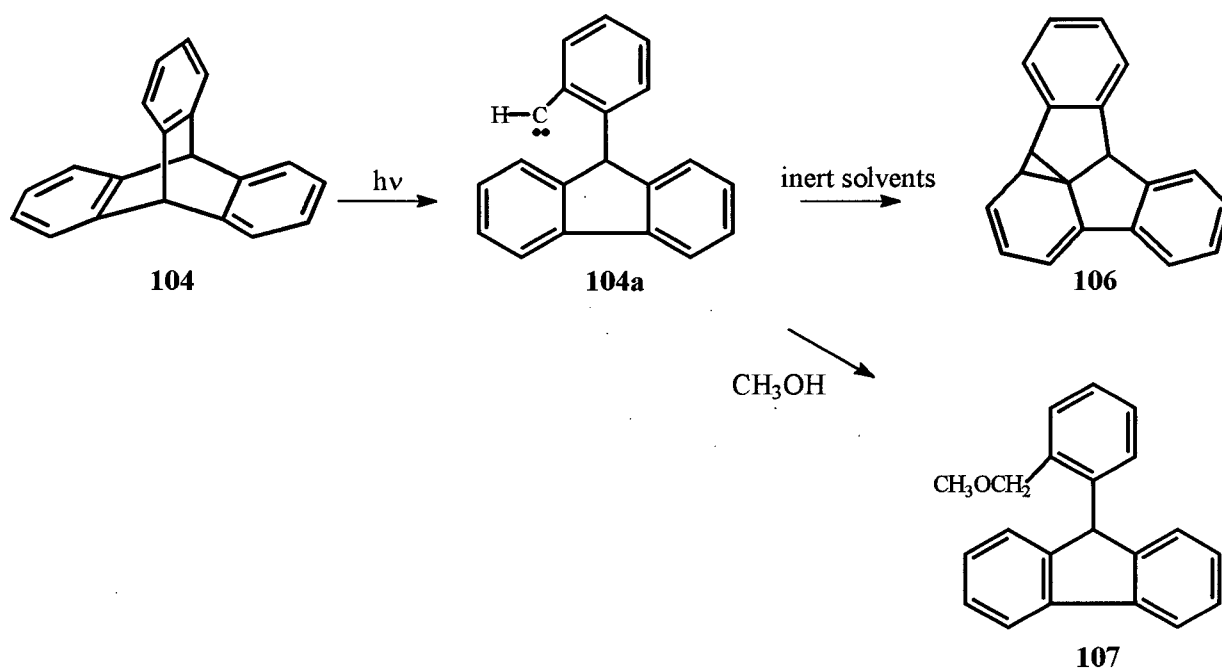


Figure 4.05. Trapping of Carbene **104a**.

The formation of norcaradiene **103** can be rationalized by applying Iwamura's mechanism to quinone **69** (Figure 4.06).

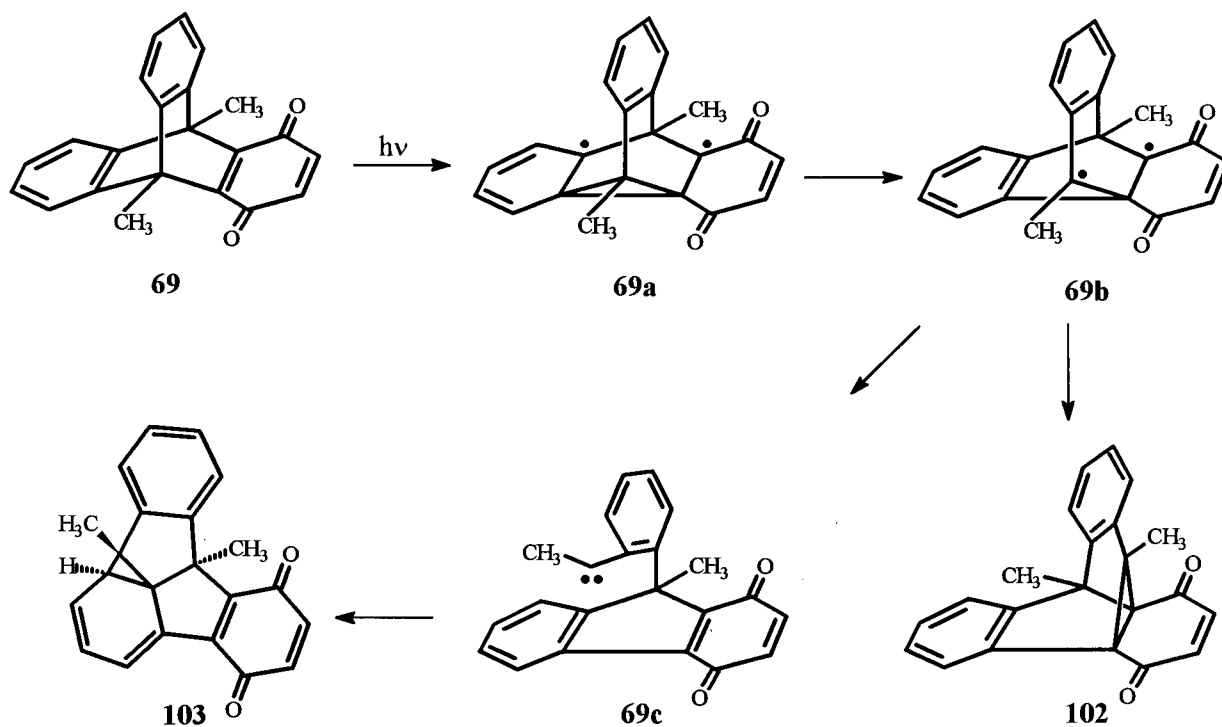


Figure 4.06. Proposed Mechanism for Formation of Photoproducts **102** and **103**.

The suggested reaction pathway involves an initial di- π -methane rearrangement giving the well established 1,3-biradical **69b** of the Zimmerman mechanism, which may either ring-close to semibullvalene **102**, or rearrange to the carbene intermediate **69c**. The carbenic center may then add internally to the aromatic ring resulting in norcaradiene **103**. This mechanism may also provide an explanation for the lack of norcaradiene formation for the previously discussed unsubstituted triptycene-1,4-quinone (**63**). In the case of quinone **69**, the methyl substituent is believed to stabilize the carbenic center of intermediate **69c**, thereby facilitating its formation from

biradical **69b**. Also, the ring closure of biradical **69b** to semibullvalene **102** could be sterically hindered by the same methyl group.

A second possible mechanism could involve carbene **69c** as the common intermediate for formation of semibullvalene **102** and norcaradiene **103**. Trapping experiments were conducted showing that upon irradiation of quinone **69** in methanol, the yield of photoproduct **103** decreased significantly (4%), whereas an increase in the amount of di- π -methane product **102** was observed (40%). The reduced formation of norcaradiene derivative **103** leads to the tentative conclusion that successful trapping of intermediate **69c** occurred, and that semibullvalene **102** was less likely to result from intermediate **69c**. Control experiments were also conducted in order to rule out the possibility of interconversion between **102** and **103** under the photolysis conditions.

4.1.3. The Midnight-Blue Color of Norcaradiene **103**

Although **69** is more commonly referred to as a triptycene-1,4-quinone derivative, it can be viewed as a 9,10-ethenoanthracene derivative. Classified as such, it is believed to be the first example to form a photostable norcaradiene product upon photolysis. All previous examples of this reaction have been produced by triptycene derivatives.¹⁰⁷ One of the unusual observations of this reaction is that norcaradiene **103** is midnight-blue in color, whereas the previously analyzed norcaradiene analogues from the triptycene reaction were reported as being yellow. The blue color results from a very broad absorption band, centered around 570 nm, as indicated by the

UV/VIS absorption spectrum (Figure 4.10). This can be explained by a charge-transfer interaction between the norcaradiene and quinone chromophores. This interaction often occurs in molecules that possess a low ionization potential (electron donor) or a high electron affinity (electron acceptor), giving a broad absorption spectrum as a result of an electron-donor-acceptor complex. Within this complex the formation of an ion pair in the excited state results. This type of electron transfer, which must be exothermic, more commonly occurs between a ground and excited state compound than two ground state molecules. The LUMO of the electron acceptor must be at a lower energy than the LUMO of the excited electron donor.¹⁰⁸ Hence, an increase in the energy difference between the LUMO of the ground and excited state would lead to a decrease in the activation energy barrier of the charge-transfer process.

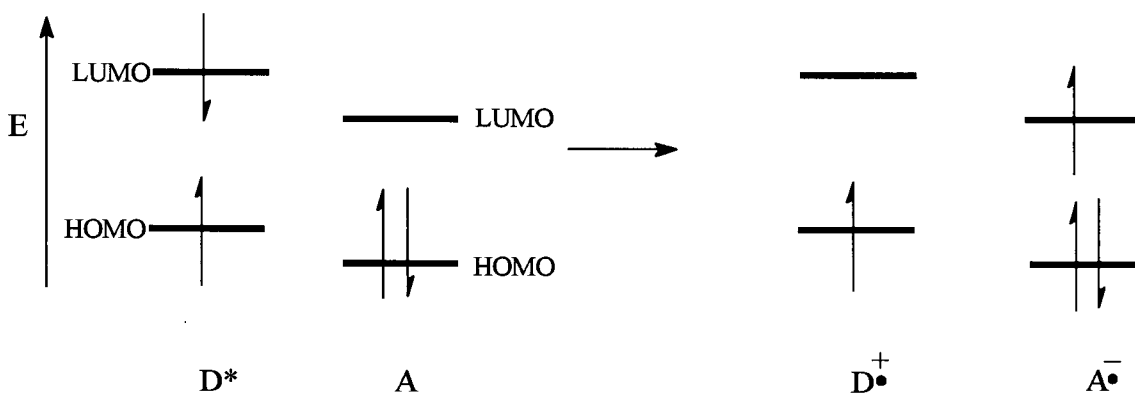


Figure 4.07. Charge-Transfer from an Excited Donor (D*) to Acceptor (A).

If both molecules are in the ground state, an electron transfer can only take place if the HOMO of the donor is higher-lying than the LUMO of the acceptor.

An example of a compound that exhibits a pronounced charge-transfer absorption band at λ_{max} (CH₃CN) 655 nm and possesses similar structural components to norcaradiene **103** is naphth[2,3-*a*]azulene-1,12-dione (**108**).¹⁰⁹ This can be explained by the interaction between the quinone which possesses acceptor properties and the cycloheptatriene which has donor properties (Figure 4.08).

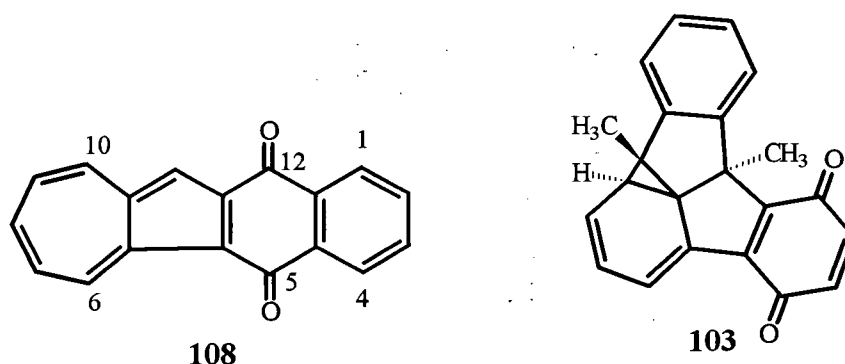


Figure 4.08. Naphth[2,3-*a*]azulene-5,12-dione (**108**) and Norcaradiene **103**.

Similar colors, which however were transient, have been detected in the crystalline state photochemistry of several 9- or 9,10-disubstituted 9,10-ethenoanthracene derivatives with electron-withdrawing esters or carboxylic acid substituents on the bridging double bond.¹¹⁰ These compounds were shown to be photochromic, a process whereby a substance changes color upon absorption of light. This appearance is by definition either thermally or photochemically reversible.¹¹¹ Compounds displaying photochromism have been studied since the end of the last century¹¹² and this process has been observed for various compounds in different media, including examples of photochromism in the solid state.¹¹⁰

A compound that exhibits photochromism is 9,10-ethenoanthracene derivative 109 (Figure 4.09), which turns dark blue upon irradiation in the crystalline state and gradually loses its color over several hours at room temperature in the dark.¹¹³ Heating as well as dissolving the colored crystals also resulted in a loss of color.

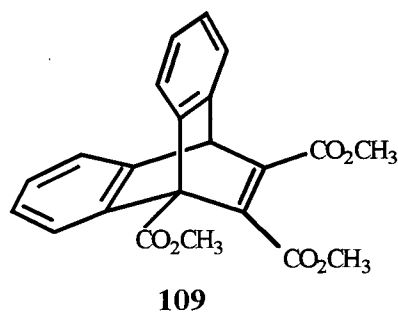


Figure 4.09. Example of a Photochromic 9,10-Ethenoanthracene Derivative 109.

In the case of norcaradiene 103, the blue-colored crystals were thermally as well as photochemical stable. The diffuse reflectance UV/VIS absorption spectrum of the irradiated crystals of compound 109 resembles the corresponding spectrum of norcaradiene 103. Hence, it is possible that irradiation of 109 leads to the formation of a small amount of the analogous norcaradiene derivative, which may break down to form colorless products. Although norcaradiene 103 was only formed under irradiation conditions in solution, and 69 was shown to be unreactive in the solid state ($\lambda \geq 290$ nm, 8 h), the isolation of norcaradiene 103 might have solved the up-to-now unsolved mystery of solid state photochromism of 9,10-substituted-ethenoanthracene derivatives. However, in order to fully understand why the coloration of triester 109 is unique to the crystalline state, and quinone 69 is photostable upon irradiation in the solid state, the medium effects have to be investigated further.

4.1.4. Solvatochromic Effect of Norcaradiene 103

A solvent effect was observed when norcaradiene 103 was dissolved in acetonitrile and in chloroform. The color of the solution of norcaradiene 103 in acetonitrile was violet, whereas in chloroform a deep blue color was obtained. This is known as the solvatochromic effect, resulting from changes in the wavelengths, intensities and shapes of the absorption band of chromophores due to the effect of the solvent.¹¹⁴

Table V UV/VIS Absorption Data for Norcaradiene 103^a

Band	Acetonitrile			Chloroform		
	λ_{\max} (nm)	$1/\lambda_{\max}$ (cm^{-1})	ϵ_{\max}	λ_{\max} (nm)	$1/\lambda_{\max}$ (cm^{-1})	ϵ_{\max}
1	569	17,570	2,066	594	16,840	2,423
2	316	31,650	3,577	324	30,860	4,157
3	232	43,100	9,756	256	39,060	8,889

(a) Concentrations of 103 in acetonitrile and chloroform were $4.10 \times 10^{-4} \text{M}$ and $4.49 \times 10^{-4} \text{M}$, respectively.

Table VI UV/VIS Absorption Data for Benzoquinone

Band	Acetonitrile $1/\lambda_{\max}$ (cm^{-1})	Dichloroethane $1/\lambda_{\max}$ (cm^{-1})
1 ($n \rightarrow \pi^*$)	29,540	29,370
2 ($\pi \rightarrow \pi^*$)	39,920	39,600

The UV/VIS absorption spectrum of 103 in chloroform shows a red shift (bathochromic shift), which can be attributed to an increase in solvent polarity. In comparing the UV/VIS absorption spectra of 103 to the spectra of benzoquinone in similar solvents, a correlation between the absorption bands is observed.¹¹⁵ In both cases, the $n \rightarrow \pi^*$ and $\pi \rightarrow \pi^*$ absorption bands of the carbonyl compounds undergo a red shift as the polarity of the solvent increases.

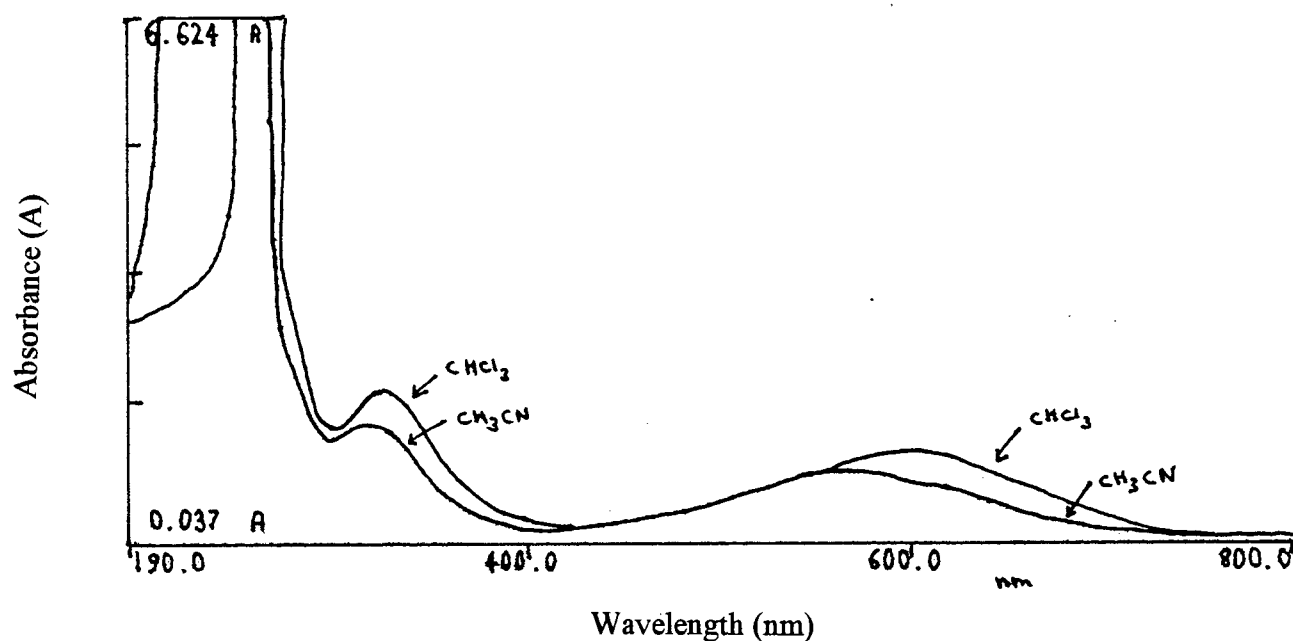


Figure 4.10. UV/VIS Absorption Spectrum of 103 in Acetonitrile and Chloroform.

By increasing the polarity of the solvent, the $\pi \rightarrow \pi^*$ transitions of aromatic carbonyl compounds undergo a red shift, whereas the $n \rightarrow \pi^*$ transitions undergo a blue shift.¹¹⁵ The blue shift observed for the $n \rightarrow \pi^*$ absorption bands of carbonyl compounds may result from cooperating effects of both electrostatic and hydrogen bonding interactions with the solute molecule.¹¹⁵ Protic solvents are thought to hydrogen-bond more strongly to the more polar ground state of the molecule than the excited state, which only has one available n-electron.¹¹⁶ This lowers the energy of the ground state more than the energy of the excited state. As a consequence the energy of the $n \rightarrow \pi^*$ transition is raised. The red shift is believed to be caused by a greater stabilization of the excited state than the ground state. In this case the excited state is thought to be more polar than the ground state, resulting in the energy lowering of the $\pi \rightarrow \pi^*$ transition.

In the case of compounds 103 and benzoquinone, the $n \rightarrow \pi^*$ absorption band does not undergo a blue shift in dichloroethane or chloroform. This may be explained by the lack of hydrogen bonding interaction between solvent and the solute molecules. Hence, the general effect on the $n \rightarrow \pi^*$ absorption of these polar solvents is also a red shift. As seen from Figure 4.10 a pronounced solvatochromic effect is observed for the absorption bands of norcaradiene 103. As before, quinone 103 can be compared with naphth[2,3-*a*]azulene-1,12-dione (108) (Figure 4.08), which demonstrates solvatochromism in acetonitrile and benzene, λ_{\max} (CH₃CN) = 655 nm, λ_{\max} (C₆H₆) = 672 nm, as a result of the quinone moiety which has acceptor properties and the cycloheptatriene moiety which has donor properties.

CHAPTER 5 PHOTOCHEMICAL STUDIES OF 9,10-BIS(METHOXYMETHYL)-9,10-DIHYDRO-9,10[1',2']BENZENOANTHRACENE-1,4-DIONE (72)

5.1. Photorearrangement of 72 in Acetonitrile

Photolysis of 9,10-bis(methoxymethyl)tritycene-1,4-quinone (**72**) at $\lambda \geq 300$ nm, in deoxygenated acetonitrile, led to the formation of three photoproducts which, after column-chromatographic separation, were identified as the dark-blue norcaradiene **110** (3%), the colorless dihydrobenzofuran **111**, (19%) and the dark red benz[*a*]aceanthrylene **112** (18%). However, the corresponding semibullvalene derivative was not isolated. When a solution of **72** was irradiated at $\lambda \geq 300$ nm in benzene, the isolated product yields changed to 10% of dihydrofuran **111** and 33% of benz[*a*]aceanthrylene **112**.

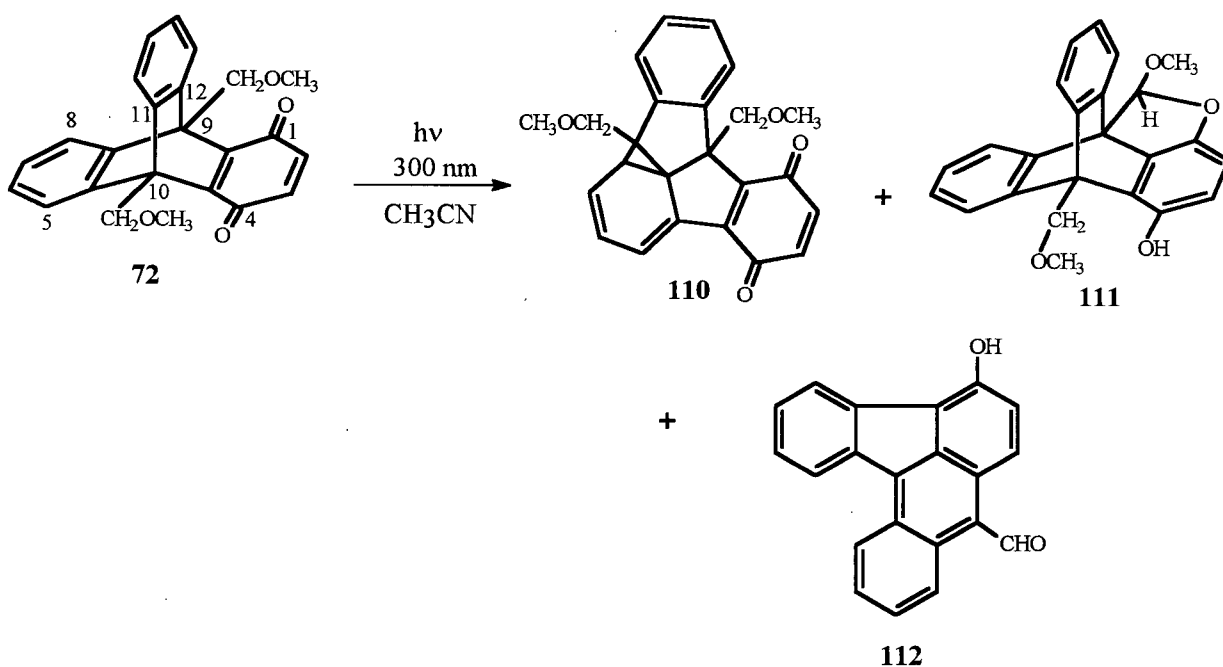


Figure 5.01. Photolysis of **72** in Acetonitrile.

5.1.1. Structure Elucidation of Photoproducts 103, 110 and 111

The structural assignment of the blue norcaradiene photoproduct 110 was simplified not only by its blue color, which had been observed earlier in the case of norcaradiene 103, but also by comparing its ^1H NMR and IR spectra to those of 103. The IR spectrum supports the structure by the presence of two carbonyl bands at 1665 and 1646 cm^{-1} . The base peak of the mass spectrum is at m/e 372, which is equivalent to the mass of the starting material. Similarities between norcaradiene 110 and 103 are mainly established by the ^1H NMR spectrum. This shows the presence of one aromatic ring between δ 7.66 and 7.19 ppm and the quinone vinyl hydrogens as an AB system at δ 6.64 ppm ($J = 8$ Hz). Furthermore, the assignment of the diene moiety was based on the coupling constants represented as a doublet at δ 6.90 ppm ($J = 6$ Hz), a doublet of doublets at δ 6.31 ppm ($J = 9$ Hz and 6 Hz), and a doublet of doublet at δ 6.16 ppm ($J = 9$ Hz and 5 Hz). Additionally, the doublets at δ 4.05 ($J = 9$ Hz) and 3.30 ppm ($J = 9$ Hz) are representing the two hydrogens of one of the methoxymethylene groups, whereas the AB system at δ 3.28 ppm ($J = 9$ Hz) depicts the remaining methoxymethylene hydrogens. The methoxymethyl substituents are confirmed by a singlet at δ 3.21 ppm and 3.17 ppm. The doublet at δ 2.85 ppm ($J = 5$ Hz) corresponds to the hydrogen at the cyclopropyl ring. As previously discussed (Chapter 4), the formation of norcaradiene derivative 110 is believed to proceed through a carbene intermediate, analogous to that of norcaradiene 103, as suggested by Iwamura.¹⁰⁵

The structure of dihydrobenzofuran 111 was assigned on the basis of the spectral data collected. The IR absorption at 3270 cm^{-1} clearly indicates the presence of an OH group. A molecular ion at m/e 372, the same as that of the starting material, was observed in the mass spectrum, suggesting that a rearrangement had occurred. The ^1H NMR spectrum of 111 is shown in Figure 5.02. Assignment of the peaks was confirmed by HMQC and HMBC NMR experiments (Table VII) as well as by a COSY NMR experiment (Table VIII). The disappearance of the CH_2 -signal of one of the methoxymethylene groups and the appearance of one hydrogen singlet at δ 6.87 ppm instead, supported the proposed formation of an acetal group involving one of the methoxymethyl substituents. Also of note is the presence of two singlets at δ 3.98 ppm and δ 3.91 ppm corresponding to two different methoxy groups, indicating a loss of symmetry. As a result of the incorporation of one of the former quinone oxygens into the dihydrobenzofuran ring, the second quinone oxygen was reduced to a phenol group corresponding to the peak at δ 8.28 ppm.

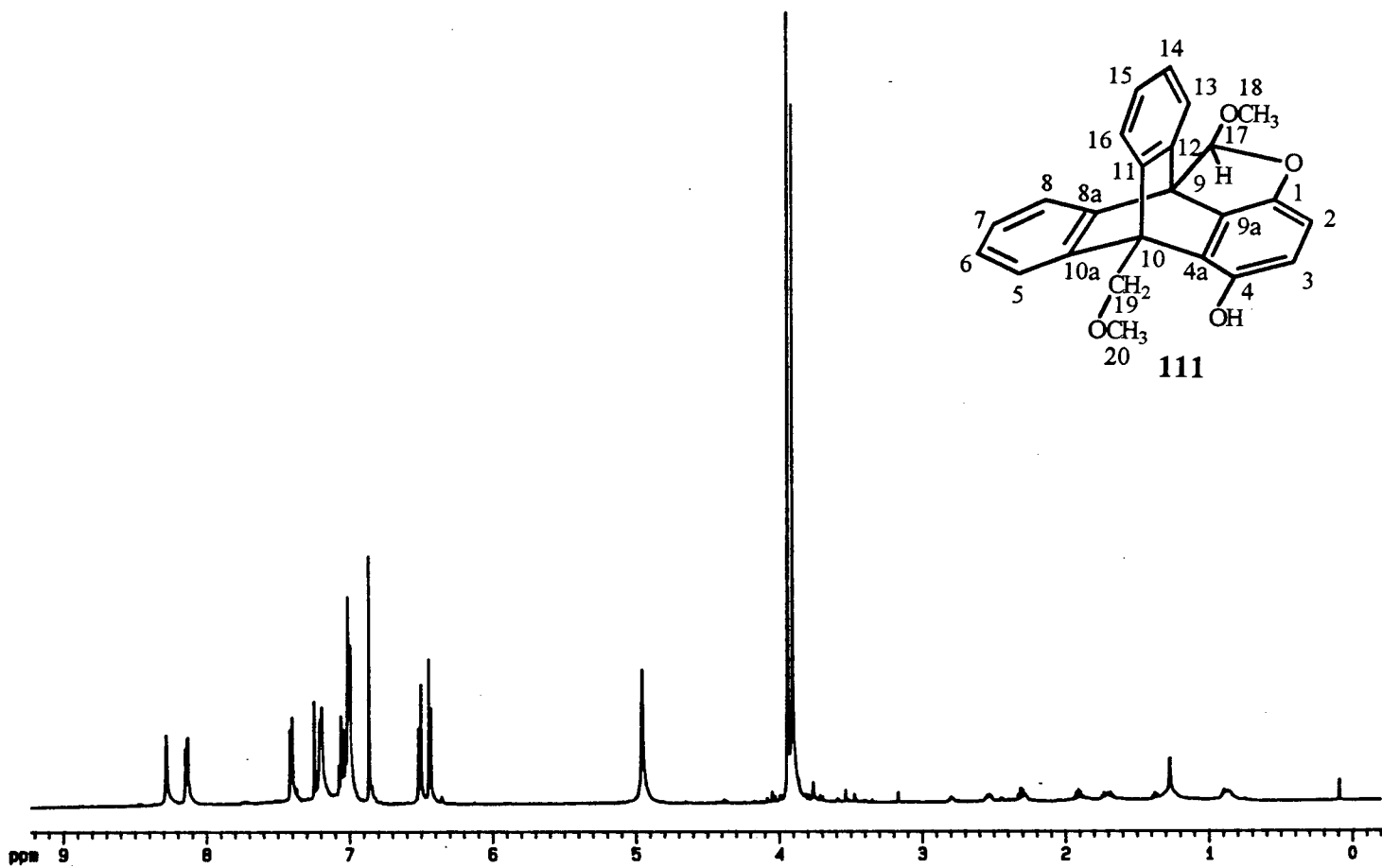
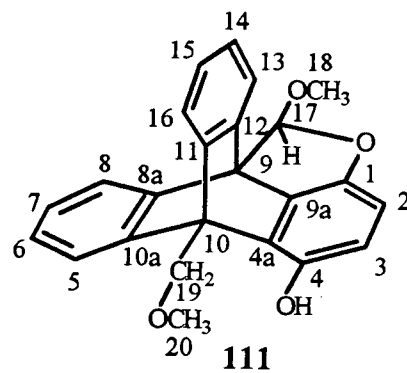
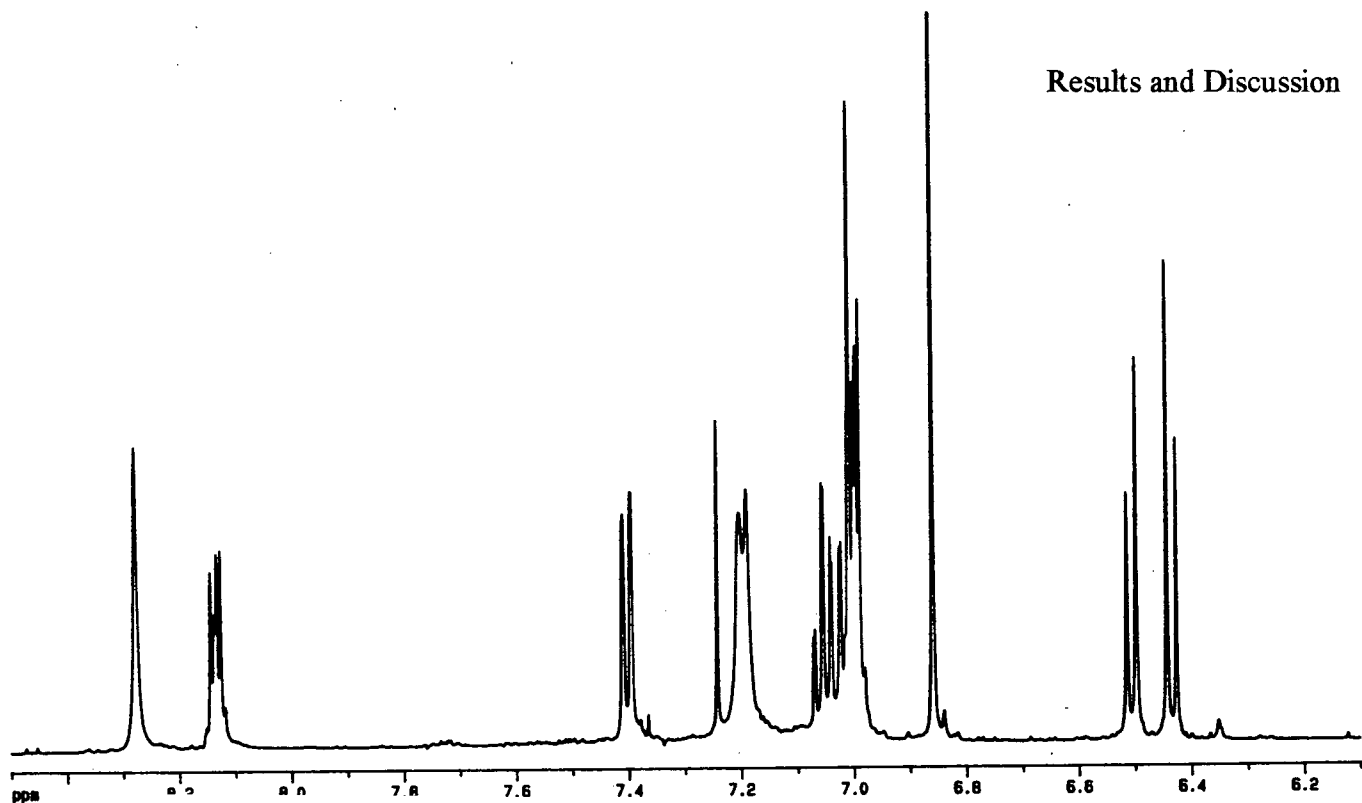
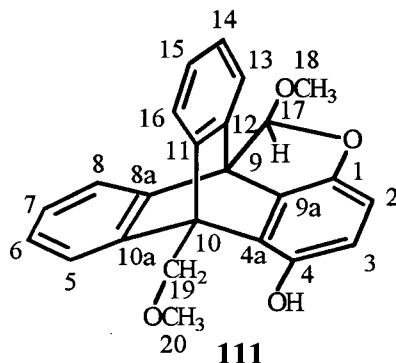


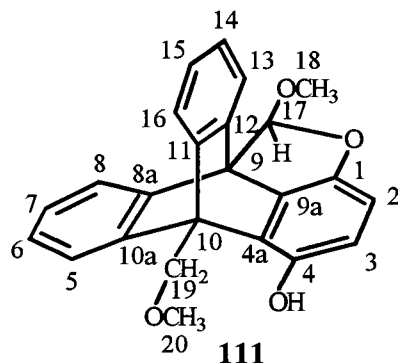
Figure 5.02. ^1H NMR (CDCl_3) Spectrum of Dihydrofuran Derivative 111.

Table VII ^1H NMR (500 MHz) and ^{13}C NMR (125 MHz) Data for Dihydrofuran 111^a

Element	Carbon Assignment	^{13}C NMR Spectrum (125 MHz) δ ppm, APT ^b	HMQC ^1H NMR Correlations (500 MHz) δ ppm (Assignment)	^1H - ^{13}C HMBC Long-range Correlations
a	1	138.24		H-2, H-3
b	2 & 3	107.83(-ve), 116.61(-ve)	6.48 (H-2 & H-3)	
c	4	126.00		H-3
d	5&16	121.31(-ve), 121.81(-ve)	7.22-7.17 (H-5 & 16)	H-7 or 6 or 14 or 15
e	6&7, 14&15	125.16(-ve), 124.97(-ve) 124.82(-ve), 124.59(-ve)	7.08-6.97 (H-6 & 7 & 14 & 15)	
f	8&13	120.48(-ve), 124.82(-ve)	7.40 & 8.22-8.16 (H-8 & 13)	H-7 or 6 or 14 or 15
g	9	57.60		H-13 or 8
h	10	53.91		CH2-19
i	11 & 10a	145.03, 145.03		
j	8a & 12	146.15, 146.17		H-8 or 13, H-13
k	17	112.06(-ve)	6.87 (H-13)	Me-18
l	18	58.22(-ve)	3.91 (Me-18)	H-17
m	19	71.43	4.96 (CH2-19)	
n	20	59.60(-ve)	3.98 (Me-20)	CH2-19

a -The assignments and chemical shifts of the ^{13}C NMR spectrum are listed in columns II and III, respectively. Column IV shows the ^1H NMR signal(s) which correlate(s) with the carbon of columns II and III, as obtained from the HMQC experiment (1 bond correlation). The last column lists the hydrogen(s) which correlate(s) with the ^{13}C NMR signal of column II and III as obtained from the HMBC experiments (2 and 3 bonds correlation(s)).

b - The results of the APT experiments are given in parentheses (-ve for CH and CH_3 carbon signals).

Table VIII ¹H NMR Data (500 MHz) for Dihydrofuran 111

Entry	Hydrogen Assignment	¹ H-NMR (500 MHz) δ ppm (mult., <i>J</i> (Hz))	COSY Correlations
a	H-2 & 3	6.48 (AB system, <i>J</i> = 8 Hz)	
b	H-5 & 16	7.22-7.17 (m)	H-6, H-15
c	H-6, 7, 14, 15	7.08-6.97 (m)	H-5, H-8, H-16, H-13
d	H-8 & 13	7.40 (d, <i>J</i> = 7), 8.16-8.12 (m)	H-7, H-14
e	H-17	6.87 (s)	
f	Me-18	3.98 (s)	
g	CH ₂ -19	4.96 (s)	
h	Me-20	3.91 (s)	
i	OH	8.28 (s)	

5.1.2. Mechanism for Formation of Dihydrobenzofuran 111

Earlier investigations of the photochemistry of quinones containing *tert*-butyl side-chains have resulted in photorearrangements similar to that found for quinone 72. One example is the photochemical conversion of *tert*-butyl-1,4-quinone 113 into the corresponding dihydrobenzofuran derivative 114, reported by Orlando *et al.*¹¹⁷ The proposed mechanism involves an initial intramolecular γ -hydrogen abstraction resulting in a semiquinone biradical 113a (Figure 5.03). Biradical 113a is suggested to undergo intramolecular cyclization to give spirocyclopropane 113b, followed by an electron demotion to yield zwitterion 113c. The cyclopropyl ring opening is believed to be initiated by a strong tendency to aromatization. Dihydrobenzofuran derivative 114 is formed as a result of a hydrogen transfer. In order to confirm the reaction pathway, Farid¹¹⁸ conducted trapping experiments of biradical 113a with sulfur dioxide. Several products were isolated, and explained by the formation of the corresponding sulfinic acid benzoquinone precursor resulting from the initial addition of sulfur dioxide to the radical side-chain of 113a followed by a hydrogen transfer.

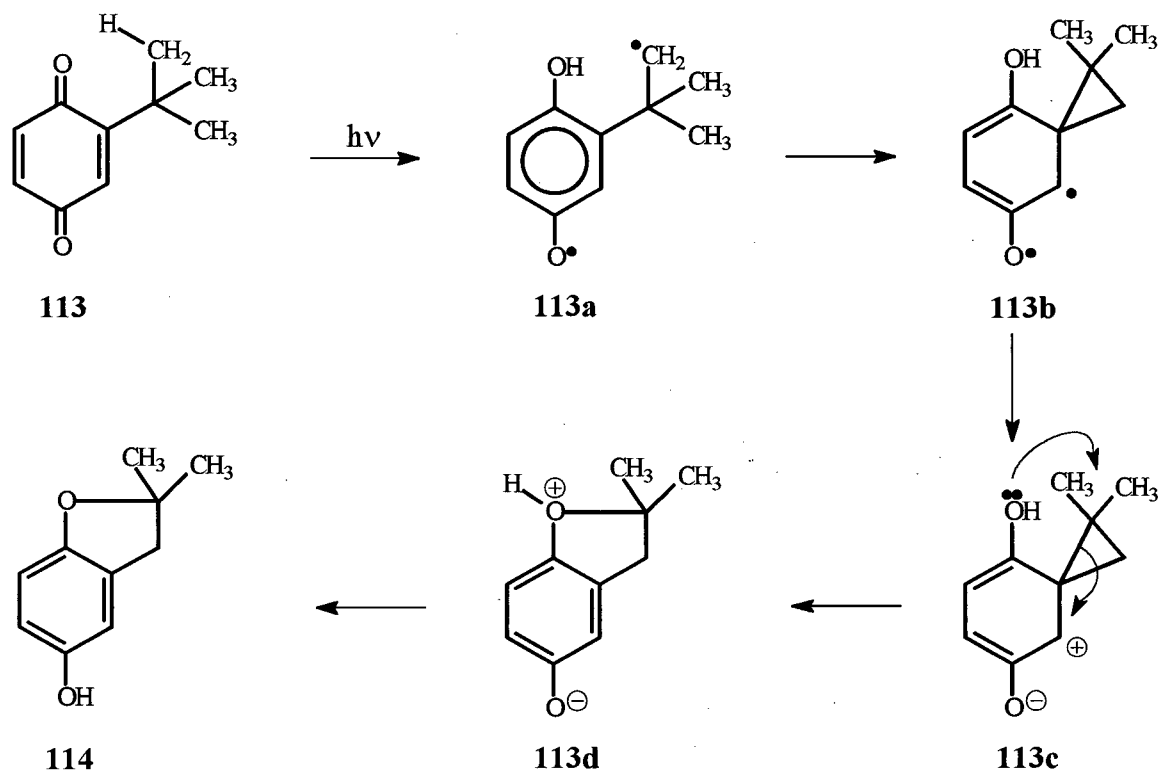


Figure 5.03. Mechanism for the Formation of Dihydrofuran Derivative 114.

Based on the structural similarities between photoproducts 114 and 111, quinone 72 is believed to undergo a photorearrangement by a mechanism analogous to that proposed by Orlando *et al.*¹¹⁷ as illustrated in Figure 5.04.

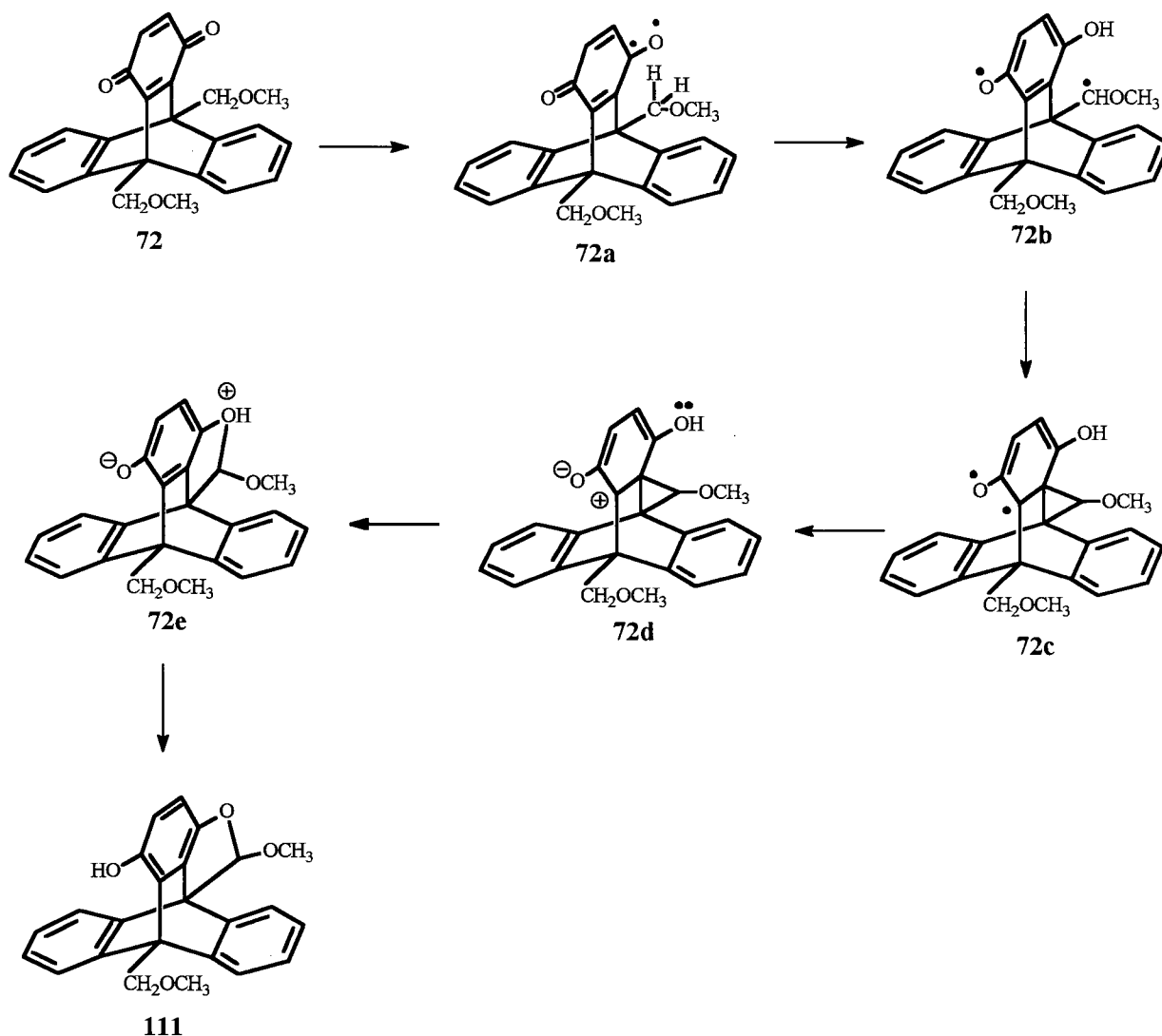


Figure 5.04. Mechanism for the Formation of Dihydrofuran Derivative 111.

The more favorable γ -hydrogen atom abstraction (Norrish type II photoreaction) involving one of the methoxymethyl groups and a quinone oxygen of 72 (Figure 5.04) may explain the low yield of norcaradiene 110 (Section 5.1). The pathway, giving rise to photoproduct 111, is believed to be preferred due to the radical-stabilizing effect of the methoxymethyl substituent. The activating effect that alkoxy groups possess in promoting hydrogen abstractions in the Norrish

type II photoreaction has clearly been demonstrated by Wagner and co-workers in arylalkyl ketones.¹¹⁹ Wagner showed that a hydrogen abstraction will be favorable if the γ -substituent stabilizes the resulting radical site. In the case of the methoxymethyl group of quinone 72, the availability of the lone pairs on the oxygen is believed to contribute to the resonance stability of radical 72b. The mechanism is assumed to proceed through dispiro compound 72c, which is thought to be formed by an intramolecular cyclization of biradical 72b. An electron demotion is believed to occur, resulting in zwitterion 72d. This is proposed to undergo cyclopropyl ring opening to yield 72e. Finally, a hydrogen transfer is suggested to take place leading to photoproduct 111.

5.1.3. Structure-Reactivity Analysis of Quinone 72

As demonstrated by the X-ray crystal structure of quinone 72 (Figure 5.05), the intramolecular distances between the γ -hydrogen (hydrogens 6 and 7) and the quinone oxygen (oxygen 1) are within the proposed abstraction distance of 2.72 Å (sum of the van der Waals radii for hydrogen and oxygen).¹²⁰ The involvement of the Norrish type II photoreaction leading to dihydrofuran 111 is geometrically favorable as indicated by the two abstractable hydrogens at C=O \cdots H distances of 2.44 and 2.53 Å and angle values in Table IX. As discussed earlier (see p 24, Introduction), the optimum range for the angle Δ is between 90-120°. Thus in quinone 72, with Δ angles at 89.0 and 102.7°, n-orbital abstraction is favored. Angles ω , at 13.02 and 24.69°, are also close to the optimum value of zero. As noted earlier, the angle θ may differ from the preferred

value of 180° , as seen in this case. This analysis is based on the assumption that the reactive excited state geometry in solution is close to the ground state geometry as determined by X-ray crystallography.¹²¹

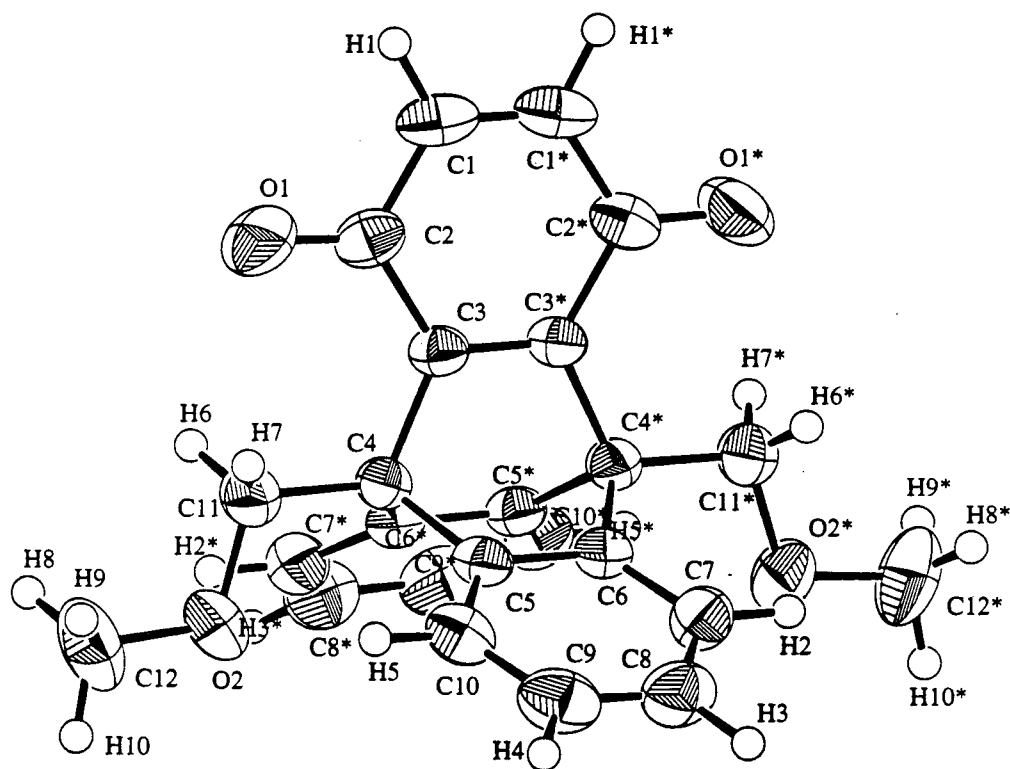


Figure 5.05. X-ray Crystal Structure of Quinone 72. Space group $C2/c$ (#15), $a = 15.772(1) \text{ \AA}$, $b = 8.000(1) \text{ \AA}$, $c = 14.7883(9) \text{ \AA}$, $\beta = 98.430(6)^\circ$, $Z = 4$; $R = 4.0\%$.

Table IX Crystallographically Determined Angles for Quinone 72

Angle	Atoms	Value (°)
Δ	C2, O1, H7	98.0
Δ	C2, O1, H6	102.7
θ	C11, O1, H7	92.1
θ	C11, O1, H6	97.5
ω	C2, O1, H7	13.0
ω	C2, O1, H6	24.7

5.1.4. Structure Elucidation of Product 112

Compound 112 was proposed as a phenolic aldehyde having the benz[*a*]aceanthrylene carbon skeleton, based on its spectral data. The IR spectrum indicates the presence of an OH group at 3332 cm⁻¹ and a carbonyl group at 1643 cm⁻¹. As a result of the conjugated π -system, the absorption of the aldehyde is shifted to a lower frequency. Structure 112 was further supported by the mass spectrum with a base peak of *m/e* 296. This mass corresponds to the loss of a methoxymethyl group as well as the loss of a methoxy group from the original quinone 72. The strongest spectral evidence supporting the structure 112 came from the ¹H NMR, COSY NMR, as well as from HMQC and HMBC NMR experiments. The absence of the methoxymethyl groups was confirmed by the presence of hydrogens in the aromatic region only. Correlating the carbon and hydrogen atoms as seen from Table X, led to the proposed assignment of benz[*a*]aceanthrylene 112. The singlet at δ 11.55 ppm is in agreement with the general region of chemical shifts expected for an aldehyde hydrogen.

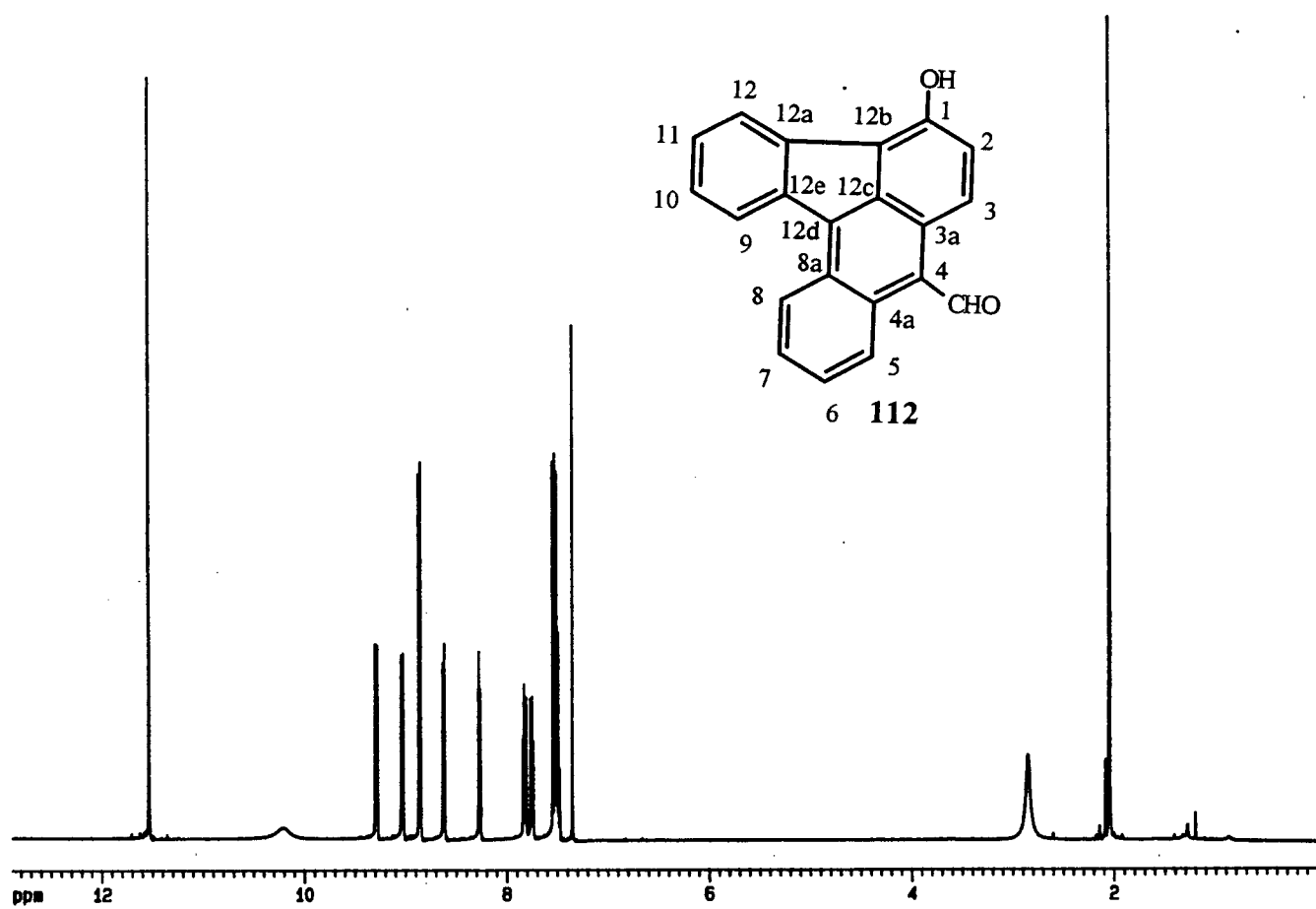
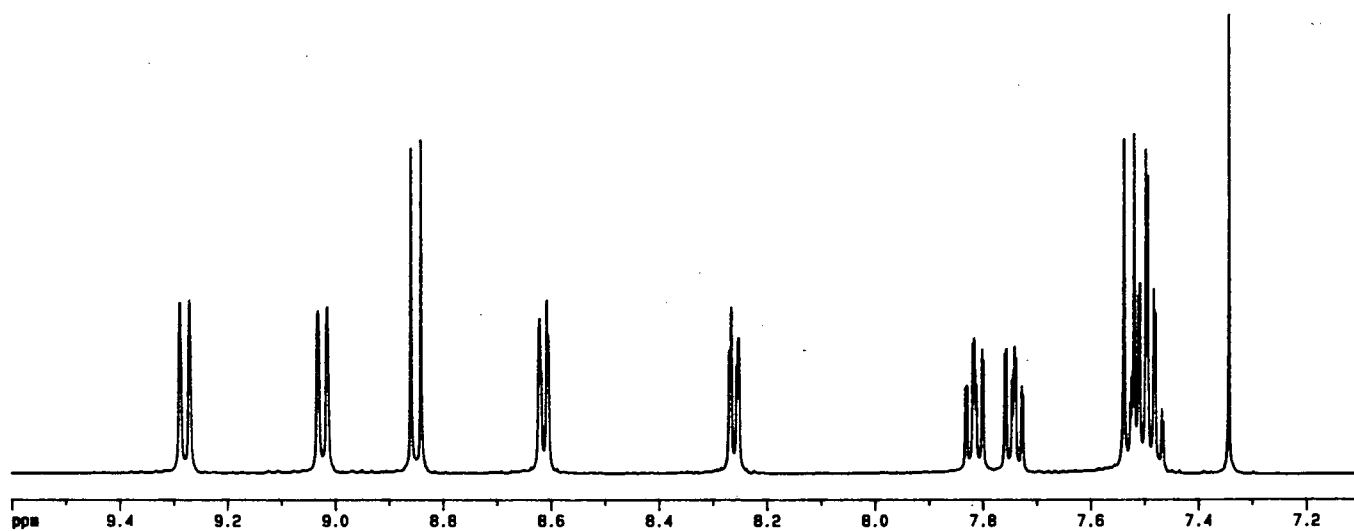
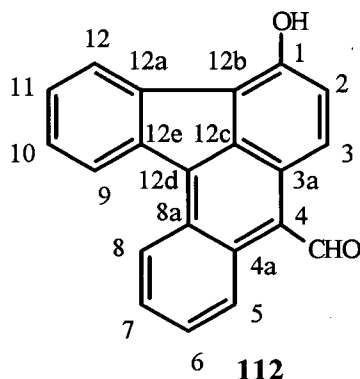


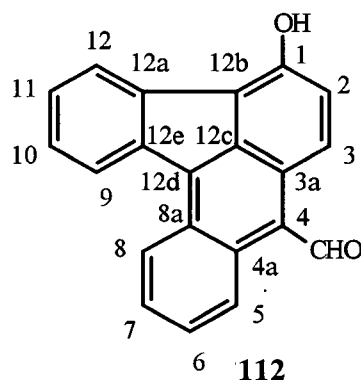
Figure 5.06. ^1H NMR (d_6 -Acetone) of Benz[*a*]aceanthrylene Derivative 112.

Table X ^1H NMR (500 MHz) and ^{13}C NMR (125 MHz) Data for Benz[*a*]aceanthrylene Derivative 112^a

ENTR Y	Carbon Assignment	^{13}C NMR Spectrum (125 MHz) δ ppm, APT ^b	HMQC ^1H NMR Correlations (500 MHz) δ ppm (Assignment)	^1H - ^{13}C HMBC Long-range Correlations
a	1	154.34		H-2
b	2	128.47(-ve)	8.85 (H-2)	
c	3	125.99(-ve)	7.55-7.46 (H-3)	
d	3a	129.12		
e	4	126.07		
f	4a	130.01		H-5, H-7(4-bonds)
g	5	126.47(-ve)	9.28 (H-5)	H-7
h	6	127.90(-ve)	7.73-7.70 (H-6)	H-8
i	7	128.32(-ve)	7.84-7.80 (H-7)	H-5
j	8	125.35(-ve)	9.02 (H-8)	H-6
k	8a	133.21		H-8, H-6(4bonds)
l	9	125.12(-ve)	8.26 (H-9)	
m	10 & 11	127.31(-ve), 128.83(-ve)	7.55-7.46 (H-10, H-11)	H-12
n	12	125.68(-ve)	8.62 (H-12)	H-11
o	12a	140.10		H-12
p	12b	138.03		
q	12c	136.36		H-8
	12d	117.12		
	12e	132.48		H-2
	13	193.26(-ve)	11.55 (H-13)	

a -The assignments and chemical shifts of the ^{13}C NMR spectrum are listed in columns II and III, respectively. Column IV shows the ^1H NMR signal(s) which correlate(s) with the carbon of columns II and III, as obtained from the HMQC experiment (1 bond correlation). The last column lists the hydrogen(s) which correlate(s) with the ^{13}C NMR signal of column II and III as obtained from the HMBC experiments (2 and 3 bonds correlation(s)).

b- The results of the APT experiments are given in parentheses (-ve for CH and CH_3 carbon signals).

Table XI ^1H NMR Data (500 MHz) for Benz[*a*]aceanthrylene Derivative 112

Entry	Hydrogen Assignment	^1H -NMR (500 MHz) δ ppm (mult., J (Hz))	COSY Correlations
a	H-2	8.85 (d, $J = 8.5$)	H-3
b	H-3	Part of m at 7.55-7.46	H-2
c	H-5	9.28 (d, $J = 9$)	H-6
d	H-6	7.73-7.70 (m)	H-5
e	H-7	7.84-7.80 (m)	H-8
f	H-8	9.02 (d, $J = 8.5$)	H-7
g	H-9	8.26 (dd, $J = 7 \text{ \& } 6$)	H-10
h	H-10	Part of m at 7.55-7.46	H-9
i	H-11	Part of m at 7.55-7.46	H-12
j	H-12	8.62 (dd, $J = 6 \text{ \& } 7$)	H-11
k	OH	10.20 (s)	
l	CHO	11.55 (s)	

5.1.5. Mechanism for the Formation of Benz[*a*]aceanthrylene Derivative 112

Benz[*a*]aceanthrylene derivatives have been commonly observed as by-products in the photochemistry of triptycenes as demonstrated by Iwamura *et al.*¹²² The photochemistry of

tritycenes was also of interest to Wheeler *et al.*¹²³ who investigated the photochemical isomerization of 1,4-dimethoxytritycene (115) in methanol (Figure 5.07). Instead of the expected norcaradiene derivative similar to that found by Iwamura (Section 4.1.2), Wheeler obtained benz[*a*]aceanthrylene 117. Wheeler suggested that triptycene 115 formed norcaradiene 116, followed by a thermal conversion to compound 117, accompanied by the loss of methanol.

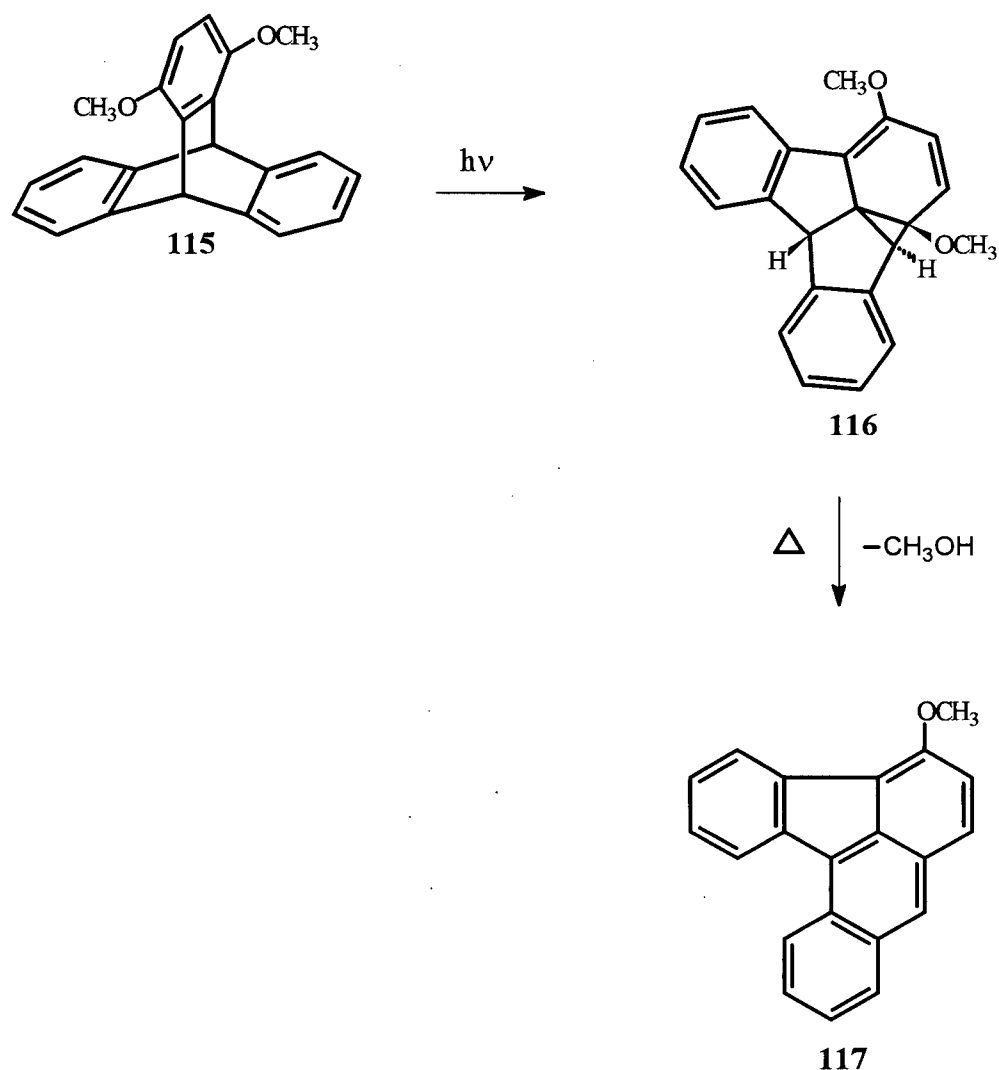


Figure 5.07. Photoreaction of 1,4-Dimethoxytritycene (115).

Applying the proposed thermal rearrangement step to a mechanism which involves dihydrofuran derivative **111** may explain the formation of benz[*a*]aceanthrylene **112** (Figure 5.08).

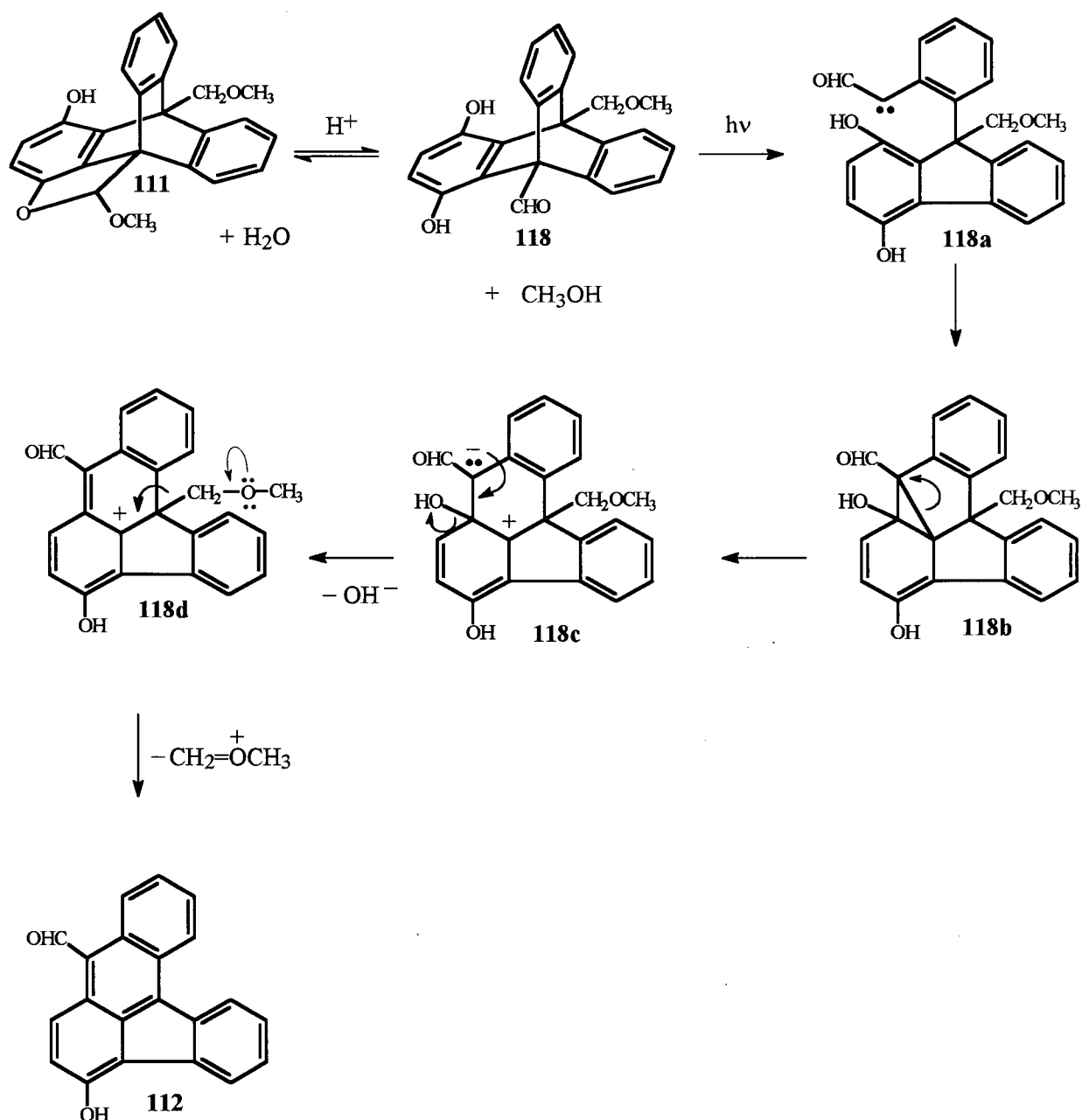


Figure 5.08. Proposed Mechanism for the Formation of Benz[*a*]aceanthrylene **112**.

Although compound 118 was not detected in the reaction mixture, it is possible that the acetal ring of 111 could open under the photolysis conditions. Compound 118 could then react further, forming the carbene intermediate 118a as discussed earlier for the formation of norcaradiene 113. Opening of the cyclopropyl ring, elimination of the methoxymethyl substituent, and loss of the hydroxy group could then give benz[α]aceanthrylene derivative 112. Two control experiments were conducted in order to determine if dihydrofuran derivative 111 was a potential precursor. Treatment of 111, dissolved in acetone, with aqueous hydrochloric acid (15%) followed by stirring the reaction mixture overnight, did not result in the formation of any major product, as the reaction contained a mixture of compounds, which could not be identified. The possibility exists that hydroquinone 118 is not a stable intermediate, as it is in equilibrium with dihydrofuran 111. Likewise, irradiation (2 h) of dihydrofuran derivative 111 under the same photolysis conditions as described at the beginning of this section, did not lead to photoproduct 112. Based on these results, it may be concluded that either the reaction conditions are very specific and were not reproduced in the control experiments, or a different pathway may explain the photoreaction. The tentative mechanism will have to be evaluated and more studies will have to be conducted in this area to fully determine the reaction pathway for the formation of photoproduct 112.

As was the case for quinones 63 and 69, quinone 72 was found to be unreactive upon irradiation (8 h) through Pyrex ($\lambda \geq 290$ nm) in the solid state. The lack of reactivity may be explained by reasoning analogous to the rationalization proposed in Section 3.4.

PART II THE CONTROL OF REACTION MULTIPLICITY IN THE SOLID STATE: IONIC SENSITIZERS AND IONIC HEAVY ATOM EFFECTS

Although the control of the multiplicity of a photochemical reaction in solution has been well established over the years by sensitization and quenching techniques, not much attention has been devoted to this area of research in the solid state. In order to enhance the photochemical triplet behavior of a probe molecule in the solid state, heavy atoms, which enhance intersystem crossing or sensitizers, which promote triplet-triplet energy transfer, could be introduced. The two components would have to be in close proximity to one another. This may be achieved by combining two functionally different molecules in the crystalline state by forming a salt. The auxiliaries chosen for this study are either inorganic cations (heavy atoms), or triplet energy sensitizer amines to populate the triplet excited state in a probe molecule containing a carboxylic acid functionality. The differential singlet/triplet reactivity of the probe molecule would then be monitored to determine the success of the energy transfer. The application of the ionic auxiliary concept would permit the investigation of how distances and orientations, determined by X-ray crystallography, affect the efficiency of energy transfer in the solid state.

CHAPTER 6 GENERAL ORGANIC SYNTHESIS

6.1. Preparation of β , γ -Unsaturated Ketones:

2-(1-Cyclopentenyl)cyclopentanone (121) and 2-(1-Cyclohexenyl)cyclohexanone (125)

The β , γ -unsaturated keto-acid 121 was first synthesized by Givens *et al.*^{124a} by alkylating 2-cyclopentylidene cyclopentanone (119) with methyl bromoacetate to yield ester 120, followed by hydrolysis with methanolic KOH. The procedure for the preparation of 2-cyclopentylidene cyclopentanone (119) was described by Varech *et al.*¹²⁵ and involves a based-catalyzed aldol condensation between two molecules of cyclopentanone (118).

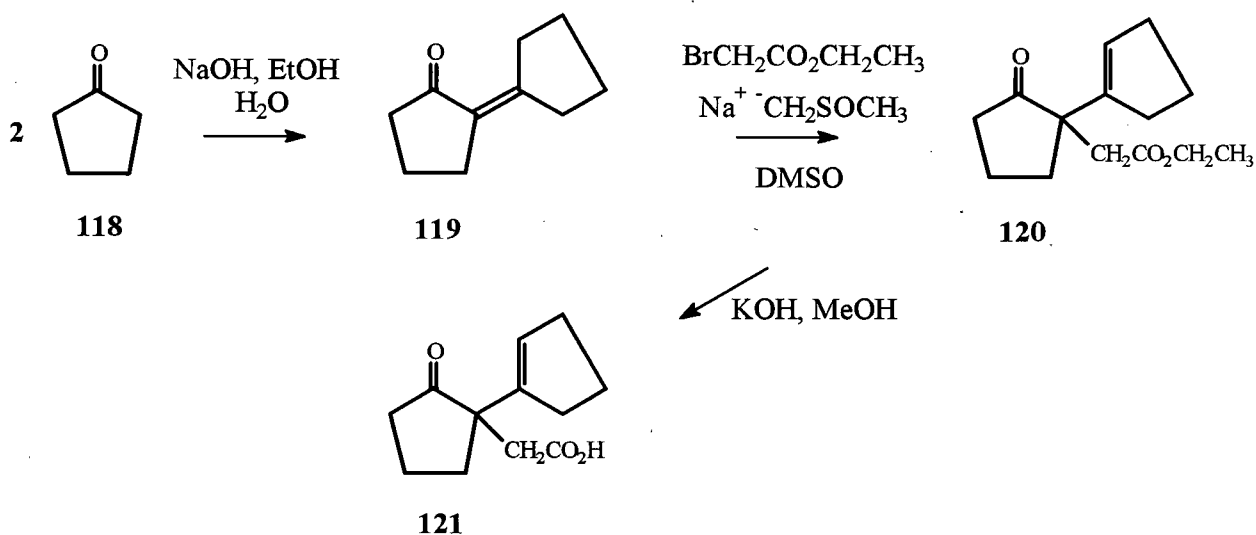


Figure 6.01. Preparation of 2-(1-Cyclopentyl)cyclopentanone (121).

The β , γ -unsaturated keto-acid **125** was prepared in an analogous manner to **121**, except for the initial aldol condensation step between two cyclohexanone molecules (**122**), which was carried out under acidic conditions according to procedures described by Gault *et al.*¹²⁶

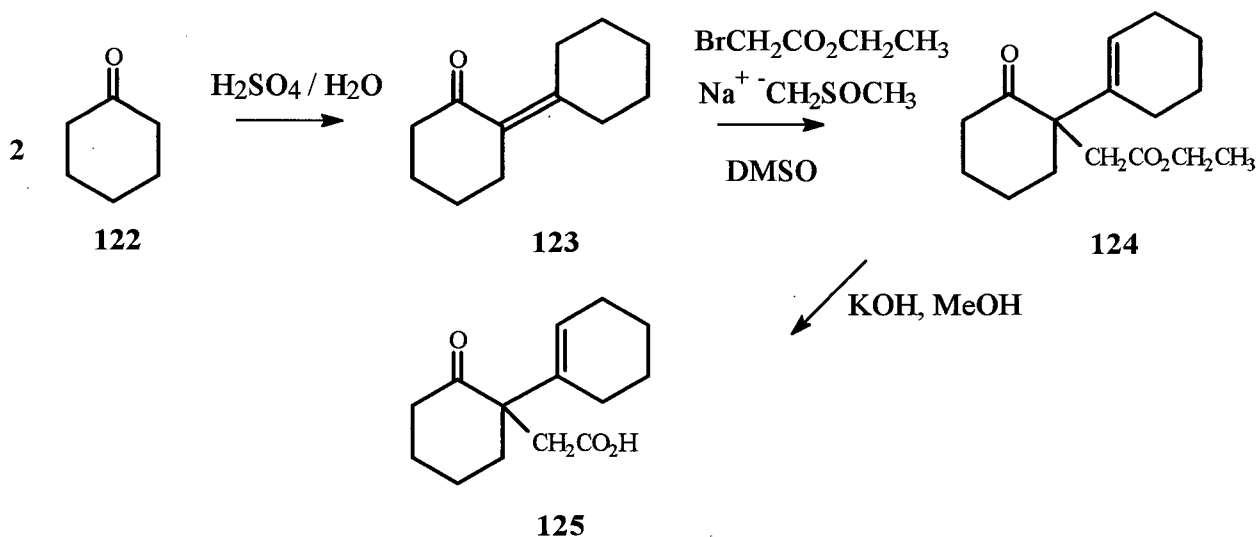


Figure 6.02. Preparation of 2-(1-Cyclohexenyl)cyclohexanone (**125**).

6.2. Preparation of *p*-Acetyl-*N,N*-dimethylbenzylamine (**128**)

The synthesis of *p*-acetyl-*N,N*-dimethylbenzylamine (**128**) involved the initial preparation of *p*-(dimethylaminomethyl)benzotrile (**127**) from α -bromo-*p*-toluonitrile (**126**) as described by Norman *et al.*¹²⁷ This entails an initial nucleophilic substitution reaction of α -bromo-*p*-toluonitrile (**126**) with dimethyl amine at -78°C and was followed by a Grignard reaction with methylmagnesium iodide to give compound **128**.

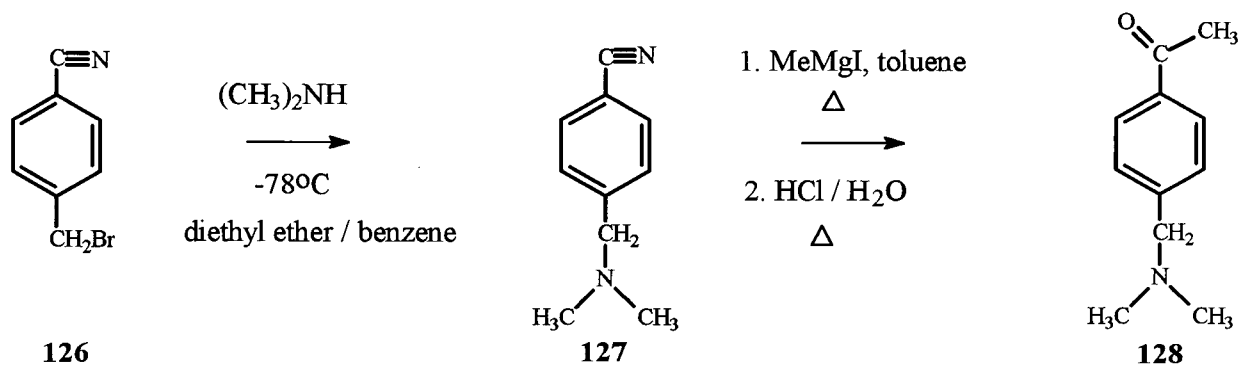


Figure 6.03. Preparation of *p*-Acetyl-*N,N*-dimethylbenzylamine (128).

6.3. Preparation of 9,10-Dihydro-9,10-ethenoanthracene Acids

Dibenzobarrelene ester **130**, originally prepared by Vaughan *et al.*,¹²⁸ was obtained by a Diels-Alder reaction between anthracene and ethyl propiolate in a sealed Carius tube. The ester was then reduced by lithium aluminum hydride-aluminum trichloride to the corresponding alcohol.¹²⁹ The introduction of the extended side-chain to obtain acid **132** was achieved by addition of succinic anhydride to a refluxing pyridine solution of alcohol **131**, a procedure described for a different system by Aries.¹³⁰ Acid **133** was prepared by reacting alcohol **131** with bromoacetic acid in the presence of sodium hydride under reflux conditions, a reaction adapted from Brady *et al.*¹³¹

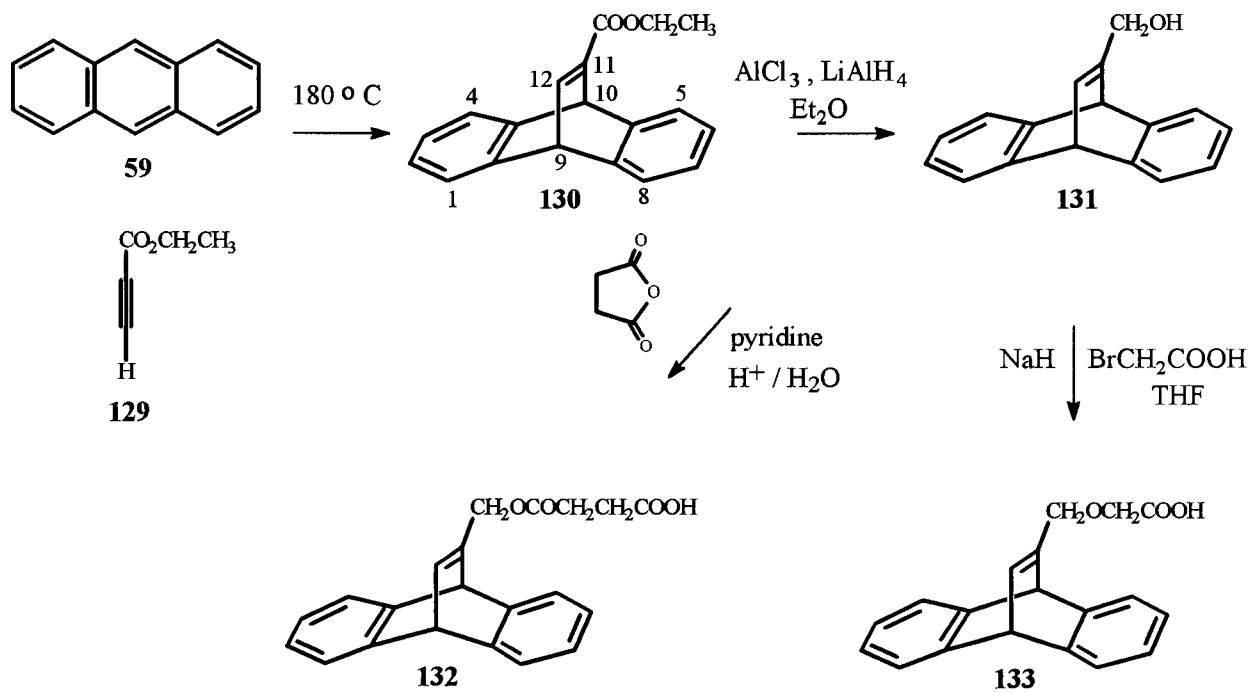


Figure 6.04. Preparation of 9,10-Dihydro-9,10-ethenoanthracene Acids 132 and 133.

CHAPTER 7 THE PHOTOCHEMISTRY OF β , γ -UNSATURATED KETONES

7.1. The Solution Phase Photochemistry of 2-(1-Cyclopentenyl)cyclopentanone Derivative

121

The first type of probe molecule chosen for testing the success of energy transfer was the β , γ -unsaturated ketone 121. The photochemistry of this acid has been investigated by Givens *et al.*,¹³² who showed that compound 121 undergoes primarily a 1,3-acyl shift (1,3-AS) reaction from the excited singlet state upon direct irradiation in solution to form β , γ -unsaturated ketone 135. However, upon triplet-sensitized photolysis, the cyclopropyl ketone derivative 134 is formed by the oxadi- π -methane (ODPM) rearrangement from the triplet excited state. Compound 121 would hence serve as a good candidate for investigating the chemical effects that a series of increasingly heavy alkali metal cations and various ionic sensitizers containing an amine functionality would have on promoting triplet state reactivity in the solid state.

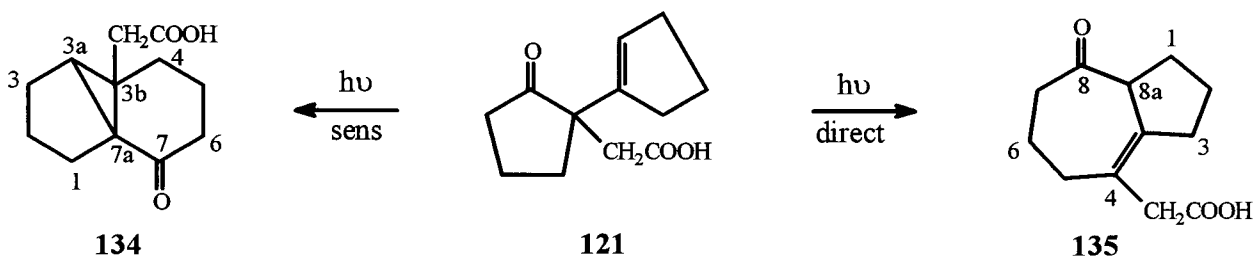


Figure 7.01. Photolysis of Keto-Acid 121.

7.2. The Solid State Photochemistry of 2-(1-Cyclopentenyl)cyclopentanone Derivative 121 and its Alkali Metal Salts

The direct irradiation of keto-acid 121 in the crystalline state was first investigated by Scheffer and Ramamurthy *et al.*,¹³³ who detected the same characteristic 1,3-acyl shift reactivity that had been observed in solution, yielding photoproduct 135. The same communication describes an investigation of the heavy-atom effect by preparing the Li⁺, Na⁺, K⁺, Rb⁺ and Cs⁺ salts of compound 121 and subjecting them to direct photolysis both in the crystalline state and solution. A significant cation effect was observed in the solid state but not in solution. The results were intriguing, showing that the Li⁺ salt afforded 9% of the ODPM product 134, the Na⁺ salt 52%, the K⁺ salt 65%, the Rb⁺ salt 60% and the Cs⁺ salt 40%. Hence the greatest perturbation of the photoproduct ratio did not result from the heaviest metal ion. This was attributed to the different crystal structures with different distances and orientations between metal ions and organic moieties. For instance, the closest contact distances between the K⁺ and oxygen atom of the ketone group of keto-acid 121 was determined to be 2.79 Å, whereas the X-ray crystal structure of the Rb⁺ salt showed a distance of 3.43 Å. The similar amounts of product arising from the triplet state were proposed to result from the nearly identical conformations of the potassium and rubidium salts in the solid state. Additionally, it was suggested that intersystem crossing was enhanced by the heavy atoms as a result of the coordination of the metal ions to the ketone oxygen atoms.

This paper also demonstrated the first example of the perturbation of unimolecular photochemical behavior as a result of heavy metal-containing zeolites. Ramamurthy investigated the photophysical behavior and photoproduct distribution of methyl ester 121 in heavy metal-

containing zeolites. The fluorescence and phosphorescence emission intensities were measured, and the photoproduct ratios were determined by gas chromatography. The decrease in singlet lifetime and fluorescence intensities and the increase in the phosphorescence intensities were observed as a result of the heavy atom effect. Furthermore, the photoproduct ratios in the zeolite systems confirmed the effects that the alkali metals exerted on the photorearrangement of the salts in the crystalline state.

7.3. The Photochemistry of Ionic Sensitizer Salts of 2-(1-Cyclopentenyl)cyclopentanone Derivative 121

The employment of ionic sensitizers to bring about triplet state reactions was the next target of investigation. The amines chosen for study were 3-(dimethylamino)propiophenone (136), commercially available as the hydrochloric salt from Aldrich, *p*-acetyl-*N,N*-dimethylbenzylamine (128), a synthesized compound, and 4-acetylpyridine (137), a compound that is obtainable from Aldrich. The selected amines contained an acetophenone group, which is a good sensitizer for most ODPM reactions.¹³⁴ This is important in order to achieve selective excitation of the sensitizer, as it is impossible to use a large excess of a sensitizer in the crystalline state compared to solution state photolysis experiments. Reaction of the keto-amines with keto-acid 121 afforded salts 138, 139 and 140 as white powders. The samples were irradiated in the solid state through a uranium glass filter ($\lambda \geq 330$ nm) at a wavelength where only the aryl ketone of the sensitizer absorbs, followed by acidic work-up and treatment with diazomethane (Figure 7.02).

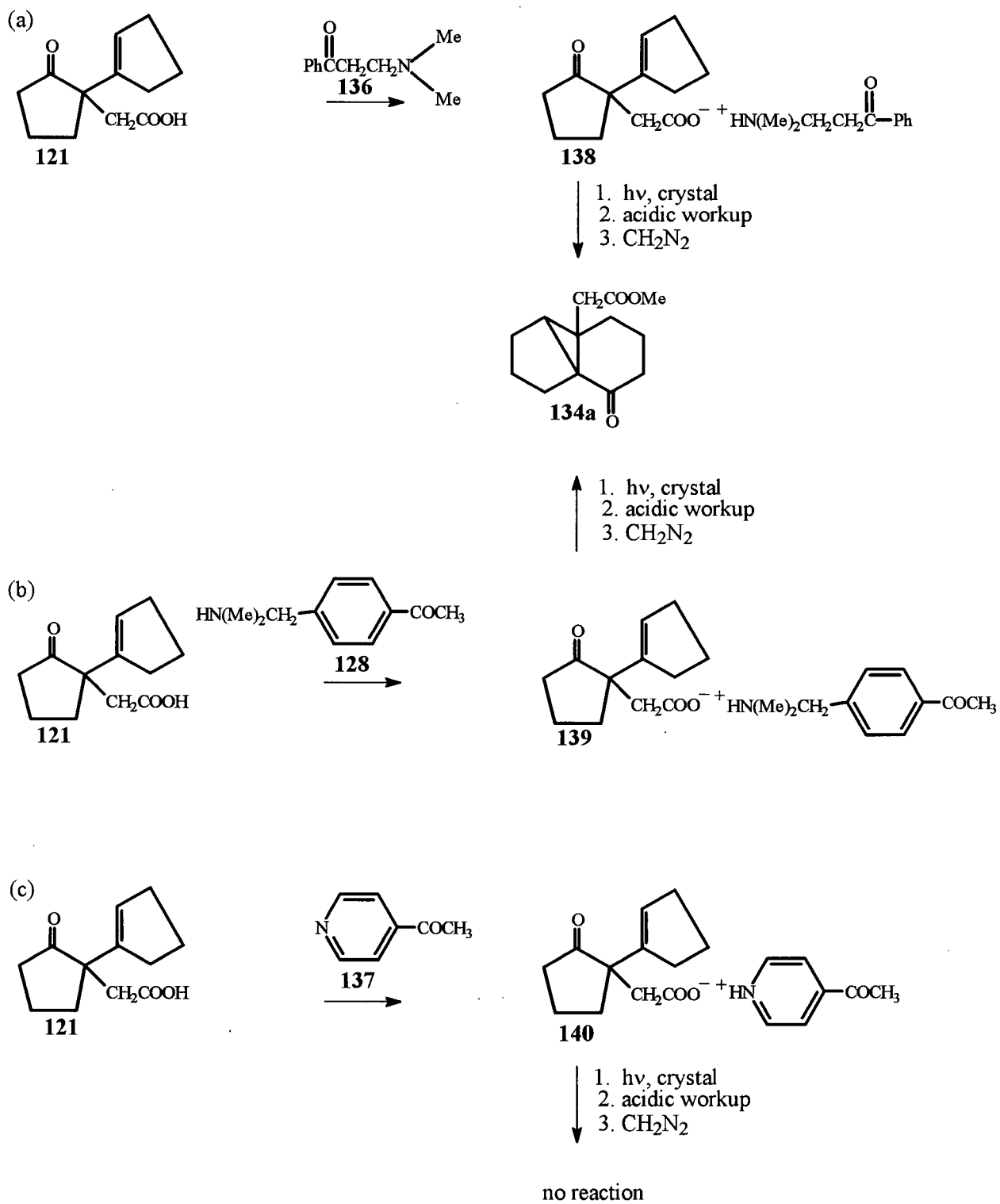


Figure 7.02. Photolysis and Work-Up of Salts 138, 139 and 140.

As shown above (Figure 7.02), amines 136 and 128 acted as ionic sensitizers, giving the ODPM ester 134a exclusively, as no singlet-mediated 1,3-AS reactivity was observed. Only traces of ODPM product 134a could be detected as a result of photolysing salts 138 and 139 in methanol. The solutions were probably too dilute (10^{-2}M) for energy transfer to occur during the excited state lifetime of the sensitizer, as the ionic pair would now be separated. Amine 137, however, did not act as an ionic triplet energy donor, leading to no reaction after irradiation (24 h) both in the solid state and solution. The detailed results of these experiments are summarized in Table XXI (Experimental, p 254). The poor quality of the crystals, even after successive recrystallizations, made it impossible to obtain X-ray crystal structures of salts 138, 139 and 140. This may be attributed to decomposition, possibly, of the sensitizer amine component to the amine oxide. However, the decomposition products were never characterized. Therefore, a correlation between the structures of the individual salts and the reactivity was difficult to establish. Although the potential of utilizing ionic sensitizers to bring about a triplet state reaction in the solid state has been demonstrated by the above examples, the full interpretation of these preliminary results had to be postponed until a more suitable probe molecule could be found.

7.4. The Solution Phase Photochemistry of 1-(1-Cyclohexen-1-yl)-2-oxocyclohexaneacetic Acid (125)

The promising results brought about by the alkali salts of the 5-membered ring keto-acid 121, encouraged us to study its 6-membered counterpart (125).

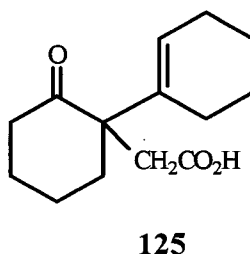


Figure 7.03. 1-(1-Cyclohexen-1-yl)-2-oxocyclohexaneacetic Acid (125).

The photochemistry of 2-(1-cyclohexenyl)cyclohexanone 123a had previously been analyzed by Cookson and Rogers,¹³⁵ who demonstrated that irradiation of a mixture of isomers 123a and 123 in cyclohexane gave cyclobutanol 141 as the major photoproduct (Figure 7.04). Hence, compound 123a undergoes a γ -hydrogen abstraction (Norrish type II reaction). However, irradiation of 123 in acetone yielded only a small amount of cyclobutanol 141, with the major product being the isomer 123a as the result of an α , β to β , γ isomerization. There was no evidence of products arising from 1,3- or 1,2-acyl shifts. Cookson and Rogers later showed¹³⁶ that upon direct irradiation, compound 123 isomerizes to 123a via the lowest excited triplet state, followed by a singlet state reaction to give cyclobutanol 141. The failure of the oxadi- π -methane reaction upon acetone-sensitized irradiation of 123a was believed to result from loss of triplet energy by ring-twisting or reaction from a different inactive lowest triplet state.

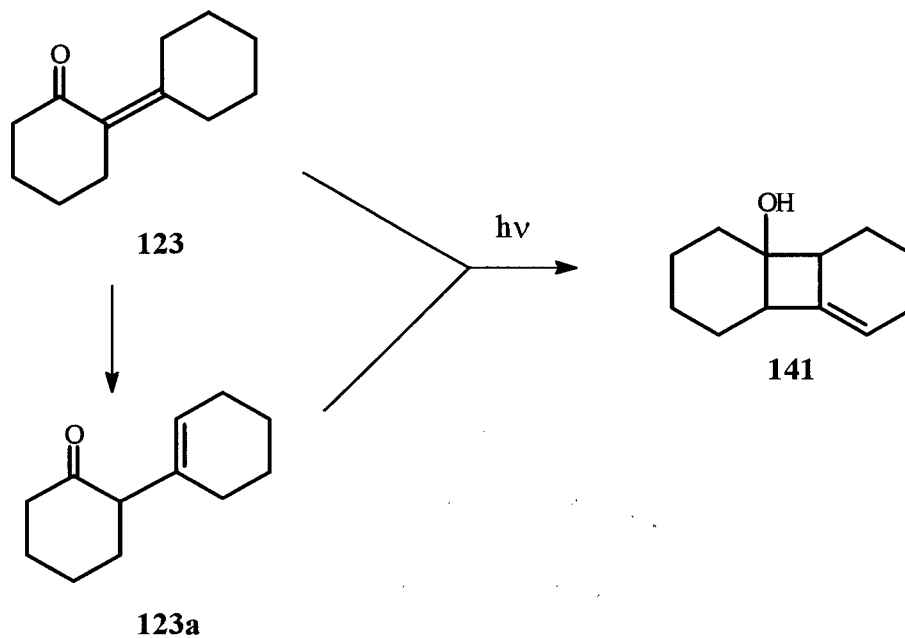


Figure 7.04. Rearrangement of 2-Cyclohexenylidenecyclohexanone (123) and 2-(1-Cyclohexenyl)cyclohexanone (123a).

The direct irradiation of $\beta,\gamma,\beta',\gamma'$ -dienones had been studied by van der Veen and Cerfontain,¹³⁷ whose results revealed that dieneone 142 was photostable at $\lambda \geq 300$ nm. The observed photostability was rationalized in terms of rapid radiationless decay of the excited singlet state, enhanced by CT-interactions between the carbonyl $^1(n,\pi^*)$ state and the homoconjugated 1,4-diene moiety.¹³⁷

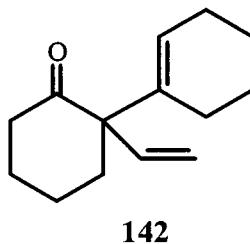


Figure 7.05. Dieneone 142 Studied by Direct Irradiation.

Although these results indicated that the 6-membered ring keto-acid **125** would not react in the same manner as the 5-membered ring keto-acid **121**, keto-acid **125** was nevertheless irradiated in the solid state (Pyrex, $\lambda \geq 290$ nm, 44 h) as well as in acetonitrile or acetone (2 h). The results in solution were analogous to dieneone **142**, as no reaction was observed. An X-ray crystal structure of **125** was obtained in order to determine the distances between the carbonyl oxygen and the γ -hydrogens that could be abstracted (Figure 7.06). The X-ray crystal structure of keto-acid **125** represented in Figure 7.06 shows the most probable orientation of the disordered molecule. The stereodiagram is also given, illustrating intermolecular hydrogen bonding (Figure 7.07).

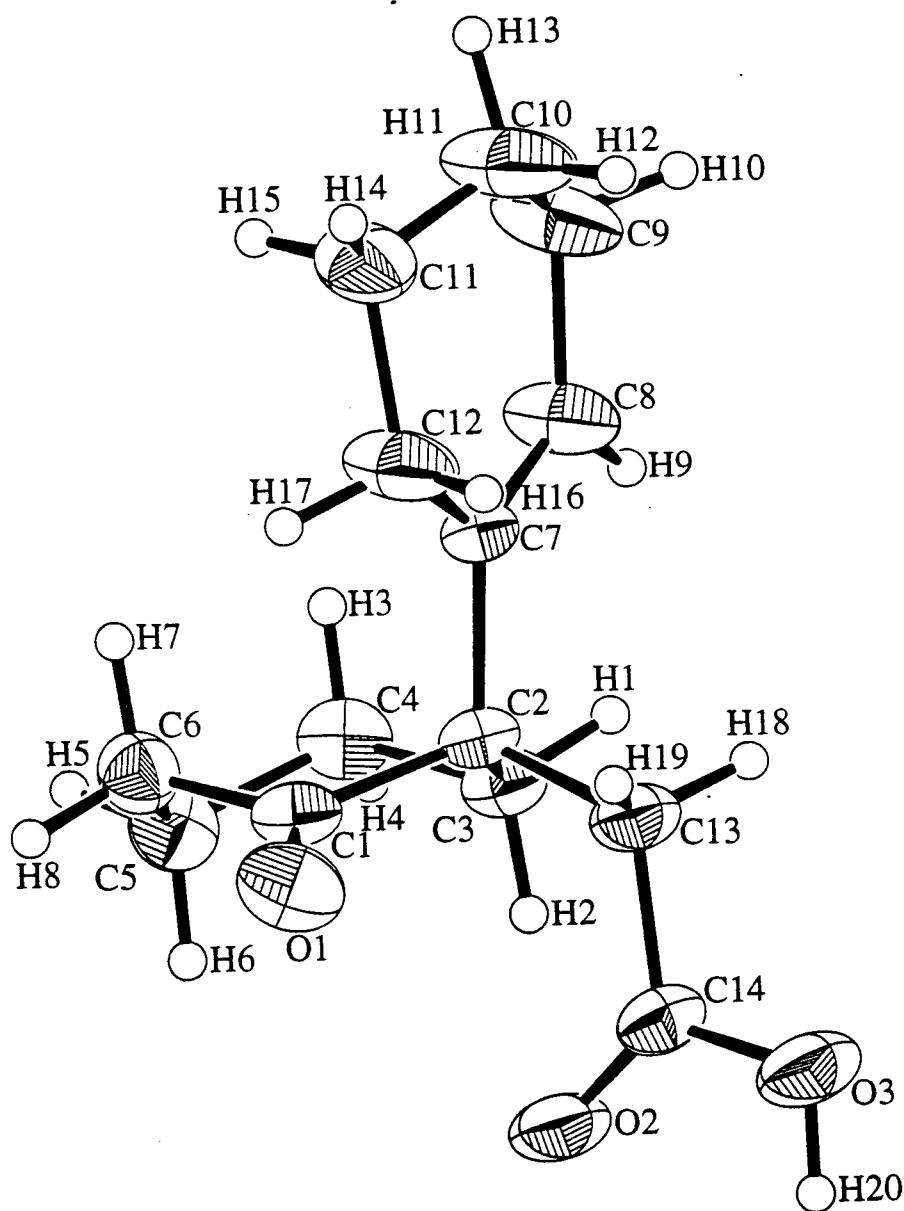


Figure 7.06. X-ray Crystallographic Structure of Keto-Acid 125. Space Group $C2/c$ (#15), $a = 26.516(2) \text{ \AA}$, $b = 6.9831(3) \text{ \AA}$, $c = 18.503(2) \text{ \AA}$, $\beta = 131.394(4)^\circ$, $Z = 8$, $R = 5.2\%$.

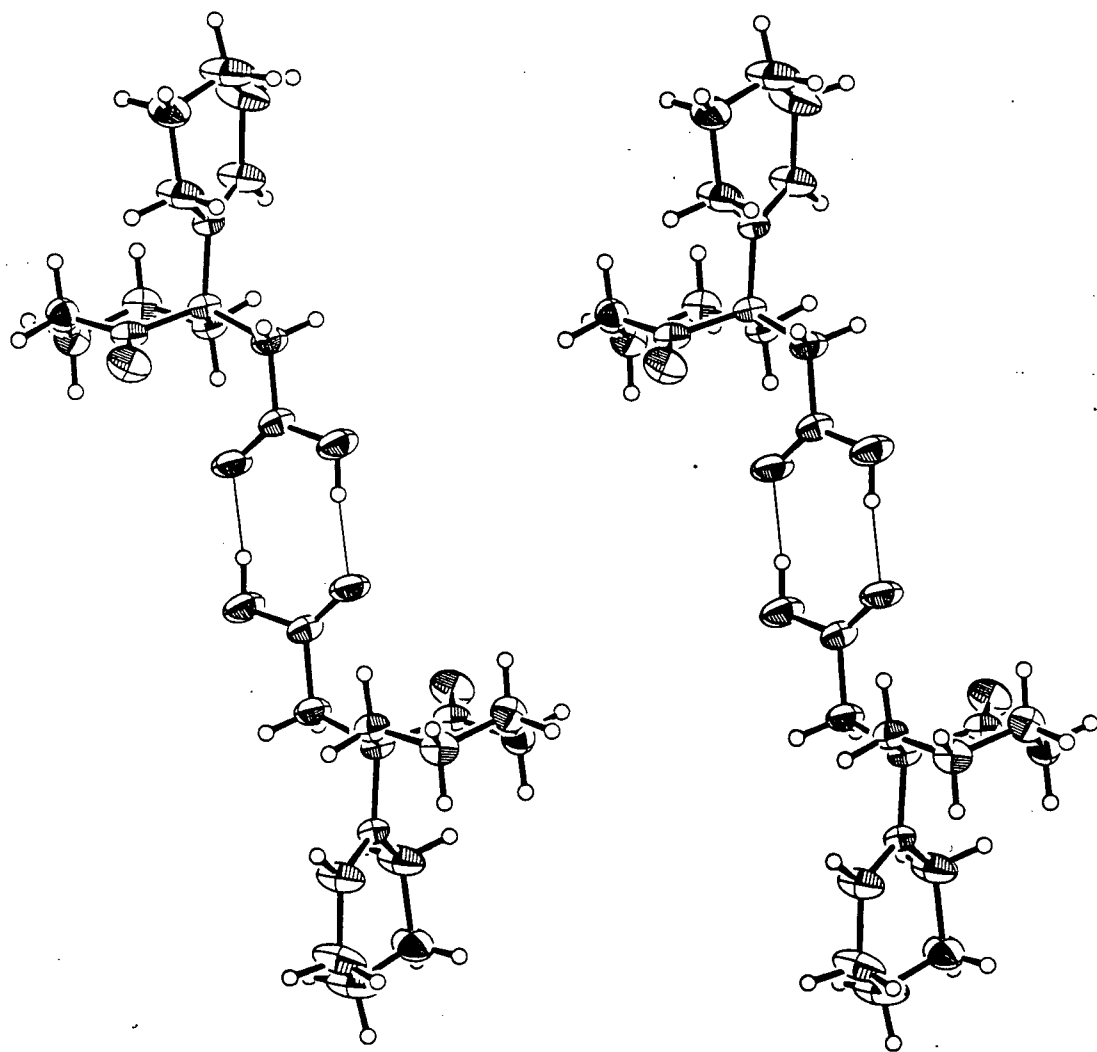


Figure 7.07. Stereo Diagram of Keto-Acid 125, Showing Hydrogen Bonding.

Despite the presence of three potential γ -hydrogens, a closer look at the distances led to only one γ -hydrogen (H17) which was within the proposed abstracting distance of 2.72 \AA^{138} from the oxygen (O1). Table XII shows the abstraction parameters obtained from the X-ray structure of **125** for non-bonded contacts less than 3.60 \AA .

Table XII Hydrogen Abstraction Geometric Parameters for **125**

Oxygen	γ -Hydrogen	d (C=O...H) (Å)	Δ (°)	ω (°)	θ (°)
O1	H17	2.67	64.43	62.25	116.50
O1	H16	3.32	76.45	52.22	76.45

As shown in Table XII, the angle between the carbonyl carbon (C1), the carbonyl oxygen (O1) and γ -hydrogen (H17), defined as Δ , is outside the favorable range of 90 - 120° . The same holds true for the angle ω , representing the degree to which the abstractable hydrogen lies outside the mean plane of the carbonyl group, which has an ideal value of 0° . In addition, angle θ , defined as the angle between the carbonyl oxygen, the γ -hydrogen, and the γ -carbon, which has an ideal parameter of 180° , is also relatively unfavorable. The lack of reactivity of **125** may therefore be explained by these geometric parameters, which do not favor a γ -hydrogen abstraction in the solid state. Hence, to study multiplicity effects in the solid state, a different system had to be chosen, in order to establish structure-reactivity relationships between a particular ionic sensitizer and a probe molecule.

CHAPTER 8 THE PHOTOCHEMISTRY OF

9,10-DIHYDRO-9,10-ETHENOANTHRACENE DERIVATIVES

8.1. Photolysis of 11-Hydroxymethyl-9,10-dihydro-9,10-ethenoanthracene (131)

Monosubstituted dibenzobarrelenes containing a methylene group at one of the vinyl positions were chosen for the study of the heavy atom effect and triplet-triplet energy transfer. In the past, 11-alkyl substituted dibenzobarrelenes have been shown to undergo the di- π -methane rearrangement upon triplet-sensitized irradiation and dibenzocyclooctatetraene formation upon direct irradiation.¹³⁹ Before carboxylic acid-substituted derivatives of the dibenzobarrelene system were prepared, the photochemical behavior of the corresponding hydroxymethyl compound 131 was determined in solution and the solid state.

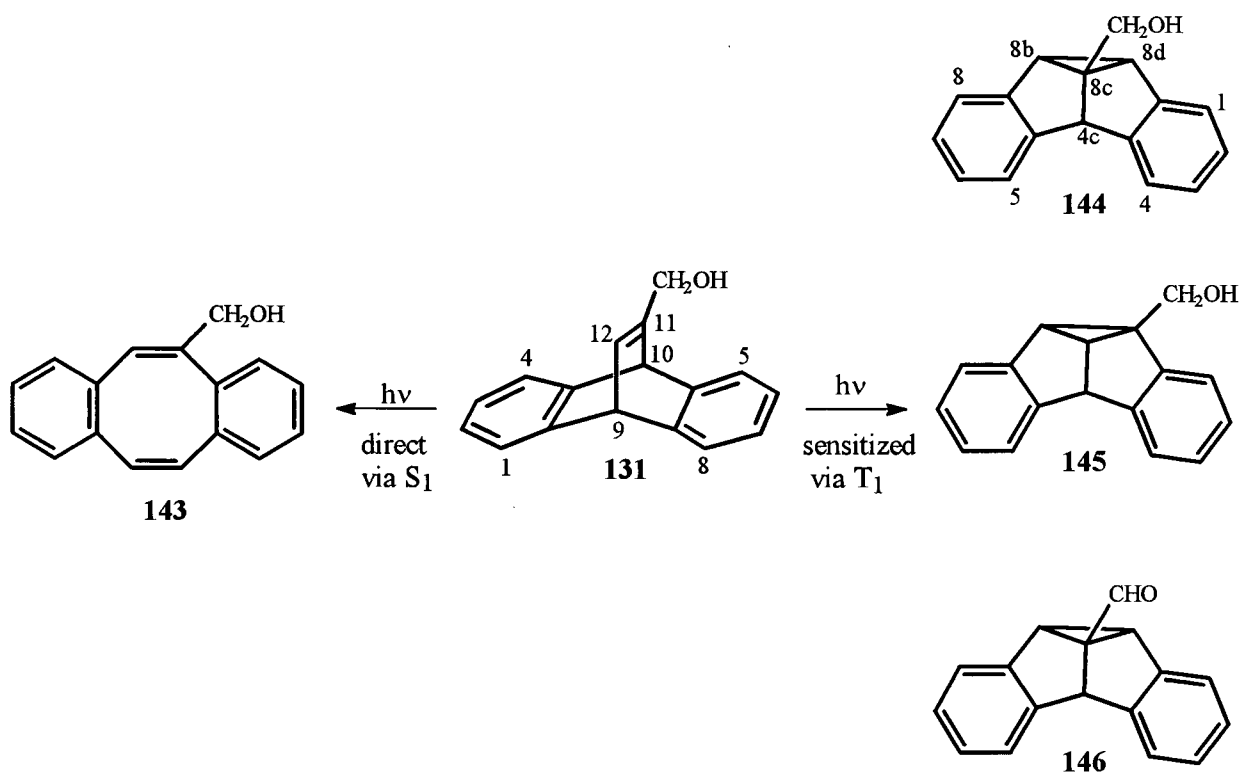


Figure 8.01. Photolysis of Dibenzobarrelene 131.

Direct irradiation of dibenzobarrelene **131** in acetonitrile with the Rayonet Photoreactor (254 nm) led to exclusive formation of the dibenzocyclooctatetraene derivative **143**. However, changing the light source to a 450-W Hanovia lamp equipped with a Vycor filter ($\lambda \geq 240$ nm) resulted in the formation of **143** as well as a small amount of dibenzosemibullvalene regioisomers **144** and **145** (Table XIII). In comparison, triplet-sensitized irradiation of alcohol **131** in acetone through a Pyrex filter ($\lambda \geq 290$ nm) gave the corresponding dibenzosemibullvalene regioisomers **144** and **145**, as well as the dibenzosemibullvalene aldehyde **146**. The aldehyde formation, which occurs only in acetone, may be explained by the presence of the potentially reactive C—H bond α to the oxygen in alcohol **131**. Such oxidation reactions are commonly observed in the liquid phase photochemistry of alcohols, as a result of abstraction by a radical or a photo-activated ketone, which could be acetone in this case.¹⁴⁰ Solid state irradiation of alcohol **131** with the Hanovia lamp gave cyclooctatetraene **143** as the sole product.

Table XIII Photolysis Results of Alcohol **131**^a

Medium (wavelength)	Alcohol 131 (%)	Photoproduct 143 (%)	Photoproduct 144 (%)	Photoproduct 145 (%)	Photoproduct 146 (%)
Acetonitrile ($\lambda \geq 240$ nm)	11	84	4	1	0
Acetonitrile (254 nm)	11	89	0	0	0
Acetonitrile (254 nm)	13	69	0	0	0
Acetone ($\lambda \geq 290$ nm)	0	0	55	34	11
Acetone ($\lambda \geq 290$ nm)	0	0	38	24	6
Solid State ($\lambda \geq 200$ nm)	92	8	0	0	0

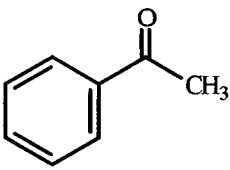
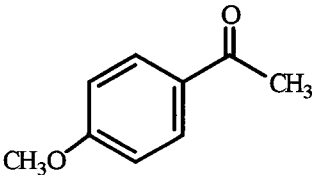
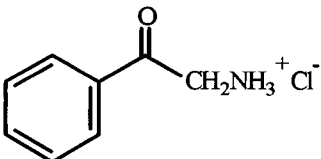
(a) All non-highlighted yields were determined by gas chromatography with an estimated error of $\pm 2\%$. The highlighted rows correspond to isolated yields.

These results differ slightly from the data obtained by Cristol *et al.*,¹⁴¹ who showed that direct (254 nm) irradiation of the corresponding acetate derivative of 131 in acetic acid or benzene led to a 4 : 1 mixture of the acetate derivatives of cyclooctatetraene 143 and semibullvalene 144.

8.2. Triplet-Triplet Energy Transfer in Zeolites

In collaboration with Dr. V. Ramamurthy and co-workers at Tulane University in New Orleans, the triplet state reactivity of alcohol 131 in the presence of a variety of sensitizers was investigated in a zeolitic environment by selectively irradiating through Pyrex ($\lambda \geq 290$ nm). The sensitizers chosen for study were acetophenone (147), *p*-methoxyacetophenone (148) and α -aminoacetophenone hydrochloride (149). The incorporation of the sensitizer and probe molecule 131 within the zeolite cage was achieved by stirring the sensitizer or probe molecule in a hexane solution with zeolite K-Y, followed by filtration, washing with hexane and vacuum drying the complex. Among the numerous naturally occurring and synthetically induced zeolites, zeolite K-Y is one of two synthetic forms of zeolites, X and Y, also known as faujasites, which differ by the typical unit cell composition: X type = $M_{86}(AlO_2)_{86}(SiO_2)_{106} \cdot 264 H_2O$, Y type = $M_{56}(AlO_2)_{56}(SiO_2)_{132} \cdot 253 H_2O$.¹⁴² The K-Y complexes were irradiated in the solid state and as a hexane slurry. Triplet-triplet energy transfer was achieved in all cases, and *p*-methoxyacetophenone (148) proved to be the most effective sensitizer as shown by the increased triplet product formation of 144 and 145 (Table XIV).

Table XIV Zeolite Photolysis Results^a

Medium	Irradiation Medium	Photoproduct 143	Photoproduct 144	Photoproduct 145
KY	slurry ^b	77	19	4
	solid ^c	84	15	1
KY + 	slurry	20	54	26
147	solid	7	65	28
KY + 	slurry	7	59	34
148	solid	<1	54	45
KY + 	slurry	51	21	28
149	solid	32	32	36

(a) All yields were determined by gas chromatography with an estimated error of $\pm 2\%$. The average loading of material in the zeolite was 25, indicating the presence of one sensitizer molecule and one probe molecule for every 25 supercages. These results were obtained by Ramamurthy *et al.* (b) Samples were irradiated for 2.5 h in a suspension of hexane. (c) Samples were irradiated as powders for 20 h.

These results may be explained by the different low-lying triplet states of the sensitizers. Compared to acetophenone, with a low-lying n, π^* triplet state at $26,900 \text{ cm}^{-1}$, the lowest energy state of *p*-methoxyacetophenone is the π, π^* triplet state.¹⁴³ This can be attributed to the methoxy substituent which raises the energy of the n, π^* triplet state to $27,800 \text{ cm}^{-1}$ and lowers the energy

of the π, π^* triplet state ($25,600 \text{ cm}^{-1}$). The π, π^* triplet state is more desirable than the n, π^* triplet state since it is relatively chemically inert towards a photochemical reaction with the acceptor molecule (i.e. alcohol 131), a process that may interfere with triplet-triplet energy transfer. Furthermore, the relatively long radiative lifetime of the π, π^* state of *p*-methoxyacetophenone ($\tau_{\text{rad}} = 0.38 \text{ s}$) versus that of acetophenone ($\tau_{\text{rad}} = 0.005 \text{ s}$) contributes to the ability of compound 148 to be the better sensitizer.¹⁴³ Additionally, the dry powder technique resulted in an enhanced triplet-triplet energy transfer compared to irradiation in the slurry. This may be explained by an increase in triplet lifetime in the solid state or a decrease in mobility between the probe molecule and sensitizer as the zeolite channels are filled with solvent.

8.3. Photolysis of 13-(11-Methyl-9,10-dihydro-9,10-ethenoanthracenyl)succinate (132)

The first carboxylic acid that was chosen for the heavy atom investigation was dibenzobarrelene 132. In order to confirm that this compound would lead to similar photochemical results as alcohol 131, it was irradiated in acetonitrile, acetone and in the solid state. The results are summarized in Table XV.

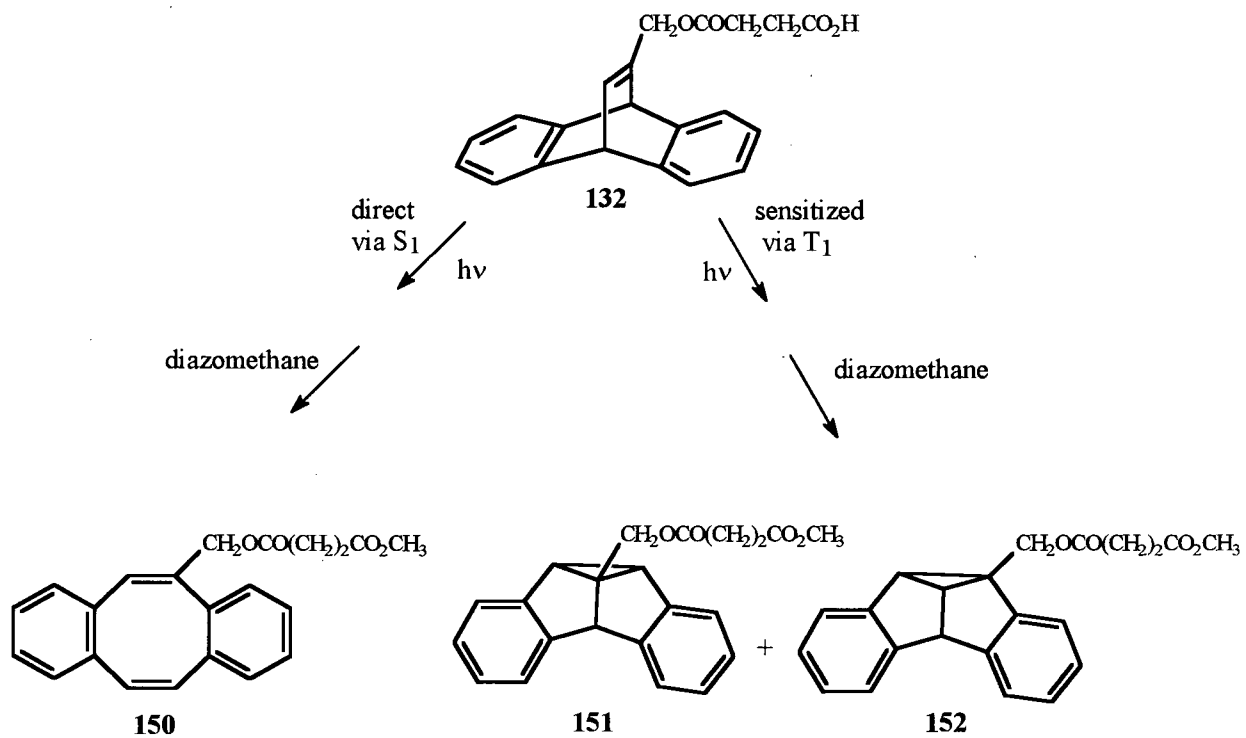


Figure 8.02. Photolysis of Succinate 132.

Table XV Photolysis Results of Succinate 132^a

Medium (wavelength)	Succinate 132 ^b (%)	Photoproduct 150 (%)	Photoproduct 151 (%)	Photoproduct 152 (%)
Acetonitrile ($\lambda \geq 240$ nm)	3	80	17	0
Acetonitrile (254 nm)	3	83	14	0
Acetonitrile (254 nm)	2	66	11	0
Acetone ($\lambda \geq 290$ nm)	5	0	75	11
Acetone ($\lambda \geq 290$ nm)	4	0	58	12
Solid State ($\lambda \geq 240$ nm)	87	6	7	0

(a) All non-highlighted yields were determined by gas chromatography with an estimated error of $\pm 2\%$. The highlighted rows correspond to isolated yields. (b) Succinate 132 was identified as the methyl ester derivative.

The methylated succinate derivative was also subjected to the same photolysis conditions and the results were determined to be equivalent to those of acid 132. As seen from Table XV, direct irradiation of 132 in acetonitrile also produces a small amount of the triplet product semibullvalene 151. Furthermore, the reaction in the solid state results in an almost equal distribution of the singlet and triplet products.

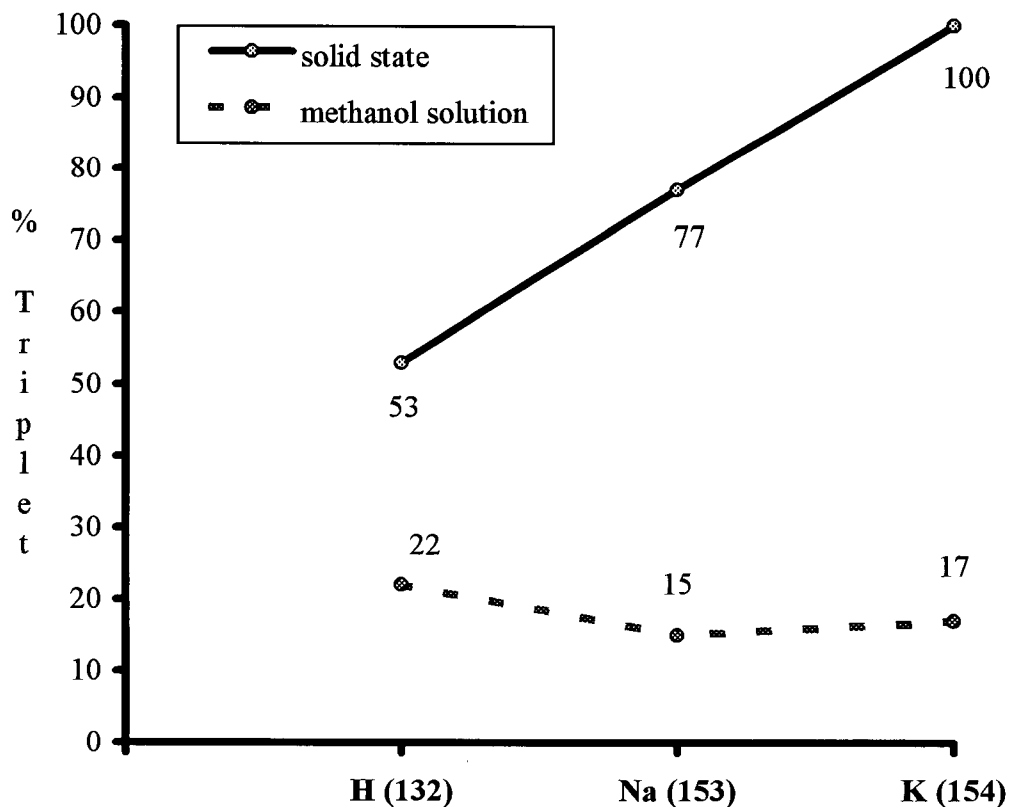
8.4. The Heavy-Atom Effect in the Photochemistry of Succinate 132

Difficulties arose in the preparation of the alkali metal salts of succinate 132, as the side chain had a tendency to cleave during treatment with sodium or potassium hydroxide. Milder conditions had to be applied, and the salts were formed by mixing equimolar amounts of sodium

or potassium bicarbonate with succinate 132. Graph I represents the results of irradiation of the sodium and potassium salts in the solid state and in solution. The cations have a significant effect on the reaction in the crystalline state, leading to a product distribution favoring the triplet-derived dibenzosemibullvalene regioisomers 151 and 152. This behavior can be attributed to an increase in the rate of intersystem crossing from S_1 to T_1 resulting from enhanced spin-orbit coupling. In solution, however, no significant effect was observed. As the salts are solvated and separated in the methanol solution, the heavy atom effect is expected to be weak, as it operates only over relatively short distances as shown by Chandra *et al.*¹⁴⁴

X-ray crystal structures of the sodium and potassium salts could not be obtained due to the amorphous, hygroscopic quality of the solids obtained.

Graph I Irradiation Results of Alkali Salts of Succinate 132



8.5. Photolysis of 13-(11-Methyleneoxy-9,10-dihydro-9,10-ethenoanthracenyl)acetic Acid (133)

As a result of the limitations inherent in the use of acid 132, a different side chain had to be utilized, which would be able to withstand treatment with alkali hydroxides, and later amines to make sensitizer salts. Dibenzobarrelene derivative 133 was prepared and subjected to irradiation experiments in solution and the solid state in order to determine the photoproducts. The results of

irradiation in solution were analogous to those found for dibenzobarrelene **132**. However, in the solid state, less triplet-derived semibullvalene **156** and **157** formed, resulting in an increase of singlet-derived cyclooctatetraene **155** (Table XVI).

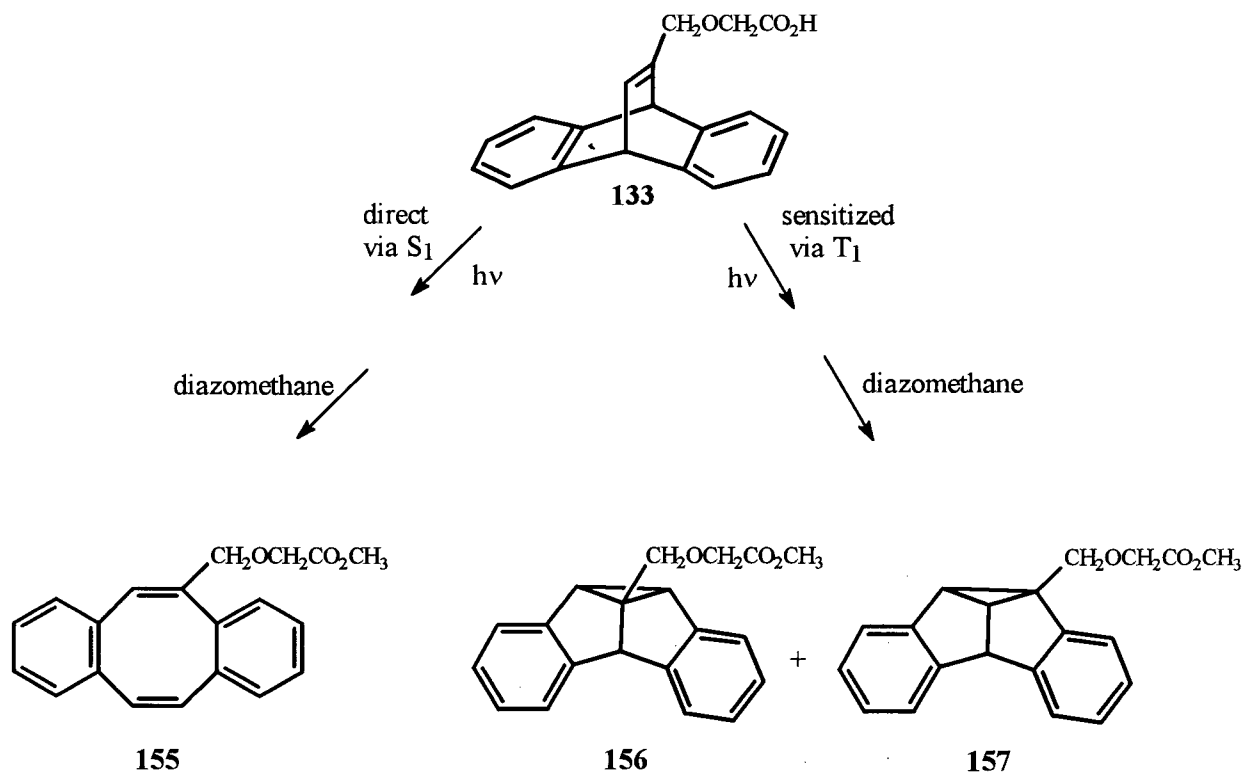


Figure 8.03. Photolysis of Acetic Acid Derivative **133**.

Table XVI Photolysis Results of Acetic Acid 133^a

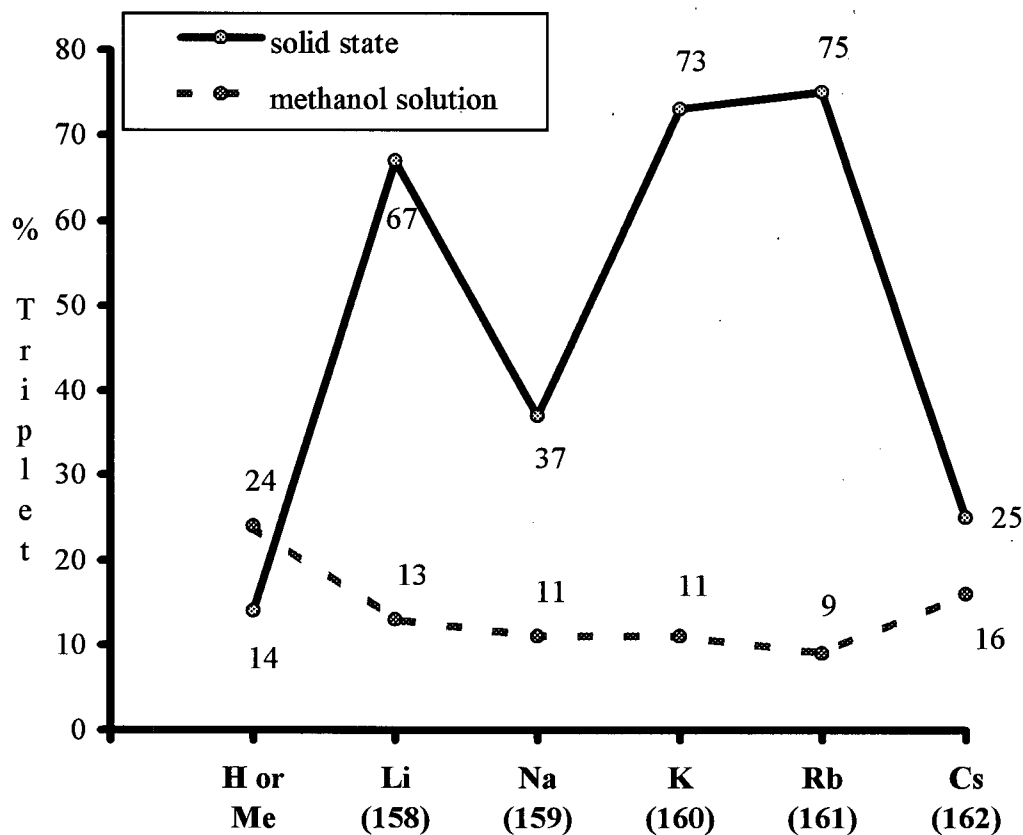
Medium (wavelength)	Acid 133 ^b (%)	Photoproduct 155 (%)	Photoproduct 156 (%)	Photoproduct 157 (%)
Acetonitrile ($\lambda \geq 240$ nm)	0	76	21	3
Acetonitrile (254 nm)	0	77	23	0
Acetonitrile (254 nm)	0	40	10	0
Acetone ($\lambda \geq 290$ nm)	0	0	72	28
Acetone ($\lambda \geq 290$ nm)	0	0	46	15
Solid State ($\lambda \geq 240$ nm)	93	6	1	0

(a) All non-highlighted yields were determined by gas chromatography with an estimated error of $\pm 2\%$. The highlighted rows correspond to isolated yields. (b) Acid 133 was identified as the methyl ester derivative.

8.6. The Heavy-Atom Effect in the Photolysis of Acetic Acid Derivative 133

The Li⁺, Na⁺, K⁺, Rb⁺ and Cs⁺ salts of acid 133 were prepared from the corresponding alkali hydroxides and subjected to direct photolysis (Vycor, $\lambda \geq 240$ nm) both in the crystalline state and as a methanol solution. Graph II is a representation of the irradiation results (2 h), showing the combined percentage of triplet-derived photoproducts 156 and 157.

Graph II Irradiation Results of Alkali Salts of Acetic Acid 133



The results summarized in Graph II reveal a strong cation effect in the solid state, but not in solution, similar to the earlier findings with succinate 132. This demonstrates again that in solution, the interaction or association between alkali ions and the organic substrate is reduced significantly, hence affecting the photochemical behavior of the probe molecule. Contrary to predictions,¹⁴⁵ the greatest perturbation of the photoproduct ratio does not result from the salt with the heaviest alkali metal ion. The lithium cation, even though it is not a heavy atom, led to a large increase in triplet-derived product formation, whereas the cesium cation effect is less than that due to rubidium. It is possible that these unexpected results may be due to differences in the

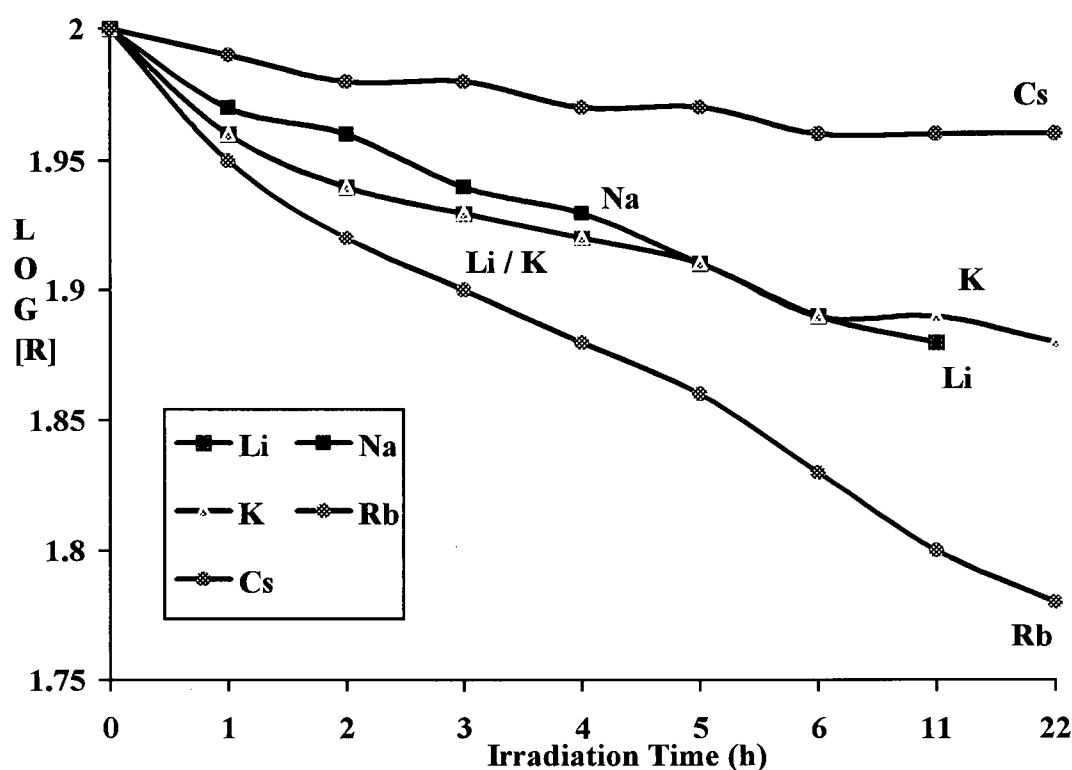
distances and orientations between the metal ions and organic moieties in the crystal structures of the salts. This concept was supported by Scheffer *et al.*¹⁴⁶ who interpreted the X-ray structures for the potassium and rubidium salts of keto-acid 121 (Figure 7.01). Hence, the observed enhancement of ISC may be explained by the more favorable positioning of the Li^+ cation in salt 158, compared to the Cs^+ ion with respect to the probe molecule 133. The deviation of these results may depend on the orientation of the heavy atom with respect to the chromophore orbital.

Another factor that could contribute to the enhanced triplet-derived product formation, apart from the heavy atom effect, could be the manner of coordination between the metal ions and the ethenoanthracene carbonyl oxygen. Triplet enhancement resulting from a lithium cation was also observed by Ramamurthy *et al.*¹⁴⁷ who investigated the Norrish type I and II reactions of macrocyclic ketones in the cavities of alkali metal-containing zeolites. The lithium cation was believed to bind more strongly to the carbonyl chromophore. Hence, the electronic interaction between the cation and the probe molecule is of importance. The strength of the bonding interaction between the cation and probe molecule is suggested by Anpo *et al.*¹⁴⁸ to be directly dependent on the charge density or electrostatic potential of the cation. The electrostatic potential in e/r (charge/radius) decreases with increasing atomic number of the cation (Li^+ (1.67), Na^+ (1.05), K^+ (0.75), Rb^+ (0.67) and Cs^+ (0.59)).¹⁴⁸ Ramamurthy *et al.*¹⁴⁹ demonstrated that higher charge densities (i.e. charge per unit volume of the cation) led to stronger binding (ΔH binding: Na^+ , 14.9; K^+ , 11.0; Cs^+ , 7.9 kcal mole⁻¹). In this case, the light Li^+ atom would have more influence on the reaction than the heavier Cs^+ atom. This is known as the light atom effect.¹⁴⁹ Anpo *et al.*¹⁴⁸ have also observed that the phosphorescence lifetimes of xanthone molecules in

alkali-metal cation-exchanged Y-zeolites are affected by the cations. The singlet-triplet transitions were proposed to be affected by alkali metal cations resulting in a prolongation of the lifetimes of the excited triplet states in the order Li^+ (0.30 s), Na^+ (0.28 s), K^+ (0.15 s), Rb^+ (0.04 s) and Cs^+ (0.03 s). Applying this observation to acid 133, the presence of the Li^+ cation may lead to a longer triplet lifetime, hence increasing the di- π -methane rearrangement product formation.

The conversion of each reactant to photoproducts was kept below 15%, as a result of 2 h of irradiation, in order to minimize changes in the crystal environment, which may lead to altered reaction selectivity. However, the photolysis experiments were conducted over a period of 22 h (Graph III) in order to detect any changes in the reaction rate resulting from changes in the crystal structure. All alkali salts followed approximately a first-order plot indicating a constant rate of conversion with time.

Graph III Conversion versus Irradiation Time Experiments

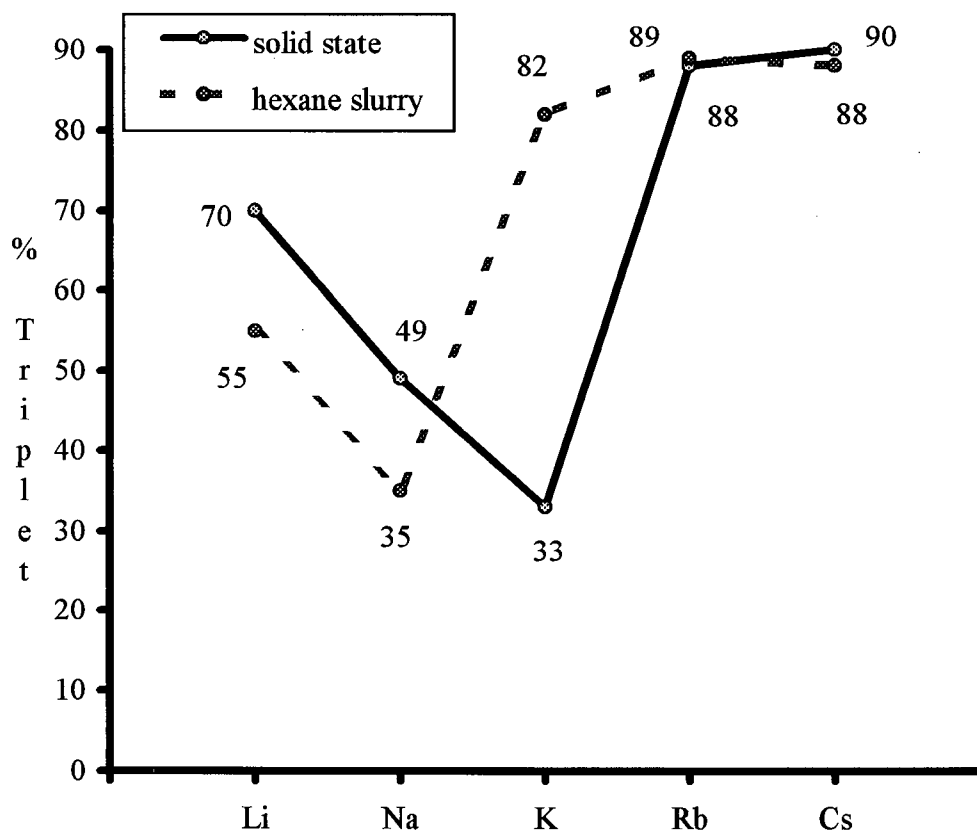


R is the percentage of starting material remaining at the different irradiation time intervals.

To confirm the heavy atom effect results, the photochemistry of the methyl ester of 133 was also investigated in alkali metal-containing zeolites in collaboration with Ramamurthy *et al.* The photochemical outcome in M^+X zeolites in the solid state or in a hexane slurry verified the strong effect earlier observed for the Li^+ cation. Overall, the results in the slurry display a similar trend in triplet product formation as shown previously (Graph II). However, in the solid state in the zeolites, the K^+ cation only exerts a minute heavy atom effect on the ester of 133. The solid state reactions in the zeolites were carried out over 20 h compared to 2 h of photolysis of the

alkali salts. However, the irradiation of the ester of 133 as a slurry in the heavy metal containing zeolites was performed over a period of 2.5 h, leading to somewhat more comparable results.

Graph IV Irradiation Results of Methyl Ester of Acid 133 in Alkali-Containing Zeolites



8.7. Structure Elucidation of Cyclooctatetraene and Semibullvalene Photoproducts

All photoproducts were isolated and fully characterized by spectroscopic and analytical methods. The ^1H NMR spectra of the cyclooctatetraene photoproducts **143**, **150** and **155** are quite similar, differing only in the side-chain. The aromatic hydrogens appear as a multiplet integrating for eight hydrogens between δ 7.20 and 7.00 ppm. The vinyl hydrogens closest to the side chain are represented by a broad singlet at δ 6.8 ppm. For alcohol **143** and succinate **150**, the remaining two vinyl hydrogens, appear as an AB system ($J = 12$ Hz) at δ 6.78 ppm. The coupling interaction between these chemically inequivalent protons results in the splitting by the adjacent protons. In the case of acid **155**, the vinyl protons give a singlet at δ 6.72 ppm, indicating that they are chemical shift equivalent. The multiplicity of the CH_2O -group at the vinyl position of the three distinct cyclooctatetraenes also differs. An AB system ($J = 14$ Hz) is observed in the spectra of alcohol **143** and acid **155** at δ 4.42 ppm and δ 4.39 ppm respectively, compared to a doublet ($J = 1$ Hz) in the spectrum of succinate **150** at δ 4.88 ppm. This doublet may actually be an AB system with the outer transitions being indistinguishable from the noise of the base line of the spectrum. Structure determination of cyclooctatetraene has shown that the molecule is tub-shaped,¹⁵⁰ and NMR studies have revealed that two dynamic processes may occur in solution, namely a conformational flip or π -bond migration (Figure 8.04).¹⁵¹ More recently, Paquette *et al.*¹⁵² have investigated the dynamics of conformational mobility of chiral cyclooctatetraenes. As a result of the substituents, the tub-shaped cyclooctatetraene derivatives **143**, **150** and **155** become chiral molecules with no plane of symmetry. Hence, the pair of hydrogens in the CH_2O -group which give rise to the AB system can be interpreted as two diastereotopic geminal hydrogens.

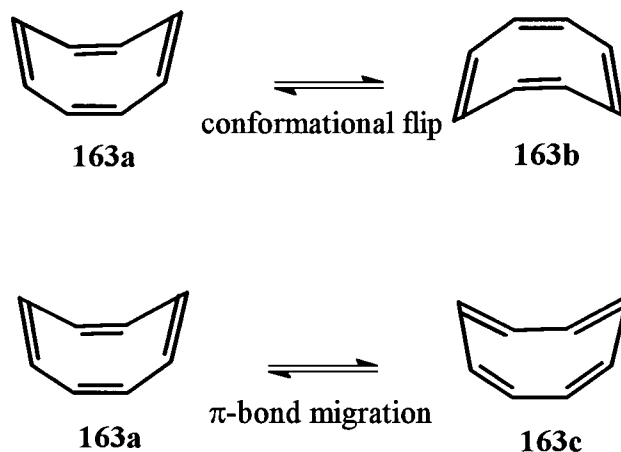


Figure 8.04. Tub-shape of Cyclooctatetraene (163a).

The ^1H NMR spectra of photoproducts 144, 151 and 156 are typical of the dibenzosemibullvalene skeleton. The multiplets in the region δ 7.25-6.85 ppm are assigned as the aromatic hydrogens. The pentalene hydrogens at carbons 4b, 8b and 8d respectively appear as two singlets in the ratio 1 : 2 at δ 4.5 ppm and δ 3.05 ppm. The spectrum of aldehyde 146 is similar to the spectrum of semibullvalene 144, differing only in the aldehyde peak at δ 9.24 ppm. The structure of the aldehyde was further confirmed by the IR spectrum with a carbonyl peak at 1686 cm^{-1} and the aldehyde C-H stretch at 2831 cm^{-1} .

The ^1H NMR spectra of the regioisomers **145**, **152** and **157** vary slightly as a result of the loss of symmetry of the semibullvalene. The aromatic hydrogens produce a multiplet centered around δ 7.36 ppm representing one hydrogen and a multiplet corresponding to the remaining seven aromatic hydrogens centered at δ 7.18 ppm. The pentalene hydrogens are assigned as a doublet ($J = 6$ Hz, H_{4b}) at δ 4.5 ppm, a triplet near δ 3.5 ppm ($J = 6$ Hz, H_{8c}) and a doublet at δ 3.14 ppm ($J = 6$ Hz, H_{8b}). The CH_2O -group at carbon 8d is represented by an AB system ($J = 12$ Hz) indicating that the protons are diastereotopic.

CHAPTER 9 TRIPLET-TRIPLET ENERGY TRANSFER IN A TWO-COMPONENT CRYSTALLINE SYSTEM

9.1. Photochemical Results Upon Irradiation of Salts 164, 166 and Complex 165

After establishing the photochemical reactivity of carboxylic acid derivative 133 in solution and the solid state, amines linked to a sensitizer moiety were selected in order to study triplet-triplet energy transfer in the resulting crystalline organic salts.

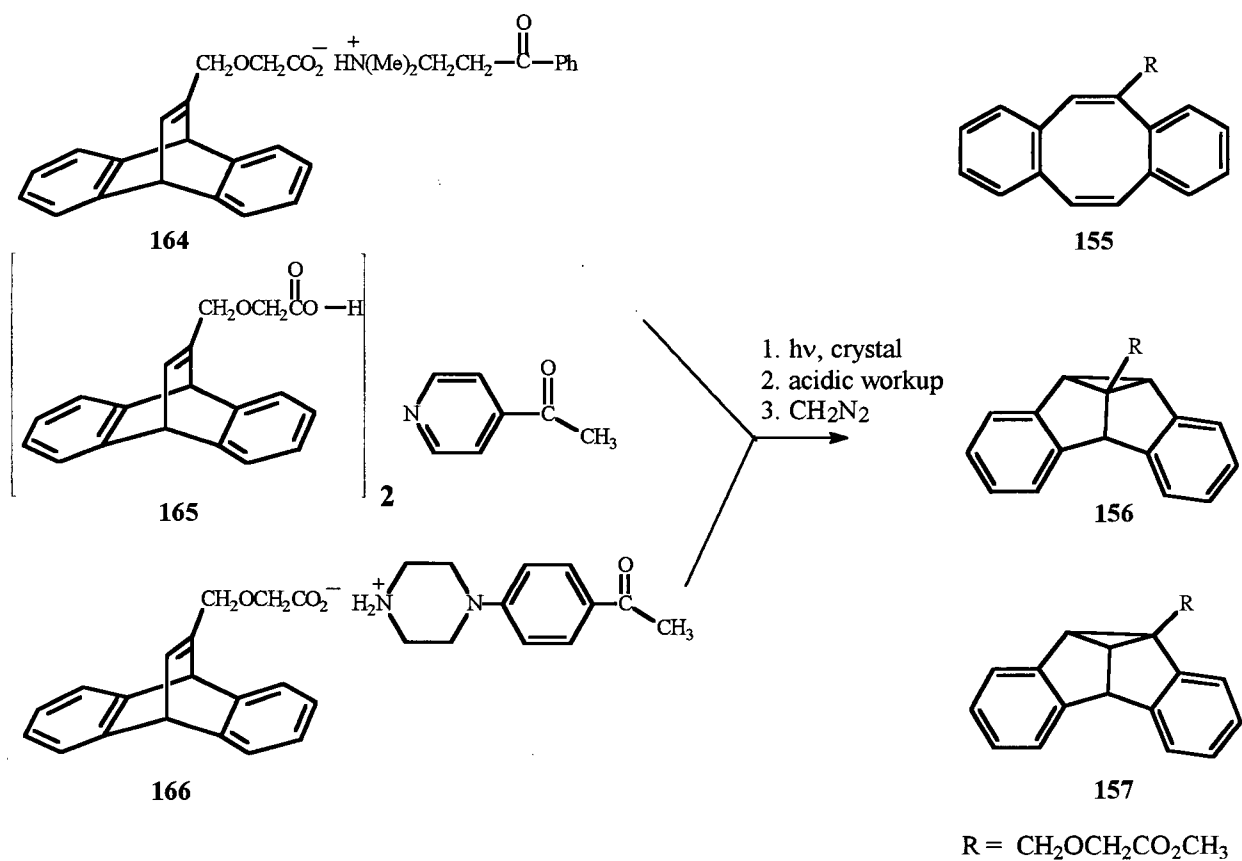


Figure 9.01. Photolysis of Salts 164, 166 and Complex 165.

The selected amines were chosen on the basis of possessing an acetophenone moiety and their commercial availability from Aldrich. These included 3-(dimethylamino)propiofenone (136), 4-acetylpyridine (137) and 4'-piperazinoacetophenone (167). The salts 164, 166 and complex 165 were prepared as described in the Experimental Section (p 218-222) by adding equimolar amounts of acid 133 dissolved in ethyl acetate to the selected amines in ethanol.

Irradiation of salts 164, 166 and complex 165 in methanol through a uranium glass filter ($\lambda \geq 330$ nm) led to the detection of 1-2% of photoproducts 156 and 157 after 6 h, following work-up. The extent of dilution (10^{-2} M) may account for the reduced efficiency of the energy transfer between the sensitizer and the probe molecule. The amine-containing acetophenone moiety, functioning as the sensitizer (donor), and the dibenzobarrelene operating as a quencher (acceptor), must be in close proximity for the triplet-triplet energy transfer to take place. Quenchers are known to accelerate the deactivation of the excited state, suppressing the photochemical reaction.¹⁵³ The relationship between quantum yields and quencher concentrations is given by the Stern-Volmer equation.¹⁵⁴ A plot of quantum yields in the absence (Φ°) and presence (Φ) of the quencher versus the concentration of the quencher should lead to a straight line with a slope of $k_q\tau$, where k_q is the quenching constant and τ the lifetime of the excited donor molecule.

$$\frac{\Phi^{\circ}}{\Phi} = 1 + k_q \tau [Q]$$

Figure 9.02. Stern-Volmer Equation.

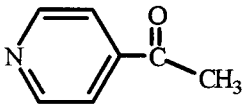
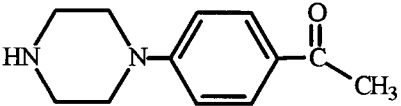
The quenching constant (k_q) is usually assumed to be diffusion-controlled.¹⁵⁵ If the lifetime of the donor is relatively short-lived, the concentration of the quencher will need to be higher to lead to efficient quenching, assigning the common value of 10^{10} l/mol s to the quenching constant (k_q).¹⁵⁶ This is illustrated by Table XVII, which suggests that quencher concentrations of greater than 10^{-3} M lead to quenching of all species with a lifetime longer than 10^{-5} s. Hence, in solution the quencher (dibenzobarrelene component) concentration is assumed to be too dilute to give rise to an efficient energy transfer during the excited state lifetime of the sensitizer (acetophenone moiety).

Table XVII Relationship between the Lifetime and Concentration of a Quencher that will lead to > 99% Quenching

Lifetime (τ) of D* (s)	Quencher Concentration (M)
10^{-9}	10
10^{-8}	1
10^{-7}	0.1
10^{-6}	10^{-2}
10^{-5}	10^{-3}
10^{-4}	10^{-4}
10^{-3}	10^{-5}

Solid state photolysis of the two salts 164, 166 and the complex 165 resulted in the exclusive formation of photoproducts 156 and 157 (Table XVIII). A control experiment showed that dibenzobarrelene 133 does not react under the same irradiation conditions in the solid state.

Table XVIII Solid State Photolysis Results of Salts 164, 166 and Complex 165^a

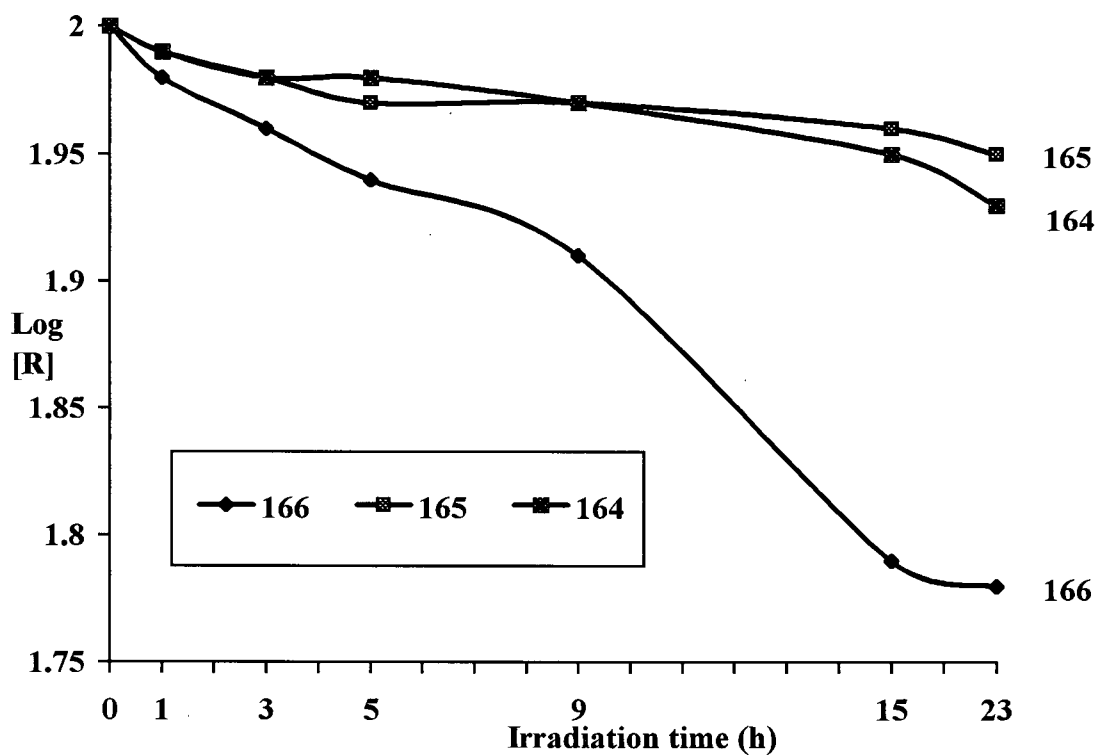
Sensitizer	Salt or Complex	Sensitizer : 133 Ratio	Photolysate Composition (%)			
			133 ^b	156	157	155
$\text{Ph}-\overset{\text{O}}{\parallel}{\text{C}}-\text{CH}_2\text{CH}_2\text{N}(\text{CH}_3)_2$ <p style="text-align: center;">136</p>	164	1 : 1	93	6	1	0
 <p style="text-align: center;">137</p>	165	1 : 2	94	5	1	0
 <p style="text-align: center;">167</p>	166	1 : 1	81	15	4	0

(a) All yields were determined by gas chromatography with an estimated error of $\pm 2\%$. (b) Compound 133 was identified as the methyl ester derivative.

A comparison of the results between salt 164 and complex 165 suggests that the ratio between the probe molecule and sensitizer does not seem to affect the efficiency of the triplet-triplet energy transfer. However, further experimentation in this area is needed.

Conversions were kept below 20% in order to minimize the possibility of melting the sample. The reaction was monitored over 23 h and the conversion of starting material is illustrated in Graph V. Salt 166 was the most reactive. In order to achieve consistent results, the reaction time was kept at 9 h. After this time, a slight increase of reactivity of 166 was observed. These results may suggest possible melting of the crystal, a process that would bring about an increase in conversion as a result of fewer physical restraints in the crystal lattice.

Graph V Reactant Conversion of Salts 164, 166 and Complex 165 versus Irradiation Time



R is the percentage of starting material remaining at the different irradiation time intervals.

9.2. Structure-Reactivity Analysis of Salts 164, 166 and Complex 165

Triplet-triplet energy transfer between the sensitizer and probe molecule clearly occurred in the solid state in all three cases as illustrated by Table XVIII. Furthermore, amine 167 proved to be the most effective sensitizer. In order to help understand the triplet-triplet energy transfer between the sensitizers and probe molecule, the X-ray crystallographic structures of the two salts and one complex were examined. In principle, the orientation of the sensitizer amine relative to the probe molecule should be important for the energy transfer process and is represented by the stereoviews and packing diagrams of salts 164, 166 and complex 165 (Figures 9.03-9.05). The stereoviews illustrate the position of the aromatic ring of the sensitizer with respect to the ethenoanthracene double bond. The orientation is most favorable in the case of salt 166, where the aromatic ring of the sensitizer points directly at the ethenoanthracene double bond of the probe molecule with a center-to-center distance of only 4.11 Å. The packing diagrams also show the ratio of probe molecule to sensitizer amine within the crystal, which is one to one for salts 164 and 166 and two to one for complex 165.

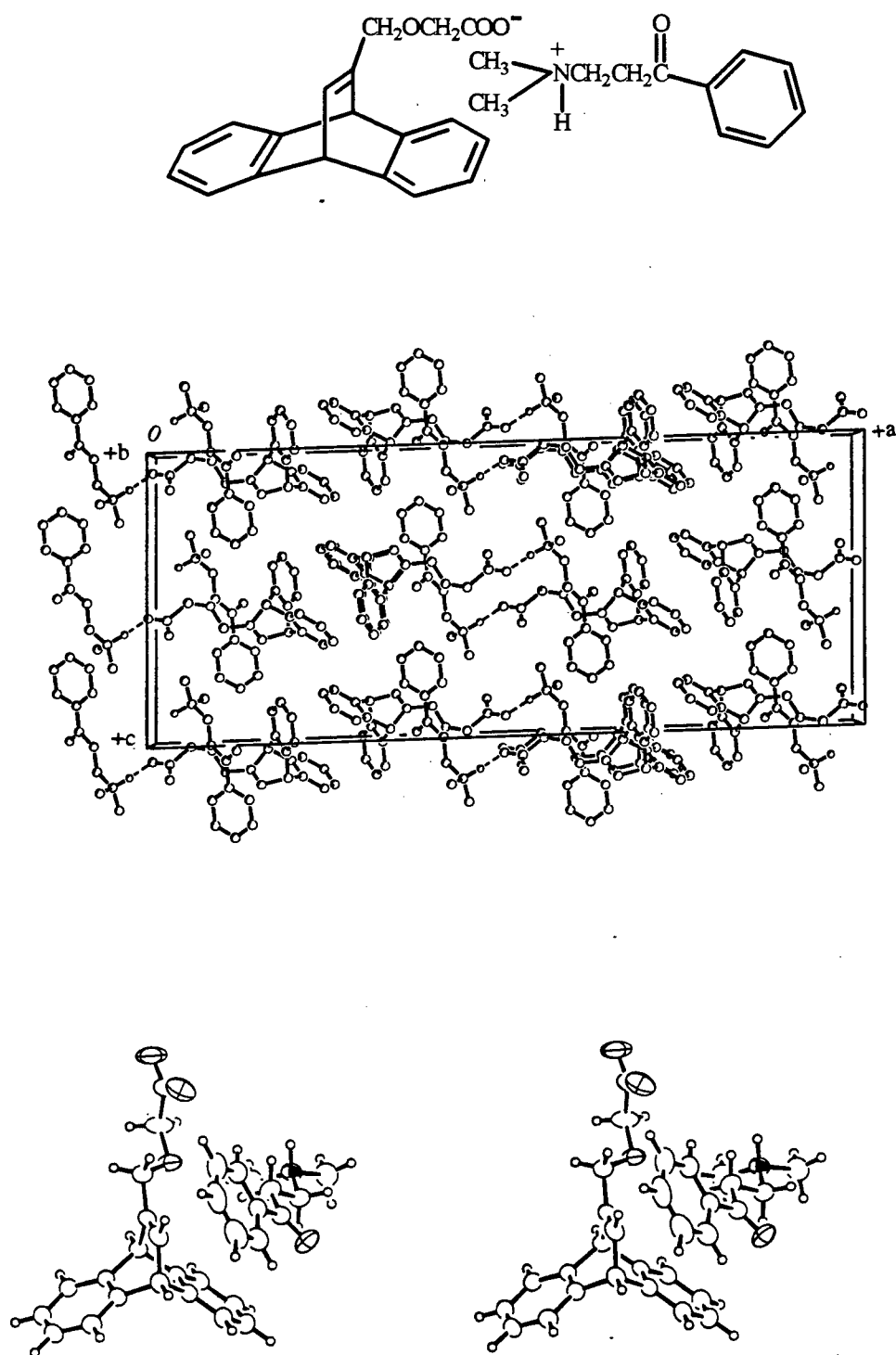


Figure 9.03. Packing Diagram and Stereoview of Salt 164. Space Group $C2/c$ (#15), $a = 37.712(3) \text{ \AA}$, $b = 8.977(1) \text{ \AA}$, $c = 15.922(1) \text{ \AA}$, $\beta = 92.055(6)^\circ$, $Z = 8$, $R = 4.5\%$.

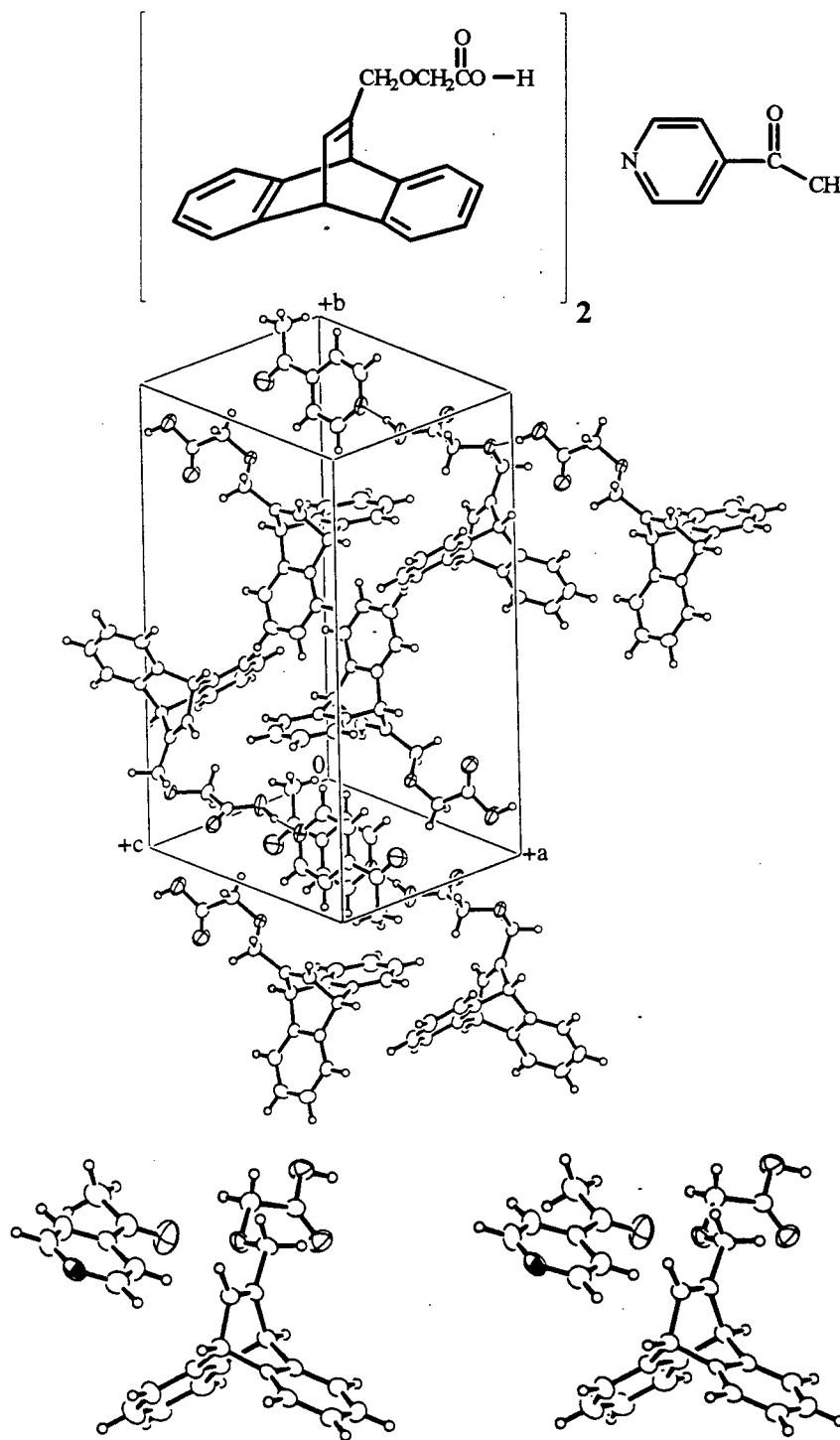


Figure 9.04. Packing Diagram and Stereoview of Complex 165. Space Group $P\bar{1}$ (#2), $a = 12.344(1) \text{ \AA}$, $b = 18.439(3) \text{ \AA}$, $c = 8.2721(7) \text{ \AA}$, $\alpha = 101.789(9)^\circ$, $\beta = 94.525(8)^\circ$, $\gamma = 95.05(1)^\circ$, $Z = 2$, $R = 5.1\%$.

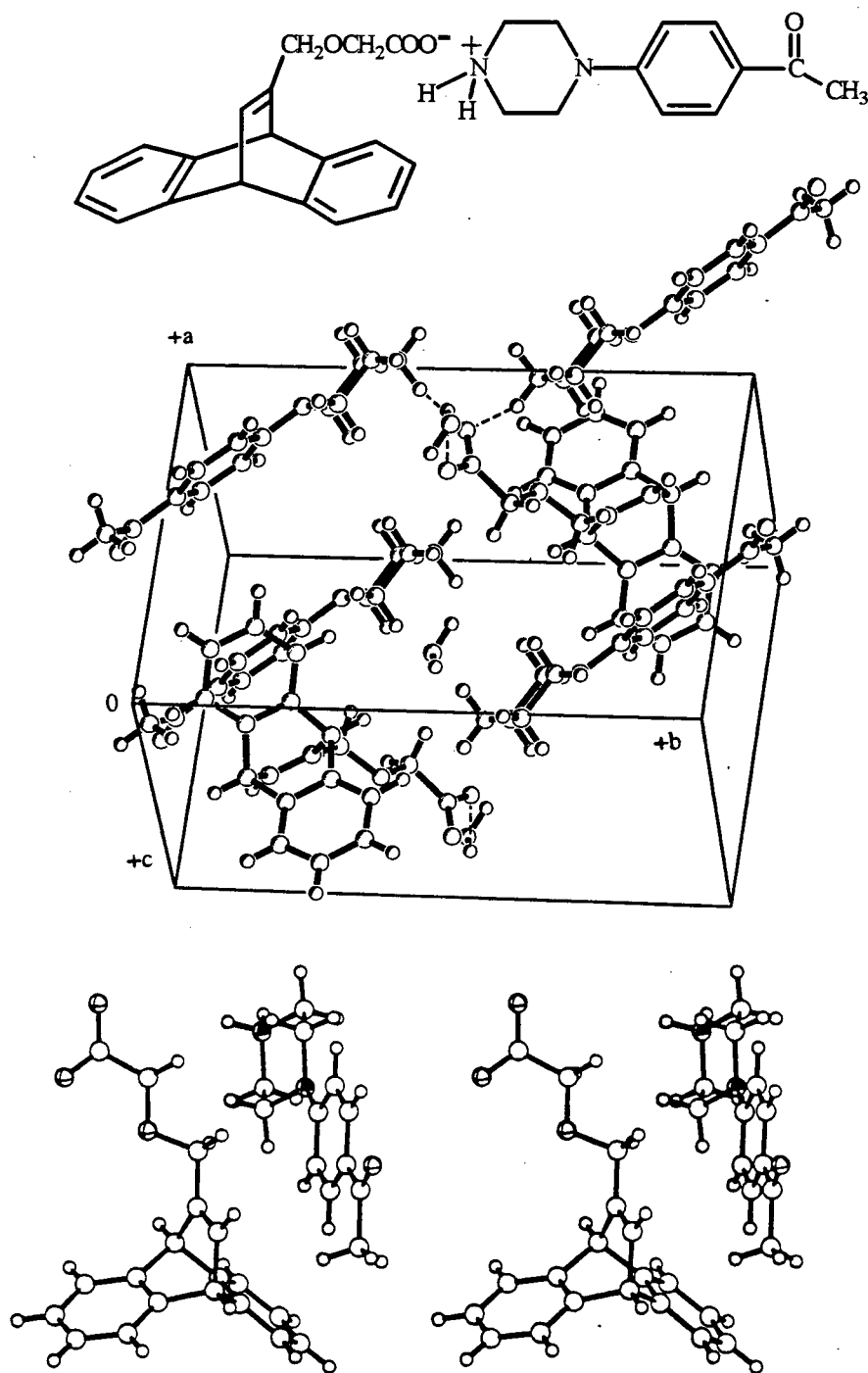
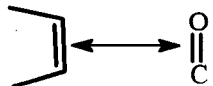
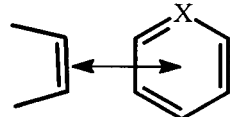


Figure 9.05. Packing Diagram and Stereoview of Salt 166. Space Group $P\bar{1}(\#2)$, $a = 9.760(1)$ Å, $b = 16.254(2)$ Å, $c = 9.114(1)$ Å, $\alpha = 99.47(1)^\circ$, $\beta = 109.17(1)^\circ$, $\gamma = 88.101(1)^\circ$, $Z = 2$, $R = 4.4\%$.

The minimum distances between the centers of the chromophores were measured with the following results:

Table XIX Distances ($< 7.5 \text{ \AA}$) Between Chromophores

Chromophores Dibenzobarrelene ^a -Amine Sensitizer ^b	Distance (\AA) in Salts or Complex		
	164	165	166
	4.62	6.08	4.59
	5.01	6.67	5.19
		6.78	7.00
	4.03	5.38	4.11
	5.95	5.48	6.79
	6.97	5.72	7.48

(a) Vinylic double bond, (b) carbonyl and aromatic functionality, where X = C, N.

The distances between the chromophore moieties were of importance, as these units are responsible for the absorption of light by the molecule. All of these distances are small enough for an efficient energy transfer to occur between the probe molecule and the sensitizer. Intramolecular triplet-triplet energy transfers were shown to take place at separations of 7 and 15 \AA as discussed in the Introduction (Section 1.5.1, p 27).

The positioning of the probe molecule with respect to the acetophenone moiety of the amine was also investigated. A different representation of the packing diagrams for salts 164 and 166 (Figure 9.06) illustrates the interaction between the dibenzobarrelene (white circles) and the acetophenone (black circles) groups. Salt 164 demonstrates that the probe molecules are sandwiched between two layers of sensitizer amines, whereas the illustration of salt 166 indicates that the sensitizer molecules are sandwiched between layers of the probe molecules. In the case of

complex 165, where two dibenzobarrelene carboxylic acids crystallized with one amine functionalized sensitizer, a similar arrangement, as described above, was not observed. Whether the reversed pattern between salts 164 and 166 affect the triplet-triplet energy transfer efficiency is not clear at this point.

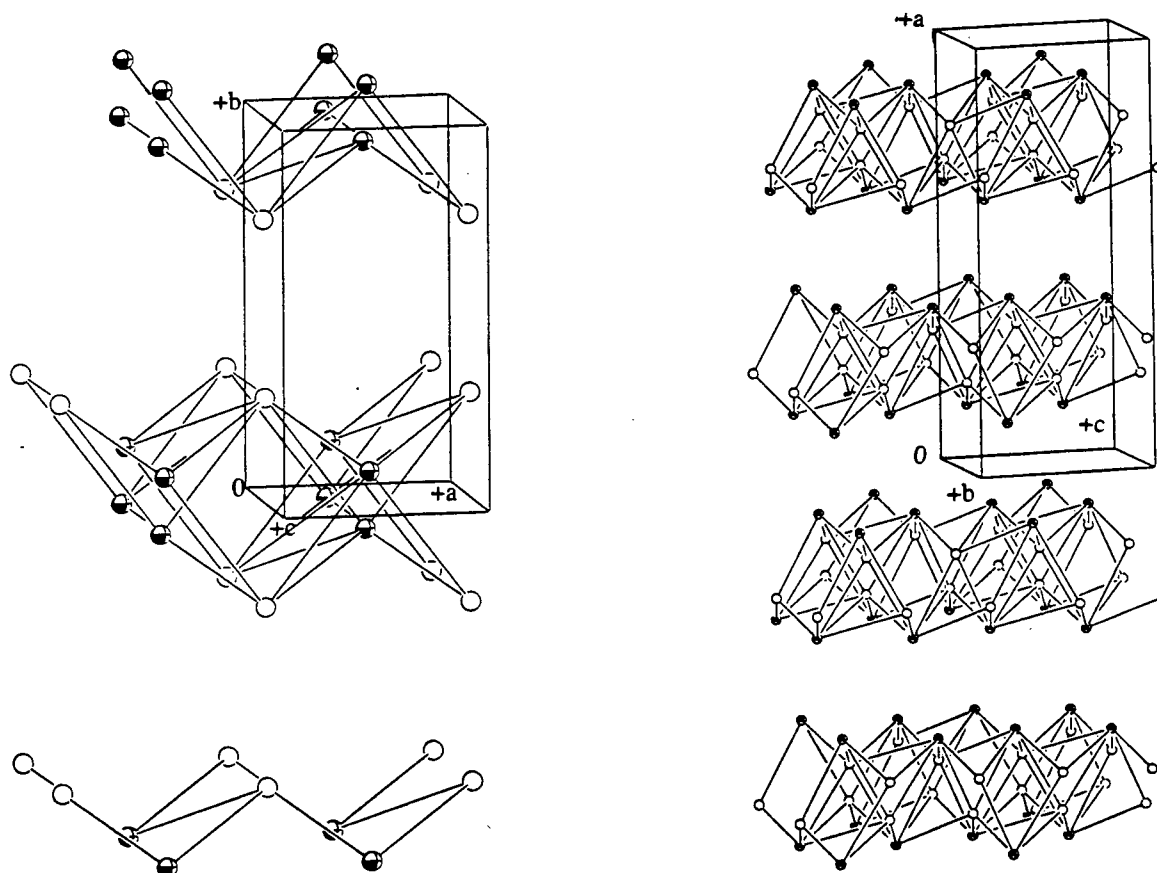


Figure 9.06. Different Representation of Packing Diagrams for Salts 164 and 166. (The white circles represent the dibenzobarrelene moiety and the black circles acetophenone). Interactions of less than 10 Å between atoms are represented by the connected lines.

9.3. UV/VIS Analysis of Salts 164, 166 and Complex 165

The increase in triplet product formation in the case of salt 166 compared to salt 164 and complex 165 may be due in part to its pronounced absorption spectrum. Examination of the UV/VIS absorption spectrum of salt 166 in methanol shows a very high molar extinction coefficient ($\epsilon = 20,700$) at λ_{\max} of 325 nm. This is not the case for salt 164 and complex 165, which exhibit extinction coefficients at λ_{\max} of 319 nm similar to that of acetophenone ($\epsilon = 50$, in cyclohexane).¹⁵⁷

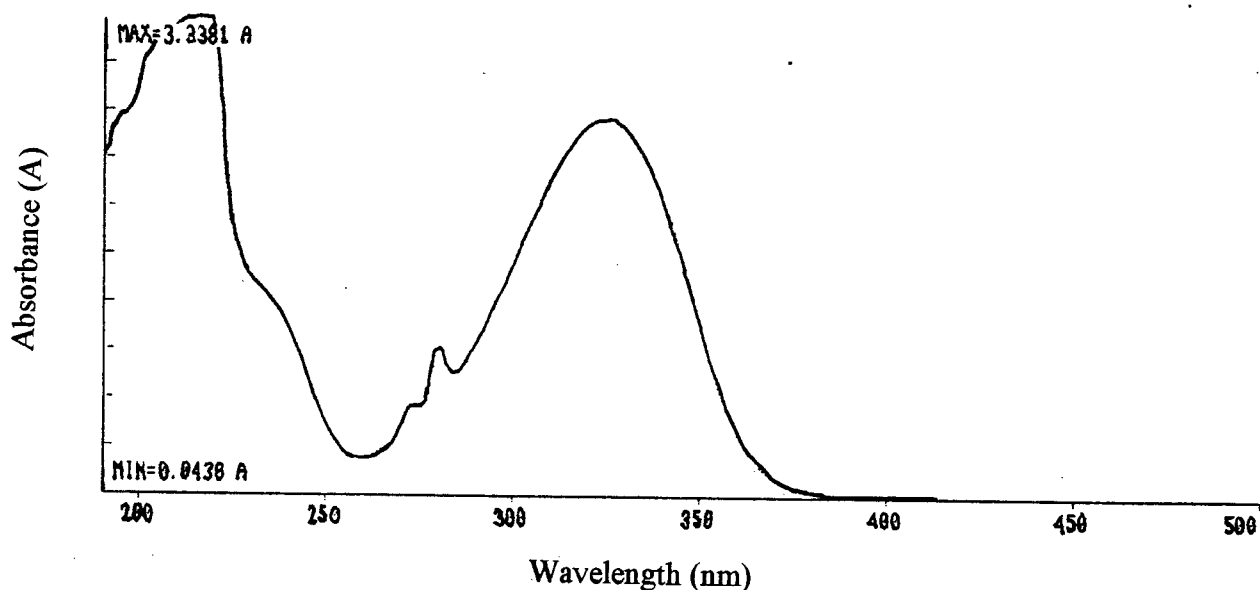


Figure 9.07. UV/VIS Absorption Spectrum of Salt 166 in Methanol.

In agreement with the results for salt 166 is the absorption spectrum of the free amine sensitizer moiety 167 in methanol, demonstrating an extinction coefficient (ϵ) of 22,600 at a λ_{\max} of 326 nm. This value may be compared to the absorption spectrum of 4'-aminobutyrophenone (168) in methanol, which exhibits a similarly strong molar extinction coefficient ($\epsilon = 20,200$) at a λ_{\max} of 316 nm.¹⁵⁸

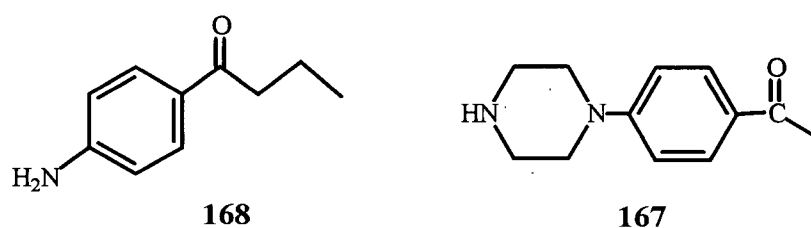


Figure 9.08. Structural Comparison of 4'-Aminobutyrophenone (168) and 4'-Piperazinoacetophenone (167).

These features of the absorption spectra are characteristic of charge transfer (see Section 4.1.3, p 86), which results from the intramolecular interaction of the electron-withdrawing and electron-donating substituents with the π -system of the aromatic ring. Furthermore, salt 166, which was initially light yellow compared to the colorless salt 164 and complex 165, turned slightly pink after one hour of irradiation. This color disappeared when the crystals were left in the dark (1 h). Hence, the crystals exhibited photochromism. Irradiation of the crystals of sensitizer amine 167 did not lead to these results. However, this was not further investigated, as it was outside the scope of the present project.

9.4. Energy State Analysis of Salts 164, 166 and Complex 165

The efficiency of the triplet-triplet energy process also depends on the relative energies of the states involved in the transfer step. These may either be n,π^* , π,π^* or CT states. Each sensitizer contains an acetophenone moiety, which possesses a carbonyl chromophore and an aromatic ring chromophore in conjugation. In such cases, the lowest energy excited state of a molecule is determined by the chromophore with the lowest energy excited state.¹⁵⁹ Experiments conducted by Lamola,¹⁶⁰ showed that acetophenone demonstrates a short-lived phosphorescence, characteristic of n, π^* triplet aromatic carbonyl compounds. The orbital composition of the T_1 state of any ketone can be represented by the following equation : $T_1 = a (n, \pi^*) + b (\pi, \pi^*)$, where "a" and "b" are the extent to which each configuration contributes to the state.¹⁶¹ The configuration of three different ketones and their corresponding excited states are illustrated in Figure 9.09.¹⁶¹ If a reaction proceeds through an n, π^* state, the triplet-excitation energy should be localized mainly on the carbonyl group (169). If the π, π^* state is involved, this implies that the excited carbonyl oxygen is not as electron deficient as in the n, π^* state and the electron density of the excited state may be partially delocalized (170). Aryl ketones that contain strong electron donating substituents and undergo efficient electron transfer from a heteroatom substituent to the carbonyl group will give rise to a more nucleophilic carbonyl oxygen. States which follow this model, are referred to as charge transfer excited states (171).

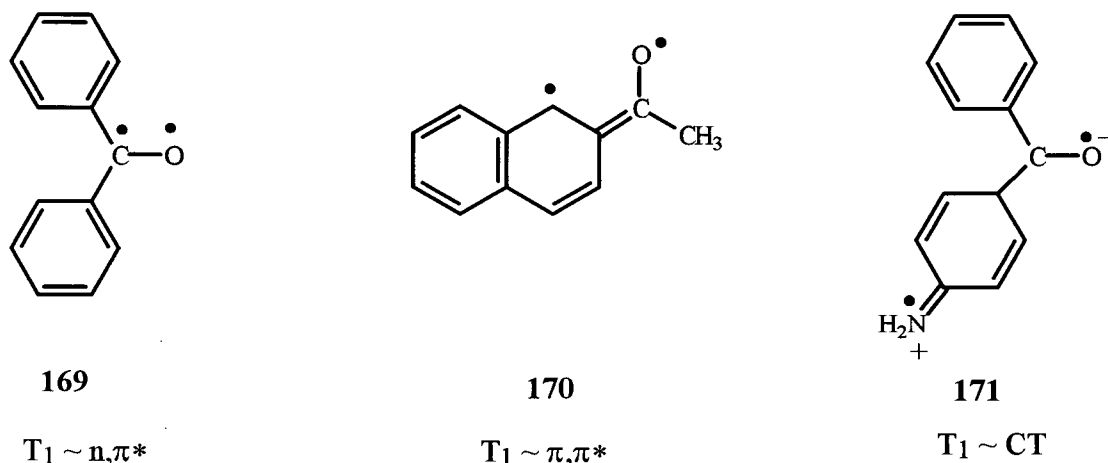


Figure 9.09. Examples of Different States for Aryl Ketones.

From the irradiation results it appears that the energy transfer for salt 164 and complex 165 occurs between the n, π^* (keto-amine) and the π, π^* (dibenzobarrelene-acid) excited states, whereas in the case of salt 166, transfer results from either the π, π^* state or CT state to the dibenzobarrelene π, π^* triplet. Electronic excitation of 4'-piperazinoacetophenone (167) could result in a transfer of charge from the electron-donating nitrogen group to the carbonyl group, as in the case of *p*-aminobenzophenone (171). Both π, π^* and CT states involve mainly π -type orbitals. However, the difference lies in the occupation of space. In the case of π, π^* states, the π and π^* electrons are commonly presumed to be positioned in similar or the same vicinity of space, whereas in the CT state, the π and π^* electrons may have different locations, resulting in a charge separation.¹⁶¹ Additionally, the ability of amine 167 to act as a more efficient triplet-triplet sensitizer may relate to its longer π, π^* triplet lifetime (seconds) versus that of the typical n, π^* states which is on the order of tenths and hundredths of milliseconds.¹⁶²

EXPERIMENTAL

CHAPTER 10 PREPARATION OF SUBSTRATES

10.1. General Procedures

Melting Points (MP)

The melting points were determined on a Fisher-Johns melting point apparatus and were not corrected.

Infrared Spectra (IR)

The infrared spectra were taken on a Perkin Elmer 1710 Fourier transform infrared spectrometer. The absorption maxima are given in cm^{-1} . Liquid samples were applied neat between two sodium chloride discs, whereas solid samples (2-5 mg) were ground with anhydrous potassium bromide (100-200 mg) and pressed into pellets in an evacuated die (Perkin-Elmer 186-0002) with a laboratory press (Carver, model B) at 15,000 psi.

Mass Spectra (MS)

A Kratos MS 50 mass spectrometer was used to determine the low and high resolution electron ionization (EI) mass spectra. A Kratos MS 80 spectrometer attached to a Carlo-Erba chromatograph recorded the data for coupled gas chromatography-mass spectral analysis (GC-MS). Electron bombardment at 70 electron volts led to ionization (EI). Fast atom bombardment

(FAB) mass spectra were taken with an AEI MS 9 mass spectrometer. Desorption chemical ionization (DCI) spectra were recorded on a Delsi Nermag R10-10C spectrometer with ammonia as the CI gas. Mass to charge ratios (m/e) are given with relative intensities in parentheses. Molecular ions are designated as M^+ .

Nuclear Magnetic Resonance Spectra (NMR)

^1H NMR

The spectrometers used to record the proton nuclear magnetic resonance spectra (^1H -NMR) were: Bruker AC-200 (200 MHz), Varian XL-300 (300 MHz), Bruker WP-400 (400 MHz) and Bruker AMX-500 (500 MHz). The positions of the signals are given as chemical shifts (δ) in parts per million (ppm) using tetramethyl silane (TMS) as an internal reference standard. The chemical shifts are reported, followed by the multiplicity of the signals, number of protons, coupling constants (J) in Hz and the molecular assignments. The multiplicities are abbreviated as follows: s = singlet, d = doublet, t = triplet, q = quartet, m = multiplet. In some cases HETCOR (Heteronuclear Chemical Shift Correlation Spectroscopy, $^{13}\text{C} - ^1\text{H}$) experiments on the Bruker AMX-500 (500 MHz) spectrometer and NOE (Nuclear Overhauser Effect) experiments on the Bruker WP-400 (400 MHz) spectrometer were conducted to verify structures.

^{13}C NMR

The spectrometers utilized to record the carbon nuclear magnetic resonance spectra (^{13}C NMR) were: Bruker AC-200 at 50.3 MHz, Varian XL-300 at 75.4 MHz, Bruker WP-400 at 100.6 MHz and Bruker AMX-500 at 125.8 MHz. Chemical shifts (δ) are given in parts per

million under broad band proton decoupling and are followed by the carbon assignment, which was confirmed by the attached proton test (APT) experiment.

Ultraviolet Spectra (UV)

A Perkin Elmer Lambda-4B UV/VIS spectrometer was used to record the ultraviolet spectra. Given are the wavelength (λ) in nanometers (nm) and the extinction coefficient (ϵ ($M^{-1} \text{ cm}^{-1}$)) of each absorption maximum.

Elemental Analysis (Anal)

The elemental analyses were carried out by Mr. Peter Borda, Department of Chemistry, University of British Columbia.

Chromatography

A Hewlett Packard 5890A gas chromatograph fitted with a flame ionization detector and a Hewlett Packard 3392 A integrator was employed for gas liquid chromatography analysis. Samples dissolved in ethyl acetate were injected (2 μ l) into one or more of the following columns: 15 m x 0.25 mm DB1 column (J & W Scientific Inc.), 15 m x 0.25 mm DB17 column (J & W Scientific Inc.), 15 m x 0.25 mm DB5 (J & W Scientific Inc.) or 30 m x 0.25 mm HP 5 column (Hewlett Packard) with helium as a carrier gas. Column head pressure was maintained at 15 psi.

Gravity column chromatography separations were conducted using silica gel 60, 230-400 mesh gel (E. Merck) with the appropriate solvent systems.

Thin layer chromatography analysis was carried out on pre-coated silica gel plates (type 5554 from E. Merck).

Solvents and Reagents

All solvents and reagents were used as supplied by Fisher Scientific, unless specified. When further purification was necessary, known methods and procedures were followed in each case.

Crystallographic Analysis

A Rigaku AFC6S 4-circle diffractometer was used to determine the crystal structures by Dr. Bozena Borecka, Tai Y. Fu, and Dr. Gunnar Olovsson under Professor James Trotter's supervision in the University of British Columbia Chemistry Department.

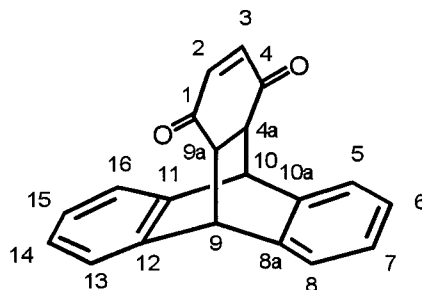
Recrystallizations

Salts (photochemical substrates) were not recrystallized due to difficulties arising from decomposition. Photoproducts were recrystallized, provided more than 10 mg of the product could be isolated by column chromatography.

10.2. Preparation of Photochemical Substrates

10.2.1. 9,10[1',2']Benzenoanthracene-1,4-dione Derivatives

4a,9,9a,10-Tetrahydro-9,10[1',2']benzenoanthracene-1,4-dione (**61**)⁷⁵



61

A Diels-Alder reaction was performed by refluxing recrystallized 1,4-benzoquinone (4.3 g, 39 mmol, Eastman Kodak Co.) and anthracene (7.0 g, 39 mmol, Eastman Kodak Co.) in 40 mL of mixed xylenes (*o*, *p* and *m*-isomers) for 2 h according to procedures described by Bartlett *et al.*⁷⁵ The mixture was cooled in an ice bath and the resulting brown solid was isolated by suction filtration. This was then recrystallized two times from a mixture of xylenes (isomers) to yield pale yellow crystals of adduct **61** (8.4 g, 29 mmol, 75%).

MP : 220-221 °C (lit.⁷⁵ 221-223 °C).

IR (KBr) ν_{\max} : 1674 (C=O), 1611 (C=C) cm^{-1} .

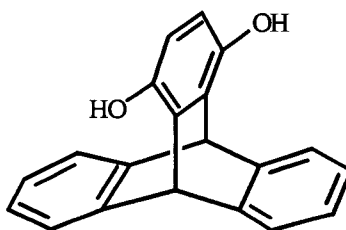
MS *m/e* (relative intensity) : 287 (M+1, 0.4), 286 (M⁺, 2), 178 (100).

Exact mass calculated for C₂₀H₁₄O₂ : 286.0994. Found : 286.0991.

$^1\text{H NMR}$ (200 MHz, CDCl_3) : δ 7.45-7.00 (m, 8H, aromatic H), 6.30 (s, 2H, vinyl H), 4.85 (s, 2H, bridgehead H_9 & H_{10}), 3.10 (s, 2H, bridgehead H_{4a} & H_{9a}) ppm.

$^{13}\text{C NMR}$ (50 MHz, CDCl_3) : δ 198.34 (C=O), 141.54 (aromatic C), 140.59 (vinyl C-H), 139.69 (aromatic C), 126.73, 126.64, 124.73, 123.88 (aromatic C-H), 49.05 & 48.90 (bridgehead C-H) ppm.

9,10-Dihydro[1',2']benzenoanthracene-1,4-diol (62)⁷⁵



62

Adduct **61** (8.4 g, 29 mmol) was dissolved in 100 mL of boiling acetic acid (Fisher Scientific) and treated with 4 drops of HBr (48%, BDH) as described by Bartlett *et al.*⁷⁵ A vigorous evolution of heat resulted and the solution turned orange. After 30 min of refluxing, the solution was cooled in an ice bath and a white solid precipitated which was filtered off by suction filtration. The resulting powder (**62**) was recrystallized from diethyl ether resulting in white needles (6.5 g, 23 mmol, 77%).

MP : 338-340°C (lit.⁷⁵ 338-340°C).

IR (KBr) ν_{max} : 3284 (O-H) cm^{-1} .

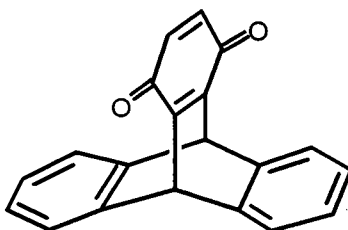
MS m/e (relative intensity) : 287 (M+1,24), 286 (M⁺,98), 269 (100), 268 (38), 256 (19), 239 (39), 226 (28), 202 (66).

Exact mass calculated for C₂₀H₁₄O₂ : 286.0994. Found : 286.1001.

¹H NMR (200 MHz, d₆-acetone) : δ 7.85 (s, 2H, OH), 7.50-7.35 (m, 4H, aromatic H), 7.05-6.90 (m, 4H, aromatic H), 6.39 (s, 2H, aromatic H), 5.95 (s, 2H, bridgehead H) ppm.

¹³C NMR (50 MHz, d₆-acetone) : δ 146.90, 146.00, 133.47 (aromatic C, aromatic C-OH), 125.48, 124.30 (aromatic C-H), 113.83 (aromatic C-H), 48.18 (bridgehead C-H) ppm.

9,10-Dihydro-9,10[1',2']benzenoanthracene-1,4-dione (63)⁷⁵



63

Adduct 62 (6.5 g, 23 mmol) was dissolved in 60 mL of hot acetic acid according to Bartlett *et al.* procedures.⁷⁵ A solution of KBrO₃ (1.3 g, 7.5 mmol, BDH) in 80 mL of hot water was added. The solution was refluxed for 5 min and 50 mL of hot water was added. The solution was cooled in an ice bath and the orange solid collected. This was then recrystallized from diethyl ether to give bright yellow crystals of 63 (4.5g, 1.6 mmol, 70%).

MP : 290-292°C (lit.⁷⁵ 292-296°C).

IR (KBr) ν_{\max} : 1660 (C=O), 1581 (C=C) cm^{-1} .

MS m/e (relative intensity) : 285 (M+1, 24), 284 (M^+ , 100), 255 (17), 226 (18), 202 (86).

Exact mass calculated for $\text{C}_{20}\text{H}_{12}\text{O}_2$: 284.0837. Found : 284.0837.

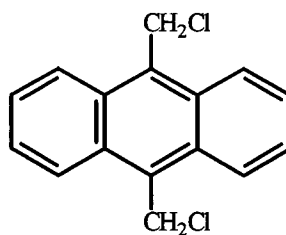
^1H NMR (200 MHz, CDCl_3) : δ 7.50-7.35 (m, 4H, aromatic H), 7.10-6.95 (m, 4H, aromatic H), 6.59 (s, 2H, vinyl H), 5.79 (s, 2H, bridgehead H) ppm.

^{13}C NMR (50 MHz, CDCl_3) : δ 183.41 (C=O), 151.82 (vinyl C), 143.49 (aromatic C), 135.28 (vinyl C-H), 125.47, 124.32 (aromatic C-H), 47.27 (bridgehead C-H) ppm.

UV (acetonitrile) λ_{\max} : 404 (ϵ 357), 330 (ϵ 993), 251 (ϵ 14,884) nm.

X-Ray Crystal Data for $\text{C}_{20}\text{H}_{12}\text{O}_2$: Space group *Pnma* (#62), $a = 13.979(2)$ Å, $b = 12.608(7)$ Å, $c = 8.024(2)$ Å, $V = 1414.2(7)$ Å³, $Z = 4$, $D_{\text{calcd}} = 1.335$ g/cm³, $R = 0.059$.

9,10- Bis(chloromethyl)anthracene (64)⁷⁷



64

A solution of 1,4-dioxane (78 mL, Fisher Scientific) and concd HCl (16 mL, Fisher Scientific) was saturated with HCl gas (Matheson Gas Products Inc.) according to Miller *et al.*⁷⁷ Anthracene (10 g, 56 mmol, Eastman Kodak Co.) and paraformaldehyde (8.4 g, Fisher Scientific)

were added to the flask and the solution was heated until it started to reflux. A fine dispersion of HCl gas was added over 2 h and the solution stirred an additional 3 h. The solution was allowed to sit for 16 h and the resulting fine yellow solid was removed via suction filtration. The solid was suspended (three times) in 1,4-dioxane, stirred, and filtered. The solid was recrystallized from toluene giving yellow plates of **64** (5.0 g, 18 mmol, 32%).

MP : 257-259 °C (lit.⁷⁷ 258-260 °C).

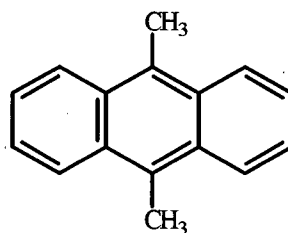
IR (KBr) ν_{\max} : 3087, 3044, 3008 (aromatic C-H), 1248 (CH₂Cl), 627 (C-Cl) cm⁻¹.

MS m/e (relative intensity) : 278 (M+4, 1), 276 (M+2, 8), 275 (M+1, 2), 274 (M⁺, 12), 239 (38), 204 (100), 101 (48).

Exact mass calculated for C₁₆H₁₂Cl₂ : 274.0316. Found : 274.0312.

¹H NMR (200 MHz, CDCl₃) : δ 8.42-8.31 (m, 4H, aromatic H), 7.75-7.64 (m, 4H, aromatic H), 5.62 (s, 4H, CH₂Cl) ppm.

¹³C NMR (75 MHz, d₅-nitrobenzene) : δ 130.93 & 130.27 (aromatic C), 127.39 & 124.90 (aromatic C-H), 39.63 (CH₂Cl) ppm.

9,10- Dimethylantracene (65)⁷⁶**65**

9,10-Bis(chloromethyl)anthracene **64** (2.5g, 9.1 mmol) was extracted (Soxhlet) into dry THF (150 mL) containing lithium aluminum hydride (580 mg, 15 mmol, Aldrich) for 18 h as outlined by Kirby *et al.*⁷⁶ The mixture was cooled to room temperature, treated cautiously with water, aqueous NaOH, diluted with ether and filtered. The yellow solid was recrystallized from benzene giving light yellow needles of **65** (1.7 g, 8.3 mmol, 90%).

MP : 181-182 °C (lit.⁷⁶ 180-181 °C).

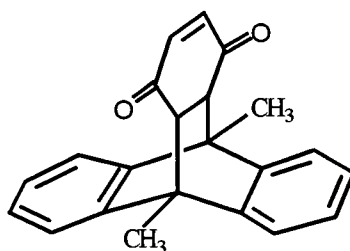
IR (KBr) ν_{\max} : 3073 (aromatic C-H) cm^{-1} .

MS m/e (relative intensity) : 207 (M+1, 18), 206 (M⁺, 100), 191 (43), 178 (8), 101 (25).

Exact mass calculated for C₁₆H₁₄ : 206.1095. Found : 206.1096.

¹H NMR (200 MHz, CDCl₃) : δ 8.40-8.23 (m, 4H, aromatic H), 7.59-7.42 (m, 4H, aromatic H), 3.09 (s, 6H, CH₃) ppm.

¹³C NMR (50 MHz, CDCl₃) : δ 129.91 & 128.35 (aromatic C), 125.33 & 124.71 (aromatic C-H), 14.09 (CH₃) ppm.

9,10-Dimethyl-4a,9,9a,10-tetrahydro-9,10[1',2']benzenoanthracene-1,4-dione (67)⁷⁹

67

A Diels-Alder reaction was performed by refluxing recrystallized 1,4-benzoquinone (415 mg, 3.8 mmol) and 9,10-dimethylantracene **65** (396 mg, 1.9 mmol) in 2 mL of benzene (1 min), according to procedures developed by Theilacker *et al.*⁷⁹ The mixture was cooled in an ice bath and the resulting yellow solid was isolated by suction filtration. This was then recrystallized two times from benzene to yield pale yellow crystals of adduct **67** (574 mg, 1.8 mmol, 95%).

MP : 213-215 °C (lit.⁷⁹ 217 °C (red), 221-222 (melting) °C).

IR (KBr) ν_{\max} : 1674 (C=O) cm^{-1} .

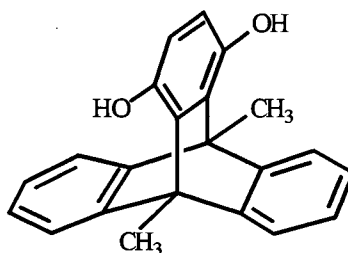
MS (DCI, NH_3 , relative intensity) : 332 (M+18, 13).

Exact mass calculated for $\text{C}_{22}\text{H}_{19}\text{O}_2$: 315.1385. Found : 315.1391 (M+1).

¹H NMR (200 MHz, CDCl_3) : δ 7.46-7.36 (m, 4H, aromatic H), 7.30-7.11 (m, 4H, aromatic H) 6.25 (s, 2H, vinyl H), 2.82 (s, 2H, bridgehead H), 2.02 (s, 6H, CH_3) ppm.

¹³C NMR (50 MHz, CDCl_3) : δ 197.75 (C=O), 141.86 (aromatic C), 140.09 (vinyl C-H), 136.53 (aromatic C), 126.71, 126.45, 121.89, 121.19 (aromatic C-H), 56.45 (bridgehead C-H) 44.92 (bridgehead C), 16.25 (CH_3) ppm.

9,10-Dihydro-9,10-dimethyl-9,10[1',2']benzenoanthracene-1,4-diol (**68**)⁷⁹



68

In a round bottomed flask fitted with a condenser, 59 mL of 10% NaOH in methanol was refluxed as described by Theilacker *et al.*⁷⁹ Compound **67** (706 mg, 2.2 mmol) was added, and the solution was refluxed for 10 min. The solution was cooled to room temperature and poured into a beaker with 59 mL of 20% aqueous H₂SO₄. This solution was then added to another beaker with 350 mL of water. A light beige powder (**68**) (565 mg, 1.8 mmol, 80%) was obtained after filtering the solution.

MP : > 300 °C (lit.⁷⁹ 332 °C (red), 340 °C (brown)).

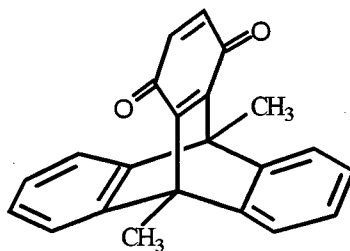
IR (KBr) ν_{\max} : 3363 (O-H) cm⁻¹.

MS m/e (relative intensity) : 315 (M+1, 4), 314(M⁺, 16), 299 (28), 284 (19).

Exact mass calculated for C₂₂H₁₈O₂ : 314.1307. Found : 314.1306.

¹H NMR (200 MHz, CDCl₃) : δ 7.47-7.35 (m, 4H, aromatic H), 7.11-7.00 (m, 4H, aromatic H), 6.17 (s, 2H, aromatic H), 3.69 (s, 2H, OH), 2.65 (s, 6H, CH₃) ppm.

¹³C NMR (75 MHz, d₆-acetone) : δ 150.29, 147.58, 134.99 (aromatic C, aromatic C-OH), 125.21, 121.45 (aromatic C-H), 115.78 (aromatic C-H), 49.68 (bridgehead C), 17.77 (CH₃) ppm.

9,10-Dihydro-9,10-dimethyl-9,10[1',2']benzenoanthracene-1,4-dione (69)⁷⁸**69**

Adduct **68** (695 mg, 2.2 mmol) was dissolved in 15 mL of hot acetic acid and refluxed for 5 min. A solution of KBrO_3 (133 mg, 0.80 mmol, BDH) in 15 mL of hot water was added. The solution was refluxed for 3 min and 8 mL of hot water was added. The solution was cooled in an ice bath and the yellow solid collected (635 mg, 2.0 mmol, 92%). This was then purified by column chromatography (silica gel, benzene) and recrystallized from ethyl acetate (444 mg, 1.4 mmol, 64%).

MP : $> 300^\circ\text{C}$ (lit.⁷⁸ not reported).

IR (KBr) ν_{max} : 1652 (C=O) cm^{-1} .

MS m/e (relative intensity) : 313 (M+1, 16), 312 (M⁺, 62), 297 (71), 284 (22), 230 (86), 215 (100).

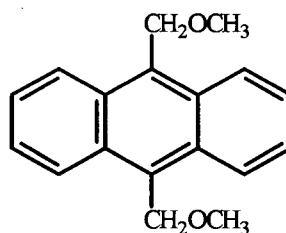
Exact mass calculated for $\text{C}_{22}\text{H}_{16}\text{O}_2$: 312.1150. Found : 312.1154.

¹H NMR (400 MHz, CDCl_3) : δ 7.42-7.40 (m, 4H, aromatic H), 7.10-7.08 (m, 4H, aromatic H), 6.40 (s, 2H, vinyl H), 2.58 (s, 6H, CH_3) ppm.

^{13}C NMR (75 MHz, CDCl_3): δ 185.46 (C=O), 153.70, 147.08 (aromatic C), 135.45 (vinyl C-H), 125.24, 121.64 (aromatic C-H), 50.32 (bridgehead C), 15.18 (CH_3) ppm.

UV (acetonitrile) λ_{max} : 399 (ϵ 564), 298 (ϵ 754) nm.

9,10-Bis(methoxymethyl)anthracene (66)⁷⁷



66

A suspension of 9, 10 bis(chloromethyl)anthracene 64 (5.5g, 20 mmol) and KOH (5.5g, 98 mmol) in 120 mL of methanol was refluxed for 2.5 h according to procedures described by Miller *et al.*⁷⁷ The solution was cooled in an ice bath and a light yellow solid precipitated out. The solid was filtered off and the filtrate was evaporated under reduced pressure. The residue was dissolved in chloroform and washed with excess aqueous HCl (15%). The organic layer was then washed with aqueous NaCl, water and dried over MgSO_4 . After the solvent was evaporated, the resulting solid was combined with the first and recrystallized from 1,4-dioxane to give yellow plates (5.1g, 19 mmol, 96%).

MP : 182-184 °C (lit.⁷⁷ 183-185 °C).

IR (KBr) ν_{max} : 3093, 3032, 2987 (aromatic C-H), 2921, 2898 (methyl C-H), 1088 (C-O-C) cm^{-1} .

MS m/e (relative intensity) : 267 (M+1, 19), 266 (M⁺, 94), 235 (100), 221 (70), 203 (27), 191 (49), 178 (16).

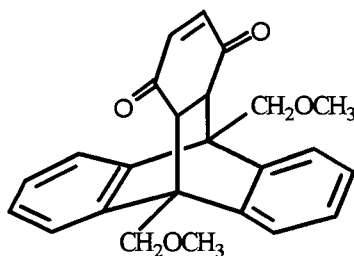
Exact mass calculated for C₁₈H₁₈O₂ : 266.1307. Found : 266.1308.

¹H NMR (200 MHz, CDCl₃) : δ 8.45-8.40 (m, 4H, aromatic H), 7.60-7.55 (m, 4H, aromatic H), 5.45 (s, 4H, CH₂OCH₃), 3.54 (s, 6H, CH₃) ppm.

¹³C NMR (50 MHz, CDCl₃) : δ 130.76 & 130.27 (aromatic C), 125.76 & 124.89 (aromatic C-H), 66.72 (CH₂OCH₃), 58.35 (CH₃) ppm.

9,10-Bis(methoxymethyl)-4a,9,9a,10-tetrahydro-9,10[1',2']benzenoanthracene-1,4-dione

(70)



70

A Diels-Alder reaction was performed by refluxing recrystallized 1,4-benzoquinone (823 mg, 7.5 mmol) and 9,10-bis(methoxymethyl)anthracene 66 (1.0 g, 3.8 mmol) in 8 mL of mixed xylenes (*o*, *p* and *m*-isomers) for 7 h. The mixture was cooled in an ice bath and the resulting yellow solid was isolated by suction filtration. This was then recrystallized two times from a

mixture of xylenes (*o*, *p* and *m*-isomers) to yield pale yellow crystals of adduct **70** (1.3 g, 3.4 mmol, 90%).

MP : 192-194 °C.

IR (KBr) ν_{\max} : 1672, 1656 (C=O) cm^{-1} .

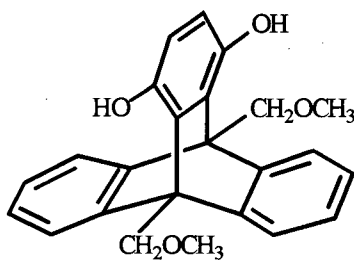
MS (DCI, NH_3 , relative intensity) : 392 (M+18, 10), 375 (M+1, 10).

Exact mass calculated for $\text{C}_{24}\text{H}_{22}\text{O}_4$ (M+1) : 375.1596. Found : 375.1585.

$^1\text{H NMR}$ (200 MHz, CDCl_3) : δ 7.49-7.42 (m, 4H, aromatic H), 7.20-7.09 (m, 4H, aromatic H) 6.08 (s, 2H, vinyl H), 4.42 (s, 4H, CH_2OCH_3), 3.65 (s, 6H, CH_3), 3.18 (s, 2H, bridgehead H) ppm.

$^{13}\text{C NMR}$ (50 MHz, CDCl_3) : δ 197.60 (C=O), 142.10 (aromatic C), 140.31 (vinyl C-H), 139.83 (aromatic C), 128.33, 126.62, 126.33, 122.84 (aromatic C-H), 70.78 (CH_2OCH_3), 59.08 (CH_3), 49.21 (bridgehead C-H) ppm.

9,10-Bis(methoxymethyl)-9,10-dihydro-9,10[1',2']benzoanthracene-1,4-diol (71)



71

Compound 70 (95 mg, 0.254 mmol) was added to 10 mL of a refluxing solution of 5% NaOH in methanol followed by refluxing for an additional 10 min. After cooling the reaction mixture down to room temperature, 10 mL of 10% aqueous H₂SO₄ was added plus an additional 60 mL of water. A light beige powder (71) (92 mg, 0.246 mmol, 97%) was obtained after filtration.

MP : 210-213°C .

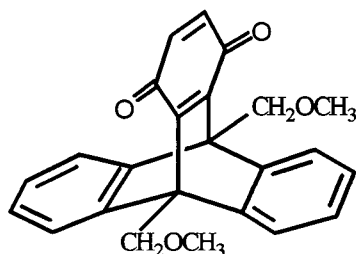
IR (KBr) ν_{\max} : 3232 (O-H) cm⁻¹.

MS m/e (relative intensity) : 375 (M+1, 27), 374 (M⁺, 100), 297 (36), 284 (41), 266 (36).

Exact mass calculated for C₂₄H₂₂O₄ : 374.1518. Found : 374.1521.

¹H NMR (200 MHz, CDCl₃) : δ 8.75 (s, broad, 2H, OH), 7.60-7.37 (m, 2H, aromatic H), 7.20-6.92 (m, 6H, aromatic H), 6.70 (s, 2H, aromatic H), 5.34-5.20 (m, 2H, CH₂OCH₃), 4.90-4.75 (m, 2H, CH₂OCH₃), 3.87 (s, 6H, CH₃) ppm.

¹³C NMR (50 MHz, CDCl₃) : δ 145.95, 145.63, 130.74 (aromatic C, aromatic C-OH), 125.27, 125.10, 123.08, 120.49, 118.68 (aromatic C-H), 72.64 (CH₂OCH₃), 59.35 (CH₃), 51.55 (bridgehead C) ppm.

9,10-Bis(methoxymethyl)-9,10-dihydro-9,10[1',2']benzenoanthracene-1,4-dione (72)

72

Adduct **71** (738 mg, 1.9 mmol) was mixed with 25 mL of hot acetic acid and refluxed until all of it dissolved. A solution of KBrO_3 (119 mg, 0.713 mmol, BDH) in 10 mL of hot water was added. The solution was refluxed for 3 min and 15 mL of hot water was added. The solution was cooled and the yellow solid collected (590 mg, 0.157 mmol, 80%). This was then purified by column chromatography (silica gel, benzene) and recrystallized from ethyl acetate giving compound **72** (403 mg, 1.1 mmol, 55%).

MP : 249-251°C.

IR (KBr) ν_{max} : 1647 (C=O) cm^{-1} .

MS m/e (relative intensity) : 273 (M+1, 10), 272 (M^+ , 40), 327 (15), 296 (23), 75 (100).

Exact mass calculated for $\text{C}_{24}\text{H}_{20}\text{O}_4$: 372.1361. Found : 372.1354.

^1H NMR (200 MHz, CDCl_3) : δ 7.72-7.41 (m, 4H, aromatic H), 7.12-7.03 (m, 4H, aromatic H), 6.41 (s, 2H, vinyl H), 5.20 (s, broad, 4H, CH_2OCH_3), 3.70 (s, 6H, CH_3) ppm.

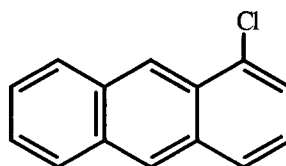
^{13}C NMR (50 MHz, CDCl_3) : δ 184.56 (C=O), 154.57, 144.16 (aromatic C), 135.13 (vinyl C-H), 125.22, 124.09 (aromatic C-H), 69.31 (CH_2OCH_3), 58.91 (CH_3), 55.11 (bridgehead C) ppm.

UV (acetonitrile) λ_{\max} : 331 (ϵ 1,246), 303 (ϵ 3,544), 248 (ϵ 10,902) nm.

Anal. calculated for $C_{24}H_{20}O_4$: C, 77.40; H, 5.41. Found: C, 77.14; H, 5.36.

X-Ray Crystal Data for $C_{24}H_{20}O_4$: Space group $C2/c$ (#15), $a = 15.772(1) \text{ \AA}$, $b = 8.000(1) \text{ \AA}$, $c = 14.7883(9) \text{ \AA}$, $\beta = 98.430(6)^\circ$, $V = 1845.8(3) \text{ \AA}^3$, $Z = 4$, $D_{\text{calcd}} = 1.340 \text{ g/cm}^3$, $R = 0.040$.

1-Chloroanthracene (79a)⁸¹



79a

1-Chloro-9,10-anthraquinone (1.0 g, 4.1 mmol, Aldrich) and zinc powder (3.2 g, 49 mmol, Aldrich) were added to a round bottomed flask containing pyridine (20 mL) according to procedures specified by Schilling.⁸¹ The solution was heated under reflux with stirring, while 80 % aqueous acetic acid (8 mL) was added through an addition funnel over 1 h. Upon completion of addition, the reaction mixture was stirred for an additional 30 min followed by cooling to room temperature. The zinc was filtered off (caution : zinc is pyrophoric, spontaneously ignites with air) and the filtrate was added to ice cold HCl (80 mL, 3 M). This solution was stirred for 15 min until a solid formed, which was filtered and recrystallized from ethanol to give light yellow crystals (720 mg, 3.4 mmol, 82%).

MP : 75-77 °C (lit.⁸¹ 77-80 °C).

IR (KBr) ν_{\max} : 3022 (C-H), 1110 (C-Cl) cm^{-1} .

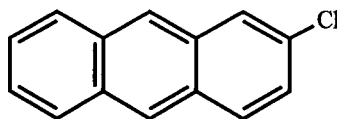
MS m/e (relative intensity) : 214 (M+2, 33), 213 (M+1, 16), 212 (M^+ , 100), 177 (13), 176 (26), 106 (18).

Exact mass calculated for $\text{C}_{14}\text{H}_9\text{Cl}$: 212.0393. Found : 212.0391.

^1H NMR (400 MHz, CDCl_3) : δ 8.84 (s, 1H, aromatic H), 8.42 (s, 1H, aromatic H), 8.11-7.95 (m, 2H, aromatic H), 7.91 (d, 1 H, $J = 9$ Hz, aromatic H), 7.56 (d, 1 H, $J = 9$ Hz, aromatic H), 7.54 - 7.46 (m, 2H, aromatic H), 7.38-7.31 (m, 1 H, aromatic H) ppm.

^{13}C NMR (50 MHz, CDCl_3) : δ 132.34, 132.16, 131.00, 131.93, 129.02 (aromatic C), 128.68, 127.91, 127.56, 126.89, 126.17, 126.03, 125.32, 124.78, 123.57 (aromatic C-H) ppm.

2-Chloroanthracene (79b)⁸²



79b

A solution of 2-chloro-9,10-anthraquinone (2.0 g, 8.2 mmol, Aldrich) and zinc powder (6.5 g, 99 mmol, Aldrich) in pyridine (40 mL) was refluxed while 80 % aqueous acetic acid (16 mL) was added over a period of 3 h as outlined in procedures by Barnett *et al.*⁸² After cooling the solution to room temperature and filtering off the zinc powder the filtrate was added to ice cold HCl (65 mL, 3 M) whereupon a light yellow precipitate formed. The solid was filtered off and purified by column chromatography with petroleum ether. After recrystallization with petroleum ether, white shiny plates (585 mg, 2.8 mmol, 33%) were obtained.

MP : 218-220 °C (lit.⁸² 221-223 °C).

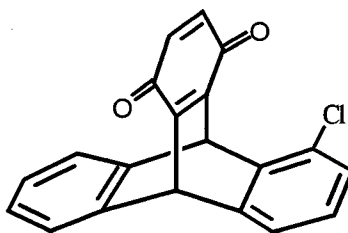
IR (KBr) ν_{\max} : 3561(C-H), 1067 (C-Cl) cm^{-1} .

MS m/e (relative intensity) : 214 (M+2, 33), 213 (M+1, 16), 212 (M⁺, 100), 177 (13), 176 (31), 106 (22).

Exact mass calculated for C₁₄H₉Cl : 212.0393. Found : 212.0395.

¹H NMR (400 MHz, CDCl₃) : δ 8.39 (s, 1H, aromatic H), 8.31 (s, 1H, aromatic H), 7.98 (d, 1 H, $J = 5$ Hz, aromatic H), 7.96 (s, 2 H, aromatic H), 7.93 (d, 1 H, $J = 9$ Hz, aromatic H), 7.50-7.44 (m, 2 H, aromatic H), 7.37 (dd, 1 H, $J = 9$ & 2 Hz, aromatic H) ppm.

5-Chloro-9,10-dihydro-9,10[1',2']benzenoanthracene-1,4-quinone (73)



73

Quinone **73** was synthesized by an initial Diels-Alder reaction between 1-chloroanthracene **79a** (279 mg, 1.3 mmol) and recrystallized 1,4-benzoquinone (142 mg, 1.3 mmol) in a mixture of refluxing xylenes (2 mL, *o*, *m*, *p*-isomers) over 3.5 h. After filtration the resulting adduct was treated with 5 mL of acetic acid, refluxed and 2 drops of HBr (48%, BDH) were added. Following a refluxing period of 30 min, and cooling the solution, the hydroquinone (49 mg, 0.153

mmol, 12%) was obtained by filtration. This compound was dissolved in acetic acid (5mL), refluxed and KBrO_3 (9.0 mg, 0.054mmol) dissolved in water (2 mL) was added. After adding an additional amount of water (2 mL) a precipitate formed which was filtered off giving the desired quinone **73** (8.1 mg, 0.025 mmol, 16%).

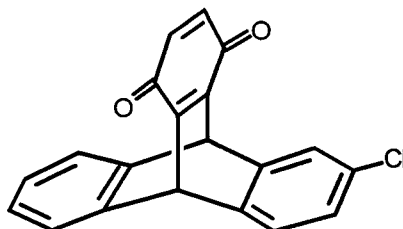
MP : 172-175 °C.

IR (KBr) ν_{max} : 3068 (C-H), 1659 (C=O), 1573 (C=C) cm^{-1} .

MS m/e (relative intensity) : 320 (M+2, 36), 319 (M+1, 28), 318 (M⁺, 100), 285 (42), 284 (35), 283 (46), 255 (80), 236 (79).

Exact mass calculated for $\text{C}_{20}\text{H}_{11}\text{O}_2\text{Cl}$: 318.0448. Found : 318.0445.

¹H NMR (400 MHz, CDCl_3) : δ 7.50-7.40 (m, 2H, aromatic H), 7.29 (d, 1H, $J = 8$ Hz, aromatic H), 7.15-6.90 (m, 4H, aromatic H), 6.61 (AB-system, 2H, $J = 10$ Hz, vinyl H), 6.25 & 5.79 (s, 1H each, bridgehead H) ppm.

6-Chloro-9,10-dihydro-9,10[1',2']benzenoanthracene-1,4-dione (74)

74

Compound **74** was prepared by a Diels-Alder reaction between recrystallized 1,4-benzoquinone (200 mg, 1.8 mmol) and 2-chloroanthracene **79b** (391 mg, 1.8 mmol) in refluxing mixed xylenes (3 mL, *o*, *m*, *p*-isomers) over 6 h. The reaction mixture was cooled and the precipitate filtered, washed with a mixture of xylenes and hot water. The resulting product was then refluxed with 4 mL of acetic acid to which a drop of HBr (48 %, BDH) was added. After 30 min of refluxing, the solution was cooled and filtered, resulting in the hydroquinone (327 mg, 1.02 mmol, 55 %). This compound was dissolved in 4 mL of acetic acid and heated until boiling. KBrO₃ (61 mg, 0.365 mmol) dissolved in hot water (4 mL) was added to the reaction mixture which was refluxed an additional 5 min. After adding more hot water (3 mL) to the solution, a precipitate formed, which was filtered off after cooling, giving the final product **74** (179 mg, 0.563 mmol, 55 %). Column chromatography with ethyl acetate / petroleum ether (5 : 95) gave a mixture of two compounds (37 mg, 0.116 mmol, 21 %), the desired product plus one or several of the 2 : 1 chloro-anthracene : benzoquinone adducts **77a-d**. A chromatotron (Model 8924, Harrison Research) using a 1mm layer plate and 2-4 mL / min rate of solvent ethyl acetate / petroleum ether (15 : 85) gave pure compound **74** (6.1 mg, 0.019 mmol, 2 %) as well as the 2 : 1 adduct(s) **77a-d** (25 mg, 0.047 mmol, 10%).

MP : 175-178 °C.

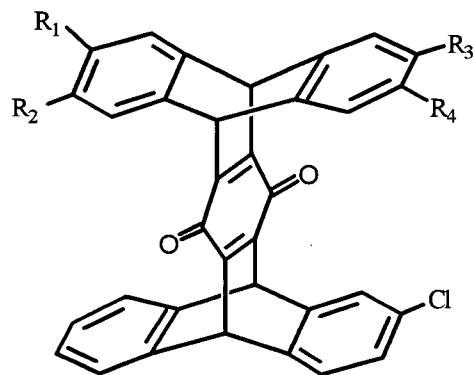
IR (KBr) ν_{\max} : 1653 (C=O) cm^{-1} .

MS m/e (relative intensity) : 320 (M+2, 33), 319 (M+1, 22), 318 (M⁺, 100), 283 (28), 255 (40), 236 (77).

Exact mass calculated for C₂₀H₁₁O₂Cl : 318.0448. Found : 318.0443.

¹H NMR (400 MHz, CDCl₃) : δ 7.42-7.37 (m, 3H, aromatic H), 7.31 (d, 1H, $J = 6$ Hz, aromatic H), 7.05-7.01 (m, 2H, aromatic H), 6.98 (AB-system, 1H, $J = 8$ Hz, aromatic H), 6.60 (s, 2H, vinyl H), 5.74 & 5.73 (s, 1H each, bridgehead H) ppm.

Possible 2 : 1 Chloroanthracene: Benzoquinone Adducts 77a-d



	R ₁	R ₂	R ₃	R ₄
a	Cl	H	H	H
b	H	Cl	H	H
c	H	H	Cl	H
d	H	H	H	Cl

77a-d

MP : > 300 °C.

IR (KBr) ν_{\max} : 3064 (C-H), 1651 (C=O) cm^{-1} .

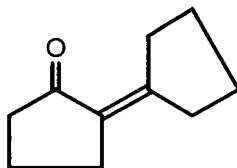
MS m/e (relative intensity) : 532 (M+4, 15), 530 (M+2, 67), 529 (M+1, 1), 528 (M⁺, 100), 494 (10), 493 (7), 472 (17), 437 (17).

Exact mass calculated for C₃₄H₁₈O₂Cl : 528.0684. Found : 528.0691.

¹H NMR (400 MHz, CDCl₃) : δ 7.36-7.32 (m, 6H, aromatic H), 7.26-7.23 (m, 2H, aromatic H), 6.92-6.70 (m, 6H, aromatic H), 5.71, 5.70, 5.69, 5.68 (s, 1H each, bridgehead H) ppm.

¹³C NMR (75 MHz, CDCl₃) : δ 179.50, 179.46 (C=O), 150.97, 150.56 (vinyl C), 145.58, 143.19, 142.85, 142.16 (aromatic C), 131.16 (aromatic C-Cl), 125.78, 125.73, 125.30, 125.09, 124.74, 124.47, 124.35 (aromatic C-H), 47.01, 46.77 (bridgehead C-H) ppm.

10.2.2. 2-(1-Cyclopentenyl)cyclopentanones and 2-(1-Cyclohexenyl)cyclohexanones

2-Cyclopentylidenecyclopentanone (119)¹²⁵

119

Cyclopentanone (52 g, 619 mmol, Aldrich) dissolved in ethanol (100 mL) and NaOH (2.5 g, 63 mmol) in water (45 mL) were stirred at room temperature for 24 h following procedures developed by Varech *et al.*¹²⁵ Ethanol was then rotary evaporated and the aqueous layer extracted with diethyl ether (three times). The combined organic layers were washed with water and brine, dried over MgSO₄ and evaporated to dryness giving a red oil (38 g, 253 mmol, 83%). The oil was then vacuum distilled resulting in a colorless oil of 119 (29 g, 193 mmol, 62%).

BP : 103-105 °C (10 mm) (lit.¹²⁵ 117-119 °C (13mm)).

IR (NaCl) ν_{\max} : 2959 (C-H), 1708 (C=O), 1641 (C=C), 1253 (C-O) cm⁻¹.

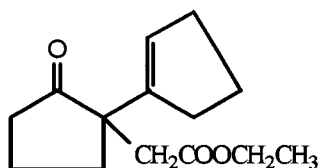
MS m/e (relative intensity) : 151 (M+1, 12), 150 (M⁺, 100), 149 (35), 135 (12), 122 (23), 121 (29), 107 (31).

Exact mass calculated for C₁₀H₁₄O : 150.1045. Found : 150.1044.

¹H NMR (200 MHz, CDCl₃) : δ 2.79-2.64 (m, 2H, CH₂), 2.55-2.40 (m, 2H, CH₂), 2.29-2.15 (m, 4H, CH₂), 1.94-1.74 (m, 2H, CH₂), 1.72-1.52 (m, 4H, CH₂) ppm.

^{13}C NMR (50 MHz, CDCl_3) : δ 207.00 (C=O), 158.27, 127.77 (vinyl C), 39.63, 34.14, 32.38, 29.40, 26.83, 25.14, 19.98 (CH_2).

Ethyl 1-(1-cyclopenten-1-yl)-2-oxocyclopentaneacetate (120)^{124a}



120

Sodium methylsulfinylmethide was synthesized by the method of Ide and Iwai^{124b} by adding anhydrous DMSO (57 mL) to sodium hydride (1.7g, 44 mmol, 60% in oil, Aldrich) in a round bottomed flask with stirring under nitrogen, followed by heating the solution to 80 °C for 30 min. To the cooled solution, compound 119 (5.7 g, 38 mmol) in DMSO (45 mL) was added dropwise and the solution was stirred for 1 h at room temperature, following the experimental procedure of Givens *et al.*^{124a} While cooling the solution in an ice bath, ethyl bromoacetate (7.4 g, 44 mmol, 98%, Aldrich) in DMSO (35 mL) was added dropwise and the solution was stirred for 30 min at room temperature. The reaction mixture was then quenched with a saturated aqueous solution of ammonium chloride (100 mL, Fisher Scientific) and extracted with *n*-pentane (three times). The organic layer was dried over MgSO_4 and the solvent evaporated leaving a golden oil (7.7 g, 33 mmol, 86%). After vacuum distillation a colorless oil (120) was obtained (5.1 g, 22 mmol, 57%).

BP : 150-153 °C (20 mm) (lit.^{124a} BP not reported).

IR (NaCl) ν_{\max} : 2958 (C-H), 1734 (C=O) cm^{-1} .

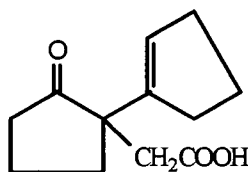
MS m/e (relative intensity): 237 (M+1, 16), 236 (M^+ , 100), 191 (75), 190 (78), 173 (36), 163 (54), 162 (54), 149 (61).

Exact mass calculated for $\text{C}_{14}\text{H}_{20}\text{O}_3$: 236.1412. Found : 236.1411.

^1H NMR (200 MHz, CDCl_3) : δ 5.36-5.34 (m, 1H, vinyl H), 3.93 (q, 2H, $J = 8$ Hz, $\text{CH}_2\text{CO}_2\text{CH}_2\text{CH}_3$), 2.53 (AB-system, 2H, $J = 16$ Hz, $\text{CH}_2\text{CO}_2\text{CH}_2\text{CH}_3$), 2.30-1.86 (m, 8H, CH_2), 1.85-1.50 (m, 4H, CH_2), 1.09 (t, 3H, $J = 8$ Hz, $\text{CH}_2\text{CO}_2\text{CH}_2\text{CH}_3$) ppm.

^{13}C NMR (50 MHz, CDCl_3) : δ 218.20 (pentanone C=O), 171.23 (ester C=O), 141.69 (vinyl C), 127.54 (vinyl C-H), 60.29 ($\text{CH}_2\text{CO}_2\text{CH}_2\text{CH}_3$), 52.81 ($\text{CH}_2\text{CO}_2\text{CH}_2\text{CH}_3$), 39.61, 37.01, 32.91, 32.39, 31.59, 23.23, 19.00 (CH_2 , C), 14.09 ($\text{CH}_2\text{CO}_2\text{CH}_2\text{CH}_3$) ppm.

1-(1-Cyclopenten-1-yl)-2-oxocyclopentaneacetic acid (121)^{124a}



121

Ester 120 (4.1g, 17 mmol) and KOH (2.9g, 52 mmol) were refluxed in methanol (100 mL) overnight as described by Givens *et al.*^{124a} The solvent was evaporated and the solid was dissolved in diethyl ether and washed with water. The aqueous layer was acidified with HCl (15%) and extracted with diethyl ether three times. The organic layer was dried over MgSO_4 , filtered and evaporated giving a white solid (3.3 g, 16 mmol, 90%). After column chromatography on silica

gel with ethyl acetate / petroleum ether (3 : 7) and recrystallization from diethyl ether / petroleum ether (1 : 1), white crystals of **121** were obtained (2.3 g, 11 mmol, 64%).

MP : 93-94 °C (lit.^{124a} 93-94 °C).

IR (KBr) ν_{\max} : 3400-2960 (OH), 2957 (C-H), 1742 (C=O), 1703 (C=O) cm^{-1} .

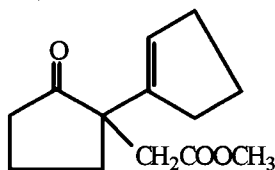
MS m/e (relative intensity): 209 (M+1, 10), 208 (M⁺, 69), 191 (13), 190 (72), 173 (16), 163 (21), 162 (42), 152 (21), 149 (37), 148 (27), 144 (14), 135 (21), 134 (28), 131 (32), 121 (31), 107 (100).

Exact mass calculated for C₁₂H₁₆O₃ : 208.1099. Found : 208.1098.

¹H NMR (200 MHz, CDCl₃) : δ 11.00 (s, 1H, broad, OH), 5.50-5.48 (m, 1H, vinyl H), 2.65 (AB-system, 2H, J = 17 Hz, CH₂CO₂H), 2.38-1.70 (m, 12H, CH₂) ppm.

¹³C NMR (50 MHz, CDCl₃) : δ 217.22 (pentanone C=O), 176.71 (acid ester C=O), 141.13 (vinyl C), 128.27 (vinyl C-H), 52.79 (CH₂CO₂H), 39.54, 36.95, 33.06, 32.49, 31.58, 23.24, 19.04 (CH₂, C) ppm. ³

UV (methanol) λ_{\max} : 296 (ϵ 222), 208 (ϵ 2,200) nm.

Methyl 1-(1-cyclopenten-1-yl)-2-oxocyclopentaneacetate (121a)^{124a}**121a**

Methyl ester **121a** was prepared by treating the corresponding acid **121** with an ethereal solution of diazomethane. The reaction was complete when the initially yellow solution remained yellow. Evaporation of the solvent resulted in total conversion to an oil corresponding to ester **121a**.

IR (NaCl) ν_{\max} : 2954 (C-H), 1738 (C=O) cm^{-1} .

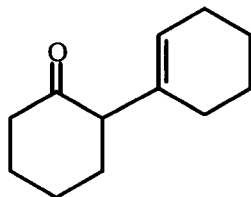
MS m/e (relative intensity) : 223 ($M+1$, 10), 222 (M^+ , 74), 191 (41), 190 (60), 173 (36), 163 (42), 162 (38), 150 (37), 149 (66), 107 (96), 91(100).

Exact mass calculated for $\text{C}_{13}\text{H}_{18}\text{O}_3$: 222.1256. Found : 222.1252.

^1H NMR (400 MHz, CDCl_3) : δ 5.41-5.39 (m, 1H, vinyl H), 3.52 (s, 3H, $\text{CH}_2\text{CO}_2\text{CH}_3$), 2.58 (AB-system, 2H, $J = 16$ Hz, $\text{CH}_2\text{CO}_2\text{CH}_3$), 2.26-1.66 (m, 12H, CH_2) ppm.

^{13}C NMR (50 MHz, CDCl_3) : δ 217.80 (ketone C=O), 171.67 (ester C=O), 141.62 (vinyl C), 127.59 (vinyl C-H), 52.74 ($\text{CH}_2\text{CO}_2\text{CH}_3$), 51.38 ($\text{CH}_2\text{CO}_2\text{CH}_3$), 39.31, 36.95, 32.84, 32.37, 31.57, 23.21, 18.98 (CH_2 , C) ppm.

UV (acetonitrile) λ_{\max} : 297 (ϵ 234), 204 (ϵ 2,980) nm.

2-(1-Cyclohexenyl)cyclohexanone (123a)¹²⁶**123a**

As outlined by Gault *et al.*,¹²⁶ H₂SO₄ (9 mL, 60%, Fisher Scientific) was added to a round bottomed flask fitted with a condenser and stirring bar. While stirring the solution at room temperature, cyclohexanone (15 g, 157 mmol, Aldrich) was added dropwise. The solution was stirred for 2 h at room temperature resulting in an increase of the temperature of the reaction mixture to 30 °C. The stirring was stopped and the solution was then left in the fumehood for 24 h. The reaction mixture was treated with water and diethyl ether and the layers were separated. The ether layer was washed three times with a saturated aqueous Na₂SO₄ solution and water. After drying the organic layer over MgSO₄, the solution was filtered and rotary evaporated. An orange oil was obtained (15 g, 81 mmol, 52%). Following distillation of the crude product (2.08g, 12 mmol), a clear oil of **123a** was obtained (1.2 g, 6.7 mmol, 60%).

BP : 130 °C (6 mm), (lit.¹²⁶ 150 °C(18-20 mm)).

IR (NaCl) ν_{\max} : 2931 (C-H), 1713 (C=O) cm⁻¹.

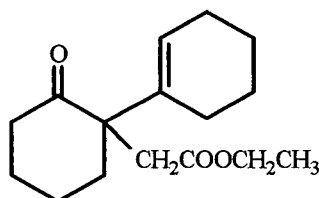
MS m/e (relative intensity) : 179 (M+1, 9), 178 (M⁺, 59), 150 (16), 149 (100), 135 (36), 121 (19), 107 (22), 98 (16), 93 (32), 92 (22), 91 (37).

Exact mass calculated for C₁₂H₁₈O : 178.1358. Found : 178.1360.

^1H NMR (200 MHz, CDCl_3) : δ 5.09-5.07 (m, 1H, vinyl H), 2.65-2.45 (m, 1H, CH), 2.10-1.93 (m, 4H, CH_2), 1.80-1.15 (m, 12H, CH_2) ppm.

^{13}C NMR (50 MHz, CDCl_3): δ 211.50 (C=O), 135.75 (vinyl C), 123.44 (vinyl C-H), 58.60 (CH_2), 41.98, 31.75, 27.56, 27.14, 25.40, 25.35, 22.74, 22.31 (CH_2 , C) ppm.

Ethyl 1-(1-cyclohexen-1-yl)-2-oxocyclohexaneacetate (124)



124

Following the procedure used to make keto-ester 120, dry DMSO (25 mL) was added to a round bottomed flask containing sodium hydride (539 mg, 13 mmol, 60% in oil, Aldrich) under nitrogen. The mixture was then heated in an oil bath to 75 °C for 30 min. Following cooling of the flask in a water bath to 30 °C, cyclohexenylcyclohexanone 123a (2.08 g, 12 mmol) in DMSO (20 mL) was added dropwise to the solution and stirred for 1 h. Ethyl bromoacetate (2.3 g, 14 mmol, Aldrich) dissolved in DMSO (15 mL) was then added dropwise to the flask. The solution was stirred for 30 min. After quenching the reaction mixture with a saturated aqueous solution of ammonium chloride, an extraction with *n*-pentane was performed. After drying the solution over MgSO_4 , filtration and rotary evaporation, a light yellow oil was obtained (2.1 g, 7.9 mmol, 68%). After column chromatography with silica gel eluting the compound with ethyl acetate / petroleum ether (3 : 97), a colorless oil of 124 (1.1 g, 4.1 mmol, 35%) resulted.

IR (KBr) ν_{\max} : 2934 (C-H), 1710 (C=O) cm^{-1} .

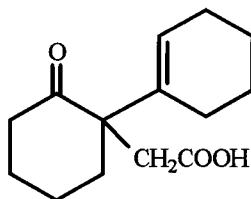
MS m/e (relative intensity) : 265 (M+1, 8), 264 (M^+ , 38), 235 (46), 219 (32), 218 (37), 190 (22), 177 (100), 91 (70).

Exact mass calculated for $\text{C}_{16}\text{H}_{24}\text{O}_3$: 264.1725. Found : 264.1732.

^1H NMR (200 MHz, CDCl_3) : δ 5.51-5.49 (m, 1H, vinyl H), 3.99 (q, 2H, $J = 7$ Hz, $\text{CO}_2\text{CH}_2\text{CH}_3$), 2.45 (AB-system, 2H, $J = 14$ Hz, $\text{CH}_2\text{CO}_2\text{CH}_2\text{CH}_3$), 2.25-2.12 (m, 2H, CH_2), 2.07-1.64 (m, 6H, CH_2), 1.63-1.43 (m, 8H, CH_2), 1.15 (t, 3H, $J = 8$ Hz, $\text{CO}_2\text{CH}_2\text{CH}_3$) ppm.

^{13}C NMR (50 MHz, CDCl_3) : δ 212.12 (ketone C=O), 171.87 (ester C=O), 135.02 (vinyl C), 125.13 (vinyl C-H), 59.90 ($\text{CO}_2\text{CH}_2\text{CH}_3$), 57.07 ($\text{CH}_2\text{CO}_2\text{CH}_2\text{CH}_3$), 41.21, 39.80, 34.11, 27.46, 25.56, 25.07, 22.98, 22.03, 21.57 (CH_2 , C), 14.20 ($\text{CO}_2\text{CH}_2\text{CH}_3$) ppm.

1-(1-Cyclohexen-1-yl)-2-oxocyclohexaneacetic acid (125)



125

To a solution of ester **124** (143 mg, 0.542 mmol) in methanol (4 mL), KOH (91 mg, 1.62 mmol) was added and the mixture was refluxed overnight. The methanol was evaporated and the remaining solid was dissolved in diethyl ether and washed with water. The aqueous layer was acidified with 15% HCl, extracted with diethyl ether (three times) and the organic layer was dried

over MgSO_4 , filtered and rotary evaporated. After column chromatography on silica gel with diethyl ether / petroleum ether (3 : 7), followed by recrystallization from the same solvent system, white crystals of **125** (70 mg, 0.297 mmol, 55%) were obtained.

MP : 101-102 °C.

IR (KBr) ν_{max} : 3400-2960 (OH), 2941(C-H), 1708 (C=O) cm^{-1} .

MS m/e (relative intensity) : 237 (M+1, 7), 236 (M^+ , 42), 207 (90), 177 (100), 149 (25), 148 (28), 133 (26).

Exact mass calculated for $\text{C}_{14}\text{H}_{20}\text{O}_3$: 236.1412. Found : 236.1412.

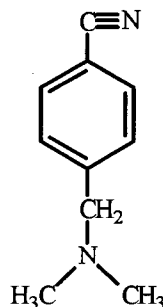
^1H NMR (200 MHz, CDCl_3) : δ 10.95-10.38 (s, 1H, broad, OH), 5.36-5.34 (m, 1H, vinyl H), 2.50 (AB-system, 2H, $J = 14$ Hz, $\text{CH}_2\text{CO}_2\text{H}$), 2.34-2.20 (m, 2H, CH_2), 2.10-1.70 (m, 6H, CH_2), 1.65-1.38 (m, 8H, CH_2) ppm.

^{13}C NMR (50 MHz, CDCl_3) : δ 215.55 (ketone C=O), 175.43 (ester C=O), 135.13 (vinyl C), 126.56 (vinyl C-H), 57.56 ($\text{CH}_2\text{CO}_2\text{H}$), 42.30, 39.74, 34.86, 27.41, 25.63, 24.68, 22.88, 21.94, 21.57 (CH_2 , C) ppm.

UV (methanol) λ_{max} : 290 (ϵ 120), 204 (ϵ 2,978) nm.

Anal. calculated for $\text{C}_{14}\text{H}_{20}\text{O}_3$: C, 71.14; H, 8.54. Found : C, 71.14; H, 8.53.

X-Ray Crystal Data for $\text{C}_{14}\text{H}_{20}\text{O}_3$: Space group $C2/c$ (# 15), $a = 26.516(2)$ Å, $b = 6.9831(3)$ Å, $c = 18.503(2)$ Å, $\beta = 131.394(4)^\circ$, $V = 2570.2(4)$ Å³, $Z = 8$, $D_{\text{calcd}} = 1.22$ g/cm³, $R = 0.056$.

***p*-(Dimethylaminomethyl)benzonitrile (127)¹²⁷****127**

A solution of α -bromo-*p*-toluonitrile (1.0 g, 5.1 mmol, Aldrich) in anhydrous diethyl ether / benzene (8 mL / 2 mL) was chilled to $-78\text{ }^{\circ}\text{C}$ in a dry ice / acetone bath as described by Norman *et al.*¹²⁷ Dimethyl amine gas (230 mg, 5.1 mmol, Aldrich) was bubbled through the solution for 10 min, the flask was sealed and was allowed to warm up to room temperature over a period of 48 h. After cooling the solution to $-10\text{ }^{\circ}\text{C}$ in a salt / ice bath, the flask was opened and the solvent rotary evaporated. The remaining solid was dissolved in a minimum amount of water, extracted with diethyl ether, the ether layer dried over MgSO_4 , filtered and evaporated to give a pale yellow oil of **127** (543 mg, 3.4 mmol, 66%).

IR (NaCl) ν_{max} : 2942 (C-H), 2361 (C \equiv N), 1018 (C-N) cm^{-1} .

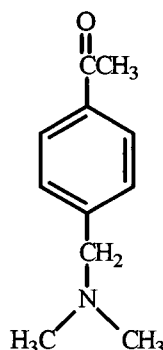
MS m/e (relative intensity) : 161 ($\text{M}+1$, 3), 160 (M^+ , 28), 116 (29), 102 (2), 58 (100).

Exact mass calculated for $\text{C}_{10}\text{H}_{12}\text{N}_2$: 160.1000. Found : 160.0996.

^1H NMR (200 MHz, CDCl_3) : δ 7.42 (m, 2H, aromatic H), 7.28 (m, 2H, aromatic H), 3.32 (s, 2H, CH_2), 2.10 (s, 6H, CH_3) ppm.

^{13}C NMR (50 MHz, CDCl_3) : δ 144.81 (aromatic C), 131.94, 129.39 (aromatic C-H), 118.90 (CN), 110.71 (aromatic C), 63.65 (CH_2), 45.31 (CH_3) ppm.

p-Acetyl-*N,N*-dimethylbenzylamine (128)¹²⁷



128

Following the procedure of Norman *et al.*,¹²⁷ compound 127 (685 mg, 4.3 mmol) dissolved in toluene (5 mL) was added to a solution of MeMgI (1.6 mL, 12 mmol, Aldrich) in toluene (10 mL) and refluxed for 48 h. The reaction mixture was poured onto crushed ice and HCl (6 M) was added until the precipitate dissolved. The solution was heated in an oil bath (100 °C) for 2 h, cooled, extracted with diethyl ether and washed with water and brine. The organic layer was dried over MgSO_4 , filtered and evaporated, resulting in a pale yellow oil of 128 (585 mg, 3.3 mmol, 77%).

IR (NaCl) ν_{max} : 2975 (C-H), 1685 (C=O), 1017 (C-N) cm^{-1} .

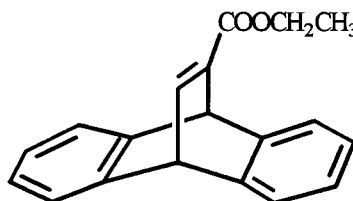
MS m/e (relative intensity) : 178 ($\text{M}+1$, 8), 177 (M^+ , 67), 133 (21), 105 (12), 58 (100).

Exact mass calculated for $\text{C}_{11}\text{H}_{15}\text{NO}$: 177.1154. Found : 177.1154.

¹H NMR (200 MHz, CDCl₃) : δ 7.75 (m, 2H, aromatic H), 7.25 (m, 2H, aromatic H), 3.25 (s, 2H, CH₂), 2.40 (s, 3H, COCH₃), 2.08 (s, 6H, NCH₃) ppm.

¹³C NMR (50 MHz, CDCl₃) : δ 197.50 (C=O), 144.69, 135.95 (aromatic C), 129.05, 128.25 (aromatic C-H), 63.77 (CH₂), 45.27 (NCH₃), 26.40 (COCH₃) ppm.

10.2.3. 9,10-Dihydro-9,10-ethenoanthracene Derivatives

Ethyl 9,10-Dihydro-9,10-ethenoanthracene-11-carboxylate (130)¹²⁸

130

Anthracene (5.0 g, 28 mmol) and ethyl propiolate (3.3 g, 34 mmol, Aldrich) were placed in a Carius tube which was then sealed and heated to 180 °C for 6 h, a reaction initially carried out by Vaughan and Milton in refluxing mixed xylenes.¹²⁸ After column chromatography (1% ethyl acetate in petroleum ether) over silica gel and recrystallization from petroleum ether, white crystals of the ester **130** were obtained (15 g, 55 mmol, 61%).

MP : 103-105 °C (lit.¹²⁸ 111.5-112.5 °C).

IR (KBr) ν_{\max} : 1700 (C=O), 1611 (C=C), 1218 (C-O) cm^{-1} .

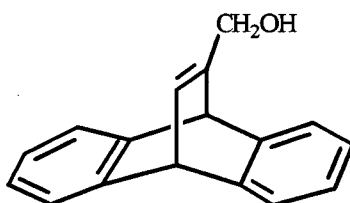
MS m/e (relative intensity): 277 ($M+1$, 7), 276 (M^+ , 35), 203 (100), 178 (12).

Exact mass calculated for $\text{C}_{19}\text{H}_{16}\text{O}_2$: 276.1150. Found : 276.1158.

^1H NMR (200 MHz, CDCl_3) : δ 7.88 (dd, 1H, $J = 2$ Hz & 7 Hz, vinyl C-H), 7.41-7.31. (m, 4H, aromatic H), 6.95-7.05 (m, 4H, aromatic H), 5.70 (d, 1H, $J = 2$ Hz, bridgehead H), 5.25 (d, 1H, $J = 7$ Hz, bridgehead H), 4.19 (q, 2H, $J = 7$ Hz, $\text{CO}_2\text{CH}_2\text{CH}_3$), 1.27 (t, 3H, $J = 7$ Hz, $\text{CO}_2\text{CH}_2\text{CH}_3$) ppm.

^{13}C NMR (50 MHz, CDCl_3) : δ 164.78 (C=O), 149.25 (vinyl C-H), 145.38 (aromatic C), 144.75 (vinyl C), 144.48 (aromatic C), 125.06, 124.88, 123.75, 123.52 (aromatic C-H), 60.70 ($\text{CO}_2\text{CH}_2\text{CH}_3$), 51.61, 50.40 (bridgehead C-H), 14.29 ($\text{CO}_2\text{CH}_2\text{CH}_3$) ppm.

11-Hydroxymethyl-9,10-dihydro-9,10-ethenoanthracene (131)¹²⁹



131

Ethyl ester 130 (3.2 g, 12 mmol) dissolved in 38 mL of anhydrous ether was added dropwise over a period of 30 min to a solution of 1.2 g (12 mmol) of aluminum trichloride (caution) and 1.0 g (26 mmol) of lithium aluminum hydride in 150 mL of anhydrous ether while stirring at room temperature. The reaction mixture was then stirred for 2 h at room temperature and quenched with a saturated solution of aqueous Na_2SO_4 . The precipitate was filtered through a Celite filter and washed with ethyl acetate. Following an extraction with ethyl acetate, the organic layer was washed with water and brine and dried over MgSO_4 . The solvent was rotary evaporated and the oil redissolved in ethanol. After evaporation of the solvent in an evaporating dish and recrystallization from ethanol, 2.2 g (9.2 mmol, 80%) of white crystals of the alcohol 131 were obtained.

MP : 121-123 °C (lit.¹²⁹ 126-127 °C).

IR (KBr) ν_{\max} : 3200 (O-H), 2980 (C-H) cm^{-1} .

MS m/e (relative intensity) : 235 ($M+1$, 9), 234 (M^+ , 45), 203 (100), 178 (67).

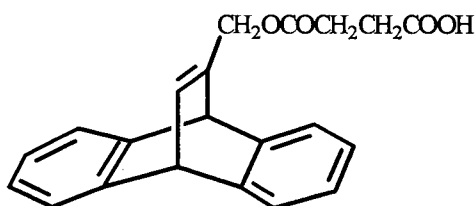
Exact mass calculated for $\text{C}_{17}\text{H}_{14}\text{O}$: 234.1045. Found : 234.1043.

^1H NMR (200 MHz, CDCl_3) : δ 7.35-7.20 (m, 4H, aromatic H), 7.04-6.90 (m, 4H, aromatic H), 6.75 (dd, 1H, $J = 2$ & 7 Hz, vinyl H), 5.11 (d, 1H, $J = 7$ Hz, bridgehead H), 5.05 (d, 1H, $J = 2$ Hz, bridgehead H), 4.28 (s, 2H, CH_2OH), 1.43 (s, broad, 1H, OH) ppm.

^{13}C NMR (50 MHz, CDCl_3) : δ 152.59 (vinyl C), 146.44, 145.80 (aromatic C), 133.58 (vinyl C-H), 124.65, 124.53, 123.07, 122.91 (aromatic C-H), 63.32 (CH_2OH), 52.51 & 50.72 (bridgehead C-H) ppm.

UV (acetonitrile) λ_{\max} : 280 (ϵ 5,870), 272 (ϵ 3,893), 253 (ϵ 2,696) nm.

13-(11-Methyl-9,10-dihydro-9,10-ethenoanthracenyl)succinate (132)



132

To a round bottomed flask fitted with a condenser, alcohol 131 (452 mg, 1.9 mmol) and succinic anhydride (396 mg, 4.0 mmol, Eastman Kodak Co.), as well as 20 mL of dry pyridine were refluxed overnight, adapting procedures described by Aries¹³⁰ and applying them to the above system. After cooling the solution to room temperature, water was added and the solution was acidified with concd HCl. The reaction mixture was then extracted three times with ethyl

acetate. The organic layer was washed with warm water and aqueous 5% Na₂CO₃ (three times). The basic layer was then acidified with aqueous HCl (15%). The acidic aqueous layer was extracted with ethyl acetate (three times) and the organic layer was washed with water and brine and dried over MgSO₄. Evaporation of the solvent resulted in a yellow oil which was column chromatographed on silica gel (3 : 7 : 1, ethyl acetate: petroleum ether: ethanol) giving a colorless oil (**132**), which solidified in the freezer (524 mg, 1.5 mmol, 81%).

MP : 90-93 °C.

IR (KBr) ν_{\max} : 3210 (O-H), 2971 (C-H), 1737 (C=O), 1713 (C=O) cm⁻¹.

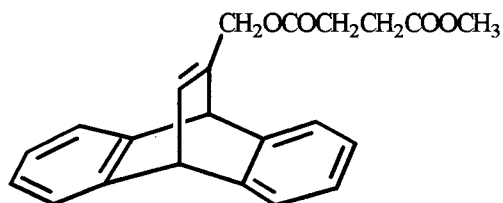
MS m/e (relative intensity) : 335 (M+1, 1), 334 (M⁺, 4), 233 (13), 216 (100).

Exact mass calculated for C₂₁H₁₈O₄ : 334.1205. Found : 334.1197.

¹H NMR (200 MHz, CDCl₃) : δ 10.55 (s, broad, 1H, OH), 7.40-7.25(m, 4H, aromatic H), 6.97-6.89 (m, 4H, aromatic H), 6.86 (m, 1H, vinyl H), 5.21 (d, 1H, $J = 6$ Hz, bridgehead H), 5.15 (d, 1H, $J = 2$ Hz, bridgehead H), 4.78 (d, 2H, $J = 1$ Hz, CH₂O), 2.57 (s, broad, 4H, COCH₂CH₂CO) ppm.

¹³C NMR (75 MHz), CDCl₃) : δ 178.17, 171.84 (C=O), 147.42 (vinyl C), 145.87, 145.42 (aromatic C), 136.82 (vinyl C-H), 124.67, 124.56, 123.00, 123.00 (aromatic C-H), 64.45 (CH₂O), 52.68 & 50.76 (bridgehead C-H), 28.75 (COCH₂CH₂CO) ppm.

UV (acetonitrile) λ_{\max} : 279 (ϵ 3,305), 272 (ϵ 2,170), 212 (ϵ 22,309) nm.

Methyl 13-(11-methyl-9,10-dihydro-9,10-ethenoanthracenyl)succinate (132a)**132a**

To carboxylic acid **132** (431 mg, 1.3 mmol) dissolved in diethyl ether, an ethereal solution of diazomethane was added until the solution remained yellow. The flask was left in the fumehood to evaporate the excess diazomethane and the solvent was rotary evaporated giving a yellow oil which was column chromatographed on silica gel (1 : 9, ethyl acetate : petroleum ether) resulting in a colorless oil (**132a**) which solidified upon standing in the freezer overnight (346 mg, 0.994 mmol, 77%).

MP : 85-86 °C.

IR (KBr) ν_{\max} : 2944 (C-H), 1727 (C=O) cm^{-1} .

MS m/e (relative intensity) : 349 (M+1, 3), 348 (M⁺, 12), 233 (14), 217 (39), 216 (100), 203 (27).

Exact mass calculated for C₂₂H₂₀O₄ : 348.1362. Found : 348.1356.

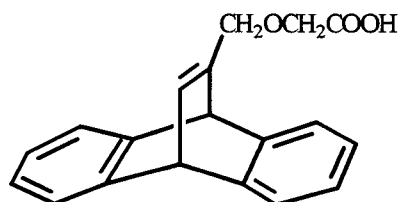
¹H NMR (400 MHz, CDCl₃) : δ 7.31-7.25 (m, 4H, aromatic H), 6.98- 6.93 (m, 4H, aromatic H), 6.85-6.83 (m, 1H, vinyl H), 5.09 (d, 1H, *J* = 6 Hz, bridgehead H), 5.02 (d, 1H, *J* = 2 Hz, bridgehead H), 4.79 (d, 2H, *J* = 1 Hz, CH₂O), 3.68 (s, 3H, OCH₃), 2.62 (s, broad, 4H, COCH₂CH₂CO) ppm.

^{13}C NMR (50 MHz), CDCl_3 : δ 172.67, 172.00 (C=O), 147.59 (vinyl C), 145.96, 145.50 (aromatic C), 136.70 (vinyl C-H), 124.72, 124.60, 123.07, 123.03 (aromatic C-H), 64.39 (CH_2O), 52.74, 50.84 (bridgehead C-H), 51.87 (OCH_3), 29.09, 28.86 ($\text{COCH}_2\text{CH}_2\text{CO}$) ppm.

UV (acetonitrile) λ_{max} : 279 (ϵ 3,180), 272 (ϵ 2,067), 252 (ϵ 1,337) nm.

Anal. calculated for $\text{C}_{22}\text{H}_{20}\text{O}_4$: C, 75.84; H, 5.79. Found C, 75.93; H, 5.79.

13-(11-Methyleneoxy-9,10-dihydro-9,10-ethenoanthracenyl)acetic Acid (133)



133

In a round bottomed two-neck flask fitted with a condenser, alcohol 131 (500 mg, 2.1 mmol) and bromoacetic acid (297 mg, 2.1 mmol, Aldrich) were dissolved in 25 mL of dry THF under nitrogen adapting procedures described by Brady and Giang¹³¹ and applying them to the above system. While cooling the flask in an ice bath, sodium hydride (256 mg, 6.4 mmol, 60% in oil) was added and the solution was stirred for 20 min at room temperature. The solution was then refluxed for 2 h. After quenching the reaction with a mixture of ethyl acetate and water, the solution was acidified with aqueous 15% HCl and an extraction with ethyl acetate was performed, followed by a wash with brine. The organic layer was dried over MgSO_4 , filtered and rotary evaporated. The resulting carboxylic acid 133 was purified by an aqueous 10 % KOH wash, followed by an acidification of the aqueous layer with 15% HCl. The acidic aqueous layer was

extracted with ethyl acetate (three times) and washed with water and brine. After drying the organic layer over MgSO_4 , filtration and evaporation of the solvent, acid **133** (487g, 1.7 mmol, 78%) was obtained.

MP : 55-57 °C.

IR (KBr) ν_{max} : 3067(O-H), 2906 (C-H), 1724 (C=O) cm^{-1} .

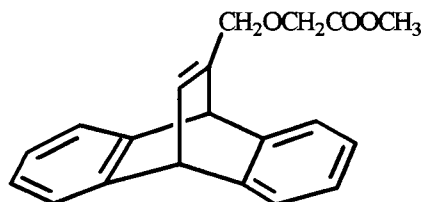
MS m/e (relative intensity) : 293 (M+1, 2), 292 (M^+ , 10), 216 (54), 215 (42), 202 (62), 178 (100).

Exact mass calculated for $\text{C}_{19}\text{H}_{16}\text{O}_3$: 292.1099. Found : 292.1094.

^1H NMR (200 MHz, CDCl_3) : δ 11.6 (s, broad, 1H, OH), 7.26-7.12 (m, 4H, aromatic H), 6.93-6.80 (m, 4H, aromatic H), 6.75 (d, 1H, $J = 6$ Hz, vinyl H), 5.06 (s, 1H, bridgehead H), 5.01 (d, 1H, $J = 6$ Hz, bridgehead H), 4.19 (s, 2H, CH_2O), 3.65 (s, 2H, $\text{CH}_2\text{CO}_2\text{H}$) ppm.

^{13}C NMR (50 MHz, CDCl_3) : δ 178.00 (C=O), 148.59 (vinyl C), 146.04, 145.55 (aromatic C), 137.73 (vinyl C-H), 124.72, 124.65, 123.14, 123.00 (aromatic C-H), 70.85, 65.70 (CH_2), 52.36 & 50.93 (bridgehead C-H) ppm.

UV (acetonitrile) λ_{max} : 279 (ϵ 3,853), 272 (ϵ 2,564), 210 (ϵ 22,331) nm.

Methyl 13-(11-methyleneoxy-9,10-dihydro-9,10-ethenoanthracenyl)acetate (133a)**133a**

The carboxylic acid **133** (635 mg, 2.1 mmol) was dissolved in diethyl ether and treated with an ethereal solution of diazomethane until the solution remained yellow. The reaction flask was left in the fumehood until the yellow color disappeared and the remaining ether was rotary evaporated leaving a yellow oil which was purified by column chromatography (silica gel, 1 : 9, ethyl acetate: petroleum ether) resulting in a colorless oil. This oil (**133a**) solidified upon standing overnight in the freezer (513 mg, 1.7 mmol, 78%).

MP : 71-73 °C.

IR (KBr) ν_{\max} : 2952 (C-H), 1753 (C=O) cm^{-1} .

MS m/e (relative intensity) : 307 ($M+1$, 8), 306 (M^+ , 38), 217 (43), 216 (100), 215 (43), 204 (16), 203 (77), 202 (34), 178 (48).

Exact mass calculated for $\text{C}_{20}\text{H}_{18}\text{O}_3$: 306.1255. Found : 306.1250.

^1H NMR (400 MHz, CDCl_3) : δ 7.40-7.25 (m, 4H, aromatic H), 7.03-6.92 (m, 4H, aromatic H), 6.84 (d, 1H, $J = 6\text{Hz}$, vinyl H), 5.19 (s, 1H, bridgehead H), 5.11 (d, 1H, $J = 6\text{ Hz}$, bridgehead H), 4.29 (s, 2H, CH_2O), 3.77 (s, 2H, $\text{CH}_2\text{CO}_2\text{CH}_3$), 3.71 (s, 3H, OCH_3) ppm.

^{13}C NMR (75MHz, CDCl_3) : δ 170.62 (C=O), 148.81 (vinyl C), 146.00, 145.53 (aromatic C), 137.15 (vinyl C-H), 124.54, 124.45, 123.05, 122.83 (aromatic C-H), 70.64, 66.05 ($\underline{\text{C}}\text{H}_2$), 52.20 (bridgehead C-H), 51.69($\text{O}\underline{\text{C}}\text{H}_3$), 50.79 (bridgehead C-H) ppm.

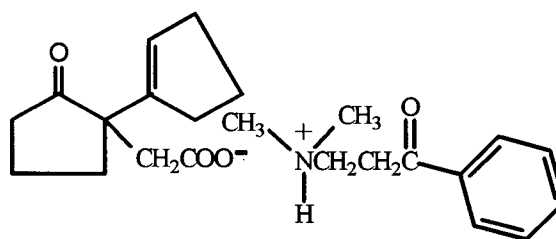
UV (acetonitrile) λ_{max} : 279 (ϵ 3,711), 272 (ϵ 2,376), 211 (ϵ 20,246) nm.

Anal. calculated for $\text{C}_{20}\text{H}_{18}\text{O}_3$: C, 78.41; H, 5.92. Found C, 78.28; H, 5.78.

10.3. Salt Formation of Photochemical Substrates

10.3.1. Sensitizer Salts Formed with 2-(1-Cyclopentenyl)cyclopentanone Derivative 121

3-(Dimethylamino)propiofenone Salt of Acid 121 (138)



138

3-(Dimethylamino)propiofenone hydrochloride (76 mg, 0.355 mmol, Aldrich) was dissolved in ethanol (5 mL), and KOH (20 mg, 0.355 mmol) in ethanol (2 mL) was added. The solution was centrifuged and the liquid pipetted off and added to a solution of acid 121 (74 mg, 0.355 mmol) in ethanol. Some of the solvent was evaporated and ethyl acetate added. After a week fine white needles (138) had formed (19 mg, 0.050 mmol, 14%).

MP : 117-118 °C.

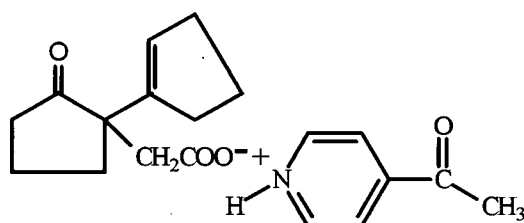
IR (KBr) ν_{\max} : 3422 (N-H), 2954 (C-H), 1736 (pentanone C=O), 1680 (C=O) cm^{-1} , 1579 (COO⁻ asym.), 1409 (COO⁻ sym.) cm^{-1} .

MS FAB (matrix : Thioglycerol) : 386 (M+1).

Exact mass calculated for C₂₃H₃₁NO₄ (Thioglycerol +M+1) : 386.2331. Found : 386.2313.

$^1\text{H NMR}$ (400 MHz, d_6 -DMSO) : δ 8.70 (s, broad, 1H, N-H), 8.05-7.85 (m, 2H, aromatic H), 7.63-7.04 (m, 3H, aromatic H), 5.38 (t, 1H, $J = 2$ Hz, vinyl H), 3.54 & 3.30 (s, broad, 2H each, CH_2CH_2), 2.62 (AB-system, 2H, $J = 16$ Hz, CH_2COO^-), 2.31-1.52 (m, 12H, CH_2), 2.30 (s, 6H, CH_3) ppm.

p-Acetylpyridine Salt of Acid 121 (140)



140

Acid 121 (100 mg, 0.481 mmol) was dissolved in ethanol (3 mL) and *p*-acetylpyridine (60 mg, 0.481 mmol, Aldrich) in ethanol (1 mL) was added dropwise to the solution. After evaporation of some of the solvent and addition of diethyl ether (3 mL) colorless plates of 140 formed (131 mg, 0.399 mmol, 83%).

MP : 68-70 °C.

IR (KBr) ν_{max} : 3059 (N-H), 2962 (C-H), 1734 (pentanone C=O), 1692 (C=O), 1606 (COO^- asym.), 1405 (COO^- sym.) cm^{-1} .

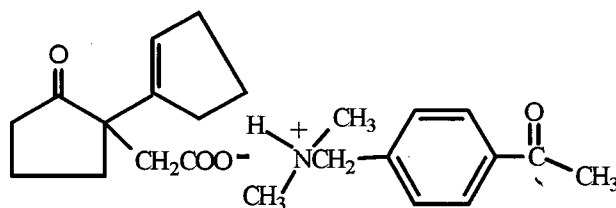
MS FAB (matrix : 3-Nitrobenzyl alcohol) : 330 (M+1).

Exact mass calculated for $C_{19}H_{23}NO_4$ (Thioglycerol + $CHCl_3$, M+1) : 330.1705. Found : 330.1695.

1H NMR (200 MHz, $CDCl_3$) : δ 10.40 (s, broad, 1H, N-H), 8.68 (s, broad, 2H, aromatic H), 7.70-7.52 (m, 2H, aromatic H), 5.36-5.34 (m, 1H, vinyl H), 2.63 (AB-system, 2H, $J = 17$ Hz, CH_2COO^-), 2.48 (s, 3H, CH_3), 2.25-1.55 (m, 12H, CH_2) ppm.

^{13}C NMR (75 MHz, $CDCl_3$) : δ 219.00 (cyclopentanone C=O), 197.06 (C=O), 175.18 (COO^-), 150.22 (aromatic C-H), 143.13 (aromatic C), 141.37 (vinyl C), 127.97 (vinyl C-H), 52.80 (CH_2), 39.70, 37.05, 33.03, 32.46, 31.59, 23.22, 19.07 (CH_2 , C), 26.64 (CH_3) ppm.

***p*-Acetyl-*N,N*-dimethylbenzylamine Salt of Acid 121 (139)**



139

To a solution of acid 121 (127 mg, 0.611 mmol) in acetone (5 mL), *p*-acetyl-*N,N*-dimethylbenzylamine (128, 325 mg, 1.8 mmol) in 5 mL of acetone was added. Upon addition of diethyl ether (10 mL) no salt formation was observed. The mixture was chromatographed on silica gel 60 (1:1, methanol : ethyl acetate) and a white solid formed after evaporation of the solvent, which proved to be the salt 139 (85 mg, 0.221 mmol, 36%).

MP : 165-167 °C.

IR (KBr) ν_{\max} : 3415 (N-H), 2961 (C-H), 1728 (pentanone C=O), 1668 (C=O), 1570 (COO⁻ asym.), 1423 (COO⁻ sym.) cm⁻¹.

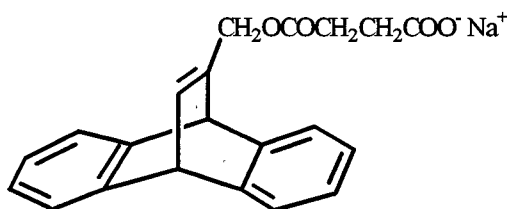
MS FAB (matrix : Thioglycerol) : 386 (M+1).

¹H NMR (400 MHz, d₆-DMSO) : δ 7.95-7.82 (m, 2H, aromatic H), 7.50-7.33 (m, 2H, aromatic H), 5.336-5.34 (m, 1H, vinyl H), 3.44 (s, broad, 3H, CH₂N & NH), 2.54 (s, broad, 5H, CH₂COO⁻ & COCH₃), 2.36-1.57 (m, 12H, CH₂), 2.14 (s, 6H, NCH₃) ppm.

10.3.2. Alkali Metal Salts Formed with 9,10-Dihydro-9,10-ethenoanthracene Derivatives

10.3.2.1. Alkali Metal Salts Formed with Succinate Derivative 132

Sodium Salt of Succinate Derivative 132 (153)



153

Succinate derivative 132 (102 mg, 0.306 mmol) was dissolved in a mixture of acetone (1mL) and diethyl ether (2 mL). A solution of NaHCO₃ (26 mg, 0.306 mmol) in water (0.5 mL) was added dropwise to the ice-cooled solution. The solution was then stirred until a white precipitate formed. After centrifuging the solution, salt 153 was obtained as a white powder (48 mg, 0.135 mmol, 44%).

MP : 205-207 °C.

IR (KBr) ν_{\max} : 3421 (O-H), 2969 (C-H), 1730 (C=O), 1580 (COO⁻ asym.), 1420 (COO⁻ sym.) cm⁻¹.

MS FAB (matrix : 3-Nitrobenzyl alcohol) : 357(M+1).

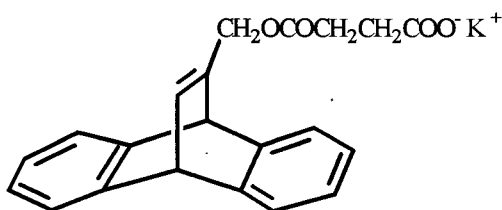
Exact mass calculated for C₂₁H₁₇O₄Na (3-Nitrobenzyl alcohol, M+1) : 357.1103.

Found : 357.1100.

¹H NMR (200 MHz, CDCl₃) : δ 7.23-7.09 (m, 4H, aromatic H), 6.94-6.76 (m, 4H, aromatic H), 6.65-6.53 (m, 1H, vinyl H), 4.92 (d, 1H, *J* = 6 Hz, bridgehead H), 4.88 (d, 1H, *J* = 2 Hz, bridgehead H), 4.52 (s, 2H, CH₂O), 2.45-2.03 (m, 4H, COCH₂CH₂COO⁻) ppm.

Anal. calculated for C₂₁H₁₇O₄ Na • 2 H₂O : C, 64.28; H, 5.39. Found : C, 64.31; H, 5.31.

Potassium Salt of Succinate Derivative 132 (154)



154

After dissolving succinate derivative 132 (78 mg, 0.234 mmol) in a mixture of acetone (1 mL) and diethyl ether (2 mL), KHCO₃ (23 mg, 0.234 mmol) dissolved in water (0.5 mL) was added dropwise to the ice-cooled solution. The mixture was stirred until a white precipitate formed. A white powder resulted which was filtered off, giving salt 154 (31 mg, 0.084 mmol, 36%).

MP : 244-246 °C.

IR (KBr) ν_{\max} : 3426 (O-H), 2968 (C-H), 1728 (C=O), 1577 (COO⁻ asym.), 1402 (COO⁻ sym.)
cm⁻¹.

MS FAB (matrix : Thioglycerol + CHCl₃) : 373 (M+1).

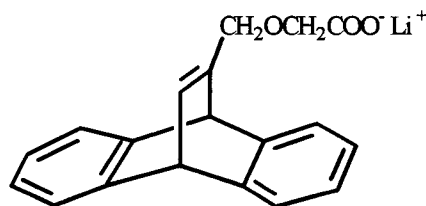
Exact mass calculated for C₂₁H₁₇O₄ K (Thioglycerol + CHCl₃, M+1) : 373.0842. Found :
373.0841.

¹H NMR (200 MHz, CDCl₃) : δ 7.23-7.09 (m, 4H, aromatic H), 7.00-6.75 (m, 4H, aromatic H),
6.70-6.55 (m, 1H, vinyl H), 4.95 (d, 1H, $J = 6$ Hz, bridgehead H), 4.90 (d, 1H, $J = 2$ Hz,
bridgehead H), 4.58 (s, 2H, CH₂O), 2.45-2.05 (m, 4H, COCH₂CH₂COO⁻) ppm.

Anal. calculated for C₂₁H₁₇O₄ K • H₂O : C, 64.60; H, 4.90. Found : C, 64.24; H, 4.45.

10.3.2.2. Alkali Metal Salts Formed with Acetic Acid Derivative 133

Lithium Salt of Acid 133 (158)



158

Dissolved acid 133 (286 mg, 0.979mmol) in ethanol (3 mL) and Li(OH)·H₂O (41 mg, 0.979 mmol) in H₂O (0.5 mL) were combined and stirred. Diethyl ether was added and the solution was placed in the freezer. A beige powder (158) resulted (240 mg, 0.805 mmol, 82%).

MP : 262-264 °C.

IR (KBr) ν_{\max} : 3400 (OH), 2967(C-H), 1609 (COO⁻ asym.), 1423 (COO⁻ sym.) cm⁻¹.

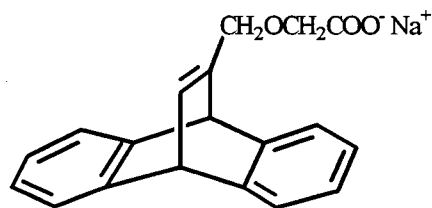
MS FAB (matrix : Thioglycerol + MeOH) : 299 (M+1).

Exact mass calculated for C₁₉H₁₅O₃Li (Thioglycerol + MeOH, M+1) : 299.1259. Found : 299.1248.

¹H NMR (400 MHz, CD₃OD) : δ 7.29-7.22 (m, 4H, aromatic H), 6.91-6.89 (m, 4H, aromatic H), 6.79 (m, 1H, vinyl H), 5.14 (d, 1H, *J* = 1 Hz, bridgehead H), 5.08 (d, 1H, *J* = 6 Hz, bridgehead H), 4.21 (s, 2H, CH₂O), 3.57 (s, 2H, CH₂COO⁻) ppm.

UV (methanol) λ_{\max} : 279 (ϵ 3,550), 272 (ϵ 2,515), 213 (ϵ 14,937) nm.

Anal. calculated for C₁₉H₁₅O₃ Li · H₂O : C, 72.15; H, 5.42. Found : C, 72.40; H, 5.33.

Sodium Salt of Acid 133 (159)**159**

Acid **133** (183 mg, 0.627 mmol) in ethanol (2 mL) and a solution of NaOH (31 mg, 0.627 mmol) in H₂O (0.5 mL) were combined. Diethyl ether (2 mL) was added and the solution was left in the freezer overnight. A white powder of **159** was obtained (153 mg, 0.487 mg, 78%).

MP : 260 °C (decomp).

IR (KBr) ν_{\max} : 3400 (O-H), 3065 (C-H), 1610 (COO⁻ asym.), 1426 (COO⁻ sym.) cm⁻¹.

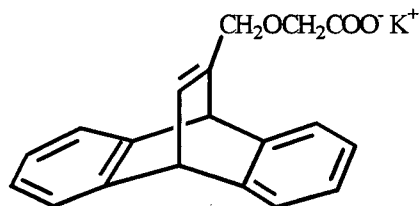
MS FAB (matrix : Thioglycerol + MeOH) : 315 (M+1).

Exact mass calculated for C₁₉H₁₅O₃Na (Thioglycerol + MeOH, M+1) : 315.0997. Found : 315.1004.

¹H NMR (400 MHz, CD₃OD) : δ 7.29-7.22 (m, 4H, aromatic H), 6.92-6.87 (m, 4H, aromatic H), 6.78 (m, 1H, vinyl H), 5.14 (d, 1H, $J = 2$ Hz, bridgehead H), 5.08 (d, 1H, $J = 6$ Hz, bridgehead H), 4.20 (d, 2H, $J = 1$ Hz, CH₂O), 3.55 (s, 2H, CH₂COO⁻) ppm.

UV (methanol) λ_{\max} : 279 (ϵ 3,895), 272 (ϵ 2,566), 211 (ϵ 25,845) nm.

Anal. calculated for C₁₉H₁₅O₃ Na • H₂O : C, 68.67; H, 5.16. Found : C, 68.82; H, 5.00.

Potassium Salt of Acid 133 (160)**160**

To a solution of acid 133 (185 mg, 0.634 mmol) in ethanol (3 mL) KOH (44 mg, 0.634 mmol) dissolved in H₂O (0.5 mL) was added. The solution was stirred and diethyl ether was added (3 mL). Small white crystals formed after 2 h in the freezer, which turned into a fine powder of 160 (177 mg, 0.476 mmol, 75 %), which was collected by filtration.

MP : 242-244 °C.

IR (KBr) ν_{max} : 3387 (O-H), 2908 (C-H), 1602 (COO⁻ asym.), 1413 (COO⁻ sym.) cm⁻¹.

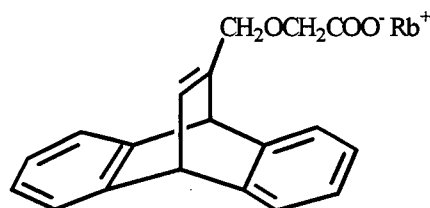
MS FAB (matrix : Thioglycerol + MeOH) : 331 (M+1).

Exact mass calculated for C₁₉H₁₅O₃K (Thioglycerol + MeOH, M+1) : 331.0736. Found : 331.0727.

¹H NMR (400 MHz, CD₃OD) : δ 7.29-7.22 (m, 4H, aromatic H), 6.92-6.87 (m, 4H, aromatic H), 6.78 (m, 1H, vinyl H), 5.14 (d, 1H, $J = 2$ Hz, bridgehead H), 5.08 (d, 1H, $J = 6$ Hz, bridgehead H), 4.20 (d, 2H, $J = 1$ Hz, CH₂O), 3.55 (s, 2H, CH₂COO⁻) ppm.

UV (methanol) λ_{max} : 279 (ϵ 4,903), 272 (ϵ 3,170), 213 (ϵ 15,981) nm.

Anal. calculated for C₁₉H₁₅O₃ K·H₂O : C, 65.49; H, 4.92. Found : C, 65.77; H, 4.81.

Rubidium Salt of Acid 133 (161)**161**

To a solution of acid **133** (265 mg, 0.908 mmol) in ethanol (3 mL) an aqueous solution of Rb(OH) (186mg, 0.912 mmol, 50% w/w) was added. The solution was stirred and diethyl ether was added (3 mL). After letting the solution sit in the freezer overnight, off-white needles corresponding to salt **161** were formed (190 mg, 0.505 mmol, 56%).

MP : 190-192 °C.

IR (KBr) ν_{\max} : 3398 (O-H), 3005 (C-H), 1597 (COO⁻ asym.), 1420 (COO⁻ sym.) cm⁻¹.

MS FAB (matrix : Thioglycerol + MeOH) : 377 (M+1).

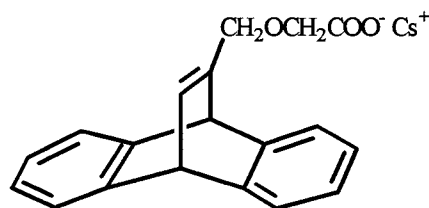
Exact mass calculated for C₁₉H₁₅O₃Rb (Thioglycerol + MeOH, M+1) : 377.0217.

Found : 377.0214.

¹H NMR (400 MHz, CD₃OD) : δ 7.29-7.22 (m, 4H, aromatic H), 6.92-6.87 (m, 4H, aromatic H), 6.78 (m, 1H, vinyl H), 5.14 (d, 1H, $J = 2$ Hz, bridgehead H), 5.08 (d, 1H, $J = 6$ Hz, bridgehead H), 4.20 (d, 2H, $J = 1$ Hz, CH₂O), 3.55 (s, 2H, CH₂COO⁻) ppm.

UV (methanol) λ_{\max} : 279 (ϵ 3,653), 272 (ϵ 2,602), 213 (ϵ 14,294) nm.

Anal. calculated for C₁₉H₁₅O₃ Rb • 1/2 [Rb(OH) • H₂O] : C, 52.22; H, 3.81. Found : C, 52.33; H, 3.69.

Cesium Salt of Acid 133 (162)**162**

Acid **133** (209 mg, 0.717 mmol) was dissolved in ethanol (5 mL) and an aqueous solution of Cs(OH) (215mg, 0.717 mmol, 50% w/w) was added. The solution was stirred and diethyl ether was added (5 mL). Off-white crystals (**162**) formed overnight in the freezer (181 mg, 0.427 mmol, 60 %).

MP : 40-42 °C.

IR (KBr) ν_{\max} : 3525 (O-H), 2906 (C-H), 1593 (COO⁻ asym.), 1417 (COO⁻ sym.) cm⁻¹.

MS FAB (matrix : Thioglycerol + MeOH) : 425 (M+1).

Exact mass calculated for C₁₉H₁₅O₃Cs (Thioglycerol + MeOH, M+1) : 425.0154. Found : 425.0142.

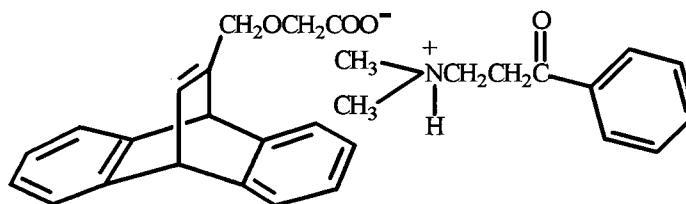
¹H NMR (400 MHz, CD₃OD) : δ 7.29-7.22 (m, 4H, aromatic H), 6.92-6.87 (m, 4H, aromatic H), 6.78 (m, 1H, vinyl H), 5.14 (d, 1H, $J = 2$ Hz, bridgehead H), 5.08 (d, 1H, $J = 6$ Hz, bridgehead H), 4.20 (d, 2H, $J = 1$ Hz, CH₂O), 3.55 (s, 2H, CH₂COO⁻) ppm.

UV (methanol) λ_{\max} : 279 (ϵ 3,285), 272 (ϵ 2,110), 213 (ϵ 12,817) nm.

Anal. calculated for C₁₉H₁₅O₃ Cs • H₂O : C, 51.60; H, 3.87. Found : C, 51.81; H, 3.84.

10.3.3. Sensitizer Salts Formed with Acetic Acid Derivative 133

3-(Dimethylamino)propiophenone Salt of 133 (164)



164

To a solution of acid 133 (157 mg, 0.538 mmol) in ethyl acetate (7 mL) 3-(dimethylamino)propiophenone was added (95 mg, 0.538 mmol, Aldrich) dissolved in ethanol (1 mL). The solution was stirred for 5 min and left in the fumehood. After two days colorless plates of the salt 164 (186 mg, 0.397 mmol, 74 %) had formed which were filtered off.

MP : 65-66 °C.

IR (KBr) ν_{\max} : 3385 (N-H), 2974 (C-H), 1681 (C=O), 1598 (COO⁻ asym.), 1401 (COO⁻ sym.) cm^{-1} .

MS FAB (matrix : 3-Nitrobenzyl alcohol) : 470 (M+1), 178 (amine + 1).

Exact mass calculated for C₃₀H₃₁NO₄ (3-Nitrobenzyl alcohol, M+1) : 470.2331. Found : 470.2337.

¹H NMR (400 MHz, CDCl₃) : δ 11.74 (s, 1H, broad, N-H), 7.94 (d, 2H, $J = 7$ Hz, aromatic H), 7.58-7.54 (m, 1H, aromatic H), 7.46-7.42 (m, 2H, aromatic H), 7.26-7.21 (m, 4H, aromatic H), 6.92-6.87 (m, 4H, aromatic H), 6.74 (m, 1H, vinyl H), 5.14 (d, 1H, $J = 1$ Hz, bridgehead H), 5.03

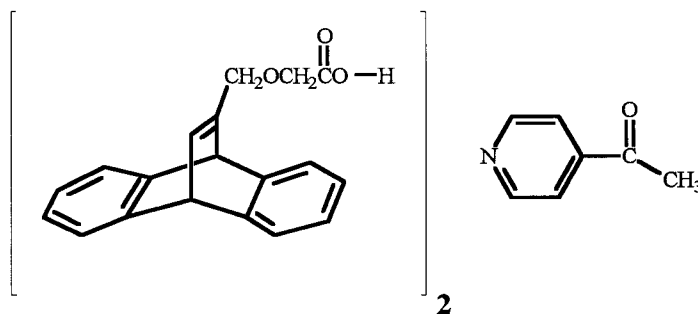
(d, 1H, $J = 6$ Hz, bridgehead H), 4.24 (d, 2H, $J = 1$ Hz, $\underline{\text{CH}_2\text{O}}$), 3.63 (s, 2H, $\underline{\text{CH}_2\text{CO}_2^-}$), 3.41, 3.18 (t, 4H, $J = 7$ Hz, $\underline{\text{CH}_2\text{CH}_2}$), 2.55 (s, 6H, $\underline{\text{CH}_3}$) ppm.

^{13}C NMR (75 MHz, CDCl_3) : δ 197.04 ($\underline{\text{COPh}}$), 175.69 ($\underline{\text{COO}^-}$), 149.76 (vinyl C), 146.32, 145.84 (acid aromatic C), 136.10 (amine aromatic C), 135.90 (vinyl C-H), 133.67 (amine aromatic C-H), 128.78, 128.16 (amine aromatic C-H), 124.48, 124.40, 123.09, 122.78 (acid aromatic C-H), 70.42, 68.16 ($\underline{\text{CH}_2}$), 52.54 ($\underline{\text{CH}_2\text{N}}$), 52.27, 50.86 (bridgehead C-H), 43.45 ($\underline{\text{CH}_3}$), 34.46 ($\underline{\text{CH}_2\text{CO}}$) ppm.

UV (acetonitrile) λ_{max} : 279 (ϵ 4,593), 272 (ϵ 3,406), 238 (ϵ 14,307) nm.

Anal. calculated for $\text{C}_{30}\text{H}_{31}\text{NO}_4$: C, 76.72; H, 6.66; N, 2.98. Found C, 76.43; H, 6.90; N, 2.99.

X-Ray Crystal Data for $\text{C}_{30}\text{H}_{31}\text{NO}_4$: Space group $C2/c$ (#15), $a = 37.712(3)$ Å, $b = 8.977(1)$ Å, $c = 15.922(1)$ Å, $\beta = 92.055(6)^\circ$, $V = 5387.0(7)$ Å³, $Z = 8$, $D_{\text{calcd}} = 1.16$ g/cm³, $R = 0.045$.

***p*-Acetylpyridine Complex with 133 (165) 2:1 ratio****165**

To a solution of acid **133** (204 mg, 0.699 mmol) in ethyl acetate (1 mL) was added *p*-acetylpyridine (85 mg, 0.699 mmol, Aldrich) dissolved in ethanol (5 mL). The solution was stirred for 5 min and left in the fumehood. After one day colorless needles of the complex **165** (130 mg, 0.185 mmol, 53%) had formed which were filtered off.

MP : 112-114 °C.

IR (KBr) ν_{\max} : 3018 (N-H), 2977 (C-H), 1698 (C=O), 1605 (COO⁻ asym.), 1414 (COO⁻ sym.) cm⁻¹.

MS FAB (matrix : Thioglycerol + CHCl₃) : 293 (acid + 1), 123 (amine + 1), 584 (2 acids).

Exact mass calculated for C₃₈H₃₂O₆ (Thioglycerol + CHCl₃, 2 acids) : 584.2199. Found : 584.2176.

¹H NMR (400 MHz, CDCl₃) : δ 10.27 (s, 1H, broad, N-H), 8.82 (s, broad, 2H, aromatic H), 7.78 (d, 2H, *J* = 6 Hz, aromatic H), 7.30-7.25 (m, 8H, aromatic H), 6.97-6.91 (m, 8H, aromatic H), 6.83 (dd, 2H, *J* = 1 & 6Hz, vinyl H), 5.14 (d, 2H, *J* = 1 Hz, bridgehead H), 5.09 (d, 2H, *J* = 6 Hz, bridgehead H), 4.29 (d, 4 H, *J* = 1 Hz, CH₂O), 3.78 (s, 4H, CH₂CO₂⁻), 2.63 (s, 3H, COCH₃) ppm.

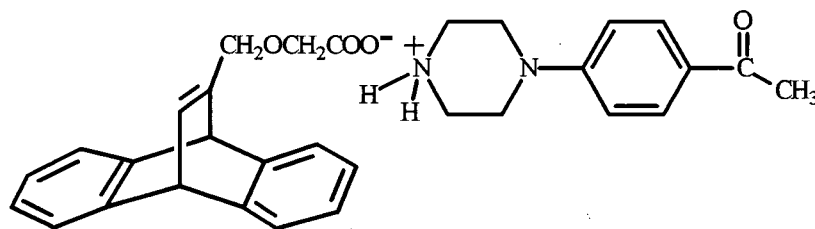
^{13}C NMR (75MHz, CDCl_3) : δ 196.84 (C=OCH_3), 174.07 (C=O^-), 149.61 (pyridine aromatic C-H), 148.62 (vinyl C), 145.96, 145.47 (acid aromatic C), 143.51 (pyridine aromatic C), 137.40 (vinyl C-H), 124.60, 124.52, 123.04, 122.89 (acid aromatic C-H), 70.70, 65.89 (CH_2), 52.24, 50.80 (bridgehead C-H), 26.63 (CH_3) ppm.

UV (acetonitrile) λ_{max} : 279 (ϵ 6,005), 272 (ϵ 4,404), 252 (ϵ 2,288), 218 (ϵ 19,829), 213 (ϵ 20,066), 208 (ϵ 19,694) nm.

Anal. calculated for $\text{C}_{45}\text{H}_{38}\text{NO}_7$: C, 76.69; H, 5.43; N, 1.99. Found C, 76.80; H, 5.33; N, 2.05.

X-Ray Crystal Data for $\text{C}_{45}\text{H}_{39}\text{NO}_7$: Space Group $P\bar{1}$ (#2), $a = 12.344(1)$ Å, $b = 18.439(3)$ Å, $c = 8.2721(7)$ Å, $\alpha = 101.789(9)^\circ$, $\beta = 94.525(8)^\circ$, $\gamma = 95.05(1)^\circ$, $V = 1826.8(4)$ Å³, $Z = 2$, $D_{\text{calcd}} = 1.283$ g/cm³, $R = 0.051$.

4'-Piperazinoacetophenone Salt of 133 (166)



166

To a solution of acid 133 (183 mg, 0.627 mmol) in ethyl acetate (15 mL) was added 4'-piperazinoacetophenone (128 mg, 0.627 mmol, Aldrich) dissolved in ethanol (15 mL). The solution was stirred for 5 min and left in the fumehood. After two days yellow crystals of the salt 166 (157 mg, 0.317 mmol, 50 %) had formed which were filtered off.

MP : 143-145 °C.

IR (KBr) ν_{\max} : 3043 (N-H), 2883(C-H), 1663 (C=O), 1597 (C=O) cm^{-1} .

MS FAB (matrix : 3-Nitrobenzyl alcohol) : 497 (M+1), 205 (amine + 1).

Exact mass calculated for $\text{C}_{31}\text{H}_{32}\text{O}_4\text{N}_2$ (3-Nitrobenzyl alcohol, M+1) : 497.2440.

Found : 497.2436.

^1H NMR (400 MHz, CDCl_3) : δ 7.89 (d, 2H, $J = 9$ Hz, aromatic H), 7.24-7.19 (m, 4H, aromatic H), 6.92-6.87 (m, 4H, aromatic H), 6.77 (d, 2H, $J = 9$ Hz, aromatic H), 6.69 (dd, 1H, $J = 1$ & 6 Hz, vinyl H), 6.60-6.30 (s, broad, 2H, NH_2), 5.03 (d, 1H, $J = 1$ Hz, bridgehead H), 4.99 (d, 1H, $J = 6$ Hz, bridgehead H), 4.16 (s, 2H, CH_2O), 3.71 (s, 2H, CH_2CO_2^-), 3.28 (m, 4H, piperazine H), 2.94 (m, 4H, piperazine H), 2.53 (s, 3H, COCH_3) ppm.

^{13}C NMR (75MHz, CDCl_3) : δ 196.54 (COCH_3), 176.32 (COO^-), 153.25 (piperazine aromatic C), 149.58 (vinyl C), 146.11, 145.59 (acid aromatic C), 135.84 (vinyl C-H), 130.31 (piperazine aromatic C-H), 128.80 (piperazine aromatic C), 124.59, 124.45, 123.06, 122.88 (acid aromatic C-H), 114.21 (piperazine aromatic C-H), 70.64, 69.32 (CH_2), 52.47, 50.70 (bridgehead C-H), 45.31, 42.70 (piperazine CH_2), 26.21 (CH_3) ppm.

UV (methanol) λ_{\max} : 325 (ϵ 20,712), 280 (ϵ 8,278), 274 (ϵ 5,116), 231 (ϵ 11,971), 215 (ϵ 26,342) nm.

Anal. calculated for $\text{C}_{31}\text{H}_{32}\text{N}_2\text{O}_4 \cdot \frac{1}{2}\text{H}_2\text{O}$: C, 73.64; H, 6.58; N, 5.54. Found C, 73.68; H, 6.53; N, 5.56.

X-Ray Crystal Data for $\text{C}_{31}\text{H}_{32}\text{O}_4\text{N}_2$: Space Group $P\bar{1}$ (#2), $a = 9.760(1)$ Å, $b = 16.254(2)$ Å, $c = 9.114(1)$ Å, $\alpha = 99.47(1)^\circ$, $\beta = 109.17(1)^\circ$, $\gamma = 88.101(1)^\circ$, $V = 1346.7(3)$ Å³, $Z = 2$, $D_{\text{calcd}} = 1.25$ g/cm³, $R = 0.044$.

CHAPTER 11 PHOTOCHEMICAL STUDIES OF SUBSTRATES

11.1. General Procedures

Irradiation Sources

Photolysis experiments were conducted either with a 450 W Hanovia medium pressure mercury lamp at room temperature through various glass filters, namely Pyrex ($\lambda \geq 290$ nm), quartz ($\lambda \geq 200$ nm), Vycor ($\lambda \geq 240$ nm) and uranium ($\lambda \geq 330$ nm), or with a Rayonet Photochemical Chamber Reactor (Model RPR-100). This light source was equipped with up to 16 lamps at 3000 Å (21 watts), 2537 Å (35 watts) or 3300 Å (24 watts) and operated at a temperature of 35 °C.

Solution State Irradiation

Solution state irradiation studies were carried out by dissolving the samples (10^{-2} M) in spectral grade solvents (Fisher). Prior to analytical runs, the samples were degassed by three freeze-pump-thaw cycles and sealed under nitrogen. In the case of preparative scale photolyses, oxygen was purged by bubbling nitrogen through the solution 30 min before and during the irradiation period, while stirring it. The photoreactions were monitored by gas chromatographic analysis. Following irradiation, the solvent was removed *in vacuo* and the photoproducts isolated by column chromatography.

Solid State Irradiation

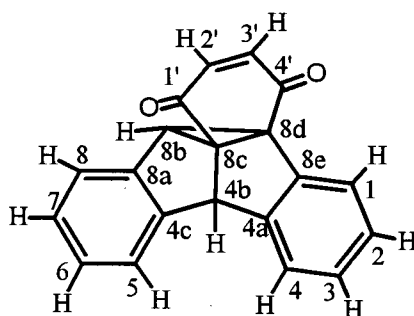
Solid state photolysis studies were carried out by crushing the crystals and distributing them evenly between two Pyrex or quartz glass plates. The samples were then placed in a polyethylene bag, which was sealed under nitrogen with a heat-sealing device. After irradiation, the samples were dissolved prior to gas chromatographic analysis and chromatographic isolation. Acid derivatives were treated with an ethereal solution of diazomethane to esterify the starting materials and photoproducts prior to GC injection and isolation. The salts were acidified with aqueous 15 % HCl (Fisher), and the resulting acids were extracted with ethyl acetate and treated with diazomethane.

11.2 Photolysis of Substrates

11.2.1. Photolysis of 9,10[1',2']Benzenoanthracene-1,4-dione Derivatives in Solution

Photolysis of 9,10-Dihydro-9,10[1',2']benzenoanthracene-1,4-dione (63) in Acetonitrile

A solution of compound **63** (250 mg, 0.880 mmol) in anhydrous acetonitrile (400 mL) was irradiated under nitrogen with a 450 W Hanovia medium pressure lamp through a Pyrex glass filter for 4 h. The solvent was removed and the remaining oil purified by column chromatography with ethyl acetate / petroleum ether (3 : 7) resulting in a light yellow crystalline photoproduct **80** (195 mg, 0.687 mmol, 78%). Compound **80** was characterized as **4b,8b,8c,8d-tetrahydrodibenzo[*a,f*]cyclopropa[*cd*]pentalene-8d,8c-benzo-1',4'-dione**.



80

MP : 167-169 °C (recryst from diethyl ether).

IR (KBr) ν_{\max} : 1677 (C=O), 1596 (C=C) cm^{-1} .

MS *m/e* (relative intensity) : 285 ($M+1$, 22), 284 (M^+ , 100), 202 (12).

Exact mass calculated for $\text{C}_{20}\text{H}_{12}\text{O}_2$: 284.0837. Found : 284.0838.

$^1\text{H NMR}$ (200 MHz, CDCl_3) : δ 8.05-7.97 (m, 1H, aromatic H), 7.35-7.03 (m, 7H, aromatic H), 6.63 (s, 2H, vinyl H), 5.13 & 4.37 (s, 1H each, pentalene H) ppm.

$^{13}\text{C NMR}$ (50 MHz, CDCl_3) : δ 191.99 (C=O), 191.07 (C=O), 150.34, 149.03 (aromatic C), 138.46, 138.09 (vinyl C-H), 133.40, 131.41 (aromatic C), 128.72, 128.16, 127.10, 127.10, 126.14, 125.51, 121.82, 121.55 (aromatic C-H), 77.28 & 58.86 (pentalene C), 58.53 & 51.43 (pentalene C-H) ppm.

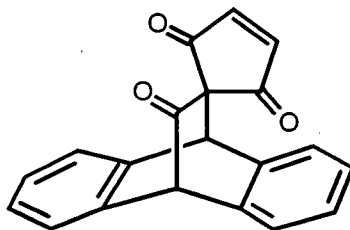
UV (acetonitrile) λ_{max} : 378 (ϵ 791), 277 (ϵ 3,366) nm.

Anal. calculated for $\text{C}_{20}\text{H}_{12}\text{O}_2$: C, 84.48; H, 4.26. Found: C, 84.26 H, 4.30.

Photolysis of 9,10-Dihydro-9,10[1',2']benzenoanthracene-1,4-dione (63) in

Air-Saturated Acetone

Compound 63 (275 mg, 0.968 mmol) dissolved in dry acetone (500 mL) was photolysed for 16 h with a Rayonet Photoreactor (11 bulbs at 3000 Å) while saturating the solution with air. Evaporation of the solvent, followed by column chromatography (ethyl acetate / petroleum ether, 3 : 7), gave the yellow crystalline triketone 81 (52 mg, 0.173 mmol, 18%).



81

MP : 171-174 °C (recryst from petroleum ether / ethyl acetate).

IR (KBr) ν_{\max} : 1709 (C=O), 1760 (C=O) cm^{-1} .

MS (DCI, NH_3 , relative intensity): 318 (M+18, 100), 301 (M+1, 10), 215 (5), 189 (15), 178 (100).

Exact mass calculated for $\text{C}_{20}\text{H}_{12}\text{O}_3$ (M+1) : 301.0864. Found : 301.0872.

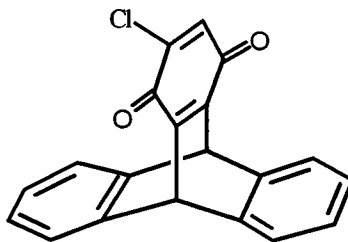
^1H NMR (400 MHz, CDCl_3) : δ 7.50-7.40 (m, 2H, aromatic H), 7.38 (s, 2H, vinyl H) 7.37-7.23 (m, 6H, aromatic H), 4.98 & 4.47 (s, 1H each, bridgehead H) ppm.

^{13}C NMR (75 MHz, CDCl_3) : δ 196.75 (C=O), 194.46 (C=O), 151.02 (vinyl C-H), 138.68, 135.65 (aromatic C), 127.53, 127.49, 125.78, 125.20 (aromatic C-H), 62.78 (bridgehead C), 61.89 & 49.61 (bridgehead C-H) ppm.

X-Ray Crystal Data for $\text{C}_{20}\text{H}_{12}\text{O}_3$: Space group $Pna2_1$, $a = 12.273(3)$ Å, $b = 7.957(3)$ Å, $c = 15.444(3)$ Å, $V = 1508(1)$ Å³, $Z = 4$, $D_{\text{calcd}} = 1.322$ g/cm³, $R = 0.037$.

Photolysis of 9,10-Dihydro-9,10[1',2']benzenoanthracene-1,4-dione (63) in Chloroform

Irradiation of compound **63** (257 mg, 0.905 mmol) in dry chloroform (150 mL) was conducted for 6 h with the Rayonet Photoreactor (16 lamps at 3000 Å). After evaporation of the solvent and column chromatography with chloroform / petroleum ether (2 : 3) two monochlorinated photoproducts, **75** (64 mg, 0.201 mmol, 25%) and **74** (62 mg, 0.195 mmol, 24%) and one dichlorinated photoproduct **76** (1 mg, 0.003 mmol, 1%) were isolated.

2-Chloro-9,10-dihydro-9,10[1',2']benzenoanthracene-1,4-dione (75)

75

MP : 275-279 °C (recryst from diethyl ether / ethyl acetate).

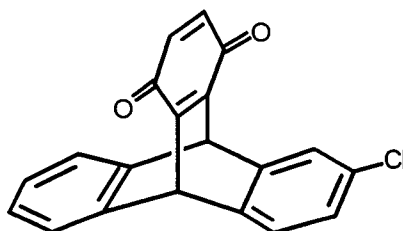
IR (KBr) ν_{\max} : 1671 (C=O), 1650 (C=O) cm^{-1} .

MS m/e (relative intensity) : 320 (M+2, 24), 319 (M+1, 17), 318 (M⁺,71), 255 (32), 226 (27), 202 (100).

Exact mass calculated for C₂₀H₁₁O₂Cl : 318.0448. Found : 318.0449.

¹H NMR (400 MHz, CDCl₃) : δ 7.48-7.36 (m, 4H, aromatic H), 7.10-6.94 (m, 4H, aromatic H), 6.79 (s, 1H, vinyl H), 5.82 & 5.75 (s, 1H each, bridgehead H) ppm.

¹³C NMR (75 MHz, CDCl₃) : δ 181.23 (C=O), 167.99 (C-Cl), 152.76, 151.98 (vinyl C) 143.24, 143.12 (aromatic C), 132.17 (vinyl C-H), 125.73, 124.47 (aromatic C-H), 47.95 & 47.43 (bridgehead C-H) ppm.

6-Chloro-9,10-dihydro-9,10[1',2']benzenoanthracene-1,4-dione (74)

74

MP : 175-178 °C (recryst from diethyl ether / ethyl acetate).

IR (KBr) ν_{\max} : 1653 (C=O) cm^{-1} .

MS m/e (relative intensity) : 320 ($M+2$, 33), 319 ($M+1$, 22), 318 (M^+ , 100), 283 (28), 255 (40), 236 (77).

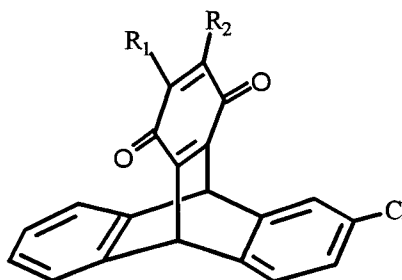
Exact mass calculated for $\text{C}_{20}\text{H}_{11}\text{O}_2\text{Cl}$: 318.0448. Found : 318.0443.

^1H NMR (400 MHz, CDCl_3) : δ 7.42-7.37 (m, 3H, aromatic H), 7.31 (d, 1H, $J = 6$ Hz, aromatic H), 7.05-7.01 (m, 2H, aromatic H), 6.98 (AB-system, 1H, $J = 8$ Hz, aromatic H), 6.60 (s, 2H, vinyl H), 5.74 & 5.73 (s, 1H each, bridgehead H) ppm.

The spectral data of photoproduct **74** was compared to the authentic sample of the quinone proving that the compounds were identical.

3,6-Dichloro-9,10-dihydro-9,10[1',2']benzenoanthracene-1,4-dione (76a)

2,6-Dichloro-9,10-dihydro-9,10[1',2']benzenoanthracene-1,4-dione (76b)



76 a $R_1 = H, R_2 = Cl$

76 b $R_1 = Cl, R_2 = H$

MP : 125-128 °C.

IR ($CHCl_3$) ν_{max} : 2927 (C-H), 1673 (C=O) 1581 (C=C) cm^{-1} .

MS m/e (relative intensity) : 356 (M+4, 3), 354 (M+2, 14), 353 (M+1, 5), 352 (M^+ , 21), 317 (8), 289 (12), 236 (25), 40 (100).

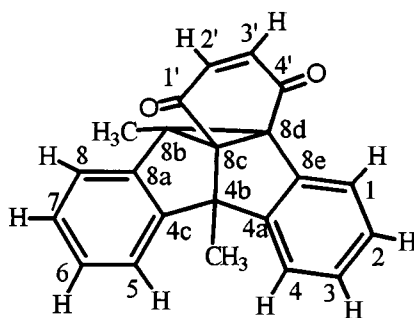
Exact mass calculated for $C_{20}H_{10}O_2Cl_2$: 352.0058. Found : 352.0068.

1H NMR (400 MHz, $CDCl_3$) : δ 7.50-7.38 (m, 3H, aromatic H), 7.35-7.29 (m, 1H, aromatic H), 7.14-6.98 (m, 3H, aromatic H), 6.82 (s, 1H, vinyl H), 5.87-5.68 (m, 2H, bridgehead H) ppm.

Photolysis of 9,10-Dihydro-9,10-dimethyl-9,10[1',2']benzenoanthracene-1,4-dione (69) in Acetonitrile

A solution of compound 69 (106 mg, 0.340 mmol) in dry acetonitrile (600 mL) was irradiated under a nitrogen atmosphere with the Rayonet Photoreactor (16 bulbs at 3000 Å) for 4.5 h. Following solvent removal and purification by column chromatography with ethyl acetate / petroleum ether (2 : 98), the yellow photoproduct 102 (31 mg, 0.099 mmol, 29%) and the midnight blue photoproduct 103 (24 mg, 0.077 mmol, 23%) as well as starting material 69 (8 mg, 0.026 mmol, 7%) were isolated. Irradiation of compound 69 (105 mg, 0.336 mmol) in dry methanol (600 mL) for 1 h under the same conditions led to the isolation of 102 (65 mg, 0.208 mmol, 63%), 103 (8 mg, 0.026 mmol, 7%) and starting material (1 mg, 0.003 mmol, 11%).

4b,8b-Dimethyl-4b,8b,8c,8d-tetrahydrodibenzo[*a,f*]cyclopropa[*cd*]pentalene-8d,8c-benzo-1',4'-dione (102)



102

MP : 130-132 °C (recryst from diethyl ether).

IR (KBr) ν_{\max} : 2927 (C-H), 1668 (C=O) cm^{-1} .

MS m/e (relative intensity): 313 (M+1, 22), 312 (M⁺, 94), 284 (18), 269(44), 242(31), 239 (32), 215 (100).

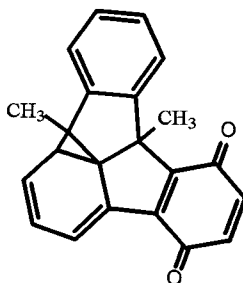
Exact mass calculated for C₂₂H₁₆O₂ : 312.1150. Found : 312.1152.

¹H NMR (400 MHz, CDCl₃) : δ 7.80 (d, 1H, *J* = 7 Hz, aromatic H), 7.20-7.02 (m, 7H, aromatic H), 6.74 (AB-system, 2H, *J* = 10 Hz, vinyl H), 2.13 & 1.98 (s, 3H each, CH₃) ppm.

¹³C NMR (75 MHz), CDCl₃) : δ 193.00, 191.87 (C=O), 153.07, 152.69, 137.45, 132.95 (aromatic C), 142.67, 140.38 (vinyl C-H), 128.66, 127.71, 127.15, 126.85, 125.01, 124.51, 119.06, 118.97 (aromatic C-H), 73.06, 61.03, 60.48, 59.08 (pentalene C), 14.96 & 13.99 (CH₃) ppm.

Anal. calculated for C₂₂H₁₆O₂ : C, 84.59; H, 5.16. Found C, 84.19; H, 5.13.

Norcaradiene Derivative 103



103

MP : 172-173 °C (recryst from petroleum ether / ethyl acetate).

IR (KBr) ν_{max} : 2922 (C-H), 1664, 1645 (C=O), 1252 (C-O) cm⁻¹.

MS m/e (relative intensity) : 313 (M+1, 8), 312 (M⁺, 32), 297 (100), 284 (6), 269 (27), 241 (23), 239 (27), 215 (44).

Exact mass calculated for C₂₂H₁₆O₂ : 312.1150. Found : 312.1157.

¹H NMR (200 MHz, CDCl₃) : δ 7.78-7.69 (m, 1H, aromatic H), 7.40-7.30 (m, 1H, aromatic H), 7.28-7.19 (m, 2H, aromatic H), 6.98 (d, 1H, *J* = 6 Hz, vinyl H), 6.65 (AB-system, 2H, *J* = 10 Hz, quinone vinyl H), 6.31 (dd, 1H, *J* = 9 & 6 Hz, vinyl H), 6.03 (dd, 1H, *J* = 9 & 5 Hz, vinyl H), 2.55 (d, 1H, *J* = 5 Hz, cyclopropyl H), 1.50 & 1.06 (s, 3H each, CH₃) ppm.

¹³C NMR (100 MHz), CDCl₃) : δ 186.11, 185.87 (C=O), 149.51, 148.17, 146.45, 141.89 (aromatic C), 137.87, 136.19 (vinyl C-H), 134.89 (vinyl C), 128.01, 127.14, 126.74, 124.97 (aromatic C-H), 126.65, 126.32, 121.84 (vinyl C-H), 61.01, 56.88 (cyclopentyl C), 37.82 (cyclopropyl C-H), 23.88 (CH₃), 21.99 (cyclopropyl C), 10.77 (cyclopropyl CH₃) ppm.

UV (acetonitrile) λ_{max} : 569 (ε 2,066), 316 (ε 3,577), 232 (ε 9,756) nm.

UV (chloroform) λ_{max} : 594 (ε 2,423), 324 (ε 4,157), 256 (ε 8,889) nm.

Anal. calculated for C₂₂H₁₆O₂ : C, 84.59; H, 5.16. Found : C, 84.40; H, 5.14.

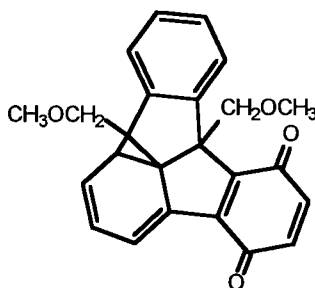
X-Ray Crystal Data for C₂₂H₁₆O₂ : Space group *P2₁/n* (#14), *a* = 8.114(3) Å, *b* = 11.966 (3) Å, *c* = 16.694(3) Å, β = 95.53(2)°, *V* = 1613.3(7) Å³, *Z* = 4, *D*_{calcd} = 1.29 g/cm³, *R* = 0.037.

Photolysis of 9,10-Bis(methoxymethyl)-9,10[1',2']benzenoanthracene-1,4-dione (72) in Acetonitrile

A solution of compound 72 (220 mg, 0.591 mmol) in dry acetonitrile (500 mL) was irradiated in a Rayonet Photoreactor (8 bulbs at 3000 Å) for 1 h while under nitrogen. Evaporation of the solvent and column chromatography with ethyl acetate / petroleum ether (3 : 7) resulted in three photoproducts. The isolated products were identified as the blue norcaradiene derivative 110 (7 mg, 0.019 mmol, 3%), the white dihydrofuran derivative 111 (42 mg, 0.113

mmol, 19%) and red benz[*a*]aceanthrylene derivative **112** (39 mg, 0.105 mmol, 18%). Upon photolysis of compound **72** (41 mg, 0.110 mmol) in benzene (100 mL) for 45 min under the above conditions, followed by the same isolation procedures, dihydrofuran **111** (4.0 mg, 0.011 mmol, 10%) and benz[*a*]aceanthrylene **112** (14 mg, 0.038 mmol, 33%) were isolated.

Norcaradiene Derivative (**110**)



110

MP : 125-128 °C.

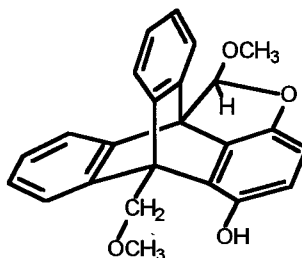
IR (KBr) ν_{max} : 2926 (C-H), 1665 (C=O), 1646 (C=O) cm^{-1} .

MS *m/e* (relative intensity) : 373 ($M+1$, 27), 372 (M^+ , 100), 343 (16), 327 (11), 311 (10), 297 (15).

Exact mass calculated for $\text{C}_{24}\text{H}_{20}\text{O}_4$: 372.1362. Found : 372.1364.

^1H NMR (400 MHz, CDCl_3) : δ 7.66 (d, 1H, $J = 7$ Hz, aromatic H), 7.58 (d, 1H, $J = 7$ Hz, aromatic H), 7.28-7.19 (m, 2H, aromatic H), 6.90 (d, 1H, $J = 6$ Hz, vinyl H), 6.64 (AB-system, 2H, $J = 8$ Hz, quinone vinyl H), 6.31 (dd, 1H, $J = 9$ & 6 Hz, vinyl H), 6.16 (dd, 1H, $J = 9$ & 5 Hz, vinyl H), 4.05 (d, 1H, $J = 9$ Hz, CH_2), 3.30 (d, 1H, $J = 9$ Hz, CH_2), 3.28 (AB-system, 2H, $J = 9$ Hz, CH_2), 3.21 & 3.17 (s, 3H each, CH_3), 2.85 (d, 1H, $J = 5$ Hz, cyclopropyl H) ppm.

Dihydrofuran Derivative 111



111

MP : 252-254 °C (recryst from benzene).

IR (KBr) ν_{\max} : 3270 (O-H), 2922 (C-H) cm^{-1} .

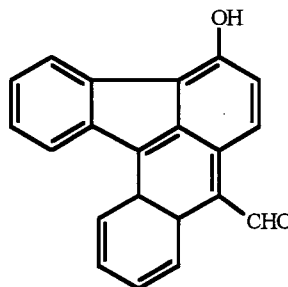
MS m/e (relative intensity) : 373 ($M+1$, 27), 372 (M^+ , 100), 310 (13), 281 (11), 258(18).

Exact mass calculated for $\text{C}_{24}\text{H}_{20}\text{O}_4$: 372.1362. Found : 372.1365.

^1H NMR (500 MHz, CDCl_3) : δ 8.28 (s, 1H, OH), 8.16-8.12 (m, 1H, aromatic H), 7.40 (d, 1H, $J = 7$ Hz, aromatic H), 7.22-7.17 (m, 2H, aromatic H), 7.08-6.97 (m, 4H, aromatic H), 6.87 (s, 1H, acetal methine H), 6.48 (AB-system, 2H, $J = 8$ Hz, aromatic H), 4.96 (s, 2H, CH_2OCH_3), 3.98 & 3.91 (s, 3H each, OCH_3) ppm.

^{13}C NMR (125 MHz, CDCl_3) : δ 146.17, 146.15, 145.96, 145.62, 145.36, 145.03, 138.24, 126.00 (aromatic C), 125.16, 124.97, 124.82, 124.59, 124.81, 121.82, 121.31, 120.48, 116.61 (aromatic C-H), 112.06 (acetal C-H), 107.83 (aromatic C-H), 71.43 (CH_2OCH_3), 59.60 (CH_2OCH_3), 58.22 (OCH_3), 57.60 & 53.91 (bridgehead C) ppm.

Anal. calculated for $\text{C}_{24}\text{H}_{20}\text{O}_4$: C, 77.40; H, 5.41. Found C, 77.28; H, 5.25.

Benz[*a*]aceanthrylene Derivative 112

112

MP : 236-238 °C (recryst from benzene).

IR (KBr) ν_{\max} : 3332 (O-H), 1643 (C=O) cm^{-1} .

MS m/e (relative intensity): 297 ($M+1$, 23), 296 (M^+ , 100), 279 (17), 268 (54), 267 (30), 240 (21), 239 (71), 238 (23), 237 (44).

Exact mass calculated for $\text{C}_{21}\text{H}_{12}\text{O}_2$: 296.0837. Found : 296.0840.

^1H NMR (500 MHz, d_6 -acetone) : δ 11.55 (s, 1H, CHO), 10.20 (s, 1H, OH), 9.28 (d, 1H, $J = 9$ Hz, aromatic H), 9.02 (d, 1H, $J = 8.5$ Hz, aromatic H), 8.85 (d, 1H, $J = 9$ Hz, aromatic H), 8.62 (dd, 1H, $J = 6$ & 7 Hz, aromatic H), 8.26 (dd, 1H, $J = 7$ & 6 Hz, aromatic H), 7.84-7.80 (m, 1H, aromatic H), 7.73-7.70 (m, 1H, aromatic H), 7.55-7.46 (m, 3H, aromatic H) ppm.

^{13}C NMR (125 MHz, d_6 -acetone) : δ 193.26 (CHO), 154.34, 140.10, 138.03, 136.36, 133.21, 132.48, 130.01, 129.12 (aromatic C), 128.83, 128.47, 128.32, 127.90, 127.31, 126.47, 125.99, 125.68, 125.35, 125.12 (aromatic C-H), 126.07 (aromatic C), 117.12 (aromatic C) ppm.

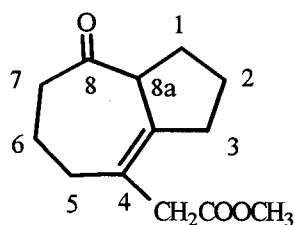
UV (acetonitrile) λ_{\max} : 484 (ϵ 14,393), 456 (ϵ 14,306), 390 (ϵ 14,891) nm.

11.2.2. Photolysis of 2-(1-Cyclopentenyl)cyclopentanone Derivative 121 in Solution

Photolysis of 1-(1-Cyclopenten-1-yl)-2-oxocyclopentaneacetic Acid (121) in Hexane^{124a}

Compound 121 (150 mg, 0.721 mmol) was dissolved in dry hexane (300 mL) and irradiated with a Hanovia medium pressure mercury lamp (Pyrex glass filter, $\lambda \geq 290$ nm) for 6 h while bubbling nitrogen through the solution. After evaporation of the solvent and treatment with diazomethane, the reaction mixture was purified by column chromatography with ethyl acetate / petroleum ether (15 : 85). The isolated products, which have been characterized by Givens *et al.*,^{124a} were the singlet product 135a, an oil (44 mg, 0.198 mmol, 28%), starting material 121 (51 mg, 0.230 mmol, 32%) and a trace of triplet product 134a, an oil (1.0 mg, 0.005 mmol, 0.6%).

Methyl 1,2,3,5,6,7,8,8a-octahydro-8-oxo-4-azuleneacetate (135a)



135a

IR (NaCl) ν_{\max} : 2952 (C-H), 1736 (C=O), 1710 (C=O) cm^{-1} .

MS m/e (relative intensity) : 223 ($M+1$, 16), 222 (M^+ , 100), 190 (62), 149 (63), 107 (73), 91 (91).

Exact mass calculated for $\text{C}_{13}\text{H}_{18}\text{O}_3$: 222.1256. Found : 222.1255.

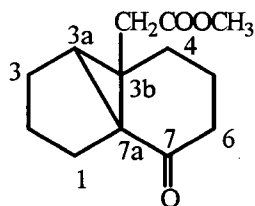
$^1\text{H NMR}$ (400 MHz, CDCl_3) : δ 3.99-3.98 (m, 1H, CH_2), 3.67 (s, 3H, CO_2CH_3), 3.02 (AB-system, 2H, $J = 15$ Hz, $\text{CH}_2\text{CO}_2\text{CH}_3$), 2.63-2.11 (m, 9H, CH_2), 1.86-1.55 (m, 3H, CH_2) ppm.

$^{13}\text{C NMR}$ (50 MHz, CDCl_3) : δ 208.46 (ketone $\text{C}=\text{O}$), 171.90 (ester $\text{C}=\text{O}$), 137.93, 125.29 (vinyl C), 52.80, 51.76 (CO_2CH_3 , CH), 43.70, 41.37, 34.41, 32.43, 27.49, 24.70, 22.24 ($\text{CH}_2\text{CO}_2\text{CH}_3$, CH_2) ppm.

Photolysis of 1-(1-Cyclopenten-1-yl)-2-oxocyclopentaneacetic Acid (121) in Acetone^{124a}

Irradiation of compound 121 (146 mg, 0.702 mmol) dissolved in dry acetone (300 mL) was carried out with a Hanovia medium pressure mercury lamp ($\lambda \geq 290$ nm) for 45 min under nitrogen. Following removal of the solvent, methylation with diazomethane and column chromatography with ethyl acetate / petroleum ether (15 : 85) the main photoproduct was 134a (98 mg, 0.441 mmol, 61%). Small amounts of the singlet product 135a (7 mg, 0.032 mmol, 4%) and starting material 121 (13 mg, 0.058 mmol, 8%) were also isolated.

Methyl octahydro-7-oxo-3b*H*-cyclopenta[1,3]cyclopropa[1,2]benzene-3b-acetate (134a)



134a

IR (NaCl) ν_{\max} : 1739 (C=O), 1675 (C=O) cm^{-1} .

MS m/e (relative intensity) : 223 ($M+1$, 6), 222 (M^+ , 39), 190 (24), 163 (47), 149 (100).

Exact mass calculated for $\text{C}_{13}\text{H}_{18}\text{O}_3$: 222.1256. Found : 222.1256.

^1H NMR (400 MHz, CDCl_3) : δ 3.72 (s, 3H, CO_2CH_3), 2.95-2.86 (m, 1H, CH_2), 2.49 (s, 2H, $\text{CH}_2\text{CO}_2\text{CH}_3$), 2.41 (d, 1H, $J = 6$ Hz, CH_2), 2.37-2.20 (m, 2H, CH_2), 2.15-1.40 (m, 9H, CH_2) ppm.

^{13}C NMR (50 MHz, CDCl_3) : δ 209.00 (ketone C=O), 172.35 (ester C=O), 51.71 (CO_2CH_3), 50.31 ($\text{CH}_2\text{CO}_2\text{CH}_3$), 37.11, 36.70 (CH), 35.70 (CH_2), 34.12 (C), 29.24, 27.19, 16.21, 24.71, 17.86 (CH_2) ppm.

11.2.3. Photolysis of 9,10-Dihydro-9,10-ethenoanthracene Derivatives in Solution

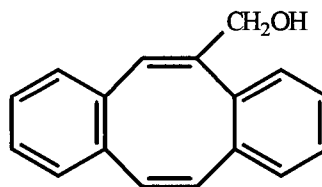
Photolysis of 11-Hydroxymethyl -9,10-dihydro-9,10-ethenoanthracene (131)

in Acetonitrile

A solution of compound **131** (204 mg, 0.872 mmol) in 100 mL of acetonitrile in a quartz vessel was irradiated for 2 h under nitrogen with the Rayonet Photoreactor (16 bulbs at 254 nm). Gas chromatographic analysis (HP5, 30m) led to the determination of a 89:11 product ratio corresponding to cyclooctatetraene derivative **143** and starting material **131**. Removal of the solvent gave a yellow oil which was purified by column chromatography with ethyl acetate /

petroleum ether (2 : 8). The resulting clear oil was identified as cyclooctatetraene derivative 143 (140 mg, 0.598 mmol, 69%); starting material 131 (27 mg, 0.115 mmol, 13%) was also isolated.

Dibenzo[*a,e*]cyclooctene-5-methanol (143)



143

IR (KBr) ν_{\max} : 3320 (O-H), 3007 (C-H) cm^{-1} .

MS *m/e* (relative intensity) : 235 (M+1, 6), 234 (M⁺, 38), 216 (28), 203(100), 202 (83), 178 (18).

Exact mass calculated for C₁₇H₁₄O : 234.1045. Found : 234.1043.

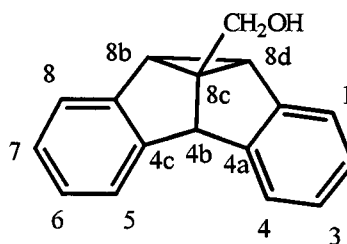
¹H NMR (400 MHz, CDCl₃) : δ 7.19-7.05 (m, 8H, aromatic H), 6.86 (s, 1H, vinyl H), 6.79 (AB-system, 2H, *J* = 12 Hz, vinyl H), 4.42 (AB-system, 2H, *J* = 14 Hz, CH₂OH), 2.10 (s, broad, 1H, OH) ppm.

¹³C NMR (50 MHz, CDCl₃) : δ 144.05 (vinyl C-H), 137.88, 137.73, 137.27, 137.27, 137.04 (aromatic C, vinyl C), 133.47, 132.69 (vinyl C-H), 128.67, 128.67, 127.83, 127.75, 127.13, 127.03, 126.84, 126.60 (aromatic C-H), 67.66 (CH₂OH) ppm.

UV (acetonitrile) λ_{\max} : 229 (ϵ 29,250), 204 (ϵ 27,426), 202 (ϵ 26,661) nm.

Photolysis of 11-Hydroxymethyl -9,10-dihydro-9,10-ethenoanthracene (131) in Acetone

Irradiation of compound **131** (231 mg, 0.987 mmol) was carried out in dry acetone with a Hanovia medium pressure mercury lamp for 5 h while maintaining a positive pressure of nitrogen in the reaction vessel. The reaction was tested by gas chromatography (HP 5, 30 m) resulting in 55% of semibullvalene derivative **144**, 34% of regioisomer **145** and 11% of aldehyde **146**. Evaporation of the solvent and column chromatography with ethyl acetate / petroleum ether (2 : 8) gave white crystalline semibullvalene derivative **144** (88 mg, 0.376 mmol, 38%) and the regioisomeric semibullvalene **145** (56 mg, 0.239 mmol, 24%) as well as the aldehyde derivative **146** (15 mg, 0.065 mmol, 6%).

4b,8b,8c,8d-tetrahydrodibenzo[*a,f*]cyclopropano[*cd*]pentalene-8c-methanol (144)**144**

MP : 132-135 °C (recryst from petroleum ether / diethyl ether).

IR (KBr) ν_{\max} : 3304 (O-H), 3017 (C-H) cm^{-1} .

MS *m/e* (relative intensity) : 235 ($M+1$, 6), 234 (M^+ , 29), 216 (18), 203 (100), 202 (56).

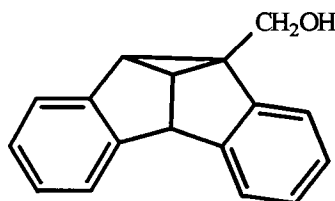
Exact mass calculated for $\text{C}_{17}\text{H}_{14}\text{O}$: 234.1045. Found : 234.1044.

$^1\text{H NMR}$ (400 MHz, CDCl_3) : δ 7.24-7.19 (m, 2H, aromatic H), 7.14-7.00 (m, 6H, aromatic H), 4.50 (s, 1H, pentalene H_{4b}), 3.96 (s, 2H, CH_2OH), 3.08 (s, 2H, pentalene $\text{H}_{8b,d}$), 1.56 (s, broad, 1H, OH) ppm.

$^{13}\text{C NMR}$ (50 MHz, CDCl_3) : δ 150.46, 138.10 (aromatic C), 126.52, 126.32, 124.78, 121.31 (aromatic C-H), 64.77 (CH_2OH), 64.07 (pentalene C), 56.08 (pentalene C- H_{4b}), 41.32 (pentalene C- $\text{H}_{8b,d}$) ppm.

Anal. calculated for $\text{C}_{17}\text{H}_{14}\text{O}$: C, 87.14; H, 6.03. Found C, 87.28; H, 5.94.

4b,8b,8c,8d-tetrahydrodibenzo[*a,f*]cyclopropa[*cd*]pentalene-8d-methanol (145)



145

MP : 135-137 °C (recryst from petroleum ether / diethyl ether).

IR (KBr) ν_{max} : 3230 (O-H), 2917 (C-H) cm^{-1} .

MS m/e (relative intensity) : 235 ($\text{M}+1$, 10), 234 (M^+ , 48), 233 (10), 217 (18), 216 (33), 215 (31), 205 (22), 204 (35), 203 (100), 202 (47).

Exact mass calculated for $\text{C}_{17}\text{H}_{14}\text{O}$: 234.1045. Found : 234.1051.

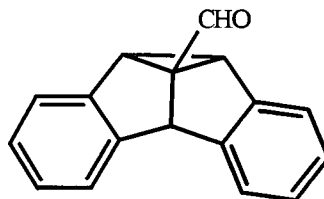
$^1\text{H NMR}$ (400 MHz, CDCl_3) : δ 7.37-7.35 (m, 1H, aromatic H), 7.24-6.98 (m, 7H, aromatic H), 4.49 (d, 1H, $J = 6$ Hz, pentalene H_{4b}), 4.12 (AB-system, 2H, $J = 12$ Hz, CH_2OH), 3.58 (t, 1H, $J = 6$ Hz, pentalene H_{8c}), 3.12 (d, 1H, $J = 6$ Hz, pentalene H_{8b}), 1.60 (s, broad, 1H, OH) ppm.

^{13}C NMR (50 MHz, CDCl_3) : δ 151.39, 138.08 (aromatic C), 126.72, 126.59, 126.36, 126.26, 124.91, 124.05, 121.17, 121.17 (aromatic C-H), 91.95 (pentalene C_{8d}), 65.26 (CH_2OH), 53.97, 52.90 (pentalene C- $\text{H}_{8c,4b}$), 42.28 (pentalene C- H_{8b}) ppm.

UV (acetonitrile) λ_{max} : 222 (ϵ 21,587), 273 (ϵ 2,534) nm.

Anal. calculated for $\text{C}_{17}\text{H}_{14}\text{O}$: C, 87.14; H, 6.03. Found C, 86.76; H, 6.03.

4b,8b,8c,8d-Tetrahydrodibenzo[*a,f*]cyclopropa[*cd*]pentalene-8c-aldehyde (146)



146

MP : 179-181 °C (recryst petroleum ether / diethyl ether).

IR (KBr) ν_{max} : 2960 (C-H), 2831 (C-H), 1686 (CHO) cm^{-1} .

MS m/e (relative intensity) : 233 ($\text{M}+1$, 1), 232 (M^+ , 6), 203 (100), 202 (51).

Exact mass calculated for $\text{C}_{17}\text{H}_{12}\text{O}$: 232.0888. Found : 232.0885.

^1H NMR (200 MHz, CDCl_3) : δ 9.24 (s, 1H, CHO), 7.25-6.95 (m, 8H, aromatic H), 4.96 (s, 1H, pentalene H_{4b}), 3.83 (s, 2H, pentalene $\text{H}_{8b,d}$) ppm.

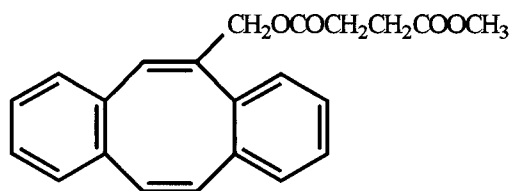
^{13}C NMR (50 MHz, CDCl_3) : δ 195.86 (CHO), 150.15, 134.51 (aromatic C), 127.41, 126.77, 124.93, 121.61(aromatic C-H), 72.52 (pentalene C_{8c}), 50.91 (pentalene C- H_{4b}), 46.46 (pentalene C- $\text{H}_{8b,8d}$) ppm.

Anal. calculated for $\text{C}_{17}\text{H}_{12}\text{O}$: C, 87.90; H, 5.21. Found : C, 87.51; H, 5.11.

Photolysis of Methyl 13-(11-methyl-9,10-dihydro-9,10-ethenoanthracenyl)succinate (132a) in Acetonitrile

Irradiation of compound **132a** (134 mg, 0.385 mmol) dissolved in dry acetonitrile (300 mL) in a quartz vessel was carried out in a Rayonet Photoreactor (15 bulbs at 254 nm) for 3.5 h under nitrogen. Gas chromatographic analysis (HP 5, 30 m) showed the presence of cyclooctatetraene derivative **150** (83%), semibullvalene derivative **151** (14%) and starting material **132a** (3%). After removal of solvent, the oil was purified on a silica gel column with ethyl acetate / petroleum ether (5 : 95) resulting in the isolation of the cyclooctatetraene derivative **150** (88 mg, 0.247 mmol, 66%, oil), the semibullvalene derivative **151** (14 mg, 0.040 mmol, 11%, oil) and starting material **132a** (3 mg, 0.009 mmol, 2%).

Methyl 13-(5-methyldibenzo[*a,e*]cyclooctenyl)succinate (150)



150

IR (KBr) ν_{\max} : 2952 (C-H), 1734 (C=O), 1155 (C-O) cm^{-1} .

MS *m/e* (relative intensity) : 349 ($M+1$, 3), 348 (M^+ , 9), 217 (37), 216 (100), 203 (15), 202 (16).

Exact mass calculated for $\text{C}_{22}\text{H}_{20}\text{O}_4$: 348.1359. Found : 348.1362.

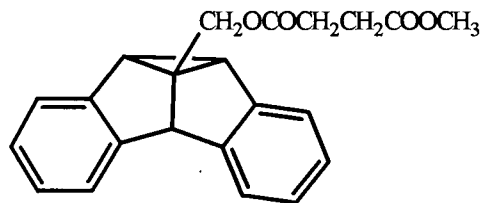
^1H NMR (400 MHz, CDCl_3) : δ 7.20-7.00 (m, 8H, aromatic H), 6.83 (s, broad, 1H, vinyl H), 6.78 (AB-system, 2H, $J = 12$ Hz, vinyl H), 4.88 (d, 2H, $J = 1$ Hz, CH_2O), 3.66 (s, 3H, s, CH_3), 2.67-2.57 (m, 4H, $\text{COCH}_2\text{CH}_2\text{CO}_2\text{CH}_3$) ppm.

^{13}C NMR (50 MHz, CDCl_3) : δ 172.64, 171.80 (C=O), 138.78, 137.75, 137.11, 137.02, 136.70 (aromatic C, vinyl C), 133.22, 132.58, 130.61 (vinyl C-H), 128.62, 128.50, 128.50, 127.83, 127.21, 126.96, 126.79, 126.79 (aromatic C-H), 68.58 (CH_2O), 51.86 (CH_3), 129.21 & 28.86 ($\text{COCH}_2\text{CH}_2\text{CO}_2\text{CH}_3$) ppm.

Photolysis of Methyl 13 -(11-methyl-9, 10-dihydro-9,10-ethenoanthracenyl)succinate (132a) in Acetone

A solution of compound **132a** (142 mg, 0.408 mmol) in dry acetone (400 mL) was irradiated with a Hanovia medium pressure mercury lamp for 2 h under nitrogen through a Pyrex glass filter. Gas chromatographic analysis showed the following photoproduct distribution: **151** (75%), **152** (11%), **132a** (5%). The solvent was removed and the oil purified by column chromatography with ethyl acetate / petroleum ether (5 : 95). The isolated photoproducts were the white crystalline dibenzosemibullvalenes **151** (83 mg, 0.238 mmol, 58%) and **152** (17 mg, 0.049 mmol, 12%) as well as starting material **132a** (6 mg, 0.017 mmol 4%).

Methyl 9-(8c-methyl-4b,8b,8c,8d-tetrahydrodibenzo[*a,f*]cyclopropa[*cd*]pentalenyl) succinate (151)



151

MP : 101-102 °C (recryst from petroleum ether / diethyl ether).

IR (KBr) ν_{\max} : 2958 (C-H), 1729 (C=O) cm^{-1} .

MS *m/e* (relative intensity): 349 ($M+1$, 1), 348 (M^+ , 4), 234 (6), 216 (100), 215 (34), 203 (34), 202 (27).

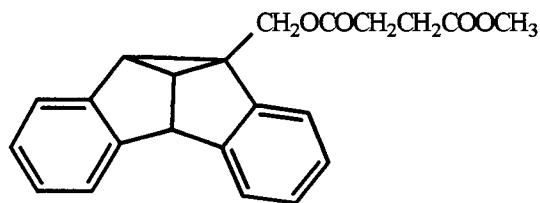
Exact mass calculated for $\text{C}_{22}\text{H}_{20}\text{O}_4$: 348.1362. Found : 348.1368.

^1H NMR (400 MHz, CDCl_3) : δ 7.22-7.20 (m, 2H, aromatic H), 7.12-7.10 (m, 2H, aromatic H), 7.04-6.99 (m, 4H, aromatic H), 4.49 (s, 2H, CH_2O), 4.47 (s, 1H, pentalene H_{4b}), 3.61 (s, 3H, CH_3), 3.13 (s, 2H, pentalene $\text{H}_{8b,8d}$), 2.54 (m, 4H, $\text{COCH}_2\text{CH}_2\text{CO}_2\text{CH}_3$) ppm.

^{13}C NMR (50 MHz, CDCl_3) : δ 172.62, 172.47 (C=O), 150.26, 137.08 (aromatic C), 126.52, 126.39, 124.82, 121.23 (aromatic C-H), 66.51 (CH_2O), 60.41 (pentalene C), 56.45, 56.45, (pentalene C-H), 51.80 (CH_3), 41.84 (pentalene C-H), 29.09, 28.90 ($\text{COCH}_2\text{CH}_2\text{CO}_2\text{CH}_3$) ppm.

Anal. calculated for $\text{C}_{22}\text{H}_{20}\text{O}_4$: C, 75.84; H, 5.79. Found : C, 75.72; H, 5.88.

Methyl 9-(8d-methyl-4b,8b,8c,8d-tetrahydrodibenzo[*a,f*]cyclopropa[*cd*]pentalenyl) succinate (152)



152

MP : 88-90 °C (recryst from petroleum ether / diethyl ether).

IR (KBr) ν_{\max} : 2968 (C-H), 1726 (C=O) cm^{-1} .

MS *m/e* (relative intensity) : 349 ($M+1$, 0.3), 348 (M^+ , 1), 217 (32), 216 (100), 215 (37), 202 (16).

Exact mass calculated for $\text{C}_{22}\text{H}_{20}\text{O}_4$: 348.1362. Found : 348.1371.

^1H NMR (400 MHz, CDCl_3) : δ 7.28-7.23 (m, 2H, aromatic H), 7.10-6.99 (m, 6H, aromatic H), 4.60 (AB-system, 2H, $J = 12$ Hz, CH_2O), 4.49 (d, 1H, $J = 6$ Hz, cyclopentyl H_{4b}), 3.64 (s, 3H, CH_3), 3.60 (t, 1H, $J = 6$ Hz, pentalene H_{8c}), 3.18 (d, 2H, $J = 6$ Hz, pentalene H_{8b}), 2.70-2.60 (m, 4H, $\text{COCH}_2\text{CH}_2\text{CO}_2\text{CH}_3$) ppm.

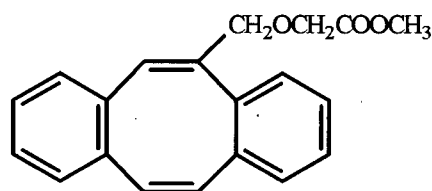
^{13}C NMR (50 MHz, CDCl_3) : δ 172.67, 172.45 (C=O), 151.27, 150.97, 137.60, 137.57 (aromatic C), 126.70, 126.53, 126.37, 126.37, 125.10, 124.11, 121.09, 121.02 (aromatic C-H), 66.93 (CH_2O), 53.90, 53.17 (pentalene C-H), 51.87 (CH_3), 46.52 (pentalene C), 42.83 (pentalene C-H), 29.17, 28.90 ($\text{COCH}_2\text{CH}_2\text{CO}_2\text{CH}_3$) ppm.

Anal. calculated for $\text{C}_{22}\text{H}_{20}\text{O}_4$: C, 75.84; H, 5.79. Found : C, 75.51; H, 5.83.

**Photolysis of 13-(11-Methyleneoxy-9,10-dihydro-9,10-ethenoanthracenyl)acetic Acid (133)
in Acetonitrile**

Compound 133 (189 mg, 0.647 mmol) was dissolved in dry acetonitrile (400 mL), saturated with nitrogen and photolysed with a Rayonet Photoreactor (16 bulbs at 254 nm) for 4 h. A yellow oil resulted (179 mg, 0.585 mmol, 90%) after solvent evaporation and esterification with diazomethane. This was purified on silica gel with ethyl acetate / petroleum ether (1 : 9). The photoproducts isolated were an oil identified as cyclooctatetraene derivative 155 (71 mg, 0.232 mmol, 40%), and the white crystalline semibullvalene analogue 156 (17 mg, 0.056 mmol, 10%). Gas chromatographic analysis showed the presence of 77% of 155, 23% of 156.

Methyl 13-(5-methyleneoxydibenzo[*a,e*]cyclooctenyl)acetate (155)



155

IR (KBr) ν_{\max} : 3013, 2952 (C-H), 1755 (C=O), 1213 (C-O) cm^{-1} .

MS *m/e* (relative intensity) : 307 ($M+1$, 1), 306 (M^+ , 5), 217 (52), 216(100), 203(37), 202 (41).

Exact mass calculated for $\text{C}_{20}\text{H}_{18}\text{O}_3$: 306.1256. Found : 306.1250.

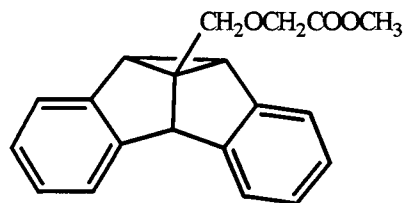
^1H NMR (200 MHz, CDCl_3) : δ 7.15-6.90 (m, 8H, aromatic H), 6.78 (s, 1H, vinyl H), 6.72 (s, 2H, vinyl H), 4.35 (AB-system, 2H, $J=13$ Hz, CH_2O), 4.11 (d, 2H, $J=2$ Hz, $\text{CH}_2\text{CO}_2\text{CH}_3$), 3.66 (s, 3H, CH_3) ppm.

^{13}C NMR (50 MHz, CDCl_3) : δ 170.79 (C=O), 139.85, 137.60, 137.08, 137.08, 137.01 (aromatic C, vinyl C), 133.50, 132.64, 130.83 (vinyl C-H), 128.61, 128.55, 128.52, 127.82, 127.09, 126.98, 126.79, 126.70 (aromatic C-H), 75.97 ($\text{CH}_2\text{CO}_2\text{CH}_3$), 66.93 (CH_2O), 51.83 (CH_3) ppm.

Photolysis of 13-(11-Methyleneoxy-9,10-dihydro-9,10-ethenoanthracenyl)acetic Acid (133) in Acetone

A solution was made up containing compound 133 (197 mg, 0.675 mmol) in acetone (400 mL). Irradiation with a Hanovia medium pressure mercury lamp for 1 h under nitrogen, followed by removal of the solvent and treatment with diazomethane, resulted in a yellow oil (174 mg, 0.569 mmol, 88%). After column chromatography with ethyl acetate / petroleum ether (5 : 95) two esterified dibenzosemibullvalene derivatives were isolated : compound 156 (80 mg, 0.261 mmol, 46%) and 157 (26 mg, 0.085 mmol, 15%). Gas chromatographic analysis (HP 5, 30 m) showed the presence of compounds 156 and 157 in a ratio of 72 : 28.

Methyl 9-(8c-methyleneoxy-4b,8b,8c,8d-tetrahydrodibenzo[*a,f*]cyclopropa[*cd*]pentalenyl) acetate (156)



156

MP : 94-96 °C (recryst petroleum ether / ethyl acetate).

IR (KBr) ν_{\max} : 2951 (C-H), 1750 (C=O), 1212 (C-O) cm^{-1} .

MS *m/e* (relative intensity) : 307 ($M+1$, 3), 306 (M^+ , 14), 217 (33), 216(100), 215 (50), 203 (98), 202 (65).

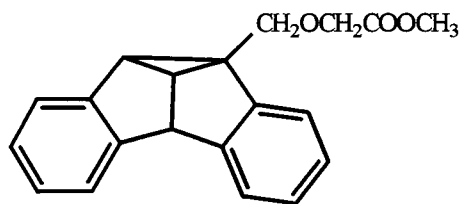
Exact mass calculated for $\text{C}_{20}\text{H}_{18}\text{O}_3$: 306.1256. Found : 306.1253.

^1H NMR (200 MHz, CDCl_3) : δ 7.25-6.85 (m, 8H, aromatic H), 4.48 (s, 1H, pentalene H_{4b}), 3.99 (s, 2H, $\text{CH}_2\text{CO}_2\text{CH}_3$), 3.90 (s, 2H, CH_2O), 3.63 (s, 3H, CH_3), 3.02 (s, 2H, pentalene $\text{H}_{8b,8d}$) ppm.

^{13}C NMR (50 MHz, CDCl_3) : δ 170.88 (C=O), 150.37, 137.21 (aromatic C), 126.48, 126.35, 124.88, 121.36 (aromatic C-H), 73.11 ($\text{CH}_2\text{CO}_2\text{CH}_3$), 67.62 (CH_2O), 61.11 (pentalene C), 56.17, 56.17 (pentalene C-H), 51.75 (CH_3), 41.53 (pentalene C-H) ppm.

Anal. calculated for $\text{C}_{20}\text{H}_{18}\text{O}_3$: C, 78.41; H, 5.92. Found : C, 78.08; H, 5.96.

**Methyl 9-(8d-methyleneoxy-4b,8b,8c,8d-tetrahydrodibenzo[*a,f*]cyclopropa
[*cd*]pentalenyl)acetate (157)**



157

MP : 74-76 °C (recryst from petroleum ether / ethyl acetate).

IR (KBr) ν_{\max} : 3039, 2952 (C-H), 1752 (C=O), 1212 (C-O) cm^{-1} .

MS *m/e* (relative intensity) : 307 (M+1, 1), 306 (M⁺, 3), 217 (37), 216(100), 215 (64), 203 (54), 202 (51).

Exact mass calculated for C₂₀H₁₈O₃ : 306.1256. Found : 306.1262.

¹H NMR (200 MHz, CDCl₃) : δ 7.43-7.33 (m, 1H, aromatic H), 7.25-7.11 (m, 1H, aromatic H), 7.10-6.85 (m, 6H, aromatic H), 4.42 (d, 1H, *J* = 6 Hz, pentalene H_{4b}), 4.15 (s, 2H, $\text{CH}_2\text{CO}_2\text{CH}_3$), 3.99 (AB-system, 2H, *J* = 11 Hz, CH_2O), 3.70 (s, 3H, CH_3), 3.50 (t, 1H, *J* = 6 Hz, pentalene H_{8c}), 3.14 (d, 1H, *J* = 6 Hz, pentalene H_{8b}) ppm.

¹³C NMR (50 MHz, CDCl₃) : δ 170.91 (C=O), 151.35, 150.93, 138.13, 137.89 (aromatic C), 126.54, 126.49, 126.26, 126.19, 125.03, 124.53, 121.03, 120.83 (aromatic C-H), 74.08 ($\text{CH}_2\text{CO}_2\text{CH}_3$), 67.89 (CH_2O), 53.86, 52.88 (pentalene C-H), 51.78 (CH_3), 47.18 (pentalene C), 42.70 (pentalene C-H) ppm.

Anal. calculated for C₂₀H₁₈O₃ : C, 78.41; H, 5.92. Found : C, 78.39; H, 5.82.

11.2.4. Photolysis 9,10-Dihydro-9,10-ethenoanthracene Derivatives in the Solid State

Photolysis of 11-Hydroxymethyl-9,10-dihydro-9,10-ethenoanthracene (131), 13-(11-Methyl-9,10-dihydro-9,10-ethenoanthracenyl)succinate (132) and Methyl 13-(11-methyleneoxy-9,10-dihydro-9,10-ethenoanthracenyl)acetate (133a) in the Solid State

Alcohol 131 was irradiated in the solid state as a powder with a Hanovia medium pressure mercury lamp through a quartz filter ($\lambda \geq 200$ nm). The product ratios were determined by dissolving the sample in ethyl acetate prior to gas chromatographic analysis (HP 5, 30m). The results are represented in Table XX.

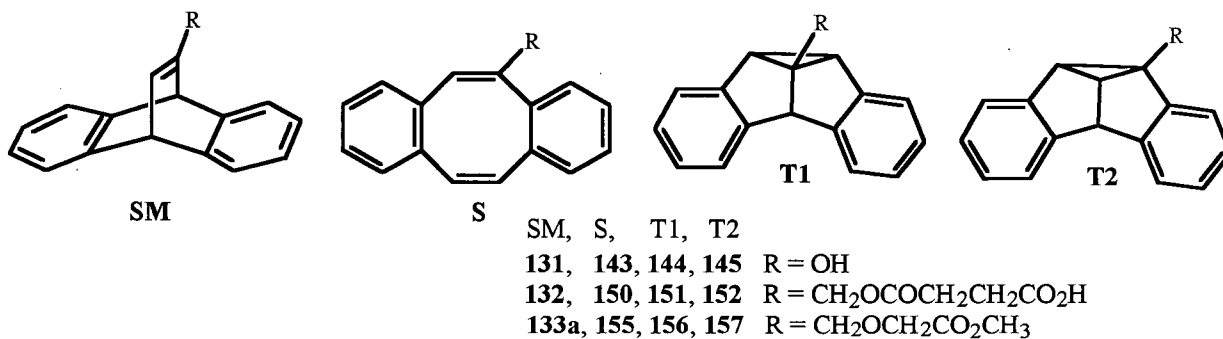
Crystals of acid 132 and ester 133a crushed between two quartz plates were photolyzed with a Hanovia medium pressure mercury lamp through a Vycor filter ($\lambda \geq 240$ nm). After methylation of 132 with diazomethane, the product ratios were determined by GC (HP 5, 30 m) and are shown in Table XX.

Table XX Photoproduct Mixture Composition of Derivatives 131, 132 and 133a

Dibenzobarrelene	Rxn time (h)	Photoproduct ratio ^a SM ^b : S: T1: T2
131	7	92: 8: 0 : 0
132	8	87: 6: 7 : 0
133a	2	93: 6: 1 : 0

(a) Estimated error in GC analysis is $\pm 2\%$. (b) Dibenzobarrelene 132 was identified as the methyl ester derivative.

T = triplet derived product, S = singlet derived product.



11.3. Photochemical Studies of Salts

11.3.1. Photolysis of Sensitizer Salts Formed with 2-(1-Cyclopentenyl)cyclopentanone Derivative 121

Photolysis of Sensitizer Salts 138, 139 and 140

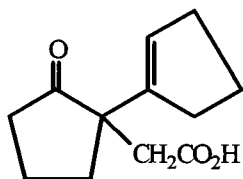
Salts 138, 139 and 140 were irradiated through a uranium glass filter ($\lambda \geq 330$ nm) in solution and the solid state with a Hanovia medium pressure mercury lamp (450 W). Following photolysis, the solvent was removed, the remaining oil dissolved in diethyl ether, washed with 15% aqueous HCl and dried over MgSO₄. After filtering off the drying agent, the acids were esterified with an ethereal solution of diazomethane to produce the corresponding methyl esters. Gas chromatography (DB 5, 15 m) was used to determine the product ratios. The results are summarized in Table XXI.

Table XXI Photoproduct Mixture Composition of Salts 138, 139 and 140 ^a

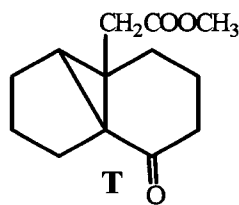
Salt (acid 121 and sensitizer moieties) :	Medium	Concentration (M)	Rxn time (h)	Photoproduct ratio 121 ^b : T : S
138 (3-dimethylamino propiophenone)	Solid State		21	72 : 28 : 0
	Methanol	1 x 10 ⁻²	24	99 : 1 : 0
140 (<i>p</i> -acetylpyridine)	Solid State		24	No Reaction
	Methanol	1 x 10 ⁻²	24	No Reaction
139 (<i>p</i> -acetyl- <i>N,N</i> -dimethylbenzylamine)	Solid State		50	83 : 17 : 0
	Methanol	1 x 10 ⁻²	24	99 : Trace : 0

(a) Estimated error in GC analysis is $\pm 2\%$. (b) Acid 121 was identified as the methyl ester derivative.

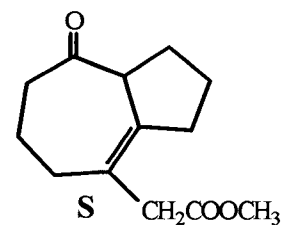
T = triplet derived product, S = singlet derived product.



121



134a



135a

11.3.2. Photolysis of Alkali Metal Salts Formed with 9,10-Dihydro-9,10-ethenoanthracene Derivatives

Photolysis of Salts Formed with Succinate Derivative 132

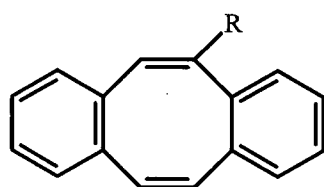
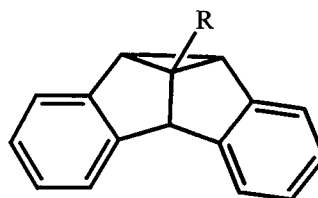
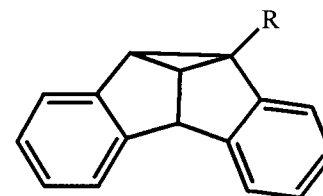
Photolysis of Alkali Metal Salts 153 and 154

Salts 153 and 154 were photolyzed in solution and the solid state through a Vycor glass filter ($\lambda \geq 240$ nm) with a Hanovia medium pressure mercury lamp (450 W). The reaction mixture was then acidified and methylated as described before. Product ratios were determined by GC analysis with a HP 5 column (30 m).

Table XXII Photoproduct Mixture Composition of Salts 153 and 154

Salt (acid 132 and alkali moiety)	Medium	Concentration (M)	Rxn time (h)	Photoproduct ratio ^a S : T1 : T2
153 (sodium)	Solid State		7	23 : 63 : 14
	Ethanol	1.0×10^{-3}	1.5	84: 15 : Trace
154 (potassium)	Solid State		8	0: 94 : 6
	Methanol	4.5×10^{-4}	2	87: 7 : 6

(a) Crystal photolyses were conducted on powders to conversions of 53-57%, whereas solution photolyses were carried out to 100% conversion. Estimated error in GC analysis is $\pm 2\%$.

**S****150****T1****151****T2****152**

Photolysis of Alkali Metal Salts Formed with Acetic Acid Derivative 133

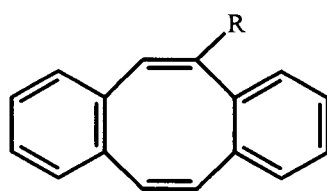
Photolysis of Alkali Metal Salts 158, 159, 160, 161, and 162

The salts 158 to 162 were irradiated in the solid state and solution through a Vycor glass filter ($\lambda \geq 240$ nm) with a Hanovia medium pressure mercury lamp. The samples were derivatized as described previously and the product ratios were determined by GC (HP 5, 30 m).

Table XXIII Photoproduct Mixture Composition of Salts 158 to 162

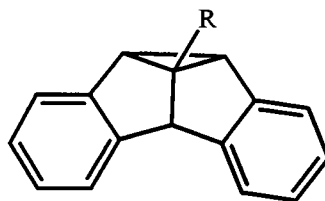
Salt (acid 133 and alkali moiety)	Medium	Concentration (M)	Rxn time (h)	Photoproduct ratio ^a S: T1 : T2
158 (lithium)	Solid State		2	33: 50 : 17
	Methanol	5.6×10^{-4}	5	87: 12 : 1
159 (sodium)	Solid State		2	62: 38 : 0
	Methanol	5.3×10^{-4}	3	89: 11 : 0
160 (potassium)	Solid State		2	27: 73 : 0
	Methanol	5.1×10^{-4}	3	89: 9 : 1
161 (rubidium)	Solid State		2	25: 63 : 12
	Methanol	4.4×10^{-4}	1	91: 9 : 0
162 (cesium)	Solid State		2	75: 25 : 0
	Methanol	4.0×10^{-4}	5	84: 14 : 2

(a) Crystal photolyses were conducted on powders to < 16% conversion. Solution photolyses were carried out to conversions of 80-95%. Estimated error in GC analysis is $\pm 2\%$.



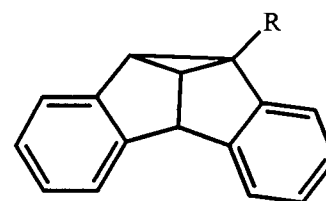
S

155



T1

156



T2

157



11.3.3. Photolysis of Sensitizer Salts Formed with Acetic Acid Derivative 133

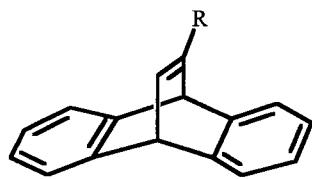
Photolysis of Sensitizer Salts 164, 166 and Complex 165

Salts 164, 166 and complex 165 were irradiated through an uranium glass filter ($\lambda \geq 330$ nm) in solution and the solid state with a Hanovia medium pressure mercury lamp. Following derivatization to the corresponding methyl ester, the reaction mixture was injected into the GC (HP 5, 30 m) to determine the product ratios.

Table XXIV Photoproduct Mixture Composition of Salts 164, 166 and Complex 165

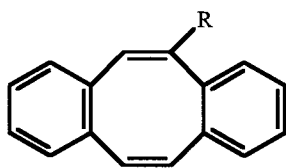
Salt or Complex (acid 133 with sensitizer moiety)	Medium	Concentration (M)	Rxn time (h)	Product ratio ^a SM : S : T1 : T2
164 (3-dimethylamino propiophenone)	Solid State		9	93 : 0 : 6 : 1
	Methanol	1.0×10^{-2}	6	96 : 0 : 3 : 1
		1.0×10^{-3}	6	98 : 0 : 1 : 1
165 (4-acetylpyridine)	Solid State		9	94 : 0 : 5 : 1
	Methanol	1.0×10^{-2}	6	98 : 0 : 1 : 1
		1.0×10^{-3}	6	98 : 0 : 1 : 0
166 (4'-piperazino- acetophenone)	Solid State		8	81 : 0 : 15 : 4
	Methanol	1.0×10^{-2}	6	98 : 0 : 1 : 1
		1.0×10^{-3}	6	98 : 0 : 1 : 0

(a) Estimated error in GC analysis is $\pm 2\%$.



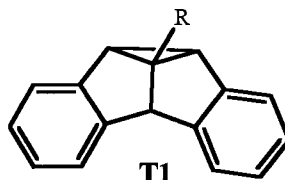
SM

133a



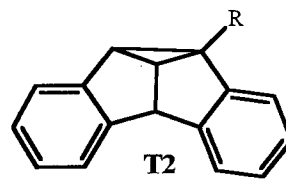
S

155



T1

156



T2

157

R = CH₂OCH₂CO₂CH₃

REFERENCES

1. Ciamician, G. *Science* **1912**, *36*, 385.
2. Emmelius, M.; Pawlowski, G.; Volmann, H.W. *Angew. Chem., Int. Ed. Engl.* **1989**, *28*, 1445.
3. *CRC Handbook of Organic Photochemistry*; Scaiano, J.C., Ed.; CRC Press: Boca Raton, FL, 1987, Vol. 2.
4. Kopecky, J. In *Organic Photochemistry: A Visual Approach*; VCH Publishers: New York, 1992, p 256.
5. Wöhler, F. *Pogg. Ann.* **1828**, *12*, 253.
6. Trommsdorff, H. *Ann. Chem. Phar.* **1834**, *11*, 190.
7. For a review of the beginnings of photochemistry, see: Roth, H.D. *Angew. Chem., Int. Ed. Engl.* **1989**, *28*, 1193.
8. Ramamurthy, V. In *Photochemistry in Organized and Constrained Media*; Ramamurthy, V., Ed.; VCH Publishers: New York, 1991.
9. (a) Dunitz, J.D. In *X-ray Analysis and the Structure of Organic Molecules*; Cornell University Press, Ithaca: New York, 1979, p 312. (b) Buckert, U.; Allinger, N.L. In *Molecular Mechanics*; Am. Chem. Soc. Monograph: Washington, D.C., 1982, p 177.
10. The following is a partial list of some of the review articles on the subject of photochemistry in organized media : (a) Ramamurthy, V.; Venkatesan, K. *Chem. Rev.* **1987**, *87*, 433. (b) Desiraju, G.R. In *Organic Solid State Chemistry*; Elsevier: Amsterdam, 1987. (c) Cohen, M.D. *Tetrahedron* **1987**, *43*, 1211. (d) *Organic Chemistry in Anisotropic Media*; Scheffer, J.R.; Turro, N.J.; Ramamurthy, V., Eds.; Tetrahedron Symposia-in-Print Number 29, *Tetrahedron* **1987**. (e) Scheffer, J.R.; Garcia-Garibay, M.; Nalamasu, O. In *Organic Photochemistry*; Padwa, A., Ed.; Marcel Dekker: New York, 1987, Vol. 8, Chapter 4. (f) Lamartine, R. *Bull. Soc. Chim. France*, **1989**, 237. (g) *Photochemistry on Solid Surfaces*; Anpo, M.; Matsuura, T., Eds.; Elsevier: Amsterdam, 1989. (h) *Photochemistry in Organized and Constrained Media*; Ramamurthy, V., Ed.; VCH Publishers: New York, 1991. (i) Scheffer, J.R.; Trotter, J.; Gudmundsdottir, A.D. In *CRC Handbook of Organic Photochemistry and Photobiology*; Horspool, W.M.; Song, P-S., Eds.; CRC Press: Boca Raton, FL, 1995, Chapter 50.
11. Kohlshutter, H.W. *Z. Anorg. Allg. Chem.* **1918**, *105*, 121.

12. (a) Cohen, M.D.; Schmidt, G.M.J. *J. Chem. Soc.* **1964**, 1996. (b) Schmidt, G.M.J. *Pure Appl. Chem.* **1971**, *27*, 647.
13. (a) Cohen, M.D. *Angew. Chem., Int. Ed. Engl.* **1975**, *14*, 386. (b) Cohen, M.D. *Mol. Cryst. Liq. Cryst.* **1979**, *50*, 1.
14. Garcia-Garibay, M.A.; Constable, A.E.; Jernelius, J.; Choi, T.; Cizmeciyan, D.; Shin, S.H. *Physical Supramolecular Chemistry*, in press.
15. Weiss, R.G.; Ramamurthy, V.; Hammond, G.S. *Acc. Chem. Res.* **1993**, *26*, 530.
16. Wegner, G. *Pure Appl. Chem.* **1977**, *49*, 443.
17. (a) Jones, W.; Nakanishi, H.; Theocharis, C.R.; Thomas, J.M. *J. Chem. Soc., Chem. Commun.* **1980**, 610. (b) Nakanishi, H.; Jones, W.; Thomas, J.M.; Hursthouse, M.B.; Motevalli, M. *J. Chem. Soc., Chem. Commun.* **1980**, 611. (c) Nakanishi, H.; Jones, W.; Thomas, J.M.; Hursthouse, M.B. Mortevalli, M. *J. Phys. Chem.* **1981**, *85*, 3636.
18. Kopecky, J. In *Organic Photochemistry: A Visual Approach*; VCH Publishers: New York, 1992, p 44.
19. Wang, W.N.; Jones, W. *Tetrahedron* **1987**, *43*, 1273.
20. (a) Zimmerman, H.E. In *Rearrangements in Ground and Excited States*; De Mayo, P., Ed.; Wiley Interscience: New York, 1980, Chapter 16. (b) Hixson, S.S.; Mariano, P.S.; Zimmerman, H.E. *Chem. Rev.* **1973**, *73*, 531.
21. (a) Zimmerman, H.E.; Grunewald, G.L. *J. Am. Chem. Soc.* **1966**, *88*, 123. (b) Zimmerman, H.E.; Binkley, R.W.; Givens, R.S., Sherwin, M.A. *J. Am. Chem. Soc.* **1967**, *89*, 3932. (c) Zimmerman, H.E., Binkley, B.W., Givens, R.S., Grunewald, ; Sherwin, R.W. *J. Am. Chem. Soc.* **1969**, *91*, 3316.
22. Zimmerman, H.E.; Kutateladze, A.G.; Mackawa, Y.; Mangette, J.E. *J. Am. Chem. Soc.* **1994**, *116*, 9795.
23. Zimmerman, H.E.; Sulzbach, H.M.; Tollefson, M.B. *J. Am. Chem. Soc.* **1993**, *115*, 6548.
24. (a) Srinivasan, R. In *Advances in Photochemistry*; Wiley Interscience: New York, 1966, Vol. 4, p 113. (b) Mousseron, M. In *Advances in Photochemistry*; Wiley Interscience: New York, 1966, Vol. 4, p 195.
25. Zimmerman, H.E.; Mariano, P.S. *J. Am. Chem. Soc.*, **1969**, *91*, 1718.

26. Saltiel, J.; D'Agostino, J.; Megarity, E.D.; Metts, L.; Neuberger, K.R.; Wrighton, M.; Zefiririov, O.C. In *Organic Photochemistry*; Chapman, O.L., Ed., Marcel Dekker: New York, 1973, Vol. 3.
27. Woodward, R.B.; Hoffman, R. In *The Conservation of Orbital Symmetry*; Verlag Chemie: Wienheim, 1970.
28. Scheffer, J.R.; Yang, J. In *CRC Handbook of Organic Photochemistry and Photobiology*; Horspool, W.M., Song, P-S., Eds.; CRC Press: Boca Raton, FL, 1995, Chapter 16.
29. Zimmerman, H.E.; Givens, R.S.; Pagni, R.M. *J. Am. Chem. Soc.* **1968**, *90*, 6090.
30. Zimmerman, H.E.; Bender, C.O. *J. Am. Chem. Soc.* **1970**, *92*, 4366.
31. Rabideau, R.W.; Hamilton, J.B.; Friedman, L. *J. Am. Chem. Soc.* **1965**, *90*, 4465.
32. Ciganek, E. *J. Am. Chem. Soc.* **1966**, *88*, 2882.
33. Grovenstein, Jr., E.; Campbell, T.C.; Shibata, T. *J. Org. Chem.* **1969**, *34*, 2418. (b) Bender, C.O.; Brooks, D.W. *Can. J. Chem.* **1975**, *53*, 1684. (c) Scheffer, J.R.; Yap, M. *J. Org. Chem.* **1989**, *54*, 2561.
34. (a) Richards, K.E.; Tillman, R.W.; Wright, G.J. *Aust. J. Chem.* **1975**, *28*, 1289. (b) Paddick, R.G.; Richards, K.E.; Wright, G.J. *ibid.* **1976**, *29*, 1005. (c) Iwamura, M.; Takuda, H.; Iwamura, H. *Tetrahedron Lett.* **1980**, *21*, 4865.
35. (a) Evans, S.V.; Garcia-Garibay, M.; Omkaram, N.; Scheffer, J.R.; Trotter, J.; Wireko, F. *J. Am. Chem. Soc.* **1986**, *108*, 5648. (b) Scheffer, J.R.; Trotter, J.; Garcia-Garibay, M.; Wireko, F.C. *Mol. Cryst. Liq. Cryst. Inc. Nonlin. Opt.* **1988**, *156*, 63. (c) Garcia-Garibay, M.; Scheffer, J.R.; Trotter, J.; Wireko, F.C. *Acta Crystallogr., Sect. B.* **1990**, *B46*, 79.
36. Dauben, W.G.; Kellogg, M.S.; Seeman, J.I.; Spritzer, W.A. *J. Am. Chem. Soc.* **1970**, *92*, 1786.
37. (a) Büchi, G.; Burgess, E.M. *J. Am. Chem. Soc.* **1960**, *82*, 4333. (b) Schuster, D.I.; Axelrod, M.; Auerbach, J. *Tetrahedron Lett.* **1963**, 1911.
38. Demuth, M. In *Organic Photochemistry*; Padwa, A., Ed.; Marcel Dekker: New York, 1991, Vol. 11, Chapter 2.
39. Houk, K.N. *Chem. Rev.* **1976**, *76*, 1.
40. Schuster, D.I. In *Rearrangements in Ground and Excited States*; de Mayo, P., Ed.; Academic Press: London, 1980, p 323.

41. Wilsey, S.; Bearpark, M.J.; Bernardi, F.; Olivucci, M. Robb, M.A. *J. Am. Chem. Soc.* **1996**, *118*, 176.
42. (a) Wagner, P.J.; Park, B-S. In *Organic Photochemistry*; Padwa, A., Ed.; Marcel Dekker: New York, 1991; Vol. 11, p 227. (b) Wagner, P.J. In *Molecular Rearrangements*; de Mayo, P., Ed.; Academic Press: New York, 1980; Vol. 3, p 381. (c) Wagner, P.J. *Top. Curr. Chem.* **1976**, *66*, 1.
43. Paquette, L.A.; Pansegrau, P.D.; Wiedeman, P.E.; Springer, J.P. *J. Org. Chem.* **1988**, *53*, 1461.
44. Johnston, L.J.; Scaiano, J.C. *Chem. Rev.* **1989**, *89*, 521.
45. Wagner, P.J.; Kelso, P.A.; Kemppainen, A.E.; Zepp, R.G. *J. Am. Chem. Soc.* **1972**, *94*, 7500.
46. Ariel, S.; Ramamurthy, V.; Scheffer, J.R.; Trotter, J. *J. Am. Chem. Soc.* **1983**, *105*, 6959.
47. (a) Scheffer, J.R. *Org. Photochem.* **1987**, *8*, 249. (b) Scheffer, J.R. In *Organic Solid State Chemistry*; Desiraju, G.R., Ed.; Elsevier: New York, 1987, Chapter 1, p 1.
48. Bondi, A. *J. Phys. Chem.* **1964**, *68*, 441.
49. (a) Kasha, M. *Radiation Research, Suppl. 2* **1960**, 243. (b) Calvert, J.G.; Pitts, J.N., Jr. In *Photochemistry*; Wiley: New York, 1966, p 249.
50. (a) Taylor, R.; Kennard, O.; Versichel, W. *J. Am. Chem. Soc.* **1983**, *105*, 5761. (b) Olovsson, I. *Croat. Chem. Acta*, **1982**, *55*, 171. (c) Taylor, R.; Kennard, O. *Acc. Chem. Res.* **1984**, *17*, 320.
51. (a) Dorigo, A.E.; Houk, K.N. *J. Org. Chem.* **1988**, *53*, 1650. (b) Dorigo, A.E.; McCarrick, M.A.; Loncharich, R.J.; Houk, K.N. *J. Am. Chem. Soc.* **1990**, *112*, 7508.
52. (a) Birks, J. In *Photophysics of Aromatic Molecules*; John Wiley: New York, 1970. (b) Wilkinson, F. In *Organic Molecular Photophysics*; Birks, J., Ed.; John Wiley: New York, 1975, p 95.
53. Turro, N.J. In *Modern Molecular Photochemistry*; Benjamin/Cummings : Menlo Park, CA, 1978, Chapter 9.
54. Zimmerman, H.E.; McKelvey, R.D. *J. Am. Chem. Soc.* **1971**, *93*, 3638.
55. Keller, R.A.; Dolby, L.J. *J. Am. Chem. Soc.* **1969**, *91*, 1293.
56. Koziar, J.C.; Cowan, D.O. *Acc. Chem. Res.* **1979**, *11*, 334.

57. Levine, I.N. In *Quantum Chemistry*; Allyn and Bacon: Boston, Mass., 1970, p 360.
58. (a) McClure, D.S.; Blake, N.W.; Hanst, P.L. *J. Chem. Phys.* **1954**, *22*, 255. (b) Ermolaev, V.L.; Svitashov, K.J. *Opt. Spect.* **1959**, *7*, 399.
59. Kasha, M. *J. Chem. Phys.* **1952**, *20*, 71.
60. (a) Cowan, D.O.; Drisko, R.L. *Tetrahedron Lett.* **1967**, 1255. (b) Cowan, D.O.; Drisko, R.L. *J. Am. Chem. Soc.* **1967**, *89*, 3068.
61. Skell, P.S.; Valenty, S.J.; Humer, P.W. *J. Am. Chem. Soc.* **1973**, *95*, 5041.
62. Givens, R.S.; Chae, W.K.; Matuszewski, B. *J. Chem. Soc.* **1978**, *104*, 2456.
63. Schuster, D.I.; Calcaterra, L.T. *J. Am. Chem. Soc.* **1982**, *104*, 6397.
64. El-Sayed, M. A. *J. Chem. Phys.* **1964**, *41*, 2462.
65. (a) Meier, W.M.; Olson, D.H. In *Atlas of Zeolite Structure Types*, 2nd revised ed.; Butterorths: Cambridge, 1987. (b) Breck, D. In *Zeolite Molecular Sieves: Structure, Chemistry, and Use*; John Wiley and Sons: New York, 1974. (c) Dyer, A. In *An Introduction to Zeolite Molecular Sieves*; John Wiley and Sons: Bath, 1988. (d) van Bekkum, H.; Flanigen, E.M.; Jansen J.C. In *Introduction to Zeolite Science and Practice*; Elsevier: Amsterdam, 1991.
66. (a) Turro, N.J.; Cheng, C-C.; Lei, X-G. *J. Am. Chem. Soc.* **1985**, *107*, 3739. (b) Turro, N.J.; Cheng, C-C.; Abrams, L.; Corbin, D.R. *J. Am. Chem. Soc.* **1987**, *109*, 2449. (c) Ramamurthy, V.; Corbin, D.R.; Johnston, L.J. *J. Am. Chem. Soc.* **1992**, *114*, 3870.
67. Nishiguchi, H.; Yukawa, K.; Yamashita, H.; Anpo, M. *Res. Chem. Intermed.* **1995**, *22*, 885.
68. Ramamurthy, V.; Caspar, J.V.; Eaton, D.F.; Kuo, E.W.; Corbin, D.R. *J. Am. Chem. Soc.* **1992**, *114*, 3882.
69. Ramamurthy, V.; Corbin, D.R.; Kumar, C.V.; Turro, N.J. *Tetrahedron Lett.* **1990**, *31*, 47.
70. Turro, N. J.; Gould, I.R.; Zimmt, M.B; Cheng, C.C. *Phys. Lett.* **1985**, *119*, 484.
71. Evans, S.V.; Garcia-Garibay, M.; Omkaram, N.; Scheffer, J.R.; Trotter, J. *J. Am. Chem. Soc.* **1986**, *108*, 5648.
72. (a) Chen, J.; Scheffer, J.R.; Trotter, J. *Tetrahedron* **1992**, *48*, 3251. (b) Chen, J.; Ph.D. Thesis, University of British Columbia, 1988. (c) Gudmundsdottir, A.D.; Ph.D. Thesis, University of British Columbia, 1993.

73. Turro, N.J. *Modern Molecular Photochemistry*; Benjamin/Cummings: Menlo Park, C.A. 1978, p 246.
74. Clar, E. *Chem. Ber.* **1931**, *64*, 1676.
75. Bartlett, P.D. *J. Am. Chem. Soc.* **1942**, *64*, 2649.
76. Kirby, G.W.; Sweeny, J.G. *J. Chem. Soc. Perkin Trans. 1* **1981**, 3250.
77. Miller, M. W.; Amidon, R.W.; Tawney, P.O. *J. Am. Chem. Soc.* **1955**, *77*, 2845.
78. Mylorie, V. L.; Stenberg, J.F. *Ann. N.Y. Acad. Sci.* **1973**, *214*, 255.
79. Theilacker, W.; Berger-Brose, U.; Beyer, K-H. *Chem. Ber.* **1960**, *93*, 1658.
80. Hashimoto, M.; Shimizu, Y.; Ogura, F.; Nakagawa, M. *Bull. Chem. Soc. Jpn.* **1974**, 1761.
81. Schilling, H. *Chem. Ber.* **1913**, *46*, 1066.
82. Barnett, E.B.; Mathews, M.A. *Rec. Trav. Chim. Pays-Bas* **1924**, *43*, 530.
83. Iwamura, H.; Makino, K. *J. Chem. Soc., Chem. Commun.* **1978**, 720.
84. Yamamura, K.; Nakasuji, K.; Murata, I.; Inagaki, S. *J. Chem. Soc., Chem. Commun.* **1982**, 396.
85. Kitaguchi, N. *Bull. Chem. Soc. Jpn.* **1989**, *62*, 800.
86. Kitaguchi, N. *Bull. Chem. Soc. Jpn.* **1989**, *62*, 3542.
87. Rattray, A.G. Ph.D. Thesis, University of British Columbia, 1992.
88. Silverstein, R.M.; Bassler, G.C.; Morrill, T.C. In *Spectrometric Identification of Organic Compounds*; Wiley and Sons: New York, 1981, Chapter 4.
89. Scheffer, J.R.; Trotter, J.; Garcia-Garibay, M.; Wireko, F.C. *Mol. Cryst. Liq. Cryst. Inc. Nonlin. Opt.* **1988**, *156*, 63. (b) Garcia-Garibay, M.; Scheffer, J.R.; Trotter, J.; Wireko, F.C. *Acta Crystallogr., Sect. B* **1990**, *B46*, 79. (c) Trotter, J.; Wireko, F.C. *Acta Crystallogr., Sect. C* **1991**, *C47*, 793.
90. Zimmerman, H.E.; Sulzbach, H.M.; Tollefson, M.B. *J. Am. Chem. Soc.* **1993**, *115*, 6548.
91. DePuy, C.H.; Zaweski, E.F. *J. Am. Chem. Soc.* **1959**, *81*, 4920.

92. Bovey, F.A. In *NMR Data Tables for Organic Compounds*; Interscience Publishers: New York, 1967, p 86. (b) De Puy, C.H.; Thurn, R.D.; Isaks, M. *J. Org. Chem.* **1962**, *27*, 744.
93. Bartlett, P.D.; Traylor, T.G. *J. Amer. Chem. Soc.* **1962**, *84*, 3408.
94. Petrellis, P.C.; Dietrich, H.; Meyer, E.; Griffin, G.W. *J. Amer. Chem. Soc.* **1967**, *89*, 1967.
95. Wöhler, F. *Justus Liebigs Ann. Chem.* **1844**, *51*, 155.
96. Adams, R.N.; Hawley, M.D.; Feldberg, S.W. *J. Phys. Chem.* **1967**, *71*, 851.
97. Cason, J.; Harman, R.F.; Goodwin, S.; Allen, C.F. *J. Org. Chem.* **1960**, *15*, 860.
98. Patai, S. In *The Chemistry of the Carbon-Halogen Bond*; Wiley and Sons: New York, 1973, Part 2, p 852.
99. Chen, J.; Scheffer, J.R.; Trotter, J. *Tetrahedron*, **1992**, *48*, 3251.
100. Ariel, S.; Askari, S.; Scheffer, J.R.; Trotter, J. *Tetrahedron Lett.* **1986**, *27*, 783.
101. Bondi, A. *J. Phys. Chem.* **1964**, *68*, 441.
102. Scheffer, J.R.; Trotter, J.; Yang, J. In *CRC Handbook of Organic Photochemistry and Photobiology*; Horspool, W.M.; Song, P.-S., Eds.; CRC Press: Boca Raton, FL, 1995, Chapter 16.
103. Walsh, T.D. *J. Am. Chem. Soc.* **1969**, *91*, 515.
104. Turro, N.J.; Tobin, M.; Friedman, L.; Hamilton, J.B. *J. Am. Chem. Soc.* **1969**, *91*, 516.
105. Iwamura, H.; Yoshimura, K. *J. Am. Chem. Soc.* **1974**, *96*, 2652.
106. Iwamura, M.; Tukada, H.; Iwamura, H. *Tetrahedron Lett.* **1980**, *21*, 4865.
107. Iwamura, H.; Tukada, H. *J. Chem. Soc., Chem. Commun.* **1975**, 969. (b) Day, R.O.; Day, V.W.; Fuerniss, S.J.; Hohman, J.R.; Wheeler, D.M.S. *J. Chem., Soc. Chem. Commun.* **1976**, 853. (c) Iwamura, M.; Nori, E.; Koike, A.; Kitagawa, T.; Koga, N.; Iwamura, H. *Chem. Lett.* **1992**, 2051 and references cited therein.
108. Lowry, T.H.; Richardson, K.S. In *Mechanism and Theory in Organic Chemistry*; Harper and Row: New York, 1987, Chapter 2, p 231.
109. Baier, M.; Daub, J.; Hasenhuendl, A.; Merz, A.; Rapp, K.M. *Ang. Chem., Int. Ed. Engl.* **1981**, *20*, 198.

110. Scheffer, J.R.; Garcia-Garibay, M.; Nalamasu, O. In *Organic Photochemistry*; Padwa, A., Ed.; Marcel Dekker: New York, 1987, Vol. 2, Part 2, Chapter 20. (b) Chen, J.; Scheffer, J.R.; Trotter, J. *Tetrahedron*, **1992**, *48*, 3251.
111. Durr, H. *Angew. Chem., Int. Ed. Eng.* **1989**, *28*, 413.
112. Exelby, R.; Grinter, R. *Chem. Rev.* **1965**, *65*, 247.
113. Gudmundsdottir, A.D. Ph. D. Thesis, University of British Columbia, 1993.
114. Burger, K. In *Solvation, Ionic and Complex Formation Reactions in Non-aqueous Solvents*; Elsevier: New York, 1983, Chapter 5.
115. Reichardt, C. In *Solvent Effects in Organic Chemistry*; Verlag Chemie: New York, 1979, Chapter 6.
116. Calvert, J.G.; Pritts, J.N., Jr.; In *Photochemistry*; Wiley & Sons: New York, 1966, Chapter 4, p 257.
117. Orlando, C.M.; Mark, H.; Bose, A.K. Manhas, M.S. *J. Am. Chem. Soc.* **1967**, *89*, 6527.
118. Farid, S. *Chem. Comm.* **1971**, 73.
119. Wagner, P.J.; Park, B-S. In *Organic Photochemistry*; Padwa, A., Ed.; Marcel Dekker: New York, 1991, Vol. 11, Chapter 4.
120. Bondi, A. *J. Phys. Chem.*, **1964**, *68*, 441.
121. Scheffer, J.R. In *Organic Solid State Chemistry*; Desiraju, G.R., Ed.; Elsevier: New York, 1987, Chapter 1.
122. Iwamrua, H.; Kawada, Y.; Tukada, H. *Tetrahedron Lett.* **1980**, *21*, 4865.
123. Wheeler, D.M.S.; Day, R.O.; Day, V.W.; Fuerniss, S.J. *J. Chem. Soc., Chem. Commun.* **1975**, 296.
124. (a) Coffin R.L.; Cox, W.W.; Carlson, R.G.; Givens, R.S. *J. Am. Chem. Soc.* **1979**, *101*, 3261. (b) Ide, J.; Iwai, I. *Organic Synthesis*, **1970**, *50*, 62.
125. Varech, D.; Ouannes, C.; Jacques, J. *Bull. Soc. Chim. Fr.* **1965**, 1662.
126. Gault, M.H.; Daltroff, L.; Ecktridon, J. *Bull. Soc. Chim. Fr.* **1945**, *12*, 952.
127. Norman, J.J.; Heggie, R.M.; Larose, J.B. *Can. J. Chem.* **1962**, *40*, 1547.

128. Vaughan, W.R.; Milton, K.M. *J. Am. Chem. Soc.* **1952**, *74*, 5623.
129. Cristol, S.J.; Schloemer, G.C.; James, D.R.; Paquette, L.A. *J. Org. Chem.* **1972**, *37*, 3852.
130. Aries, R. Patent 2,311,030, 1976; *Chem. Abstracts*, **1977**, *87*, 168265.
131. Brady, W.T.; Giang, Y.F. *J. Org. Chem.* **1985**, *50*, 5177.
132. Givens, R.S.; Coffin, R.L.; Cox, W.W.; Carlson, R.G. *J. Am. Chem. Soc.* **1979**, *101*, 3261.
133. Borecka, B.; Gudmundsdottir, A.D.; Olovsson, G.; Ramamurthy, V.; Scheffer, J.R.; Trotter, J. *J. Am. Chem. Soc.* **1994**, *116*, 10322.
134. Reviews: (a) Schuster, D.I. In *Rearrangements in Ground and Excited States*; de Mayo, R., Ed.; Academic Press: New York, 1980, Vol. 3, Chapter 17. (b) Demuth M. In *Organic Photochemistry*; Padwa, A., Ed.; Marcel Dekker: New York, 1991, Vol. 11, Chapter 2.
135. Cookson, R.C.; Rogers, N.R. *J. Chem. Soc., Chem. Comm.* **1972**, *13*, 809.
136. Cookson, R.C.; Rogers, N.R. *J. Chem. Soc. Perkin Trans 1* **1974**, *10*, 1037.
137. Van Der Veen, R.H.; Cerfontain, H. *Tetrahedron* **1985**, *41*, 585.
138. Bondi, A. *J. Phys. Chem.* **1964**, *68*, 441.
139. Scheffer, J.R.; Yang, J. In *CRC Handbook of Organic Photochemistry and Photobiology*; Horspool, W.M., Song, P-S., Eds.; CRC Press: Boca Raton, FL, 1995; Chapter 16.
140. Wells, C.H.J. *Introduction to Molecular Photochemistry*; Halsted Press: New York, 1972, p 128.
141. Cristol, S.J.; Braun, D.; Schloemer, G.C.; Vanden Plas, B.J. *Can. J. Chem.* **1986**, *64*, 1081.
142. *Photochemistry in Organized and Constrained Media*; Ramamurthy, V., Ed.; VCH Publishers: New York, 1991, p 444.
143. Yang, N.C.; McClure, D.S.; Murov, S.L.; Houser, J.J.; Dusenberry, R. *J. Am. Chem. Soc.* **1967**, *89*, 5466.
144. Chandra, A.K.; Turro, N.J.; Lyons, A.L., Jr.; Stone, P. *J. Am. Chem. Soc.* **1978**, *100*, 4964.
145. Koziar, J.C.; Cowan, D.O. *Acc. Chem. Res.* **1978**, *11*, 334.
146. Borecka, B.; Gudmundsdottir, A.D.; Olovsson, G.; Ramamurthy, V.; Scheffer, J.R.; Trotter, J. *J. Am. Chem. Soc.* **1994**, *116*, 10322.

147. Ramamurthy, V.; Lei, X-G.; Turro, N.J.; Lewis, T.J.; Scheffer, J.R. *Tetrahedron Lett.* **1991**, *32*, 7675.
148. Anpo, M.; Nishiguchi, H.; Yukawa, K.; Yamashita, H. *Res. Chem. Intermed.* **1995**, *21*, 885.
149. *Photochemistry in Organized and Constrained Media*; Ramamurthy, V., Ed.; VCH Publishers: New York, 1991, p 450.
150. Traetteberg, M. *Acta Chem. Scand.* **1966**, *20*, 1724.
151. (a) Anet, F.A.L.; Bourn, J.R.; Lin, Y.S. *J. Am. Chem. Soc.* **1964**, *86*, 3576. (b) Paquette, L.A. *Pure Appl. Chem.* **1982**, *54*, 987.
152. Paquette, L.A.; Trova, M.P. *J. Am. Chem. Soc.* **1988**, *110*, 8197.
153. Gilbert, A.; Baggot, J. In *Essentials of Molecular Photochemistry*; CRC Press: Boca Raton, FL, 1991, p 111.
154. Kopecky, J. In *Organic Photochemistry: A Visual Approach*; VCH Publishers: New York, 1991, p 45.
155. Lowry, T.H.; Richardson, K.S. In *Mechanism and Theory in Organic Chemistry*; Harper and Row: New York, 1987, Chapter 12, p 996.
156. Lamola, A.A.; Turro, N.J. In *Energy Transfer and Organic Photochemistry*; Leermakers, P.A.; Weissberger, A., Eds.; Interscience Publishers: New York, 1969, p 83.
157. Silver, R.M.; Bassler, G.C.; Morrill, T.C. In *Spectrometric Identification of Organic Compounds*; John Wiley and Sons: 1981, p 308.
158. *The Sadtler Handbook of Ultraviolet Spectra*; Simmon, W.W., Ed.; Heyden and Son: London, England, 1979, p 580.
159. (a) Turro, N.J. In *Modern Molecular Photochemistry*; Benjamin Cummings: Menlo Park, CA, 1978, Chapter 9, p 340. (b) Ermolaev, V.L.; Sveshnikova, E.B. *J. Chim. Phys.* **1958**, *55*, 698.
160. Lamola, A.A. *J. Chem. Phys.* **1972**, *47*, 4810.
161. Turro, N.J. In *Modern Molecular Photochemistry*; Benjamin Cummings : Menlo Park, CA, 1978, Chapter 10, p 376.
162. Kopecky, J. In *Organic Photochemistry: A Visual Approach*; VCH Publishers: New York, 1992, p 26.